Modeling Ice Thickness Distribution and Glacier Bed Topography from Sparse Input Data to Assess Future Glacier Changes

---

Dissertation

zur

Erlangung der naturwissenschaftlichen Doktorwürde

(Dr. sc. nat.)

vorgelegt der

Mathematisch-naturwissenschaftlichen Fakultät

der

Universität Zürich

von

Andreas Linsbauer

von

Erschmatt VS

Promotionskomitee

Prof. Dr. Wilfried Haeberli (Vorsitz)

Dr. Frank Paul (Leitung der Dissertation)

Prof. Dr. Martin Hoelzle

Zürich 2013

Summary

Glaciers are considered to be both extremely sensitive and reliable terrestrial indicators of climate change. Over the last 150 years the general retreat of glaciers is consistent world-wide. Due to their proximity to melting conditions, glaciers are especially sensitive to small changes in climatic conditions, causing the observed, often kilometer-long glacier retreat and extensive volume loss that is well visible and even physically understandable to everybody. Considering scenarios of future climate change, glaciers will further continue to retreat and lose mass with increasing temperatures.

The observed shrinkage and even disappearance of glaciers in high-mountain regions can have strong environmental impacts at local, regional and even continental scales. In this regard, changes in seasonal water supply, potentially hazardous situations due to formation of new lakes or hydropower production are important aspects for the people living in the Alps and downstream of glaciers. To be able to answer important questions by the public, policymakers, hydropower companies and others, knowledge about the state and future evolution of the glaciers in the Alps is a prerequisite.

Information about ice thickness distribution and bed topography is of central importance in this regard. However, related data is very scarce and can be obtained by (a) geophysical measurements with a subsequent spatial inter- and extrapolation or by (b) modeling. For the latter several approaches with different complexity have been developed and applied, but none provide ice thickness distributions and bed topographies over an entire mountain range from a single model run. With the model *GlabTop* (*Gla*cier *b*ed *Top*ography) this gap can be closed: using only three input data sets (a DEM, glacier outlines and a set of glacier branch lines) the ice thickness distribution and hence bed topographies of a large glacier sample can be derived within one model run. Ice thickness is derived from an ice dynamical approach, relating glacier thickness to its surface slope and a glacier specific mean basal shear stress.

The modeled ice thickness distribution is applied in order to (a) estimate total glacier volume, (b) to analyze characteristics of the modeled glacier bed topography, (c) to detect overdeepenings in the glacier beds, and (d) to model future glacier evolution. The results of these applications can be summarized as follows.

The total ice volume for all Swiss glaciers is estimated to be $75\pm22\,km^3$ for 1973 and $65\pm20\,km^3$ in 1999 with an uncertainty range of $\pm30\%$. Ice thickness values are unequally distributed; about 60% ($800\,km^2$) of glacierized area is less than 50 m thick, whereas about a quarter of the volume is related to an area of about 5% ($60\,km^2$), with ice thickness values exceeding 200 m. Most of the ice is stored in the largest glaciers and often found in their comparably flat glacier tongues. As a consequence, the elevations of the glacier beds are comparably low and furthermore, weakly inclined, indicating that large glaciers have only limited possibilities to retreat to higher elevations during shrinkage. The geomorphometric analysis revealed 500–600 overdeepenings with a total area of 50–60 km^2. If they fill up with water, they are highly relevant for hydropower-production, hazard investigations, and tourism.

A variety of methods exist to model future glacier evolution. Although the details of these approaches are different, all models foresee a strong (to almost complete) loss of glaciers in the European Alps by the end of the 21^{st} century. In this thesis, three regional-scale approaches to model future glacier evolution are compared, confirming the above trends in glacier loss, and additionally revealing that the uncertainties in the climate scenarios cause the largest spread (about 40%) in the total area loss compared to other uncertainties (ice thickness, albedo change, etc.).

If all involved uncertainties are considered, the results produce a comprehensive overview of the current conditions and characteristics, as well as the potential future evolution of the Swiss glaciers.

Zusammenfassung

Gletscher werden allgemein als sehr sensitive aber auch zuverlässige terrestrische Indikatoren für den Klimawandel betrachtet. Der generelle Gletscherrückgang während der letzten 150 Jahre ist demzufolge ein weltweites Phänomen. Aufgrund ihrer Nähe zu Schmelzbedingungen, reagieren Gletscher äusserst empfindlich auf bereits kleine klimatische Veränderungen. In der Folge kommt es zu Gletscherrückzug im Kilometerbereich und massiven Volumenverlust. Diese Änderungen sind auch für Laien sichtbar und in ihren physikalischen Prinzipien verständlich. Angesichts zukünftiger Klimaänderungs Szenarien mit steigenden Temperaturen, werden sich die Gletscher weiter zurückziehen und an Masse verlieren.

Der beobachtete Gletscherschwund in Gebirgsregionen hat schon jetzt Auswirkungen auf die Umwelt, sowohl auf lokaler und regionaler als auch auf kontinentaler Skala (Meeresspiegleanstieg). Die saisonalen Veränderungen in der Wasserversorgung, potenziell gefährliche Situationen durch neue Seen oder die Energieproduktion aus Wasserkraft sind schon jetzt sichtbare Auswirkungen für die Bevölkerung in den Alpen. Um diesbezügliche Fragen der Öffentlichkeit, von Politikern, von Wasserkraft- und anderen Unternehmen beantworten zu können, ist das Wissen über den Zustand und die Entwicklung der Gletscher in den Alpen eine wichtige Voraussetzung.

Von zentraler Bedeutung ist hier die Kenntnis der Eisdickenverteilung bzw. der Gletscher Betttopographie. Allerdings sind darüber nur spärlich Informationen vorhanden. Letztere können durch (a) geophysikalische Messungen, mit anschliessender räumlicher Inter-und Extrapolation der Messungen, oder durch (b) Modellierung gewonnen werden. Für letzteres wurden bereits verschiedene Ansätze unterschiedlicher Komplexität entwickelt und angewandt. Das hier beschriebene Modell *GlabTop* (*Gla*cier *b*ed *Top*ography) schliesst dabei eine Lücke. Basierend auf nur drei Eingabe-Datensätzen (DHM, Gletscherumrisse und Fliesslinien) ermittelt es in einem einzigen Modelllauf, die Eisdickenverteilungen und Betttopographien aller Gletscher einer Region. Die Eisdicke wird dabei aus einem eisdynamischen Ansatz abgeleitet, welcher die Neigung der Oberfläche und eine mittlere basale Schubspannung für jeden Gletscher verwendet.

Die modellierte Eisdickenverteilung wird verwendet um (a) das gesamte Gletschervolumen zu schätzen, (b) die Eigenschaften der modellierten Betttopographien zu analysieren, (c) Übertiefungen in den Gletscherbetten zu detektieren, und (d) die zukünftige Entwicklung der Gletscher zu modellieren. Die Ergebnisse können wie folgt zusammengefasst werden:

Das totale Eisvolumen aller Schweizer Gletscher ist $75\pm22\,\mathrm{km}^3$ für 1973 und $65\pm20\,\mathrm{km}^3$ für 1999 mit einem Unsicherheitsbereich von $\pm30\%$. Die Eisdickenwerte sind sehr ungleich verteilt; etwa 60% ($800\,\mathrm{km}^2$) der vergletscherten Fläche ist weniger als 50 m dick, aber ein Viertel des Eisvolumens ist unter einer Fläche von nur $60\,\mathrm{km}^2$ gespeichert, mit Eisdicken grösser als 200 m. Das meiste Eis ist damit in den flachen Zungen der grössten Gletscher zu finden. Als Konsequenz sind Gletscherbetten vergleichsweise tief gelegen und nur schwach geneigt, dass heisst grosse Gletscher haben nur sehr begrenzte Möglichkeiten, sich bei einem Rückzug in höhere Lagen zurückzuziehen. Insgesamt wurden 500–600 Übertiefungen mit einer Gesamtfläche von 50–60 km^2 gefunden. Mit Wasser gefüllt sind sie von Interesse für die Wasserkraft, aber auch im Bezug auf Naturgefahren und Tourismus.

Obwohl die Methoden um zukünftige Gletscherentwicklungen zu modellieren recht unterschiedlich sind, ermitteln alle Modelle bis zum Ende des 21. Jahrhunderts einen starken bis fast vollständigen Verlust von Gletscherfläche und Volumen. Die in dieser Arbeit verglichenen regionalen Modelle bestätigen den starken Gletscherverlust. Sie zeigen auch, dass die Unsicherheiten in den Klimaszenarien im Vergleich zu anderen Unsicherheiten (Eisdicke, Albedo Veränderung, etc.) die grösste Streuung (etwa 40%) des modellierten Flächenverlustes ausmachen.

Trotz aller Unsicherheiten geben die in dieser Arbeit entwickelten Modelle einen umfassenden Überblick der aktuellen Bedingungen und Eigenschaften, sowie eine Abschätzung der möglichen zukünftigen Entwicklung der Schweizer Gletscher.

Contents

Part I Synopsis

List of Figures

Abbreviations

AAR	Accumulation Area Ratio
ASTER	Advanced Spaceborne Thermal Emission and Reflection Radiometer
ASTER GDEM	ASTER Global DEM
BAFU	Bundesamt für Umwelt
CC-ClinCH	Climate Change Impacts on Glaciers in Switzerland (CH)
CCHydro	Climate change and hydrology
CGIAR	Consultative Group on International Agricultural Research
CH2011	Swiss Climate Change Scenarios CH2011
CHy	Schweizerische Hydrologische Kommission
DEM	Digital Elevation Model
DHM25	Digital Height Model of Switzerland (25 m resolution)
ESRI	Environmental Systems Research Institute
FMV	Forces Motrices Valaisannes
FOEN	Federal Office for the Environment
GCM	General Circulation Model
GCOS	Global Climate Observing System
GIS	Geographic Information System / Geographic Information Science
GlabTop	Glacier Bed Topography
GLIMS	Global Land Ice Measurements from Space
GPR	Ground Penetrating Radar
GTN-G	Global Terrestrial Network for Glaciers
GTOS	Global Terrestrial Observing System
ICSI	International Commission on Snow and Ice
IDW	Inverse Distance Weighting
IPCC	Intergovernmental Panel on Climate Change
LIA	Little Ice Age
NELAK	New lakes in deglaciating high-mountain areas
NRP 61	Swiss National Research Programme 61 "Sustainable Water Management"
NSIDC	National Snow and Ice Data Center

RCM	Regional Climate Model
RGI	Randolph Glacier Inventory
SFOE	Swiss Federal Office of Energy
SGHL	Schweizerische Gesellschaft für Hydrologie und Limnologie
SGI	Swiss Glacier Inventory
SRES	Special Report on Emissions Scenarios
SRTM	Shuttle Radar Topography Mission
TIN	Triangular Irregular Network
TSL	Temporal Snow Line
TTS/WGI	Temporary Technical Secretariat of the World Glacier Inventory
WGI	World Glacier Inventory
WGMS	World Glacier Monitoring Service

Part I

Synopsis

1 Introduction

1.1 Motvation

Observations and measurements all over the world confirm that the ongoing warming of the atmosphere is unequivocal, resulting in rising global air and ocean temperatures, enhanced melting of snow and ice, and a rising global sea level (*IPCC*, 2007). Considering scenarios of climate change, temperatures will further rise, independent of the future emission scenarios applied in climate models (*IPCC*, 2007). As a consequence, the Alpine environment will also continue to depart from equilibrium (*Watson and Haeberli*, 2004).

Glaciers, which form a significant part of the mountain cryosphere, are considered as very sensitive and reliable, terrestrial indicators of climatic change, due to their proximity to the melting point (*Oerlemans*, 1994, *Haeberli and Beniston*, 1998). The retreat of glaciers during the last century appears to be coherent all over the globe (e.g., *Watson and Haeberli*, 2004, *WGMS*, 2008b) which is not astonishing in the context of the observed increased global temperatures. Today, most glaciers are far from equilibrium and not adapted to the current temperatures (e.g., *Pelto*, 2006, *Paul et al.*, 2007b, *WGMS*, 2008b, *Bahr et al.*, 2009) and therefore glaciers will continue to retreat and lose mass.

Accelerated glacier shrinking or even vanishing in high-mountain regions (e.g., *Paul et al.*, 2007a) can have strong environmental impacts at local to regional and even con-

tinental to global scales (e.g., *Zemp et al.*, 2007, *WGMS*, 2008b). At a global scale, progressive melting of glaciers and ice caps leads to a rise in global sea levels (e.g., *Meier et al.*, 2007, *Hock et al.*, 2009, *Radic and Hock*, 2011). On a continental to regional scale, seasonal water supply can change substantially (e.g., *Zappa et al.*, 2003, *Kaser et al.*, 2010, and references therein) and on local scales, landscape appearance and natural hazards are even now undergoing changes far beyond historical precedence in many regions, particular, in the densely populated Alps (e.g., *Haeberli and Beniston*, 1998, *Rothenbühler*, 2006, *Haeberli and Hohmann*, 2008, *Oppikofer et al.*, 2008).

The consequences of a changed perception of the landscape due to lost glaciers is an important point, as glaciers are a symbol of an intact mountain environment, an innocent nature and an important cultural component for people living in mountain regions (*Carey*, 2007). In the 18^{th} century the European Alps became an important international tourist attraction, due especially to the contrast between the "untouched and eternal" glaciers and the cultivated Alpine garden landscapes (*Haeberli et al.*, 2011). At this time a majority of Alpine glaciers showed a strong advance reaching their maximum extent during the so called Little Ice Age (LIA) around 1850 (*Zumbühl et al.*, 2008). Beginning with the second half of the 19^{th} century glaciers started to retreat until today. Between 1850 and 1975 the European glaciers lost about half of their total volume ($0.5\%\,a^{-1}$), about 25% ($1\%\,a^{-1}$) of the remaining amount between 1975 and 2000, and an additional 10 to 15% ($2–3\%\,a^{-1}$) in the first 5 years of the 21^{st} century (*Paul et al.*, 2004, *Zemp et al.*, 2006, *Haeberli et al.*, 2007). Between ca. 1965 and 1985 a time period with small positive overall mass changes is reported and several medium sized glaciers even started to advance as a consequence of the better nourishment (*Zemp et al.*, 2009, *WGMS*, 2011). This period was followed by accelerated and sustained glacier mass loss until present, where disintegration and down-wasting are becoming predominant processes of glacier decline (*Paul et al.*, 2004, *Zemp et al.*, 2006, *Haeberli et al.*, 2011). For the future development even increasing loss rates are expected (partly due to self-reinforcing feedbacks), ultimately leading to an almost complete loss of glaciers in the Alps (e.g., *Zemp et al.*, 2006, *Huss*, 2012).

Of major interest in combination with climate and glacier change is the development of future run-off regimes and hydrological aspects. The hydrological system of the Alps is complex, but it is the major water resource for several major European river catchments (*Viviroli et al.*, 2009). The abundant water availability is an important natural resource of the Alps (and above all of Switzerland) and of a high economic value for hydropower production (e.g., *Schädler et al.*, 2011, and related articles) and tourism. Of particular interest in regard to hydropower is the water volume that is stored in the glaciers (*Jansson et al.*, 2003). Futhermore, extreme events related to precipitation often cause floods which result in high damages (e.g., *Jaeggi*, 2007) that might further increase after glaciers

have disappeared (leaving unconsolidated rocks in their forefields). The impacts due to the expected climate change in the Alps are complex and tend to be a large challenge for science, politics and economy. Considering scenarios of future climate change with further increasing temperatures (*IPCC*, 2007), a continuation if not acceleration of the current glacier shrinkage has to be anticipated. Hence, the ongoing glacier shrinkage in the Alps is of increasing concern for the expected changes in the hydrologic regime of major river catchments (e.g., *Mauser and Bach*, 2009, *Huss*, 2011), as well as for its influence on hydropower production (e.g., *Schaefli et al.*, 2007, *Terrier et al.*, 2011, *Farinotti et al.*, 2012), tourism (*Fischer et al.*, 2011), and natural hazards (e.g., *Moore et al.*, 2009, *Frey et al.*, 2010, *Haeberli et al.*, 2010, *Künzler et al.*, 2010).

At the time when this thesis started, comprehensive modeling scenarios of the future hydrological cycle based on high-resolution climate scenarios and spatially distributed quantitative declarations on the development of existing ice reserves were not available for Switzerland. To address this issue, two research projects were launched in 2009:

1. **CCHydro**: The Federal Office for the Environment (FOEN) "commissioned various research institutes to investigate how the water balance in Switzerland, the frequency of floods and low water as well as the water temperature might change by the end of this century. These studies were carried out on the basis of national climate scenarios developed at the same time" (*BAFU*, 2012). The main goal of this study was to provide – based on recent climate change scenarios – high-resolution scenarios of the water cycle and run-off for different climatic regions in Switzerland.

2. **Climate change and hydropower**: The Swiss Federal Office of Energy (SFOE), Swisselectric Research (an organization of Swiss electricity grid companies), the Canton of Valais and Forces Motrices Valaisannes (FMV) funded research institutes to conduct research on the future of the hydrologic cycle in context with climate change and hydropower production (*SGHL and CHy*, 2011). The main goal of this study was (1) to clarify the climate change impacts on hydropower use in Switzerland, to recognize the need for action in time, and to define related strategies and mitigation measures, as well as (2) in an additional sectoral study in the Canton of Valais to analyze the future development of glaciers and sediment bed loads.

Because run-off from glaciers plays a hydrologically important role (e.g., *Stahl et al.*, 2008) and a strong reduction in future glacier area and volume is likely to occur (e.g., *Zemp et al.*, 2006, *Huss*, 2012), the modeling of the future hydrologic regime has to include a glacier response module. For current distributed hydrological models that operate on a regional scale (e.g., *Verbunt et al.*, 2003, *Koboltschnig et al.*, 2008, *Viviroli et al.*,

2009), this implies that glacier surface areas have to be periodically updated according to a given climate change scenario, leading to the fundamental question, how will the Swiss glaciers develop (collectively), under recent climate change scenarios? Several transient retreat models for glaciers already exist (e.g., *Huss et al.*, 2008b, *Jouvet et al.*, 2009, 2011), but they require a large amount of specific input data and tuning and are thus difficult to apply to a greater region with a large number of glaciers. This thesis – under the abbreviation of CC-GlinCH (***C****limate* ***C****hange Impacts on* ***Gl****aciers* ***in*** *Switzerland (****CH****)*) – was carried out and funded within the framework of the two research projects presented above and aims at modeling glacier thickness, bed topography and future glacier development with simplified approaches and techniques that only require a minimum of (easily available) data and can thus be rapidly applied on a large regional scale (e.g., entire Switzerland).

1.2 Objectives and research questions

The main goal of this thesis is to model the ice thickness distribution and glacier bed topography of all Swiss glaciers to assess future glacier change. As the modeling focus is on a regional scale, simple but robust approaches are used, working with sparse but widely available input data. This requires working with digital elevation models (DEMs), glacier inventories, and climate data. The processing and modeling tool used is a Geographic Information System (GIS). The theoretical background for these topics is provided in chapters 2 to 4 and objectives and research questions are related to these topics.

The first and most important input is the spatial distribution of the glacier ice thickness. There are already several approaches existing – at different levels of complexity and spatial scales – addressing this issue (e.g., *Driedger and Kennard*, 1986, *Haeberli and Hoelzle*, 1995, *Clarke et al.*, 2009, *Farinotti et al.*, 2009b, *Li et al.*, 2012, and section 2.3), but none of these studies provide the ice thickness distribution and bed topography over an entire mountain range from a single model run. This leads to the first research question:

(**1**) ***What is the total volume of the glaciers in Switzerland and how is the ice thickness spatially distributed?***

While the total ice volume of a mountain range can be used to estimate the stored water volume for run-off or to determine its potential contribution to sea level rise (e.g., *Radic and Hock*, 2010, *Huss and Farinotti*, 2012), the derived ice thickness distribution is an important input for modeling future glacier evolution (e.g., *Salzmann et al.*, 2012) and

future run-off changes (e.g., *Mauser and Bach*, 2009, *Huss*, 2011). Furthermore the modeled ice thickness distribution enables a computation of a first approximation of the glacier bed topography in three dimensions leading to the second research question:

(**2**) ***What are the characteristics of the glacier bed topography and where are potential overdeepenings located?***

Whereas absolute values of the local ice thickness as modeled from different approaches can vary largely (due to different input data and model assumptions) and are related to high uncertainties, the principle shape of a glacier bed is rather robust (*Clarke et al.*, 2009), as the relative distribution of ice thickness is a function of the basal shear stress and therefore depends on surface slope as given by the DEMs. This is very important in the context of another phenomenon observed over the last decades: the formation of new lakes in the glacier fore-fields and at the tongues of retreating glaciers (*Frey et al.*, 2010). Lakes developing in glacial overdeepenings at the terminus of glaciers can accelerate glacier retreat but can also be a source of serious natural hazards. Due to the expected vanishing of glaciers in this century, a large number of overdeepenings will be exposed, which can be seen as potential sites of lake formation (*Frey et al.*, 2010). Such new lakes form a new potential hazard source (e.g., *Moore et al.*, 2009, *Künzler et al.*, 2010), but they are also of interest for hydro power production (e.g., *Schaefli et al.*, 2007, *Terrier et al.*, 2011) and tourism (e.g., *Fischer et al.*, 2011). As the temporal scale of glacier retreat and lake development is of fundamental interest for early anticipation of these future changes, the third research questions is:

(**3**) ***How does climate change influence the future development of glacier area (and volume) on a regional scale and what are the uncertainties?***

The variety of approaches to model future glacier retreat is large (e.g., *Le Meur et al.*, 2007, *Paul et al.*, 2007b, and section 2.4.4) and correct anticipation of future glacier evolution must be linked to climate scenarios and must provide time dependent glacier extents. As this thesis has a focus on simplified models and regional scales, the time dependence has to be implemented based on the constraints of the respective model and are rather steady state step functions.

In Figure 1.1 the framework of the thesis is schematically shown to illustrate how the research questions are treated. Basically, the thesis can be divided into three scientific parts. *Part A* is dedicated to the development and validation of the GlabTop (**Gla**cier **b**ed **Top**ography) model, which allows the estimation of ice thickness distribution and bed topography for large samples of glaciers and is thus the foundation of the entire thesis. The application of the so called GlabTop to all Swiss glaciers and the findings and

analysis accomplished from this forms *Part B*. The derived ice thickness distribution is also a major input data set for the various glacier evolution models investigated. Three simplified approaches modeling the glacier evolution of the Swiss glaciers until the end of the century are applied and compared in *Part C*.

All methods, models and results of this thesis are developed, applied and thus focused on the glaciers in the Swiss Alps.The focus of this thesis is on the general application of simple and robust approaches working with both sparse and widely available data; the application of the developed approaches to other mountain ranges is therefore possible (and already tested).

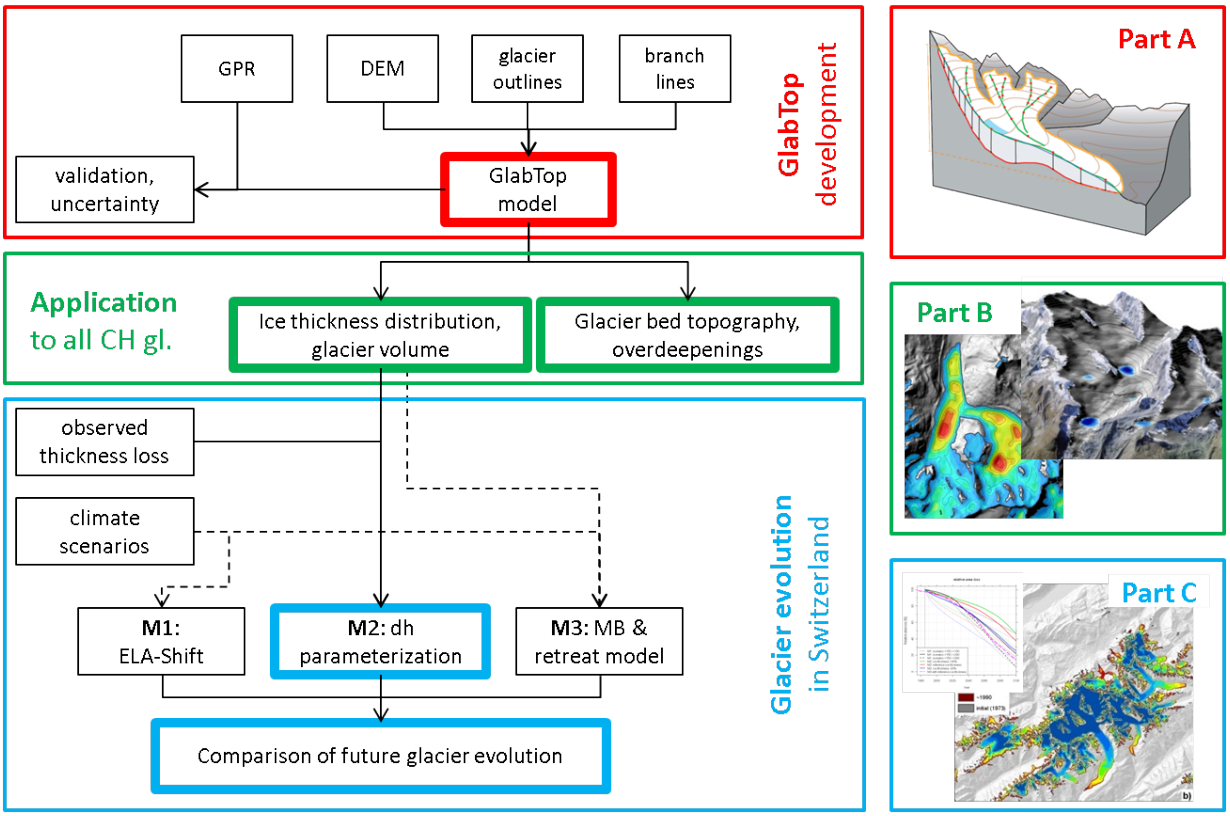

Figure 1.1: *Schematic overview of the elements of this thesis and their connections and relations. The framework of the thesis is divided into three parts (A, B and C) to answer the research questions.*

1.3 Organization of the thesis

The thesis is divided into three parts:

Part I provides a synopsis of the entire thesis. After the Introduction, the thematic and scientific background of the methods applied is explained and compared to the current state of research (chapter 2 to 3). Chapter 4 describes the data sets used and the implementation of the developed and applied models, while in chapter 5 the research papers of this thesis are summarized. A general discussion of the applied methods and findings is given in chapter 7, relating the outcomes of the research papers to the scientific context described previously. Chapter 8 concludes the synopsis and provides an outlook on potential future research.

Part II contains full versions of the research papers which constitute the main part of the thesis.

Part III consists of the appended material (CV, personal bibliography, and the acknowledgments).

2 Glaciers

2.1 Some background on glaciers

2.1.1 The glacier as a result of climate and topography

Glaciers are defined as "a perennial mass of ice, and possibly firn and snow, originating on the land surface by the recrystallization of snow or other forms of solid precipitation and showing evidence of past or present flow" (*Cogley et al.*, 2011). They can evolve where mass gain (e.g., by snowfall, avalanches and wind drift) exceeds mass loss (e.g., by melting). As a first approximation three major factors determine the presence and distribution of mountain glaciers (for convenience ice caps as well as cold and dry climate regions are neglected): (i) annual air temperature, (ii) precipitation and (iii) topography (cf. Figure 2.1). Low temperatures and large amounts of snowfall favor the persistence of a snow cover. Therefore, the occurrence of glaciers is related to wet and cold places, where wet is defined as regions not too far from a moisture source (the ocean) and cold implies high latitude or altitude (*Oerlemans*, 2001). Both factors alone do not create a glacier and the topography is as fundamental to allow snow to accumulate. In this case, the deposited snow gradually becomes denser and transforms through different processes of snow metamorphosis into firn (snow older than a year) and ultimately into ice that is not permeable for air anymore (*Paterson*, 1994). Under

the influence of gravity, the (transformed) ice masses move downhill via viscous creep (*Nye*, 1952, *Glen*, 1958) and basal sliding (*Lliboutry*, 1971). Thereby, mass is transferred by glacier flow from the accumulation area at high elevations, to the ablation area at low elevation, where ablation (mainly melting) predominates. The accumulation and ablation area are separated by the equilibrium line (EL), where accumulation equals ablation. If the sum of accumulation and ablation over a year and the entire glacier surface are equal, the mass budget is zero.

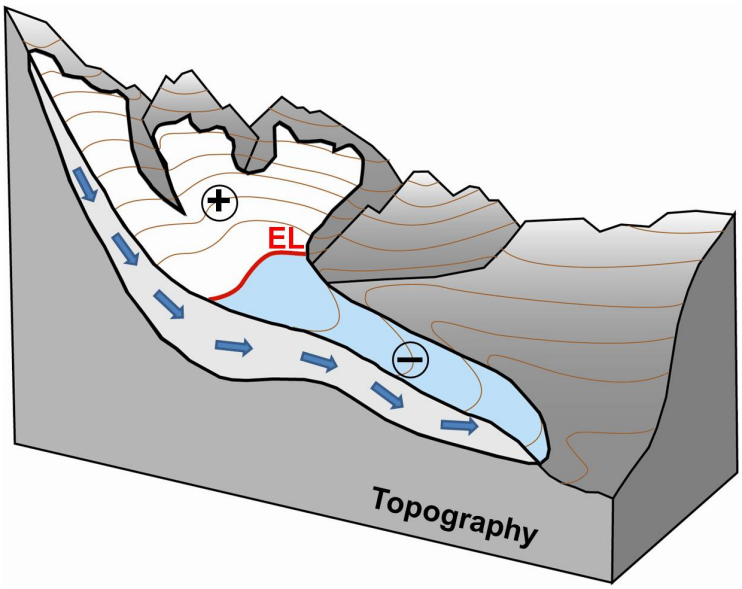

Figure 2.1: *The glacier as a function of climate and topography: In the accumulation area* $(+)$ *the glacier is nourished mainly by snowfall and in the ablation region* $(-)$ *mass loss is due to melting (and sometimes calving). The equilibrium line* (EL) *separates the glacier area into these two parts and glacier flow* $(\Rightarrow)$ *transfers the mass from the accumulation to the ablation area.*

The equilibrium line altitude (ELA) is primarily a function of mean annual air temperature (which is related to altitude and latitude) and annual precipitation amounts (*Oerlemans*, 2001). This is also shown in the cryosphere model (Figure 2.2, *Haeberli*, 1983, *Shumsky*, 1964, *Haeberli et al.*, 1989, *Haeberli and Burn*, 2002, *Zemp et al.*, 2007), a diagram illustrating the relation between temperature, precipitation and the equilibrium line (cf. *Ohmura et al.*, 1992). In humid-maritime regions the equilibrium line (EL) is at relatively low elevations with high annual air temperature, and therefore high accumulation is required to compensate for the high ablation rates.

In such regions mainly active, thick and temperate glaciers, with relatively rapid flow, high mass turnover, strong reactions to atmospheric warming enhanced by excessive melt and run-off can be found that may even extend into forested valleys. With de-

creasing precipitation towards more continental climates, there is less accumulation and the ELA is found higher up in regions with lower temperatures (altitudes above the tree line). Glaciers in such regions might be polythermal or cold, have a low mass turnover and are often surrounded by permafrost (*Haeberli and Burn*, 2002, *Zemp et al.*, 2007). Hence mass turnover, glacier activity and temperatures of glaciers are directly related to the prevailing climatic conditions. While mean temperature is decreasing from low to high altitudes and latitudes, the precipitation pattern is driven by large scale atmospheric circulation patterns and regionally influenced by topography.

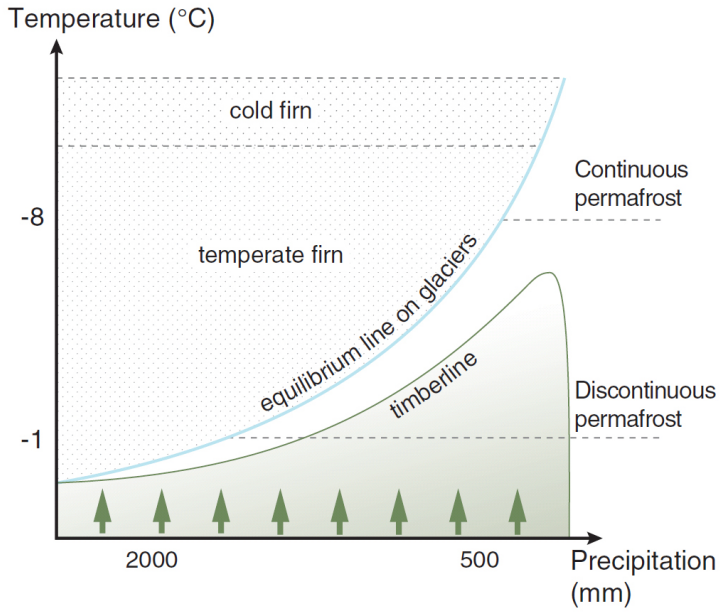

Figure 2.2: *The cryosphere scheme describes glacier, permafrost and forest limits as a function of mean annual air temperature and average annual precipitation. Forests verge on glaciers in humid-maritime climates and grow above permafrost in dry-continental areas. (after* Haeberli and Burn, *2002).*

2.1.2 Glacier types

Apart from climatic conditions, topography is primarily responsible for the size, shape and profile of a glacier. Although glaciers can have all imaginable shapes, it is in the nature of science to classify them. Following the first guidelines for a World Glacier Inventory as suggested by *UNESCO* (1970), *Müller et al.* (1977) prepared "Instructions for Compilation and Assemblage of Data for a World Glacier Inventory". Therein, the following categories for the primary classification of an ice mass were used: ice sheet, ice field, ice cap, outlet-, valley- and mountain glacier, glacierets, ice shelf and rock glacier.

As in the Alps not all of these glacier types exist, *Maisch* (1992) and *Maisch et al.* (2000) designed, following the principle of *Müller et al.* (1977), a glacier classification scheme (considering glacier type, shape, front, profile, retreat and the morphology of the fore field) for Alpine glaciers and applied it to all Swiss glaciers. In this scheme every glacier is classified with respect to four different types (*Maisch et al.*, 2000, *Alean*, 2010):

- **Valley glaciers** are the largest glaciers in terms of surface area. They often consist of several cirques covering a wide accumulation area and finally lead into a narrow valley where the glacier tongue is situated.
- **Mountain glaciers** are often located in one larger cirque. The shape of these glaciers is arbitrary, often similar to valley glaciers, but smaller in size. Mountain glaciers can be divided into an upper accumulation and a lower ablation area and during the LIA they typically showed a pronounced tongue.
- **Glacierets** are the next smaller type of glaciers, also with an arbitrary shape, but frequently without a distinct tongue-shaped terminus. They do not show a clear flow feature and there is no clear distinction between accumulation and ablation area, this is also because of the vertical extent of these glaciers, which is less than 500 m. Glacierets are often nourished by avalanches and/or wind related snow drift and are situated in the shadow of mountain flanks or at slope toes.
- **Firn patches** are small perennial ice bodies with little vertical and horizontal extent and are mostly not real glaciers anymore (no flow and smaller than 0.01 km^2). Firn patches usually exist only due to special local conditions.

Considering all glaciers in a mountain range (e.g., the Swiss glaciers) the valley glacier class is by number rather small, but in terms of glacierized area and stored ice volume they dominate the sample. In Figure 2.3 three types of valley glaciers are sketched, to visualize the storage of the main volume of ice. Also displayed are a mountain glacier and a glacieret. Most of the larger valley glaciers have a rather steep accumulation area at high elevations and a flat tongue located in a U-shaped valley at low elevations, where the thickest ice (and thus the main part of the glacier ice volume) can be found. Typically, the bedrock of these glaciers have low slopes in the ablation region, until it ascends steeply to the higher accumulation region (Figure 2.3a). Some larger glaciers lie on a bed with a more or less equal slope over the entire elevation range, with the ice volume being more equally distributed (Figure 2.3b). For a small number of larger valley glaciers the thickest ice is found in their accumulation region. These glaciers have comparably steep and thus thin tongues and a wide and flat (and hence thick) accumulation area at high altitude (Figure 2.3c).

Mountain glaciers contribute considerably to the surface area and volume of the glaciers in a mountain range like the Alps, but mostly due to their high number. Glacierets on the other hand account for the smallest amount of surface area and ice volume, but they represent by far the largest class in terms of glacier number.

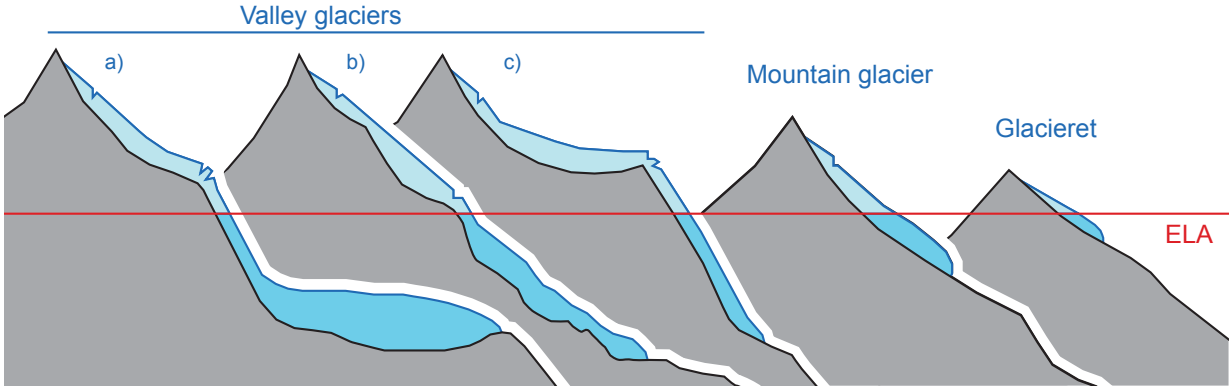

Figure 2.3: *Schematic view of the glacier types valley glacier, mountain glacier and glacierets according to the classification scheme of* Müller et al. *(1977) and* Maisch et al. *(2000). The class of the valley glaciers is further divided into three subtypes a), b) and c) to illustrate where the main volume of the ice within the glacier is stored. The equilibrium line altitude (ELA) divides the glaciers into accumulation and ablation area.*

In the Bernina test region, all glacier types listed above can be found. The Morteratsch glacier (Figure 2.4) stretches from nearly 4000 m down to 2020 m a.s.l., covers an area of about 16 km^2 and is (due to its easy access and impressive appearance) maybe the most famous valley glacier in the region, but also the target of several field and modeling studies (e.g., *Hoelzle and Haeberli*, 1995, *Klok and Oerlemans*, 2002, *Paul et al.*, 2007b, *Machguth et al.*, 2008, *Nemec et al.*, 2009). The Morteratsch glacier was used as a test site within this thesis (***Paper I*** and ***Paper II***) and for sensitivity tests (section 6.1.2). But this glacier also nicely illustrates some major issues about valley glaciers (a representative of type a) in Figure 2.3). First of all, the U-shaped valley cross section between the impressive LIA moraines is remarkable. The glacier tongue in the valley is situated at low elevations (below the treeline) on a flat bed and has therefore also a small surface slope. The tongue is flat and thus thick with few crevasses and at the margins debris covered (brought in by tributaring glacier-branches). Glacier retreating and downwasting are clearly evident from measurements, but also for everyone visible from photo comparisons (e.g., http://www.swisseduc.ch/glaciers/). The slope of the glacier surface (and hence the glacier bed) increases with elevation and around the temporal snow line (TSL) visible in Figure 2.4 the glacier is very steep and thus highly crevassed. At its highest

elevations Morteratsch glacier is nourished from a rather steep accumulation area with different cirques and prominent hanging glaciers.

Figure 2.4: *Morteratsch glacier in the year 2007, a characteristic valley glacier of type a) according to Figure 2.3. The picture shows the flat and thick glacier tongue lying in a U-shaped valley on a vegetation-free, low inclined glacier forefield between the impressive LIA moraines, illustrating the massive ice volume loss within the last century. On the contrary, the wide accumulation area is rather steep, crevassed and thin. (source:* `http://de.wikipedia.org/wiki/Morteratschgletscher`*, accessed July 2012)*

2.1.3 Energy balance at the glacier surface

Over their large surfaces, glaciers interact with the atmosphere by energy and mass fluxes. According to the principle of energy conservation, the sum of the fluxes must balance at all times. Phase changes, in particular melting and freezing, couple the energy balance strongly to the mass balance of a glacier. Thus the **energy balance** at the surface of a glacier is defined as the sum of all energy fluxes at the surface and can be expressed as (e.g., *Oerlemans*, 2001, *Hock*, 2005):

$$M = Q(1-\alpha) + L_{in} - L_{out} + H_S + H_L + G \tag{2.1}$$

where M is the energy available for melting, Q the global shortwave radiation, α the albedo, L_{in} and L_{out} the incoming and emitted longwave radiation, H_S the turbulent sensible heat flux, H_L the turbulent latent heat flux and G the ground heat flux.

Solar radiation (Q, mainly in the form of shortwave radiation) is the primary source of energy (up to several hundred W m^{-2}), reaching the glacier surface as direct or diffuse

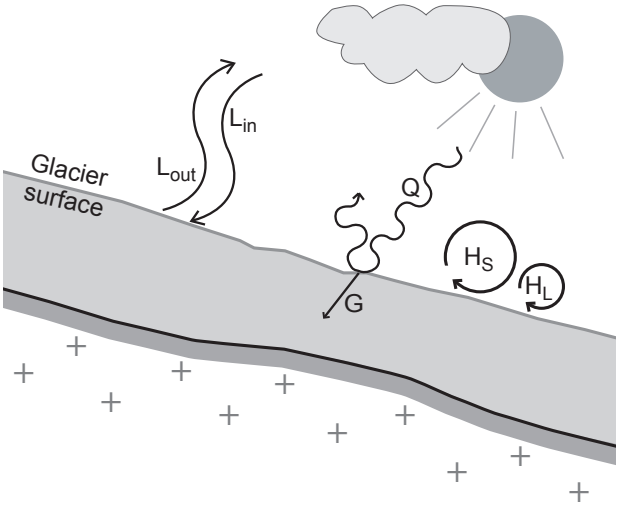

Figure 2.5: *The most important processes determining the energy fluxes at the glacier surface (modified after* Oerlemans, *2001)*

radiation, which is scattered by the atmosphere (especially clouds). Part of the solar radiation is reflected by the glacier surface, but the largest part is still used for melting the ice. The percentage of short-wave radiation that is reflected is called *albedo* (α) and is highest for fresh snow and low for bare and dirty ice (*Paterson*, 1994). Therefore, less energy is available for ablation of snow compared to bare ice. The amount of short-wave radiation received by a glacier also depends on its topographic setting, i.e. slope, aspect, shading and altitude are important for the overall radiation receipts (*Benn and Evans*, 1998, *Oerlemans*, 2001).

The incoming solar shortwave radiation is also heating up surrounding rocks and surfaces and reaches glaciers in the form of (infrared) longwave radiation and turbulent sensible heat flux. The *incoming longwave radiation* (L_{in}) is approximately compensated by the *outgoing longwave radiation* (L_{out}). With the amount emitted by a glacier surface being slightly larger most of the time. Longwave radiation is an important part of the energy budget when the air is humid and warm and clouds are present (*Benn and Evans*, 1998, *Oerlemans*, 2001).

Turbulent sensible heat (H_S) is the thermal energy exchange at the interface between atmosphere and glacier surface and is transported by warm air masses, originating from local air circulation (i.e. warm valley winds, Föhn winds, monsoon winds). The sensible heat flux is controlled by temperature and wind speed, which stimulates turbulence and thus heat flow. When the atmosphere is warmer than the glacier surface and thus favoring strong winds, sensible heat transfer is most efficient. Furthermore, as the glacier surface temperature can not be positive the gradient between warm air and glacier sur-

face can become extremely large and accordingly influence the sensible heat flux highly (*Benn and Evans*, 1998).

Phase changes of water (ice – water – vapor) requires or provides energy and is known as *turbulent latent heat* (H_L). Freezing or condensation of water on a glacier surface results in large amounts of energy being released, which can raise the temperatures and increase ablation. The latent heat flux is driven by differences in vapor pressure between surface and atmosphere and is controlled by temperature and wind speed (*Benn and Evans*, 1998).

Finally, the *melt energy* (M) is the results of the entire energy balance at the glacier surface. If the sum of radiation and sensible and latent heat fluxes is positive, the energy is used for the heating of snow and ice when the snow/ice temperature is negative, and melting when the snow/ice temperature at the surface is zero. When the sum of radiation and sensible and latent heat fluxes is negative, the glacier cools (*Hock*, 2005).

In detail, the energy balance at the glacier surface is rather complex but can be simplified if the essential aspects are considered (e.g., roughly parametrized longwave radiation, but a more complex determination of shortwave radiation, cf. *Machguth*, 2008). Energy balance and mass balance of a glacier are connected by melting, freezing, sublimation and deposition. To model ablation and thus glacier evolution (cf. section 2.4.4), the energy balance must be determined using either an energy-balance model (as used for the study in ***Paper IV***) or a temperature-index model.

2.1.4 Glacier mass balance

Accumulation processes are all events at the glacier surface, which lead to mass gain (mainly the deposition of solid precipitation), whereas ablation processes (melting and calving) result in mass loss. The sum of *accumulation* (c) and *ablation* (a) over any period is the *mass budget* (b) (*Kuhn*, 1981, *Paterson*, 1994):

$$b = c - a, \tag{2.2}$$

where b is the change in mass (expressed as local thickness change in meters water equivalent (m w.e.)) per unit area relative to the previous summer surface. The mass balance at the end of the balance year is the *net balance* (b_n) for the year, which is further divided into a *winter balance* (b_w), which is positive and a *summer balance* (b_s), which is negative (*Anonymus*, 1969, *Paterson*, 1994):

$$b_n = b_w + b_s. \tag{2.3}$$

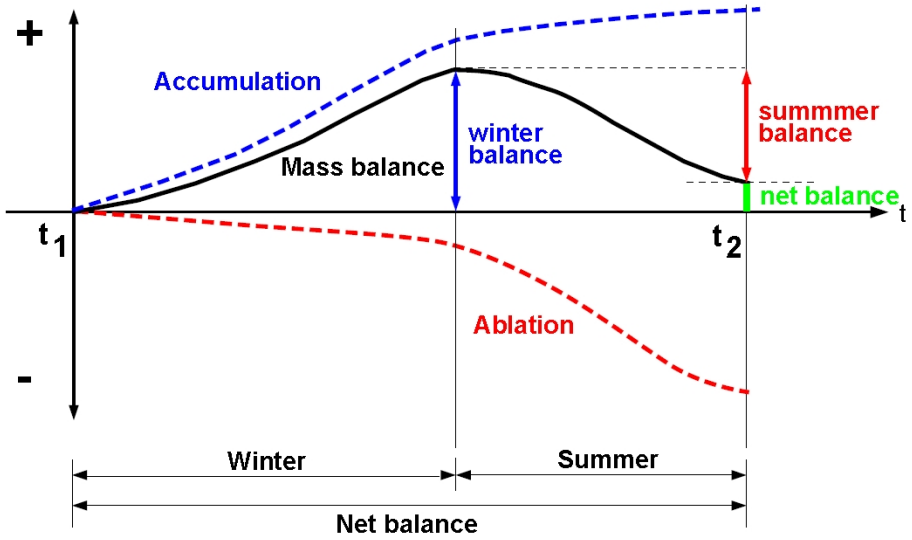

Figure 2.6: *Definition of mass balance terms for a given point (x, y) on the glacier surface (Figure originating from* Huss *(2009), modified after* Paterson *(1994)).*

Mass balance can be defined for an area, analogous to its definition for a point and have the dimension of a volume (m^3 water equivalent). The *average net balance* ($\bar{b}_n$), where the net balance over the entire glacier is divided by its surface area, is the most useful parameter for comparing mass changes of glaciers worldwide (*Paterson*, 1994, *WGMS*, 2011).

2.1.5 Measuring glacier mass balance

Different techniques can be applied to measure glacier mass balance. The most important ones are the *direct glaciological method* and the *geodetic method* and are shortly explained in the following.

The direct glaciological method is based on in-situ measurements of accumulation in snow pits (including density sampling) and ablation at stakes (*Cogley et al.*, 2011). The measurements are related to a point-scale and have to be extrapolated and integrated to derive the surface mass balance over the total glacier area, which is actually a main source of uncertainty inherent to the method (*Machguth*, 2008). As for these measurements field work on the glacier is required and therefore they are restricted to accessible terrain (i.e. in crevassed zones, steep regions and avalanche terrain no measurements are carried out). The denser the network of sampling points, the more reliable is the extrapolated surface mass balance and hence the accuracy of the method (*Fountain and*

Vecchia, 1999). More crucial and challenging is the choice of locations where representative measurements are possible (*Cogley*, 1999). The advantage of the direct glaciological method is that it processes information at the point-scale and with high temporal resolution.

If only volume changes rather than mass changes are required, laser scanning can provide annual and overall changes at a similar level of accuracy (e.g. *Baltsavias et al.*, 2001, *Geist and Stötter*, 2007, *Joerg et al.*, 2012). Though proper conversion to mass changes requires field measurements of density, the pattern of derived volume changes might be useful for the spatial interpolation of in-situ measurements nevertheless.

When determining the mass balance with the geodetic method, the surface elevation of entire glaciers at two points in time (usually several years apart) are compared. The observed changes in elevation within the time interval are multiplied with (an assumed) density to derive the mass budget over the entire glacier (*Cogley et al.*, 2011). Geodetic mass balances can be derived from the comparison of topographic maps (e.g., *Finsterwalder*, 1954, *Østrem and Haakensen*, 1999) or recently more often from DEMs derived from remote sensing data. The method is also applicable to large glacier samples and entire mountain ranges (*Paul and Haeberli*, 2008). The accuracy of the method is above all dependent on the accuracy of the used topographic maps or DEMs and the time period considered. By the different time scale covered and the entire glacier being considered, the geodetic method complements the direct method by also providing changes for unmeasured or poorly constrained regions. In this way a potential systematic bias in the field measurements can be detected and corrected (e.g., *Huss et al.*, 2009, *Haug et al.*, 2009). Of course, assumptions on density which have to be made to convert volume changes into mass changes might introduce an error. At least over long time scales (a few decades) the density of ice can be used without introducing too large an error.

The geodetic method has its strengths where the direct glaciological method has its weaknesses and vice versa (*Machguth*, 2008). In regard of long time monitoring of glacier mass balance, the combination of methods is the most reasonable way to obtain distributed mass balance time series (e.g., *WGMS*, 2008a, *Haeberli*, 2006). The geodetic method allows to derive long-term cumulative mass budgets over large regions and to minimize the systematic errors of the direct measurements, whereas the direct glaciological method provides process information and high temporal resolution (seasonal) for selected glaciers. (e.g., *Østrem and Haakensen*, 1999, *Haeberli*, 2006).

2.2 Basic processes of glacier dynamics

A major characteristic of glaciers is their ability to flow. Through deformation and sliding, snow and ice is transported from the accumulation to the ablation area, with erosion and debris transport taking place at the same time.

2.2.1 Driving forces/stresses

The Earth's gravitational pull (gravity) is the driving force which is responsible for glacier motion (*Nye*, 1952). The mass of the glacier is accelerated by gravity towards the center of the Earth, and the resulting normal stress (σ) acting on the glacier is mainly the result of the weight of the overlying ice:

$$\sigma = \rho_i \cdot g \cdot h \tag{2.4}$$

where ρ_i is the density of ice (ca. 900 kg m^{-3}), g is gravitational acceleration (9.81 m s^{-2}), and h is the ice thickness (m) (*Benn and Evans*, 1998). The glacier bed redirects glacier flow downslope, and the terrain under the glacier with its characteristics (e.g., slope, geology, geomorphology, topography) influencing the flow speed and direction of the glacier. At the glacier bed, resistance forces (shear stresses) are introduced, as a function of the slope (*Paterson*, 1994). The average shear stress (τ) at the base of a glacier results from the weight of the overlying ice and the slope of the ice surface and can be approximated as:

$$\tau = \rho_i \cdot g \cdot h \cdot \sin \alpha \tag{2.5}$$

where α is the surface slope of the ice (*Benn and Evans*, 1998) with increasing ice thickness, i.e. both, normal and shear stresses in a glacier increase linearly with ice thickness. Based on simplified assumptions and models, these stresses can be calculated, but they cannot be measured within real glaciers (*Paterson*, 1994).

In summary, the gravitational force acting on a glacier and causing a glacier to flow, can be divided into a force normal to the plane and a force parallel to the plane (Figure 2.7). Therefore, they are also known as the driving forces of glacier flow.

2.2.2 Resisting forces – basal shear stress

Figure 2.7 also illustrates a first simplified model of a glacier: a parallel-sided slab, resting on a plane with slope α (without sliding). Compared with the thickness h, the length

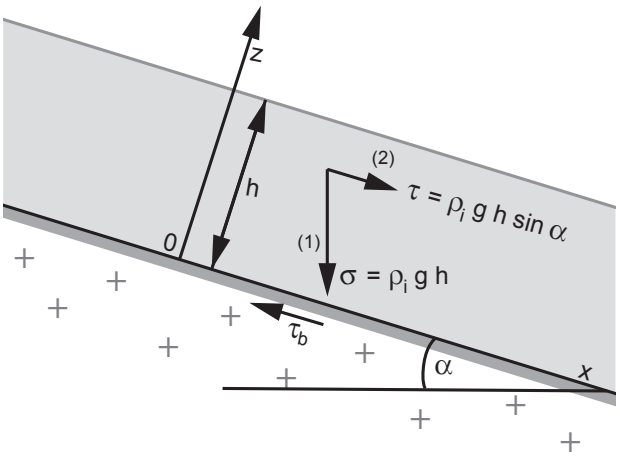

Figure 2.7: *Gravitational forces compositing the driving stress of a glacier: (1) pressure gradient force and (2) down-slope component of weight, where basal shear stress (τ) equals basal drag (τ_b) (modified after* Paterson, *1994).*

and width of the slab are assumed to be large in this example. The weight of an ice column perpendicular to the plane is calculated according to equation 2.5 and is called driving stress. To be in equilibrium it is balanced by the basal drag, the shear stress (τ_b) across the base of the column. Equation 2.5 thus leads to three important implications (*Paterson*, 1994):

1. The basal shear stress (τ_b) can be calculated from measurements of ice thickness h and surface slope α. According to *Paterson* (1994) these values are normally between 50 and 150 kPa; as a reasonable approximation glaciers can be considered to be a *perfectly plastic* material with a yield stress of about 100 kPa.

2. If perfect plasticity is assumed, and slope is calculated as the average value over distances several times the ice thickness, the latter can be estimated from the surface slope:

$$h = \frac{\tau_b}{\rho_i \cdot g \cdot \sin \alpha} \tag{2.6}$$

3. With the assumption that the product $h \cdot \sin \alpha$ is constant, a glacier is thin where the surface is steep, and thick where the surface slope is small.

The surface slope – together with the ice depth – determines the shear stress at the bed. Ice flows in the direction of maximum surface slope even when the glacier bed slope leads in the opposite direction. As a consequence ice in glaciers can flow upwards and

glacial valleys are often overdeepend. It also follows that flow-lines can be determined from contour lines of the ice surface (*Paterson*, 1994).

The resistance to flow in the simple glacier model Figure 2.7 originates from friction at the glacier bed (basal drag (τ_b)), but in a real glacier also the lateral margins of a glacier (lateral drag) as well as the spatial alteration of pushing or pulling forces (longitudinal stress gradients) are acting. Hence, basal shear stresses should be averaged over the whole cross-section profile of the glacier bed. To account for this *Nye* (1965) introduced a dimensionless shape factor f to the equation of basal shear stress

$$\tau_b = f \cdot \rho_i \cdot g \cdot h \cdot \sin \alpha, \tag{2.7}$$

Thereby *Nye* (1965) applied Glen's flow law (*Glen*, 1958) and modeled numerical solutions for the flow of ice along uniform cylindrical channels of rectangular, semi-elliptic and parabolic cross-sections. The values for the shape factor f are between 0.5 and 0.9, depending on the shape of the cross-section and the width-to-depth ratio of the glacier (*Paterson*, 1994). For alpine glaciers *Maisch and Haeberli* (1982) postulate – based on empirical evidence – a shape factor of 0.7 for the glacier tongues in the ablation area and 0.9 for the much wider accumulation areas. *Haeberli and Hoelzle* (1995) chose $f = 0.8$ as an average value for the entire glacier.

If ideal plasticity of the ice is assumed, the poorly known basal sliding is neglected, and the ice body has a horizontal extent that is much larger (about 10 times) than its vertical extent, equation 2.7 can be solved for h, the ice thickness can be derived in the following way:

$$h = \frac{\tau_b}{f \cdot \rho_i \cdot g \cdot \sin \alpha}. \tag{2.8}$$

Here, the basal shear stress (τ_b) and the surface slope (α) are the important variables. While slope can easily be averaged over a specific distance over the glacier surface, the determination of the basal shear stress is more challenging. Referring to *Nye* (1952) and *Paterson* (1994), in several studies a constant basal shear stress of 100 kPa was assumed (e.g., *Binder et al.*, 2009, *Clarke et al.*, 2009, *Marshall et al.*, 2011). Some recent studies adjusted the basal shear stress for individual glaciers (e.g., *Giesen and Oerlemans*, 2010, *Immerzeel et al.*, 2012, *Li et al.*, 2012).

Maisch and Haeberli (1982) calculated shear stress values for 62 vanished late-glacial glaciers and *Haeberli and Hoelzle* (1995) derived an empirical relation from this dataset by relating the basal shear stress τ_b to the vertical extent (ΔH) and hence mass turnover of a glacier (cf. Figure 2.8). This approach was also used by several subsequent studies (*Hoelzle et al.*, 2007, *Baumann and Winkler*, 2010, *Paul and Svoboda*, 2010):

$$\tau_b = 0.005 + 1.598\Delta H - 0.435\Delta H^2, \qquad (2.9)$$
$$and\ \tau_b = 150\ kPa\ for\ \Delta H > 1600\ m.$$

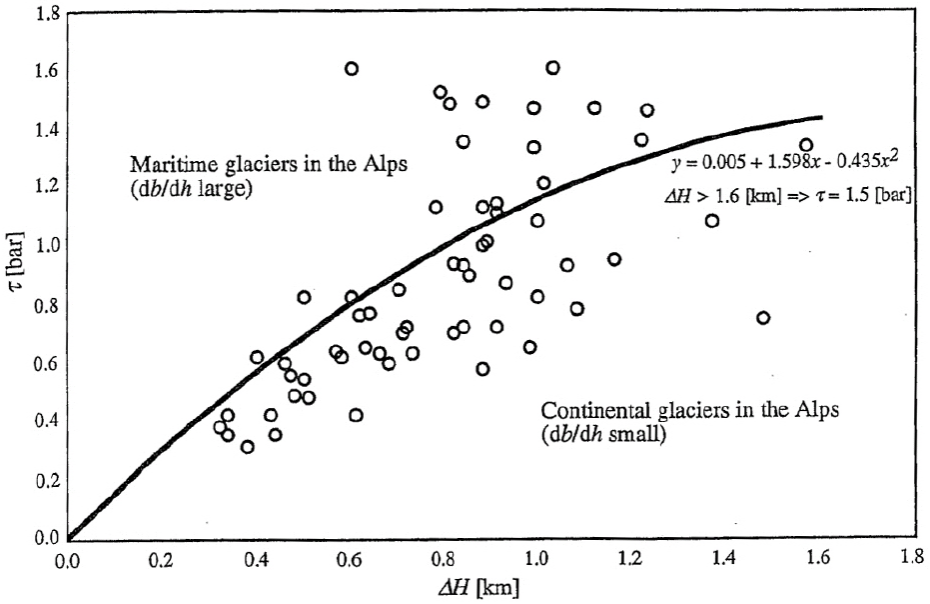

Figure 2.8: *Average basal shear stress along the central flowline vs. altitudinal extent of (reconstructed late-Pleistocene Alpine) glaciers. The polynomial fit on the data gives the function in equation 2.9. A maximum value of 150 kPa is assumed for the largest glaciers (from* Haeberli and Hoelzle, *1995)*

A maximum value of 150 kPa is assumed for glaciers with $\Delta H > 1600$ m and the basal shear stress of the smallest glaciers is set to 0.005 kPa. The maximum value of 150 kPa is empirically estimated (*Maisch and Haeberli*, 1982, *Haeberli and Hoelzle*, 1995) and 50% higher than the 100 kPa used in other studies as a mean value for all glaciers. For example *Marshall et al.* (2011) mentioned that the value of 100 kPa tends to underestimate the shear stress for large glaciers and overestimate it for small glaciers. This is in line with the study by *Driedger and Kennard* (1986) who found size-dependent values between 30 and 160 kPa for a group of comparably steep glaciers on the Cascade volcanoes and *Li et al.* (2012) who found values between 50–175 kPa for five Chinese glaciers.

The large spread of the data points visualized in Figure 2.8 reflects the high variability of ice flow. The scatter relates to an uncertainty of ±30% and for some individual glaciers even ±45%. This scatter cannot easily be overcome in any quantitative approach as the rate factor for ice deformation and the relative amount of sliding are largely unknown.

While for an approximation a mean value per glacier can be assumed, it has to be considered that basal shear stresses vary with slope (*Haeberli and Schweizer*, 1988). Stresses averaged longitudinally (within one and the same glacier) are considerably higher in the steep ice falls than for the adjacent flatter parts of the glacier.

As mentioned earlier, basal shear stress of contemporary glaciers is not a directly measurable variable, as accessing the glacier bed is not possible (an exception is Engabreen in Norway, where tunnels allow access to the glacier bed (*Cohen et al.*, 2000)). *Fischer* (2012) modeled basal shear stresses of LIA fore fields for a large sample of Swiss glaciers on the basis of equation 2.8 that largely confirmed the range of values shown in Figure 2.8.

2.2.3 Glacier dynamics

The flow of glaciers is the cumulative effect of three processes: deformation of the ice; sliding at the ice/bed interface; and deformation of the bed underlying the glacier, acting individually or in combination (*Benn and Evans*, 1998, *Hambrey and Alean*, 2004).

1. **Internal deformation**: Snow turns into firn and then into ice by being buried and compressed under the weight of the overlaying material. The resulting stresses deform the ice in a plastic manner, as ice is an incompressible and viscous material. Deformation happens through the movement between or within individual ice crystals. The strain rate increases with depth and increasing ice pressure. If the (tensile) strain rate exceeds a certain threshold, the glacier ice breaks and crevasses develop (*Paterson*, 1994). This occurs whenever there is a rapid change of flow direction and therefore a major change in the main strain direction. Glen's flow law (*Glen*, 1958) is the most widely used flow law adapted for glaciers, and describes the response of ice to stress:

$$\dot{\epsilon} = A \cdot \tau^n, \tag{2.10}$$

   where $\dot{\epsilon}$ is the strain rate, τ is the shear stress set up in the ice, and A and n are parameters defining the relationship between stress and strain, where the rate factor A increases exponentially with temperature, and the flow law exponent is usually set to $n = 3$.

2. **Basal sliding**: When large quantities of melt water build up high water pressures, the friction between the glacier and its bed is reduced and the glacier slips over its rocky bed. This process is called basal sliding and is an important component of flow in polythermal glaciers. Sliding velocities are generally related to the amount

of melt water available and the corresponding water pressure at the glacier bed. That means, a temperate glacier moves faster in summer and at daytime.

3. **Deformation of subglacial sediments** has to be taken into account if the glacier lies upon soft, unconsolidated, deformable till. When saturated with water, this sediment deforms more easily than the basal ice. Glacier movement is supported by shearing within the soft, deformable sediments, rather than by sliding.

Glacier flow is the result of permanent strain of the ice and the bed in response to stress. The contribution of these three mechanisms to the total motion of the ice masses varies according to the temperature regime and availability of subglacial melt water, as well as according to the bed characteristics (*Benn and Evans*, 1998).

2.3 Glacier thickness – measuring and modeling

The knowledge of ice thickness distribution and volume of glaciers is fundamental for a variety of glaciological application, for instance for estimates of their contribution to sea-level rise (e.g., *Meier et al.*, 2007, *Radic and Hock*, 2010), a more realistic modeling of glacier retreat (e.g., *Huss et al.*, 2010b, *Jouvet et al.*, 2009, 2011, *Salzmann et al.*, 2012), modeling future run-off from glacierized catchments (e.g., *Huss et al.*, 2008a, *Kaser et al.*, 2010), or to assess future hazard potential (e.g., *Frey et al.*, 2010, *Künzler et al.*, 2010). While quantifying the ice thickness and especially its distribution all over the glacier is challenging, the glacier surface can be investigated directly (e.g., by photogrammetry). Ice thickness is only indirectly available by application of geophysical methods or by the drilling of bore holes (cf. section 2.3.1 and *Clarke*, 1987). Recently, different estimation and modeling approaches have been developed to determine ice thickness and its distribution from glacier outlines and digital elevation models (section 2.3.2).

2.3.1 Measuring ice thickness

Clarke (1987) summarizes the evolution of investigating ice thickness, from the first glaciologists (L. Agassiz in 1948), who drilled through the glacier, to the various geophysical measurement approaches like seismic, gravimetric and electromagnetic methods as used until the middle of the 1980s. Nowadays the most often used technology to derive ice thickness measurements of glaciers is radio-echo sounding with ground penetrating radar (GPR) (e.g., *Bauder et al.*, 2003, *Binder et al.*, 2009).

Drilling a bore hole reveals an exact ice thickness at a distinct location (errors can occur due to a change in the angle of the bore hole). However, drilling is "a brutish approach

to measuring ice thickness and as a mapping technique it is completely unsatisfactory" (*Clarke*, 1987). Nevertheless, with the advent of hot-water drilling, campaigns were rather popular from the 1950s to the 1970s. In many cases the focus of hot-water or ice core drilling projects was not the measurement of the ice thickness directly, but analyses on temperatures, stratigraphy, isotopes, radioactivity contents and composition of gases (e.g., *Oeschger et al.*, 1977).

Seismic measurements were the earliest used geophysical method to determine glacier ice thickness and already *Mothes* (1927) sounded ice as thick as 792 m at Konkordia Platz on Grosser Aletschgletscher (*Clarke*, 1987). It was for decades the preferred method to derive measurements about ice thickness. Despite the slow and troublesome business with seismics, an advantage of the method in contrast to radar sounding is that it can yield more complete information about the glacier substrate and the water content distribution (*Clarke*, 1987, *Navarro et al.*, 2005). Therefore, the seismic method is still in use above all in investigating permafrost (e.g., *Hilbich*, 2010) but partly also for glaciers (e.g., *Shean et al.*, 2007).

Geoelectric techniques used to derive the ice thickness came into focus in the 1960s (e.g., *Röthlisberger and Vögtli*, 1967). *Haeberli and Fisch* (1984) placed electrodes in ice bore holes at the ice/bed interface on Grubengletscher to compare ice thickness with measurements from radio echo-sounding and to exploit the lithological characteristics of the bed. Although *Clarke* (1987) predicted a bright future, this technique was never employed extensively and became obsolete.

Radio-echo sounding (Radar) on glaciers was first used in the 1960s. The development of impulse radar systems (*Watts and England*, 1976), its application on temperate glaciers (*Haeberli et al.*, 1982, *Narod and Clarke*, 1994), and the subsequently airborne version (*Watts and Wright*, 1981) were responsible for causing radar technology to become the routine method for measuring ice thickness since the 1980s (*Clarke*, 1987). Ground Penetrating Radar (GPR) is now state of the art and extensive measurement campaigns were performed on glaciers all over the world (e.g., *Span et al.*, 2005, *Fischer et al.*, 2007) resulting in more or less dense distribution of profile measurements over the glaciers. Compared with seismic techniques, radar profiling is easier and faster and allows researchers to carry out a larger amount of measurements with the same resources (*Navarro et al.*, 2005).

Nevertheless, the availability of direct ice thickness measurement data is still sparse. All methods are based on field work and are thus expensive, laborious and time-consuming. Increasingly GPR measurements are carried out airborne (with airplanes or helicopters, e.g., *Blindow et al.*, 2011) but still a large part of available measurements performed directly on glacier surfaces are restricted to accessible parts of glaciers. Measurements in very steep, crevassed, avalanche- or ice-/rockfall affected areas of a glacier are dif-

ficult to carry out. For simple logistical reasons, ice thickness measurements mainly cover the crevasse-free flat (and thick) parts of glaciers with compressing flow (often in overdeepend parts of the bed) and might thus not be representative of the entire glacier. The point density of measurements per km^2 of a glacier can vary within orders of magnitude and the bed between the measured data remains unknown and so has to be inter- and extrapolated and is thus a modeled product (e.g., *Binder et al.*, 2009, *Fischer*, 2009).

2.3.2 Modeling ice thickness

To obtain information about subglacial topography, the glacier bed can be reconstructed from more or less dense field measurements of glacier thickness (cf. section 2.3.1), by spatially inter- and extrapolating them to a continuous bed using a variety of methods (e.g., *Welch et al.*, 1998, *Bauder et al.*, 2003, *Span et al.*, 2005, *Binder et al.*, 2009, *Fischer*, 2009). In principle, only the GPR profiles can be considered as validation data for results from other methods, as for regions without measurements glacier thickness is only a computed product and might thus be rather different from reality. Nevertheless, estimates of ice thickness and volume are also required for unmeasured glaciers. Hence, over the last decades several approaches have been developed to estimate or model ice thickness for individual as well as large samples of glaciers. Basically two different types of approaches can be distinguished:

(**A**) Scalar approaches yielding only one (mean thickness or total volume) value per glacier.

(**B**) Modeling and interpolation methods which provide 3-dimensional ice thickness distributions for each glacier.

These two classes can be further differentiated as outlined in Figure 2.9. The scaling approaches used in studies belonging to **A1** are originally based on empirical relations between measured surface areas and (geophysically) measured ice depths (e.g., *Müller et al.*, 1976, *Maisch and Haeberli*, 1982, *Driedger and Kennard*, 1986, *Maisch et al.*, 2000). In a wide range of studies the so-called area-volume scaling was applied to estimate ice volume and hence the potential sea-level rise contribution of glaciers at a global scale (e.g., *Van de Wal and Wild*, 2001, *Raper and Braithwaite*, 2005, *Ohmura*, 2009, *Radic and Hock*, 2010). This might be a suitable approach when applied to a large sample of glaciers (as the large uncertainties of the individual values average out), but deriving glacier volume (V) from its area (A) is problematic as it relates a variable (area) with itself (area in volume) resulting in high correlations and suppresses the large scatter,

in particular when plotted with a double-logarithmic scale (*Haeberli et al.*, 2008). So the problem of this method is not the physical basis of the scaling theory behind the approach (cf. *Bahr et al.*, 1997), but the requirement to derive the scaling parameter c in $V = cA^{\gamma}$ from a statistical relation that correlates a variable with itself. A further problem when using area to determine glacier thickness or volume is that physically the variability of thickness is controlled by glacier slope and mass turnover rather than area (e.g., *Paterson*, 1994, *Oerlemans*, 2001). So approaches considering these factors (**A2** in Figure 2.9) should give more realistic results than the others (**A1** in Figure 2.9) for glaciers of the same size but with different mean slopes.

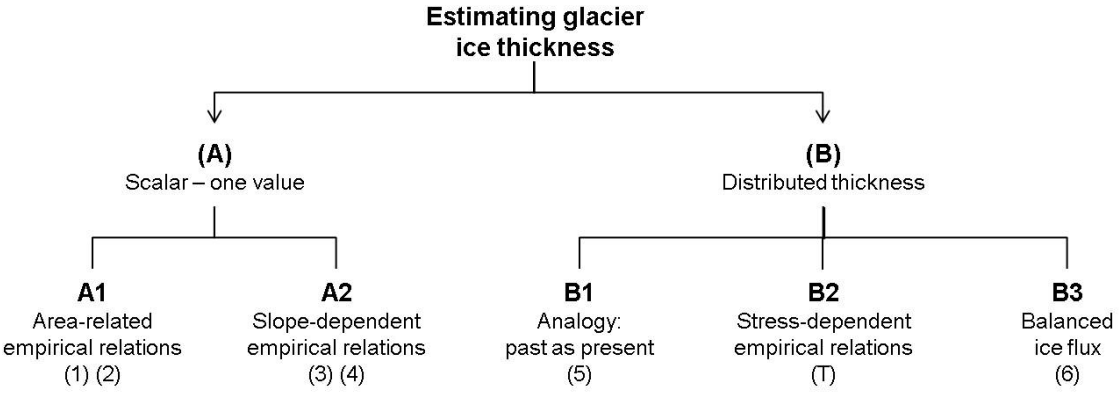

Figure 2.9: *Classification scheme to separate different approaches to estimate glacier ice thickness. A selection of studies dealing with ice thickness assessment is denoted by numbers in brackets: (1)* Müller et al. *(1976); (2)* Chen and Ohmura *(1990); (3)* Driedger and Kennard *(1986); (4)* Haeberli and Hoelzle *(1995); (5)* Clarke et al. *(2009); (6)* Farinotti et al. *(2009b). (T) refers to the approach developed and applied within this thesis.*

With the topographic information available in detailed glacier inventories it is possible to use glacier length and elevation range to derive a slope-dependent mean thickness for large samples of glaciers (*Haeberli and Hoelzle*, 1995, *Hoelzle et al.*, 2007). Studies applying this approach build the group **A2** in Figure 2.9. Corresponding thickness estimates for individual glaciers are considered to be more realistic than area-dependent estimates, because flow-related glacier thickness is strongly slope-dependent (*Kamb and Echelmeyer*, 1986, *Paterson*, 1994). In different studies (e.g., *Driedger and Kennard*, 1986, *Haeberli and Hoelzle*, 1995, *Benn and Hulton*, 2010, *Ng et al.*, 2010, *Marshall et al.*, 2011, *Li et al.*, 2011, 2012, *Immerzeel et al.*, 2012), ice thickness and surface slope are related to stress, by applying the perfect-plasticity assumption to estimate the ice thickness of glaciers (cf. section 2.2). The so-derived mean thickness of glaciers having the same size will get different values and volumes (in contrast to **A1**-approaches).

The area-related estimates and scalar methods from type **(A)** yield only one value per glacier (either a mean thickness or a total volume), but no information about subglacial topography. Simplified modeling approaches, based on application of DEMs in combination with vector outlines of glacier extent, were developed to obtain distributed ice thickness estimated and build type **(B)**. Already *Driedger and Kennard* (1986) made ice-depth estimates for individual parts of glaciers, but with presently available data and geoinformatic techniques further approaches were developed and applied to large samples of glaciers to obtain distributed ice thickness estimates and thus information about the subglacial topography.

The **B1**-class (Figure 2.9) represents approaches dealing with analogy of past and present glacierization. *Clarke et al.* (2009) trained an Artificial Neural Network (ANN) to transfer the characteristics of now ice free glacier beds to contemporary glaciers. The method yielded plausible, though not necessarily accurate, estimates of the bed surface. The obtained estimates of total glacier ice volume might be superior to the values calculated with **(A)**-approaches. Nevertheless, until today the ANN-approach was not further applied, because of the required workload and computational resources.

The concept of methods belonging to the **B2**-class (Figure 2.9) is based on the transformation of the perfect plasticity assumption of the **A2**-approaches averaged over the entire glacier to a spatially explicit reconstruction of the glacier bed. Thereby, ice thickness is computed as a function of local slope and a basal shear stress derived from the vertical glacier extent. Locally derived ice thickness are spatially interpolated and provide an approximated glacier bed. DEMs and polygons with glacier outlines basically provide all important information for this approach. In ***Paper I*** and ***Paper II*** a method following this idea is presented, applied to the Swiss Alps in ***Paper III*** and the related strengths and weaknesses are discussed in the papers and the discussion of this thesis.

Methods in the **B3**-class are based on mass conservation and principles of ice flow dynamics to estimate the ice thickness distribution. *Farinotti et al.* (2009b) presented a method established on this foundation. In contrast to the approaches from **B1** and **B2** it requires a detailed parameterization of the involved physical processes and rough assumptions about several only vaguely determined processes (e.g., surface accumulation, mass balance gradient, rate factor in the ice flow law, basal sliding velocity). As a consequence, the model must be tuned for each glacier by comparing it with selected glacier cross sections derived from GPR profiles to make it realistic. The originally envisaged complexity and process understanding is thereby reduced to an empirically calibrated approach.

All ice thickness-estimation methods presented above have their shortcomings and uncertainties (e.g., not applicable to large samples, lack of data for application, complexity of the model, computational resources required, etc.). A critical step for the use of

modeled glacier beds in other applications is the assessment of their quality, which requires a validation procedure with reference data. As the real glacier bed of still existing glaciers becomes only visible after the respective glacier has disappeared (*Vanuzzo and Pelfini*, 1999), validation data (i.e. bedrock information) has to be provided from field measurements (cf. section 2.3.1). Such reference information is only sparsely available and in most cases biased towards crevasse-free, flat and thus thick glacier parts with compressing flow.

2.4 Climate and glacier change in the past and future

2.4.1 Glacier fluctuations due to climate change

The retreat of glaciers is a very obvious signal of the ongoing climate change. Thus, the monitoring of worldwide glacier changes is a key element of global climate-related monitoring programs (*Haeberli et al.*, 1999). If on a glacier ablation is the dominant process over several years (i.e. the mass balance is always negative), the mass flux from the accumulation area is reduced and the glacier starts to retreat. In contrast, when accumulation is dominating over a longer time period (positive mass balance), the flow speed of a glacier increases and it starts to advance. Retreat (and also advance) of glaciers are a response to climate change in the past, as the response of the terminus is delayed by flow dynamics. Glacier length change is thus an indirect, delayed and enhanced reaction to a long-term climate forcing. The glacier mass balance (controlled by the energy balance and precipitation) on the other hand is the direct and undelayed reaction to annual conditions (*Watson and Haeberli*, 2004). Length and area changes are thus harder to interpret in climatic terms than mass changes, but the latter are more difficult to measure.

The climatic interpretation of a change in glacier length is hampered because response times are different for each glacier; the larger and flatter the glacier, the longer the delay of the response is under equal climatic conditions (*Oerlemans*, 1994). Nevertheless, some assumptions about glacier length change due to a change in local climate and the related response times are possible from steady-state conditions using simplified concepts (*Nye*, 1960, *Johannesson et al.*, 1989, *Haeberli*, 1991): A step change in mass balance δb (which results from a shift in ELA) is followed by a change in glacier length δL after a glacier specific reaction time t_r. After the response time t_a (and under the assumption that no further climate change occurs within this time) a glacier can reach a new steady-state. According to *Johannesson et al.* (1989) the response time (t_a) can be related to the maximum ice thickness (h_{max}) and ablation at the terminus (b_t):

$$t_a = \frac{h_{max}}{b_t}. \tag{2.11}$$

The change in glacier length is according to *Nye* (1960) a function of the change in mass balance (δb) and the original glacier length (L_0), divided by the balance at the tongue of the glacier (b_t):

$$\delta L = \frac{L_0 \cdot \delta b}{b_t}. \tag{2.12}$$

Hoelzle et al. (2003) interpreted the data of cumulative glacier length change from a large sample of glaciers selected worldwide by an intercomparison between curves from geometrically similar glaciers and by an application of continuity concepts for assumed step changes between steady-state conditions reached after the dynamic response time. The study revealed the possibility to roughly estimate secular mass balance changes by using length change measurements.

In the studies of (*Oerlemans*, 2005) and (*Leclercq and Oerlemans*, 2012) a large sample of glacier length records was used to reconstruct global and hemispherical temperatures with a simple glacier model. The obtained temperature fluctuations are in good agreement with the measured temperature records of the last century and with existing multi-proxy reconstructions in the pre-instrumental period.

2.4.2 Climate change in the Alps

The evidences of a changing climate on a global as well as a regional scale are strong and parts of these changes are very likely caused by anthropogenic greenhouse gas emissions (*IPCC*, 2007). The causal link between the increasing concentrations of greenhouse gases in the atmosphere and the observed changes in temperature can be seen as being scientifically established. Related scenarios of possible future climates reveal that impacts from climate change on natural and human systems may increase, especially if anthropogenic emissions continue to rise unabatedly. Due to the lifetime of emissions and the nature of the climate system, some of these impacts are already unavoidable (*van der Linden and Mitchell*, 2009).

The variations of surface temperature over the last millennium, as reconstructed from proxy data (tree rings, corals, ice cores and historical records) and calibrated with measurements, show a general negative temperature trend from the 1st century until the middle of the 19^{th} century (the Little Ice Age LIA) followed by a distinctive warming until present (*IPCC*, 2007). This warming is unprecedented on a hemispheric scale and

can only be explained by anthropogenic, greenhouse gas forcing (*Jones and Mann*, 2004, and references therein).

Reconstruction of temperature and precipitation in the Alpine region since 1500 show that warming is also very prominent in the Alps (*Casty et al.*, 2005). Due to interactions between the complex topography and the general circulation, climatic conditions of mountainous regions are highly variable. The climate in the Alps is also special as several very different climatic regimes (Mediterranean, Continental, Atlantic, and Polar) all come together here. The effects of climate change on high-mountain environments and living conditions are well documented, because the Alps are among the most densely populated and most intensively studied mountain region of the world (*Haeberli and Beniston*, 1998). The reported warming since the LIA occurred mainly in two stages: between 1880 and 1945 and since 1975 (*Casty et al.*, 2005). The experienced warming in the Alps since 1975 is synchronous with global warming, but of far greater amplitude (*Beniston*, 2005). According to *Ceppi et al.* (2012) the surface temperature in Switzerland has increased by a rate of 0.35 °C/decade over the last 30 years. Precipitation patterns have also changed but precipitation shows a larger variability in space than temperature (*Begert et al.*, 2005).

The Swiss Climate Change Scenarios (*CH2011*, 2011) provide a new assessment of how climate may change over the 21st century. In this study, the Swiss climate is projected to depart significantly from present and past conditions, with increasing temperatures in all regions and seasons and decreasing precipitation in Southern Switzerland (cf. Figure 2.10). Due to the complex topography and the highly localized climate within the Alps, the grid points of the central Alps are not included in the regional averages. Thus for the Alps, the determination of future climate change is a challenging task with many uncertainties (cf. section 3.2).

2.4.3 Glacier change in the Alps

Since glaciers reached their maximum extent at the end of the Little Ice Age (around 1850), Alpine glaciers lost roughly 35% of their volume until the 1970s, and almost 50% by 2000 (*Zemp et al.*, 2006). In the time period between 1975 and 2000 about 1% of the remaining ice volume was lost per year and subsequently the annual losses increased to about 2–3% per year between 2000 and 2005 (*Haeberli and Maisch*, 2007), culminating in an annual ice loss of 5–10% in the extraordinarily warm year of 2003 (*Zemp et al.*, 2008). Due to the strong warming, the predominant processes of glacier decline during the past years/decades have been downwasting and disintegration (*Paul et al.*, 2004, 2007b). Even with a moderate atmospheric warming, Alpine glaciers are expected to

shrink to about 10–20% of their present extent by the end of the 21st century (e.g., *Zemp et al.*, 2006, *Huss*, 2012).

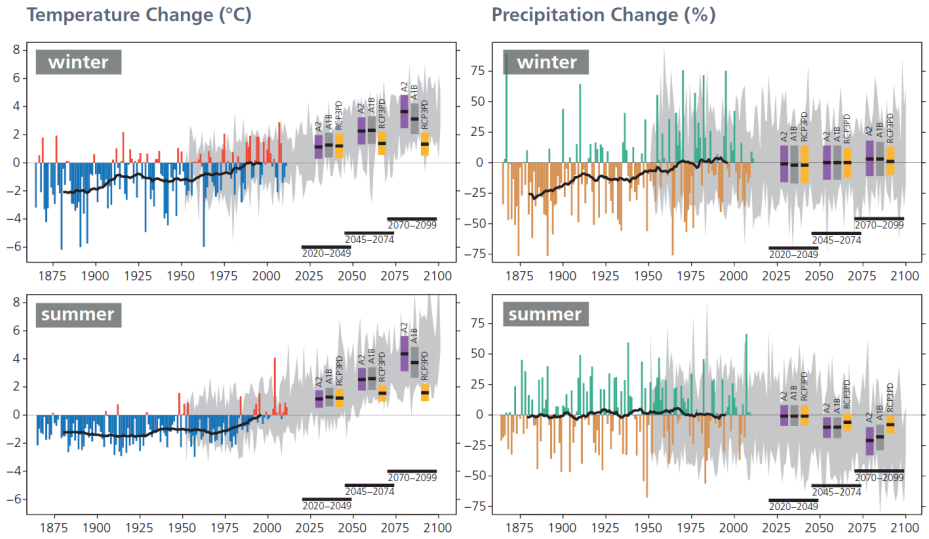

Figure 2.10: *Past and future changes in seasonal temperature (°C) and precipitation (%) over northeastern Switzerland. The changes are relative to the reference period 1980–2009. The thin colored bars display the year-to-year differences with respect to the average of observations over the reference period, the heavy black lines are the corresponding smoothed 30-year averages. The grey shading indicates the range of year-to-year differences as projected by climate models for the A1B scenario (specifically, the 5–95 percentile range for each year across the available model set). The thick colored bars show best estimates of the future projections, and the associated uncertainty ranges, for selected 30-year time-periods and for three greenhouse gas emission scenarios. (Figure and caption after* CH2011, *2011).*

2.4.4 Approaches to model future glacier evolution

Future glacier evolution, as a consequence of future climate change with further increasing temperatures (*IPCC*, 2007, and chapter 3), is of growing concern for the expected changes in the hydrologic regime of major river catchments (e.g., *Mauser and Bach*, 2009, *Huss*, 2011), as well as for its influence on hydropower production (e.g., *Schaefli et al.*, 2007, *Terrier et al.*, 2011, *Farinotti et al.*, 2012), tourism (*Fischer et al.*, 2011), and natural hazards (e.g., *Moore et al.*, 2009, *Frey et al.*, 2010, *Haeberli et al.*, 2010, *Künzler et al.*, 2010). Numerical modeling is thereby often the only possibility to provide simulations on future glacier change (*Haeberli and Dedieu*, 2004). Accordingly, several methods – based on different basic concepts, complexity and application scales – have been developed to determine future glacier evolution.

According to *Hoelzle et al.* (2005) glacier models combine stochastic with deterministic elements and can be divided into two main types: regionally calibrated empirical-statistical models and process-oriented models (which are more physically based). Between model complexity and process understanding as well as the number of modeled glaciers, a relationship can be found: simple models require only few input data and are easy to apply on both large regions and glacier samples, whereas more complex models are the contrary. However, sophisticated models can depict the involved physical processes on a higher level (Figure 2.11).

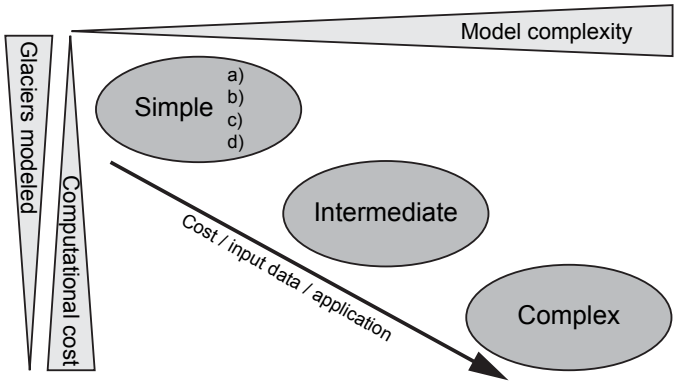

Figure 2.11: *Scheme showing the relationship between model complexity and computational costs and number of modeled glaciers, respectively for different types of models. (modified after* Hoelzle et al., *2005)*

The models developed and applied in this thesis are characterized by a rather low complexity, but they can be applied at large spatial scales. They are thus treated as simple methods. *Kuhn* (1993) suggested a classification scheme of four groups, where such simple approaches can be further divided, according to the information content of the input, the formulation of the cause and- effect relation or the practical applicability:

a) The analogy concept that is based on a search for similar events in the past;

b) Multivariate analysis of past data as basis for procedures that range from black box to calibrated models;

c) Deterministic models with explicit treatment of processes linking causes and effects;

d) Inclusion of changes in prevalent synoptic patterns.

For modeling glacier evolution at the scale of entire mountain ranges, a variety of simple techniques can thus be applied. An example for type c) are approaches where a shift of the ELA according to a change in temperature leads to a change in the size of the accumulation area and a subsequent adjustment of the glacier geometry (e.g., *Lie et al.*, 2003, *Zemp et al.*, 2006, *Condom et al.*, 2007, *Paul et al.*, 2007b) or the application of various spatio-temperal extrapolation techniques (*Huss*, 2012). The parameterization scheme presented by *Haeberli and Hoelzle* (1995) is based on simple mathematics, mass conservation physics and listed inventory data to estimate glaciological characteristics and to simulate potential climate change effects on the inventoried glaciers and also belongs to the type c). To model glacier evolution on a global scale, very simplified methods are also applied to assess the future contribution of glaciers to sea-level rise, mostly as a combination of types a) and b) (e.g., *Raper and Braithwaite*, 2005, *Bahr et al.*, 2009, *Radic and Hock*, 2011, *Giesen and Oerlemans*, 2012, *Marzeion et al.*, 2012a). *Radic and Hock* (2011) and *Raper et al.* (2000) considered the change in a standardized area-elevation distribution (hypsometry) to account for the adjustment of glacier area to future climate conditions.

A more direct way to determine future glacier evolution is the calculation of glacier volume loss based on observed overall changes in glacier thickness as derived from geodetic measurements (e.g., differencing of two digital elevation models) over a longer time period (e.g., *Huss et al.*, 2010b). These past observations can be used to develop a simple parameterization of future glacier thickness evolution, combined with the spatial distribution of glacier thickness (e.g., from a model approach as described in section 2.3.2), and applied to a large glacier sample (e.g., *Huss*, 2011, *Huss and Farinotti*, 2012, *Machguth et al.*, 2013, *Salzmann et al.*, 2012).

A variety of more complex approaches exist to model future glacier evolution, based on mass balance determination and glacier flow (e.g., *Leysinger Vieli and Gudmundsson*, 2004, *Le Meur et al.*, 2007, *Jouvet et al.*, 2009, 2011). These models are computationally intensive and only applicable to individual and well studied glaciers, where sufficient calibration and validation data exist.

Glacier mass balance and annual meteorological conditions are closely linked (cf. section 2.1.4) and as such mass balance is a key variable in understanding glacier-climate relations and is modeled with distributed mass balance models based on the temperature index method (e.g., *Braithwaite*, 1989, *Hock*, 2003) or on a energy balance approach (e.g., *Oerlemans*, 1991, 1992, *Arnold et al.*, 1996, *Brock et al.*, 2000). Depending on their complexity, such model approaches (cf. *Paul et al.*, 2008, and references therein) mostly belong to the group of models with intermediate complexity (cf. Figure 2.11).

The more simple temperature-index or degree day models use the high correlation of temperature with various energy balance terms (e.g., incoming long-wave radiation and

turbulent fluxes (cf. section 2.1.3)) (e.g., *Kuhn*, 1990, *Braithwaite*, 1981, *Braithwaite and Zhang*, 2000, *Ohmura*, 2001). Surface ablation is thereby estimated as a function of temperature (measured on the glacier or at weather stations nearby) and empirically calibrated with measured run-off. These models can be improved by incorporating a factor for solar radiation calculated from DEMs (*Hock*, 1999). Several recent studies related to the future evolution of glaciers are based on temperature-index models (e.g., *Hirabayashi et al.*, 2010, *Huss*, 2011, *Marzeion et al.*, 2012b), as temperature is the only variable in climate models that have a clear trend and limited spatial variability over larger regions (*Auer et al.*, 2007) at the same elevation. On the other hand, an averaged and constant degree-day factor has to be applied, which is not realistic for at least two reasons: (1) the degree-day factor varies from glacier to glacier (*Hock*, 2003) and (2) is not constant in time (*Huss et al.*, 2010a). As an additional drawback albedo is not considered which may introduce a systematic bias for the future evolution of glaciers.

Energy balance models calculate the components of the energy balance (cf. section 2.1.3) explicitly and determine glacier melt and run-off from a positive energy balance (cf. *Hock*, 2005). First mass balance models calculated the energy balance at a point scale (e.g., *Greuell and Oerlemans*, 1987) and were later widely applied to entire glaciers using a DEM as a representative of the glacier surface (e.g., *Oerlemans*, 2001, *Klok and Oerlemans*, 2002, *Greuell and Genthon*, 2004). An application of mass balance models to a larger sample of glaciers requires that the climatic input data must be interpolated from point observations to continuous fields (e.g., *Paul et al.*, 2008) or directly obtained from gridded RCM output (e.g., *Machguth et al.*, 2009). These models are based on some well known physical rules and can thus also be applied under future climate conditions. However, they require more (meteorological) input data that have either to be parameterized or held constant (*Paul et al.*, 2008).

All models have their advantages and disadvantages in regard to specific applications (e.g., temporal and spatial scales) and should thus be selected for their respective purpose. As a governing principle, a balance between computational effort and the quality of the results has to be found. More sophisticated models do not provide a priori better results than simple ones (*Hoelzle et al.*, 2005), if the latter consider the most important processes correctly and with the required level of detail. Thus, if for a remote region only mean annual temperature data and a coarse DEM is available, it is of limited value to run a physically complex model. If possible, models of different complexity should be applied to the same region and compared to each other. This would help finding sensitivities of the processes involved and systematic differences between the approaches but also common trends.

3 Climate modeling

3.1 Climate scenarios

Projections of future climate are based on scenarios, a plausible description or an alternative image of how the future climate might evolve. Crucial for climate scenarios are thus assumptions on future greenhouse gas emissions. In this context the economic and demographic development on Earth and measures for reduction of emissions are important. These developments are captured with the Special Report on Emissions Scenarios (SRES), a set of plausible events, developments or circumstances under which the world could evolve, ranging from variants of sustainable development, to the collapse of social, economic, and environmental systems (*Nakicenovic and Swart*, 2000, *IPCC*, 2007). The SRES emission scenarios are based on four different narrative (qualitative) storylines (A1, A2, B1, B2), which consistently describe the relationships and evolution between the driving forces of the greenhouse gas emission (e.g. economic and population growth, hypotheses related to technological advances, the rate at which the energy sector may reduce its dependency on fossil fuels, socio-economic projections related to deforestation and land use changes). Within the A1 family three different realizations were drawn, featuring alternative developments of energy technologies: A1FI (fossil fuel intensive), A1B (balanced), and A1T (predominantly non-fossil fuel). Accordingly,

the increase in global mean temperature by the end of the 21st century ranges from 1.1 °C to 6.4 °C (Figure 3.1).

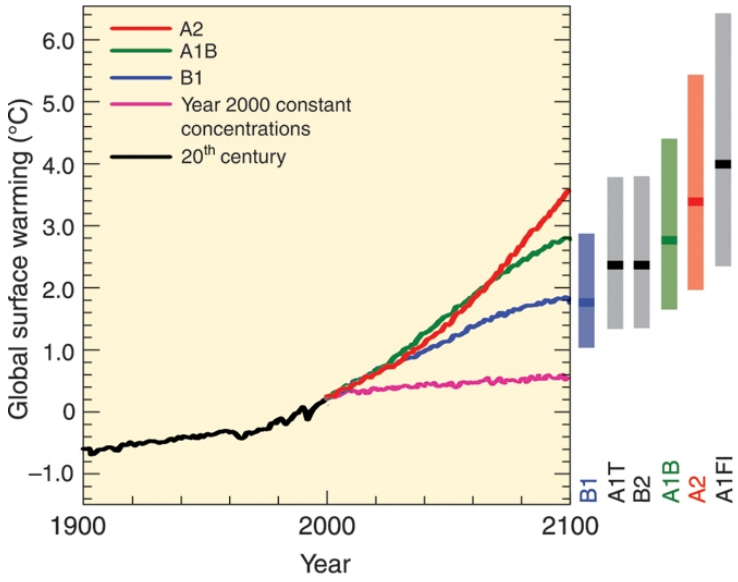

Figure 3.1: *Solid lines are multi-model global averages of surface warming (relative to 1980–1999) for the SRES scenarios A2, A1B and B1, shown as continuations of the 20th century simulations. The orange line is for the experiment where concentrations were held constant at year 2000 values. The bars in the middle of the figure indicate the best estimate (solid line within each bar) and the likely range assessed for the six SRES marker scenarios at 2090–2099 relative to 1980–1999. The assessment of the best estimate and likely ranges in the bars includes Atmosphere-Ocean General Circulation Models (AOGCMs) in the left part of the figure, as well as results from a hierarchy of independent models and observational constraints. (Source:* IPCC, *2007)*

For the modeling of future glacier evolution in this thesis, the **A1B emission scenario** is especially relevant. It is characterized by a balance across fossil-intensive and no fossil energy sources. It belongs to the A1 scenario family describing a future world of very rapid economic growth, global population that peaks in the mid-century and declines thereafter, and the rapid introduction of new and more efficient technologies (*IPCC*, 2007, *CH2011*, 2011).

3.2 Climate models

Projections of future climate change are based on comprehensive models of the Earth's climate system and on physical laws represented by mathematical equations. The so

called **General Circulation Models (GCMs)** describe in a three dimensional grid the most important processes and feedbacks in the atmosphere, the oceans and on the Earth's surface (*McGuffie and Henderson-Sellers*, 2001). GCMs run decades and centuries into the future. The computational capacities are still a limiting factor and therefore the spatial resolution of the GCM-grids is restricted to about 100 km. Nevertheless GCMs are the best available tools for assessing future climate on a global scale (*Randall et al.*, 2007).

Due to the grid spacing of current GCMs, regional climatic variations cannot be appropriately represented, the complexity of topography and land surfaces is smoothed and small-scale atmospheric processes such as fronts and precipitation systems are not or only poorly resolved (*CH2011*, 2011). With **Regional Climate Models (RCMs)** the coarse data of GCMs can be downscaled to a limited-area domain. Typically the RCMs have a grid size of 10 to 50 km and cover a distinct region (i.e. Europe), but also describe – similar to the GCMs – the processes and interactions within a climate system. RCMs allow to better characterize the regional variability of climate parameters. This is essential for a topographically highly structured terrain like the Alps and the related modeling of climate change impacts on a regional scale.

At their lateral boundaries, a high-resolution RCM is forced with information from a low-resolution GCM. The large-scale information about global scale characteristics of the atmospheric circulation thus drives the small-scale processes in the RCM (*Giorgi and Mearns*, 1999). This one way process is also called nesting. The RCM dynamically downscales the coarse GCM information and thereby represents atmospheric and surface processes in a higher resolution. Errors originating from the GCMs cannot be corrected and the RCM does not return anything to the GCM, but they simply better represent the observed spatial patterns of climate variables (*Leung and Ghan*, 1999). The combination of a specific GCM with an RCM is called a model chain (Figure 3.2).

Although not all processes of the complex climate system are fully understood and thus yet implemented, the current models are capable of reproducing the climate of the past decades. They furthermore allow estimation of the influence of greenhouse gas emissions on the global climate on Earth. Hence, to run a climate model into the future, assumptions on future greenhouse gas emission are required and captured with the Special Report on Emissions Scenarios (SRES) (cf. *Nakicenovic and Swart*, 2000, and section 3.1). Therefore, climate change model results are projections rather than predictions, they are dependent on a given scenario of anthropogenic emissions.

The European research project ENSEMBLES was initiated to provide climate information obtained through the use of the latest climate modeling and analysis tools for use in research, policy, business and public. The core of the project was in running multiple climate models ('ensembles' with several GCM-RCM model chains). This ensemble

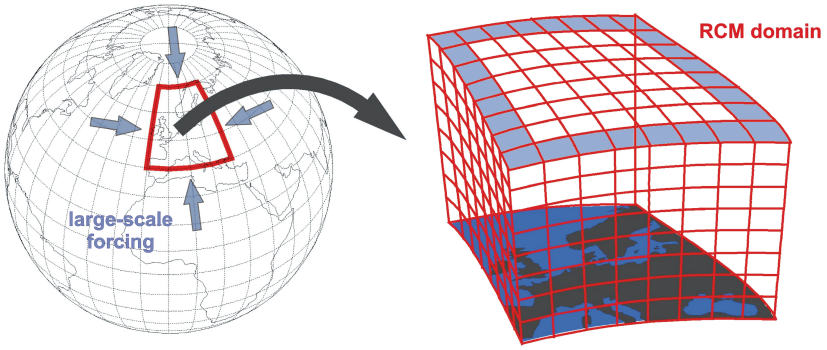

Figure 3.2: *The principle of model nesting: A RCM (red) is nested in a GCM (blue) with its coarser resolution. The RCM computes the climate for a limited model domain (e.g. Europe) with a higher spatial resolution. (source:* Bosshard et al., *2011b)*

prediction system gives the first probabilistic climate projections of temperature and rainfall changes within this century for Europe (*van der Linden and Mitchell*, 2009).

The RCM resolution of 10 to 50 km (as given from the ENSEMBLES project) enables a more detailed representation of the spatial variability of temperature and precipitation in terms of e.g. topography, ocean-land separation and land surface use, but comes to its limits when modeling a mountain range like the Alps. The topographic fine-scale structures like the Engadin or the Valais (with the valley of Rhone) could not be captured with current RCM resolutions (Figure 3.2). Information with a higher spatial resolution is required for impact models on glaciers or hydrology. This gap can be closed e.g. with a statistical downscaling, which is based on the assumption that the local climate is conditioned from the large-scale climate state on the one hand and regional/local factors (e.g. topography) on the other (*Wilby et al.*, 2004, *Fowler et al.*, 2007). A variety of methods of different complexity exists, many of them applicable to both GCM and RCM output. Two of them (de-biasing and delta change approach), which are used for the study described in ***Paper IV***, are shortly summarized in the following. *Salzmann et al.* (2007) already explored the application of these two downscaling approaches on RCM data for impact modeling on permafrost simulations in high-mountain area.

Machguth et al. (2009, 2012) for instance downscaled a whole field of RCM output to a higher resolution and applied these data to run directly a distributed mass balance model for glaciers. Thereby the centers of the RCM grid cells were treated as virtual weather stations and the downscaling procedure consists of two steps: (1) the values between the grid boxes are interpolated to the DEM resolution and (2) the application of sub-grid parameterizations. For accurate application of RCM output to impact models, the downscaled RCM grids require additional bias correction. De-biasing for each grid

cell and each variable is based on comparison and adjustment to observations at 14 high-mountain weather stations (*Machguth et al.*, 2012).

Alternatively, *Bosshard et al.* (2011a) used 10 GCM-RCM model chains from the ENSEMBLES project for a statistical downscaling of temperature and precipitation with an extension of the widely used delta change method (e.g. *Prudhomme et al.*, 2002) to the locations of MeteoSwiss weather stations. Relative to the control period 1980–2009 a climate change signal is determined from the RCM data for the scenario periods 2021–2050 and 2070–2099. All model chains use the A1B emission scenario (*IPCC*, 2007), cover the period 1951–2099 and have a grid size of 25 km. The downscaled results from *Bosshard et al.* (2011a) show, considering temperature change, peaks in winter and summer in both scenario periods for the ensemble mean. At all stations a considerable warming is expected (about +1.5 °C for the period 2021–2050 and about +3.0 to 4.5 °C for 2070–2099). Generally, the temperature change signal is distinctively above the estimated natural variability range for both scenario periods (Figure 3.3). In the case of precipitation the range of natural variability is much larger. The ensemble mean does not show a distinct trend and the uncertainties regarding the sign of precipitation change are rather large. Only a decrease of precipitation in summer of the second scenario period exceeds the range of the natural variability (Figure 3.3).

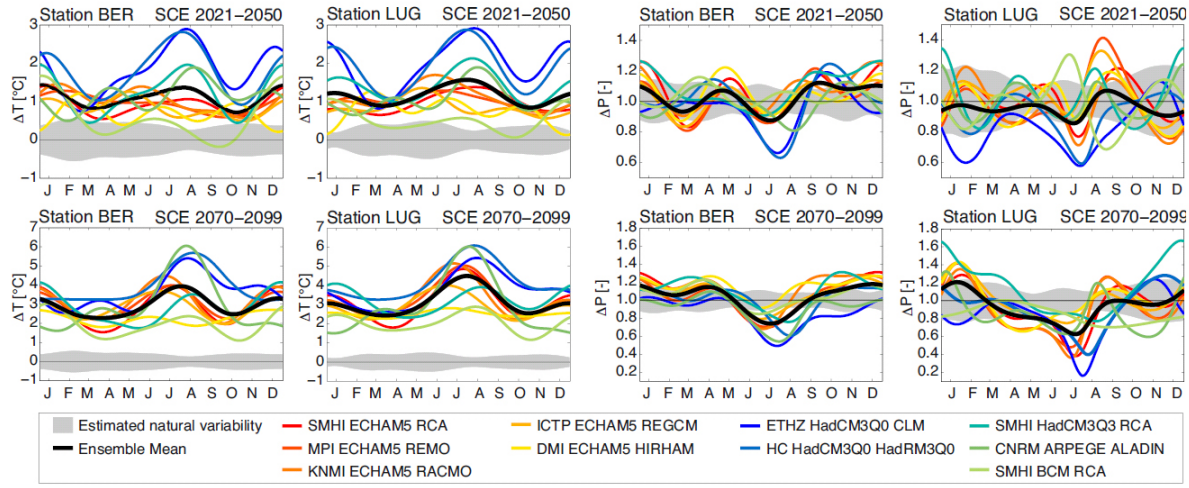

Figure 3.3: *Annual cycle of ΔT (left panel group) and ΔP (right panel group) for the scenario period 2021–2050 (top) and 2070–2099 (bottom) at the two exemplary stations Bern (BER) and Lugano (LUG). Each of the 10 GCM-RCMs is shown with an individual color. The ensemble mean is indicated by a black line. The grey band shows the range of the estimated natural variability as $\pm\alpha$ of the resampled ΔTs or ΔPs at the station site. Note the different scales in upper and lower panels. (source:* Bosshard et al., *2011a)*

3.3 Uncertainties when applying climate models for impact modeling

Due to the imperfect knowledge of the boundary conditions, emission scenarios, and the required simplifications of the governing physical processes in climate models, all climate scenarios are subject to uncertainties (*Bosshard*, 2012). There are three further main uncertainties concerning climate modeling: (1) the natural variability of the climate system, (2) the trajectories of future greenhouse gas emission, and (3) the response of the climate system to the future emissions (e.g., *Hawkins and Sutton*, 2009, *Mearns*, 2010). According to *Mearns* (2010) the emission scenarios contribute the largest amount to the uncertainty by the end of the 21st century. All these uncertainties propagate through the entire model chain and may be further amplified in the subsequent impact modeling (cf. *Bosshard*, 2012, and Figure 3.4).

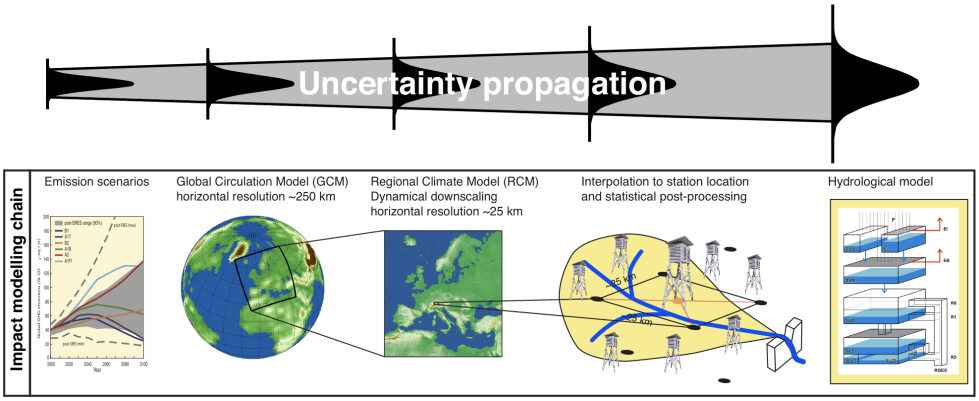

Figure 3.4: *Schematic representation of the uncertainty propagation in a climate model-hydrological impact modeling chain (source:* Bosshard, *2012).*

On the other hand, climate model data also offers major advantages for using them in impact models (*Machguth*, 2008). Appropriate meteorological properties data are not always available in remote regions and climate models provide physically consistent and already grided input datasets with a temporal and spatial resolution that is high compared to climatologies derived from measurements. When driving impact models with climate model output, the key uncertainties of the climate model contributing to the uncertainty of the final impact assessment must be known (*Mearns et al.*, 2001). Hence in ***Paper IV*** future climate scenarios based on climate models form the ENSEMBLES project were used to force three different glacier evolution models, to compare the model results and evaluate the uncertainty range induced by different climate scenarios.

4

Datasets and implementation

This chapter is closely related to the research papers, the main part of the thesis (cf. summaries in chapter 5 and full versions in Part II). On the one hand, the data used are introduced and explained (section 4.1) and on the other hand the concepts and model approaches developed and applied for the scientific work are outlined (section 4.2).

4.1 (Model) Input data

4.1.1 Digital Elevation Models (DEMs)

In geosciences, information about the Earth surface is indispensable for modeling processes and describing landscapes. Usually this information is provided by a digital elevation model (DEM), where every surface point consists of three coordinate values representing its location in the x, y, (horizontal) and z (vertical) dimension. There are two ways for representing surface in a DEM: either with a triangular irregular network (TIN), or as a equally-spaced raster dataset with an elevation value for each grid cell (*Burrough and McDonnell*, 1998). In this thesis exclusively DEMs in gridded format are used as they are more easy to handle and to combine with other raster based applications (e.g. surface derivates).

In principle, the purpose defines the use of a specific DEM, but there are several other criteria which can restrict the choice: spatial resolution (cell size), spatial extent, acquisition technique, acquisition date and availability (cf. *Frey*, 2011). For the intention and models of this thesis, a DEM with a high resolution (10 to 50 m) and a spatial extent covering the Swiss Alps was required and given by the DHM25 from swisstopo (*swisstopo*, 2005). In consideration of applying the developed methods to other glacierized mountain ranges of the world, the two free (and almost) global DEMs from SRTM and ASTER (GDEM) are investigated as well.

The **DHM25** was produced by the Swiss Federal Office of Topography (swisstopo) from aerial photography and has a cell size of 25 m. The DEM is based on the interpolation of contour lines from the Swiss topographic map sheets (1:25 000) and includes digitized lake perimeters, main break lines and spot heights (*Rickenbacher*, 1998). Two versions of this data set are available: a Level 1 (DHM25L1) from around 1985 and a Level 2 (DHM25L2) from around 1995. Apart from the acquisition date, the two DEMs primarily differ regarding the algorithms used for the contour line interpolation and the partly updated glacier elevations (in general in the ablation region only) in the Level 2 version (*swisstopo*, 2005). For the Bernina region both DEMs refer to 1991.

The deviations between the digitized and the original map contours (accuracy in x and y direction) are according to *swisstopo* (2005) 2.5–7.5 m. The vertical accuracy (z direction) is reported to be less than 10 m in the Alps. For the DHM25L2 the acquisition date and the mean error of the data can be checked for every 1:25 000 map sheet in the product description.

For sensitivity tests, three further DEMs from two sources were applied: On the one hand, two versions of the **SRTM DEM** acquired in February 2000, with 90 m spatial resolution (e.g., *Rabus et al.*, 2003, *Farr et al.*, 2007), with the data voids included and data voids filled by the *Reuter et al.* (2007) algorithm. On the other hand, the **ASTER GDEM** (version 1) with 30 m spatial resolution, which was produced by stereo photogrammetry with all scenes from the ASTER sensor acquired between 2000 and 2007 (*Hayakawa et al.*, 2008, *Toutin*, 2008). All three DEMs are available for free from public ftp-sites and were projected to the Swiss map projection (Oblique Transverse Mercator with Bessel Ellipsoid) using a bilinear resampling from their original resolution to 25 m. How the different DEMs influence the topographic characteristics of glacier entities is discussed in *Frey and Paul* (2012) and thus not repeated here.

For the SRTM DEM, validation by comparison with ground control points revealed vertical and horizontal errors of approximately 10 m (*Farr et al.*, 2007). In high-mountain topography, radar shadow and layover effects result in numerous data voids of various sizes (e.g., *Eineder*, 2001). The Consultative Group on International Agricultural Re-

search (CGIAR), which offers the void-filled version of the SRTM3 dataset, reports the vertical error to be less than 16 m (`http://srtm.csi.cgiar.org`, accessed July 2012).

For DEMs produced by photogrammetry from the ASTER sensor, vertical accuracies of ±15–30 m are reported (*Toutin*, 2008, and references therein), but in rough mountainous conditions with steep slopes and snowfields with little optical contrast, RMS values of ±60 m are reported (*Kääb et al.*, 2002). For the ASTER GDEM the standard deviation of vertical elevation errors is expected to be 7–14 m, but the spatial detail resolved by the ASTER GDEM is only slightly better than 120 m (*METI/NASA/USGS*, 2009).

4.1.2 Glacier elevation change (in the Swiss Alps)

For determination of the geodetic mass balance, two DEMs with different dates are required (cf. section 2.1.5). For Switzerland the DHM25L1 (from around 1985) and the SRTM3 DEM (from February 2000) are available for this purpose. *Paul and Haeberli* (2008) exploited this and derived the spatial variability of glacier elevation changes in the Swiss Alps from DEM differencing (SRTM3-DHM25L1). Apart from very few regions with data voids over glaciers, this data set covers nearly all glaciers in the Swiss Alps. This study reveals extreme thickness losses for flat low-lying glacier tongues and a strong overall surface lowering in the time period 1985–1999. A comparison of the DEM differencing with the mean cumulative mass balance of nine glaciers with measured mass balances revealed the representativeness of these glaciers for a mean value of all Swiss glaciers.

4.1.3 Glacier data (fluctuations and inventories)

In the context of the Hydrological Decade (1965–1974) the World Glacier Inventory (WGI) was established to assess the amount, distribution and variation of all snow and ice masses to better understand the role of the cryosphere in the global water balance (*Ohmura*, 2009). By combining the former ICSI (International Commission on Snow and Ice) services PSFG (Permanent Service on Fluctuations of Glaciers) and the TTS/WGI (Temporal Technical Secretariat/World Glacier Inventory) into the World Glacier Monitoring Service (WGMS) in 1986, the WGMS continued to maintain and collect information on glacier changes (*WGMS*, 1989, 2008a). More specifically, the tasks of the WGMS are to collect "standardized observations on changes in mass, volume, area and length of glaciers with time (glacier fluctuations), as well as statistical information on the distribution of perennial surface ice in space (glacier inventories)" (`http://www.wgms.ch/about.html`, accessed June 2012). Within the Global Climate/Terrestrial Observing Systems (GCOS/GTOS), the WGMS is in charge of the Global Terrestrial Network for

Glaciers (GTN-G) together with the Global Land Ice Measurements from Space (GLIMS) initiative and the National Snow and Ice Data Center (NSIDC). At the NSIDC in Boulder, Colorado, the GLIMS initiative maintains a database of glacier inventories where the mapped glacier outlines are stored as polygons in a digital vector format (*Raup et al.*, 2007), while the WGI data is available in a tabular format with up to 40 parameters per glacier, including geographic location, area, glacier type, topographic parameters, morphological classification, date, source material, and accuracy estimations.

In 2009, according to *Ohmura* (2009), 54% of the global glacier area were covered by the WGI and GLIMS databases (WGI: 46%, GLIMS: 34%, overlap: 26%). In the tabulated WGI data, a large amount of glacier information can be stored in an efficient manner and can be used for various applications that only require scalar information (e.g. the parameterization scheme from *Haeberli and Hoelzle* (1995)). However, the WGI data are a 'snapshot' of the late 20th century, with partially unknown accuracy (*Cogley*, 2009). Glacier outlines in a digital vector format (as stored in the GLIMS database) are a key dataset for hydrologic modeling (e.g., *Huss et al.*, 2008b), change assessment (e.g., *Andreassen et al.*, 2008), and distributed mass balance modeling (e.g., *Machguth et al.*, 2009, *Paul et al.*, 2009).

In this thesis the outlines from (1) the Swiss Glacier Inventory from 1973 by *Müller et al.* (1976) and from (2) the new Swiss Glacier Inventory 2000 (SGI2000) (*Paul*, 2007) are used:

1. *Müller et al.* (1976) compiled from aerial photography taken by the Swiss Army (mostly acquired in September 1973) a first glacier inventory for all Swiss glaciers. The photos were interpreted by stereo-photogrammetry and transferred to topographic map sheets with an $1 : 25\,000$ scale. *Benz* (1995) and *Wipf* (1999) transformed parts of the inventory to GIS-based vector layer by digitizing the glacier outlines of all glaciers north of the Rhone River. Within the work of *Maisch et al.* (2000) and *Paul* (2007) the digitizing work was completed for all glaciers, including a reassessment of the inventory from *Müller et al.* (1976). These glacier outlines fit well to the glacier extent in the DHM25L1, as only small overall area changes took place for most glaciers in the Alps between 1973 and 1985 (*Paul et al.*, 2004).

2. The Swiss Glacier Inventory 2000 (SGI2000) (*Paul*, 2007) was derived from Landsat images acquired in the years 1998 and 1999. Glaciers were separated from other terrain by dividing the high reflectance values of ice and snow in the visible band (TM3) by the very low reflectance values in the shortwave infrared (TM5) (*Paul et al.*, 2002). An additional threshold in TM1 to improved the classification in shadow regions (e.g. *Paul and Kääb*, 2005). As glacier ice under thick debris cover is not mapped by this approach, debris-covered glacier tongues and other misclas-

sification (lakes, shadow, seasonal snow) were corrected manually. In this case the DHM25L2 corresponds much better to the extent of the glaciers from the SGI2000.

Considering only perennial ice bodies larger than 0.01 km^2 from these two glacier inventories samples containing 2365 glaciers and glacierets for 1973 and 1182 for 1998/1999 were created. The difference in number is mainly due to the different number of small glaciers considered ($< 0.1\,km^2$) with many of them having disappeared during this time period or not being recognizable in the satellite images anymore (e.g. due to debris cover) (*Paul et al.*, 2007a).

4.2 Geographic Information System (GIS) and implementation

Burrough and McDonnell (1998) define a Geographic Information System (GIS) as "a powerful set of tools for collecting, storing, retrieving at will, transforming and displaying data from the real world for a particular set of purposes". In this regard a GIS helps to visualize, question, analyze, interpret, manipulate and understand all types of geographical and spatial (geocoded) data and to reveal relationships and patterns between them (*Jones*, 1997, *O'Sullivan and Unwin*, 2002, *Longley et al.*, 2011). But a GIS is much more powerful than this. It allows manipulating, calculating and computing further data and is thus highly suitable for geo-spatial modeling.

In a GIS-environment a large range of standardized tools are available and can be easily applied and combined to process different kind of geographic data (e.g. raster, vector, tabular information) to produce data and maps. Within this thesis a GIS was the main tool used for modeling and data production. Beside the more specific tools, of particular value for the computations performed here was the possibility for script-based data processing. The most important (GIS-)operations used in the model scripts of this thesis (represented as flowcharts in Figures 4.1 and 4.2) are the concepts of Map Algebra and of spatial inter- and extrapolation. In the following, technical details about these two concepts are presented, ensued by a short description of the modeling approaches developed and applied.

4.2.1 Map algebra

With raster data, where each attribute is stored in a separate dataset and in similar dimensions (cell size, reference system), any mathematical operation on one or more

attributes can easily be performed and result in a new raster layer. Methods using algebraic expressions for manipulating geographic data are called map algebra (*Tomlin*, 1991). The same algebraic notation as used for scalar values can be used on gridded data. Thus map algebra can easily be included in models operating with spatial data (e.g. *Etzelmüller and Björnsson*, 2000).

GIS transformations with map algebra are categorized into four classes depending on the spatial neighborhood: local, focal, zonal, and global (*Longley et al.*, 2011). Local operations examine rasters on individual cells, where the pixel value is a function of the value(s) at that location (i.e. reclassification). In focal operations the neighborhood of a cell is used to derive a new value for the cell (e.g. smoothing data, calculating slope and aspect). In zonal operations the cell value is a function of all cells in a zone, defined as a cluster of cells with the same value (e.g. zonal statistics). In global operations the output for a cell is a product of a calculation involving (potentially) all cells of a raster (e.g. mean value).

In this thesis, focal operations were used e.g. for smoothing DEMs or deriving the surface slope of glaciers. Of high importance was also the use of the zonal statistics tool, to calculate for example the volume of glaciers from their modeled ice thickness distribution, to extract the parameters area, volume, minimum and maximum depth of modeled overdeepenings, or to derive hypsographic distribution (area-elevation distributions) of glacier area and volume and the corresponding mean ice thickness for distinct elevation intervals related to the modeled glacier bed (cf. ***Paper II*** and ***Paper III***).

4.2.2 Spatial interpolation

Interpolation operations are pervasive in a GIS, often applied explicitly by the user, but also implicitly involved in various operations (*Longley et al.*, 2011). According to *Burrough and McDonnell* (1998), interpolation is "the procedure of predicting the values of attributes at unsampled sites from measurements made at point locations within the same area or region. Predicting the value of an attribute at sites outside the area is called extrapolation." Inter- and extrapolation methods are hence used to make a reasonable guess of the value of a continuous field at places where no measurement exists. Based on the assumption that values at a specific location are more similar to values measured nearby than further away, most of these interpolation methods include a distance measure (*Longley et al.*, 2011).

In GIS applications, interpolation methods have been designed to transform irregular point or line data to raster representation, or to resample between different raster resolutions (*Mitas and Mitasova*, 1999). Therefore, a large number of interpolation and approximation methods exist to predict values of spatial phenomena in unsampled lo-

cations, using a variety of mathematical calculations, each with its own strengths and weaknesses and therefore restricted in its use.

Mitas and Mitasova (1999) listed important demands which reliable interpolation tools in GIS applications should satisfy: "accuracy and predictive power, robustness and flexibility in describing various types of phenomena, smoothing for noisy data, direct estimation of derivatives (gradients, curvatures), d-dimensional formulation, applicability to large datasets, computational efficiency, and ease of use." As there is no method which fulfills all the mentioned requirements, the selection of an appropriate method and parameter for particular data and application is crucial. *Mitas and Mitasova* (1999) distinguishes three sets of approaches:

1. **Local neighborhood approaches**: These deterministic methods are based on the assumption that each point influences the resulting surface only up to a certain finite distance. The interpolated values are based on the surrounding measured values and on specified mathematical equations that determine the smoothness of the resulting surface (*ESRI*, 2011). The selection of points and the way the interpolation is implemented differs among the various methods (e.g. IDW (inverse distance weighting), Natural Neighbor, Trend). However, the results are reproducible and unique, but without declaration on the quality of the interpolation. Thereby, IDW is one of the simplest and most widely available methods and works on the "assumption that the value at an unsampled point can be approximated as a weighted average of values at points within a certain cut-off distance, or from a given number m of closest points" (*Mitas and Mitasova*, 1999). These methods have limitation in reproducing local shapes and often generate local extrema at data points (*Watson and Philip*, 1985).

2. **Geostatistical approaches**: Statistical models that include auto-correlation (the statistical relationship among the measured points) are key elements of geostatistical methods (e.g. Kriging) (*ESRI*, 2011). "Kriging is based on a concept of random functions: the surface is assumed to be one realization of a random function with a certain covariance" (*Mitas and Mitasova*, 1999). Kriging can provide a statistical quality of its predictions and is able to predict the spatial distribution of uncertainty, but is less favorable for applications where local geometry or smoothness have to be considered (*Mitas and Mitasova*, 1999).

3. **Variational approaches**: Spline tools belong to the category of variational approaches where "interpolation and approximation is based on the assumption that the interpolation function should pass through (or close to) the data points and, at the same time, should be as smooth as possible" (*Mitas and Mitasova*, 1999). When

interpolating with Spline tools, a mathematical function is used to minimize overall surface curvature, resulting in a smooth surface that passes exactly through the input points (*Wahba*, 1990). Effects of natural variation and measurement error may produce local artifacts using exact splines. Using thin plate splines (TPS) can help to remove these artifacts by replacing exact slpines by a locally smoothed average (*Burrough and McDonnell*, 1998). Thin plate splines are often used to interpolate DEMs where it is necessary to process large datasets and areas quickly and efficiently (*Hutchinson*, 1995).

Topo to Raster (an interpolation tool implemented in ESRIs ArcGIS environment) is the most prominently used interpolation method in this thesis (cf. Figure 4.1, ***Paper II*** and ***Paper III***). It is a computationally efficient interpolation method specifically designed for the creation of hydrologically correct digital elevation models (DEMs) from point (e.g. spot heights), line (e.g. elevation contours) and polygon (e.g. lake outlines) data. Its base is the ANUDEM algorithm developed by *Hutchinson* (1989) and is optimized to have the computational efficiency of local interpolation methods such as IDW (1), without losing the surface continuity of global interpolation methods, such as Kriging (2) and Splines (3) (*ESRI*, 2011). Topo to Raster interpolates elevation values to a raster while imposing constraints that ensure a connected drainage structure and a correct representation of ridges and streams from input contour data (*Hutchinson*, 1989). For continuous depth data inside an outer polygon with a constant elevation (e.g., the glacier outline, with a prescribed ice thickness of 0 m), Topo to Raster automatically generates a depression with a parabolic shape and is thus well suited to mimic the typical shape of glacier beds.

4.2.3 Modeling approaches

The model approaches developed and applied in this thesis are based on physically robust assumptions, applicable to large glacier samples and requiring only few input data, mainly the DHM25 from swisstopo (cf. section 4.1.1) and the glacier outlines form the Swiss Glacier Inventory (cf. section 4.1.3):

1. Figure 4.1 shows the scheme of the model workflow of GlabTop, the model used to determine the spatial distribution of ice thickness (cf. ***Paper I***, ***II*** and ***III***). With only three input data sets (glacier outlines, a DEM and a set of digitized central branch lines), GlabTop calculates thickness values at point locations and spatially interpolates them to a continuous bed within the limits of the respective glaciers. The interpolation with Topo to Raster thereby reconstructs a smoothed parabolic bed, which approximates the shape of a glacier bed very well (cf. section 4.2.2).

The calculation of ice thickness is based on the perfect plasticity assumption (cf. section 2.2 with equations 2.8 and 2.9), the concept of simple map algebra (cf. section 4.2.1) and spatial interpolation algorithms (cf. section 4.2.2) and can be applied to large samples of glaciers in a computationally efficient manner within a GIS. The model output is the ice thickness distribution for the entire glacier sample. This dataset is further used to derive ice volume, glacier bed topographies, and potential overdeepenings in the modeled beds (cf. ***Paper III***). More details concerning the implementation of this model can be found in ***Paper I*** and ***Paper II***.

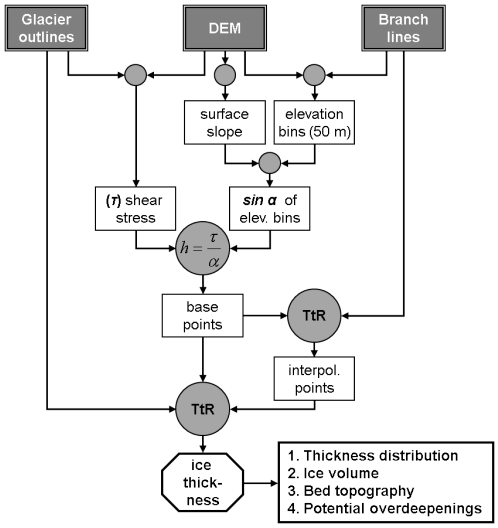

Figure 4.1: *Schematic overview of the basic processing steps for glacier bed interpolation with GlabTop using a flowchart (squares denote datasets and circles denote GIS-based calculations), with TtR (TopoToRaster) beeing the spatial interpolation algorithm used.*

2. To assess future glacier evolution on a regional scale, three simplified models were applied to the Swiss glaciers. All three models require only few input data and are illustrated schematically in Figure 4.2. The first model (**M1**) calculates (based on a DEM and glacier outlines), the change in the accumulation area following a shift in the ELA for given changes in temperature. These changes are converted to new total glacier areas (using a constant balanced-budget AAR_0 of 60%) according to three different scenarios of climate change (high, moderate or low temperature increase) derived from the ten model chains (described in *Bosshard et al.*, 2011a). For the models M2 and M3 the ice thickness distribution as derived with GlabTop (Figure 4.1) for all Swiss glaciers (***Paper III***) are required. In the second model (**M2**) the observed elevation-dependent thickness change (cf. section 4.1.2) over a 15 year period (1985–1999) is related to an observed temperature increase and

this trend is linearly extrapolated into the future. The third model (**M3**) can be separated into two model steps which are linked. First, the glacier mass balance is derived directly from RCM output (cf. section 3.2) and subsequently glacier retreat is estimated with an implemented elevation change (Δh) parametrization following *Huss et al.* (2010b). Both M2 and M3 provide future area and volume changes and the geodetic mass budgets between the time steps can be analyzed. M1 is based on *Paul et al.* (2007b), M2 is developed within this thesis (***Paper III***) and M3 is based on *Machguth et al.* (2009, 2012) and *Salzmann et al.* (2012). In ***Paper IV*** the three models are compared and analyzed.

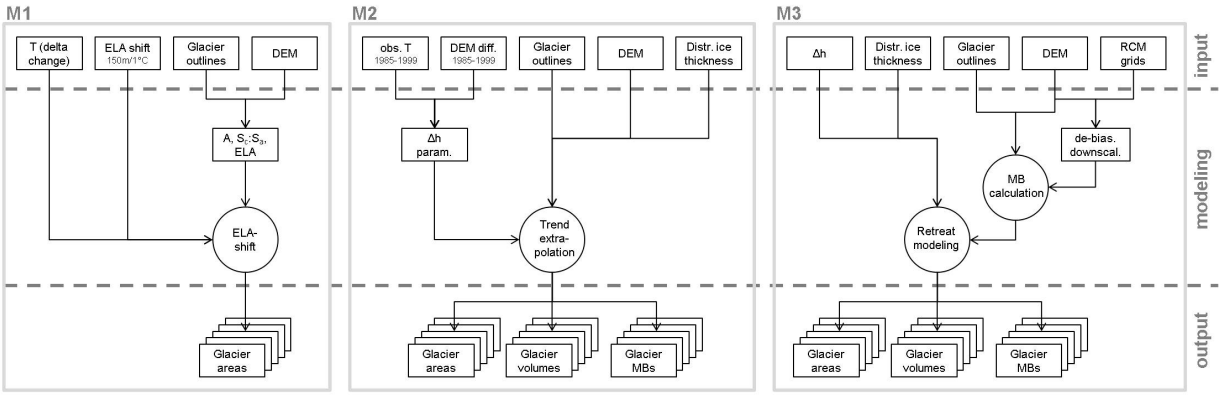

Figure 4.2: *Flowcharts of the three approaches (M1, M2 and M3) which are used to model the future glacier evolution on a regional scale.*

5
Summary of research papers

This thesis consists of four research papers that are published in or are in review at peer-reviewed scientific journals and a proceedings volume of a conference. The papers consecutively build up on each other. ***Paper I*** introduces the modeling principle of modeling ice thickness distribution and the potential fields of application, whereas in ***Paper II*** the methodological aspects are explained in detail. In ***Paper III*** the approach is validated and applied to all Swiss glaciers, leading to an extended analysis of ice distribution and glacier bed topographies in the Swiss Alps as well as a detection of potential overdeepenings. The derived ice thickness distribution is an input data for two of the three applied glacier evolution models compared in ***Paper IV***. In the following the papers are briefly summarized; the full versions can be found in Part II.

Paper I: Introducing a modeling approach for reconstruction of glacier beds

Linsbauer, A., Paul, F., Hoelzle, M., Frey, H., and Haeberli, W. (2009). The Swiss Alps without glaciers – a GIS-based modelling approach for reconstruction of glacier beds. In: *Proceedings of Geomorphometry 2009*, (edited by Purves, R., Gruber, S., Straumann, R., and Hengl, T.), pp. 243–247. University of Zurich, Zurich, Switzerland

This short paper opens the bracket for the present thesis by introducing the methodological principle of modeling ice thickness distributions and bed topographies with GlabTop and by listing the potential fields of applications of the approach.

With a glacier surface being a smoothed image of the underlying bed, the basic parameter that influences the variability in glacier thickness is surface slope. The basic principle "the steeper the glacier, the thinner the ice and vice versa" is also obvious from the perfect plasticity approach (also known as the shallow ice approximation (SIA) in glaciological text books). Together with a glacier-specific mean value of basal shear stress (τ) derived from an empirical relation with elevation range, local ice thickness is estimated in 50 m elevation bins and spatially interpolated within a GIS. For the here-introduced approach only three datasets (DEM, glacier outlines, branch lines) are required, and model results are calculated automatically for a large glacier sample using map algebra and a specific tool for spatial extrapolation.

The model output opens the door to a wide field of applications. The direct results are the interpolated ice thickness distribution (1) and the derived glacier bed topography (2). Further applications listed below are shortly explained in the paper:

1. Spatial distribution of glacier ice thickness (for large samples)
2. A DEM without glaciers (glacier bed topographies)
3. Mean glacier thickness
4. Resulting glacier volumes
5. Detection of overdeepenings as potential sites for future lake formation
6. Modeling flow paths of potential outburst floods once the glacier disappeared
7. Realistic visualization of landscapes without glaciers
8. Improved modeling of ongoing and potential future changes in run-off
9. Input for glacier flow models

Paper II: A method to model glacier bed topography and ice thickness distribution from sparse input data

Paul, F. and Linsbauer, A. (2012). Modeling of glacier bed topography from glacier outlines, central branch lines, and a DEM. *International Journal of Geographical Information Science*, 26 (7): 1173–1190. doi: 10.1080/13658816.2011.627859

For various applications in the field of glaciology it is becoming more and more important to have estimates of mean glacier thickness and total glacier volume as well as approximate knowledge about the subglacial topography. In this study, the method to model glacier bed topography (GlabTop) is described in detail and applied to the glaciers in the Bernina region.

Ice thickness is basically derived from an ice dynamical approach, based on the assumption of perfect plasticity of ice, which relates glacier thickness to its local surface slope via the basal shear stress estimated for each glacier and based on an empirical relation between shear stress and elevation range, which implicitly includes mass turnover and hence a mass balance gradient. While the glacier-wide estimated basal shear stress value determines the general/overall thickness of the glacier, the modeling of thickness variability for local glacier parts is governed by the zonal mean of the surface slope in 50 m elevation bins.

Only three data sets are required as an input: a DEM, glacier outlines and a set of manually digitized center lines of glacier branches (branch lines). DEMs and glacier outlines are widely available and the digitizing of the branch lines is based on elevation contour lines, the shaded relief of the DEM and digitizing rules as explained in the study.

With a set of artificial branch lines at a specific depth and rectangular outer polygons on flat and inclined planes, empirical tests were performed to set up digitizing rules for the branch lines and the implementation in a GIS. Key points of the GIS implementation are: (1) the raster based modeling approach which can be applied in a computationally efficient manner, (2) averaging of the surface slope in 50 m elevation bins in 100 m buffers around the branch lines, and (3) the interpolation to a continuous grid of ice thickness distribution with the TopoToRaster interpolation. This tool was developed to generate hydrologically correct DEMs and reproduces a parabolic shape of glacier beds.

The model generated ice thickness distribution and the glacier bed topographies for all 38 glaciers in the sample. The results were compared to three other datastets, revealing ice thickness values and spatial distributions in good agreement with the respective studies. Overall the accuracy of the modeled ice thickness with GlabTop is estimated to be in the $\pm$20–30% range for individual glaciers.

Paper III: Application of GlabTop: Modeling glacier thickness distribution and bed topography for all Swiss glaciers

Linsbauer, A., Paul, F., and Haeberli, W. (2012b). Modeling glacier thickness distribution and bed topography over entire mountain ranges with GlabTop: Application of a fast and robust approach. *Journal of Geophysical Research*, 117: F03007. doi: 10.1029/2011JF002313

The work presented in this paper is based on the application of GlabTop (the model introduced in ***Paper I*** and described in ***Paper II***) to the Swiss Alps resulting in modeled ice thickness distribution and bed topographies for all Swiss glaciers. The total glacier volume calculated with GlabTop for all Swiss glaciers is $75\pm22\,km^3$ for 1973 and $65\pm20\,km^3$ for 1999 and is in good agreement with earlier studies.

The analysis of the spatial distribution of ice thickness and the derived bed topographies provide further results. The ice of 60% of the ca. $1300\,km^2$ glacierized area in Switzerland (1973) is less than 50 m thick and contributes about 20% to the total ice volume. Another 20% of the total volume is stored in the small glacierized area (60–70 km^2) with ice thicknesses exceeding 200 m. Overall 1/4 of the total ice volume is stored in the largest three glaciers and 1/2 in the 15 largest. It was revealed that in regions with large ice thickness (mostly the tongues of the large valley glaciers), the elevations of the glacier beds are comparably low. The ice in the flat and thick low-lying tongues already suffers from strong melt down possibly due to positive feedbacks; because of the low mean slope of the bedrock a retreat of the terminus to higher elevations is hardly possible.

Furthermore, the geomorphometric characteristics of the modeled glacier beds are analyzed with a focus on overdeepenings. This analysis revealed a high number of sites (around 500–600 with a total area of 50–60 km^2) with a potential for future lake formation. Shallow overdeepenings might be rapidly filled with sediment, but for a high number of overdeepenings with volumes larger than 10 million m^2 and a considerable mean depth, lake formation is highly probable and relevant for hydro-power-production, hazard investigations, and tourism. The location of the modeled overdeepenings is rather robust, i.e. does not change much when another DEM or method of spatial interpolation between the base points of the local thickness estimates is used.

The model performance was evaluated by comparison to GPR profiles, analysis of the uncertainties in input parameters (sensitivity study) and a model intercomparison. The evaluation revealed that GlabTop reproduces the parabolic shape of glacier beds in good agreement with the shape of the GPR measurements, and that the measured and mod-

eled ice thickness values are within an uncertainty range of ±30%. This also results from the sensitivity analysis of the input parameters. The basal shear stress, the parameter with the highest uncertainty, governs the uncertainty of the thickness estimates. While the ice volume estimates for individual glaciers with the compared models (*Haeberli and Hoelzle*, 1995, *Farinotti et al.*, 2009b) can vary by about 20–30%, the total volume for all Swiss glaciers has an estimated uncertainty in the range of ±10%. The overall pattern of the ice thickness distribution as modeled by GlabTop and with the method developed by *Farinotti et al.* (2009b) reflects a highly similar picture.

Paper IV: Model scenarios of future glacier change for the Swiss Alps

---

Linsbauer, A., Paul, F., Machguth, H., and Haeberli, W. (2013). Comparing three different methods to model scenarios of future glacier change in the Swiss Alps. *Annals of Glaciology*, 54 (63): 241–253. doi: 10.3189/2013AoG63A400

For large-scale scenarios of the glacier contribution to sea-level rise or to the regional hydrological cycle, a variety of simplified but robust and transparent approaches were applied to consider future glacier evolution. The input data, the modeling approach and the climate forcing differ but the overall goal is rather similar: to consider future area and/or volume changes of glaciers. This study presents a comparison of three contrasting approaches with different levels of complexity, but all working at a regional scale to model the geometric evolution of glaciers. Two of these models are applied to all Swiss glaciers, whereas the third one is restricted to 101 selected larger glaciers.

The underlying climate scenarios are based on RCM simulations from the *ENSEMBLES* project and the A1B emission scenario, but are differently implemented in each of the models. Considering temperature development only, all three moderate model scenarios use the same +2 °C temperature increase until the first scenario period (2020–2050) and +4 °C increase for the second period (2070–2100). For all three models the initial glacier extent and DEM used relate to the 1980s.

The first model (M1) provides future glacier area only and is based on an adjustment of the hypsometric area distribution following an upward shift of the ELA (150 m per °C) according to three different scenarios of temperature increase (high, moderate and low). For simplicity, a constant 50-year response time for all glaciers is implemented to make the model time dependent and glaciers are reacting retrospectively, i.e. to a forcing that has taken place in the past.

The second model (M2) uses the modeled ice thickness distribution provided by GlabTop in combination with observed elevation changes (*Paul and Haeberli*, 2008) for an extrapolation of the elevation-dependent thickness change into the future assuming a constant trend. The observed thickness loss is related to a 1 °C temperature increase and a time period of 20, 25 and 30 years. These trends are assumed to continue into the future (linear extrapolation).

The last model (M3), is based on a distributed glacier mass balance model that is directly forced with gridded, downscaled and de-biased RCM data (considering temperature, precipitation, and cloudiness). Glacier retreat is simulated based on modeled mass balance and the so-called Δh approach developed by *Huss et al.* (2010b).

The comparison of these three models confirm a general trend: a strong to almost complete loss of glaciers by the end of the 21st century. Glaciers will only remain at the highest of elevations and the relative area loss considering the moderate scenarios is between 60 to 80% compared to the initial glacier extent in the 1980s and probably represents a lower bound estimate.

Furthermore, uncertainties from the ice thickness estimation ($\pm$30%) and the variability in the climate scenarios are investigated. The former directly impacts on the time scale of the modeled future glacier development, but the spread of the final glacier volumes due to this uncertainty range is smaller (20%) than the one resulting from the climate scenario variability (40%). Therefore, it is concluded that the uncertainties in the climate models have a stronger influence on future glacier evolution than the chosen glacier retreat model. All three model approaches lead to quite similar results with respect to the long-term evolution of large glacier samples at regional scale.

6 Discussion

In this chapter, the findings of the research papers (chapter 5) are put in context and discussed in view of previous studies and the current state of the art as presented in chapters 2 to 4. First, in section 6.1 the GlabTop model evaluation is extended with unpublished material. Section 6.2 analyses the storage of the large ice masses within glaciers. In section 6.3 the focus is on the detected overdeepenings, the sites of potential future lake formation. Finally, in section 6.4 the future glacier evolution of models applicable at regional scales are discussed.

6.1 GlabTop model evaluation

The performance of the GlabTop model was already evaluated in ***Paper III*** by a comparison with GPR profiles, by testing the uncertainties in input parameters and by model intercomparison. While absolute values of ice thickness estimates are still affected by a relatively large uncertainty range (±30% on average and even more in individual cases and locally), relative spatial patterns of modeled glacier-bed topography primarily depend on surface slope as given by the DEMs and are therefore quite robust.

6.1.1 Comparison with ITEM

In ***Paper III***, the GlabTop model results were compared to GPR-profiles of the three glaciers Rhone, Zinal and Corbassière. At these profiles and along the glaciers central flowlines the results as modeled with ITEM (*Farinotti et al.*, 2009a,b) can be compared to the GlabTop results (Fig. 6.1).

The comparison of the profiles reveals that GlabTop and ITEM reproduce the parabolic shape of glacier beds in good agreement with the radar measurements. At most profiles the measured values are within the uncertainty range of ±30% from the GlabTop model. At two profiles of Rhone glacier (b, c) the measured ice thickness is much larger than the modeled one. Both GlabTop and ITEM are not cabable to reproduce these large thickness values. Whereas at Zinal glacier GlabTop rather underestimates the ice thickness at certain profiles compared to the GPR-measurements, at Corbassière glacier ITEM overestimates the depths. For Corbassière and Zinal glacier GlabTop is actually often closer to the GPR measurements than ITEM. This is also visible from the profiles along the central flow lines of the glaciers.

Compared to GlabTop, the ice volume estimates with ITEM are about 20–30% higher for individual, and about 10% higher for the sample of all Swiss glaciers (whereby in the study of *Farinotti et al.* (2009a) ITEM was applied to 62 glaciers and the rest of the sample of the Swiss glaciers was estimated by a scaling relation), probably due to the stronger smoothing of ITEM and higher basal shear stresses. Nevertheless, the overall structure of the ice thickness distribution is rather similar in both studies and the found values are in the range of the expected uncertainties.

Both models also show very similar curves along the three long profiles (Fig. 6.1). Overdeepenings can be found at more or less the same locations indicating robustness of the methods in modeling the general patterns of glacier beds, but the stronger smoothing of the applied TopoToRaster-interpolation (compared to the IDW-algorithmn, cf. ***Paper III***) is also visible. Therewith, the mean ice thickness and volume becomes slightly higher and the number of modeled overdeepenings is smaller (for all Swiss glacier between 400–500 overdeepenings resulted with the TopoToRaster-interpolation, compared to 500–600 sites with the IDW-interpolation), but their locations remain unchanged.

The main conclusions from this comparison are:

1. The modeled general pattern of the glacier bed topography is robust.

2. The local uncertainties of ice thickness estimates are large (±30%) and are difficult to overcome with both approaches, also because parameters of ice flow are difficult to quantify.

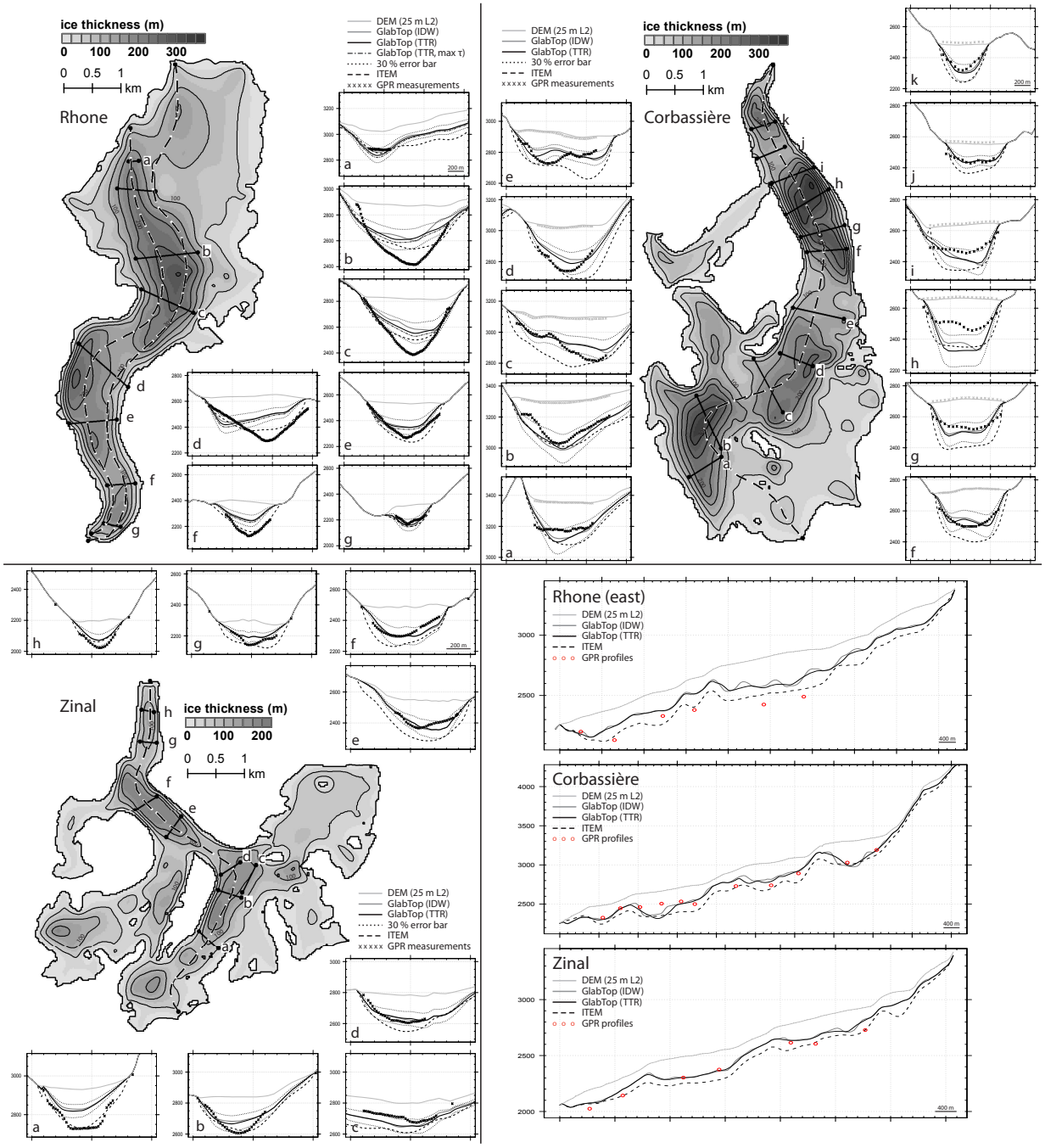

Figure 6.1: *Modeled ice thickness distribution with GlabTop for the three glaciers Rhone, Corbassière and Zinal within their extent from 1999. The black solid lines marked with letters denote the location of the measured GPR profiles and the dashed lines the central flowlines. The small graphs depict the profiles at the GPR measurements and the three graphs on the bottom right the profiles along the central flowlines. (source:* Linsbauer et al., *2012a)*

3. The results from GlabTop and ITEM deviate from the GPR measurements within the range of expected uncertainties.

4. Both approaches match to the GPR measurements similarly well.

5. The modeled ice thicknesses of individual glaciers are about 20–30% higher with ITEM than with GlabTop.

6.1.2 Sensitivity Tests on the Input Data

One of the advantages of GlabTop is that the model runs with sparse input data: a DEM, glacier outlines and a set of digitized branch lines (cf. ***Paper I***, ***II*** and ***III***). As GlabTop is designed to model the subglacial topography for large samples of glaciers, the application of the model to other mountain regions of the world is likely to provide promising results. Above all because the required input data is widely available. Digital glacier outlines exist for several other regions of the world in the GLIMS glacier database (*Raup et al.*, 2007) and the Randolph Glacier Inventory (RGI) (*Arendt et al.*, 2012) and with the SRTM DEM (*Farr et al.*, 2007) and ASTER GDEM (*Hayakawa et al.*, 2008) two DEMs with (nearly) global coverage are freely available (cf. section 4.1). The suitability of these DEMs for modeling ice thickness with GlabTop can thus be tested. Existing national DEMs might have a lower spatial resolution than the DHM25 used in this thesis. As the mean slope derived from the DEM is the most important parameter for estimating glacier thickness in GlabTop, the influence of a coarser DEM resolution (50 m) on the GlabTop output can be analyzed. Apart from the glacier outlines and the DEM, GlabTop also requires branch lines. The digitizing of theses lines is the most time-consuming part of the work in the pre-processing step. The glacier branch lines determine in which regions of the glacier the surface slope is averaged and thus, their position and number is likely to influence the model output.

The sensitivity tests described in the following have the goal to determine the change of the GlabTop output due to the variability of both input data sets, DEM and digitized branch lines.

Data

In Figure 6.2 the baseline data and the derived model output for the reference model run (hereafter REFrun) for the sensitivity tests as used at Morteratsch glacier are shown. For this purpose an 8 by 6 km subset from the DHM25L1 (`DEM_ref`), the glacier outlines from 1973, and the digitized branch lines (`bl73_ref`) from ***Paper II*** were selected.

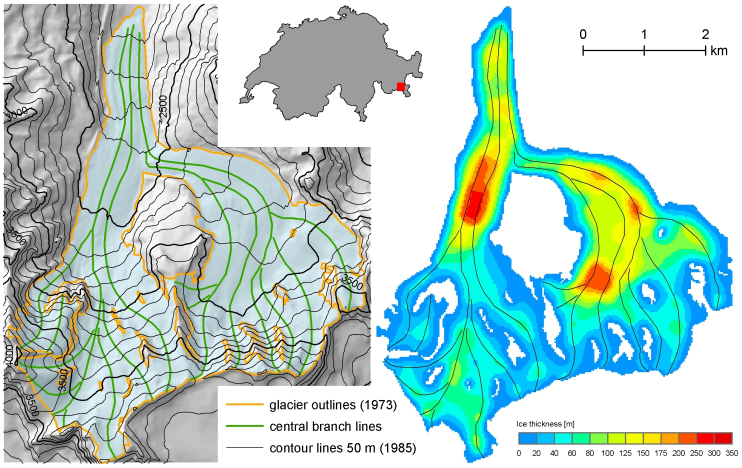

Figure 6.2: *(a) Input data: DEM, glacier outline and central branch lines, as used for the GlabTop reference model run (REFrun) for the sensitivity tests and (b) the corresponding modeled ice thickness distribution of Morteratsch glacier.*

For the DEM sensitivity tests, three further DEMs from two sources were applied: On the one hand, two versions of the SRTM DEM, with the data voids included and data voids filled by the *Reuter et al.* (2007) algorithm were used. On the other hand, the new ASTER GDEM with 30 m spatial resolution was used. All three DEMs were projected to the Swiss map projection (Oblique Transverse Mercator with Bessel Ellipsoid) using a bilinear resampling from their original resolution to 25 m. How the different DEMs influence the topographic characteristics of the glacier surface is discussed in *Frey and Paul* (2012).

Methods

To test the sensitivity of the DEMs, GlabTop was run with eight different DEM versions. At first, the `DEM_ref` was resampled to a resolution of 50 m with three standard resampling methods (cubic, bilinear, nearest neighbor), which resulted in three versions. Moreover the `DEM_ref` was smoothed with two different filters (low pass filter, Gauss filter), which gives two additional DEMs. Three further DEMs come from ASTER and SRTM.

The sensitivity of the branch lines is tested with five variations of the `bl73_ref` dataset. The first variation includes a single additional branch line and in the second version two branch lines are removed. A further data set uses a maximum number of branch lines that are snapped to each other and joined with the outline. The fourth and fifth versions consist of branch line numbers between the minimum and the maximum and one version with the lines snapped to each other.

For the obtained ice thickness distributions of each model run, difference-grids to the REFrun (Fig. 6.2b) were computed. These were then colour-coded in steps of one standard deviation (SD) around the mean to visualize the sensitivity of the model on the input data and to quantify the deviations in the calculated mean glacier thickness.

Results

The difference grids obtained with five of the eight DEMs are illustrated in Figure 6.3 and the volume (V), maximum (h_{max}) and mean thickness (h_{mean}) and their differences ($\Delta V, \Delta h_{max}$ and Δh_{mean}) to the REFrun are listed in Table 6.1. The tests with the two filtered DEMs (Fig. 6.3a/b) revealed a very similar pattern of differences, though the overdeepenings tended to be somewhat (up to 20 m) deeper than in the REFrun and there was less ice at the confluence of the Pers and Morteratsch glaciers. The minimum and maximum deviations are both around 20 m and are thus rather small. The smoothing of the DEMs also had an effect on the derived slope grids which are now more generalized and thus less susceptible to extreme values. Hence, in flat parts the mean slope is smaller and the ice is getting thicker, which results in a slightly larger mean ice thickness and glacier volume (both +2%).

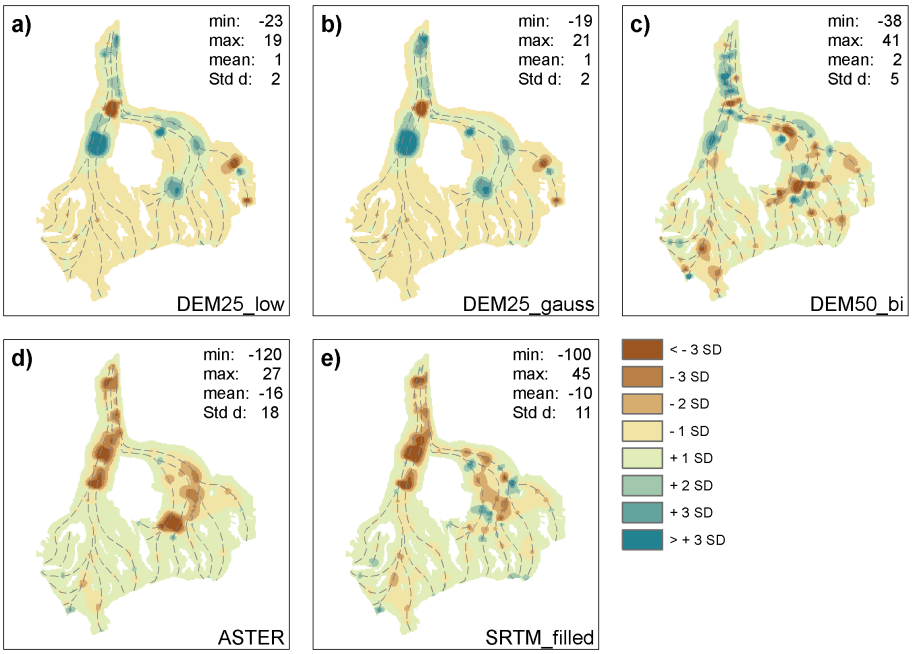

Figure 6.3: *Results of the sensitivity tests with all DEMs shown as the difference between the reference run and the respective sensitivity test in steps of 1 standard deviation (SD). Positive SDs indicate thicker values in the reference run.*

Table 6.1: *Three selected values (maximum (h_{max}) and mean ice thickness (h_{mean}) and total ice volume (V) of the Morteratsch glacier derived from the ice thickness distribution of the sensitivity tests with 8 different DEMs and 5 different versions of central branch lines. Additionally listed are the differences in percent to the reference model run which is given in the first row*

Fig.	Version	$h_{max}(m)$	$\Delta h_{max}(\%)$	$h_{mean}(m)$	$\Delta h_{mean}(\%)$	$V(km^3)$	$\Delta V(\%)$
6.2 b	REFrun	268		61		1.024	
6.3 a	DEM25_low	287	+7	62	+2	1.039	+2
b	DEM25_gauss	289	+8	62	+2	1.042	+2
-	DEM50_cu	276	+3	60	-1	1.016	-1
c	DEM50_bi	276	+3	60	-1	1.016	-1
-	DEM50_nn	272	+2	60	-1	1.011	-1
d	ASTER	210	-21	44	-27	0.747	-27
e	SRTM_voids	246	-8	48	-20	0.814	-21
-	SRTM_filled	240	-10	50	-17	0.849	-17
6.4 a	cbl_1973_plus1	268	0	62	+2	1.047	+2
b	bl73_minus2	268	0	60	-1	1.017	-1
c	bl73_max	261	-2	71	+16	1.191	+16
d	bl73_mid	269	+1	67	+10	1.126	+10
e	bl73_mid_snap	269	+1	67	+11	1.134	+11

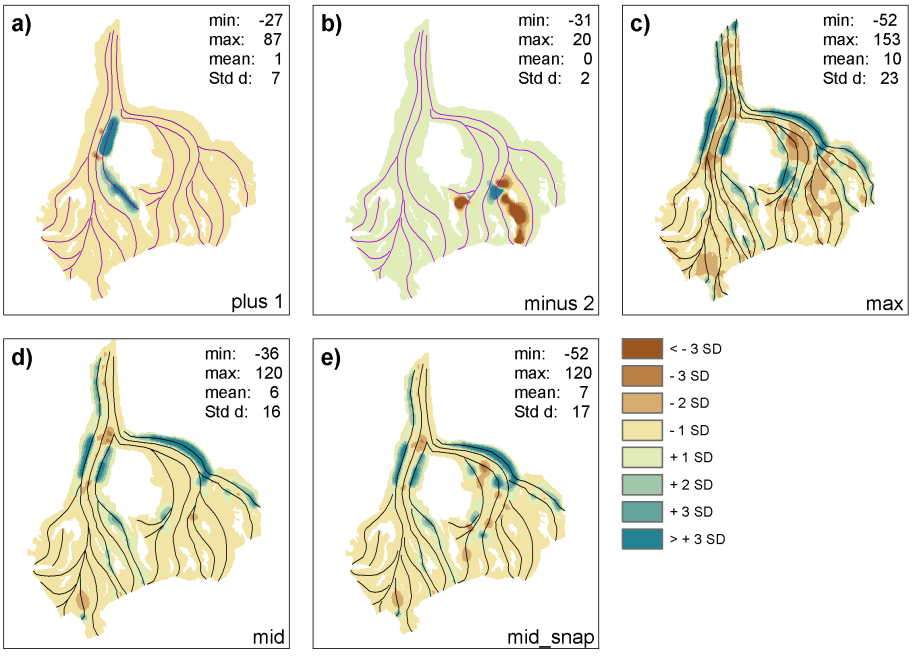

Figure 6.4: *Results of the sensitivity tests with all branch lines shown as the difference between the reference run and the respective sensitivity test in steps of 1 standard deviation (SD). Positive SDs indicate thicker values in the reference run.*

There are minor variations between the results which were achieved with the DEMs resampled using three different methods. Therefore only one result is depicted (bilinear resampled) in Figure 6.3c. What is remarkable is the resulting highly variable pattern of positive and negative differences. There is no clear structure visible, indicating that the ice thickness is locally over- or underestimated compared to the REFrun. The deviations of $\pm$40 m lie in a medium range and cancel each other out in the mean (Table 6.1).

The test with the ASTER GDEM and the SRTM DEMs confirm that both suffer from local artifacts, in particular in the flat glacier parts where the surface is not as smooth as in the DHM25. Hence, ice thickness is underestimated due to locally higher mean slope values. This observation is confirmed by differences of up to 120 and 100 m and is also expressed in a mean ice thickness and volume that lies between 20% and 30% under the values of the REFrun. Using the SRTM DEM with filled data voids creates a small change in both directions and gives somewhat better results.

As the empirical tests in ***Paper II*** have shown, the central branch lines used in the REFrun represent a minimum of lines to model the bed of the Morteratsch glacier. In Figure 6.4a–f, the sensitivity to variations in the number and position of branch lines are shown (cf. Table 6.1 for differences).

The additional branch line considered for the model run shown in Figure 6.4a resulted in thicker ice at this location, in particular at the flat part before the confluence with the Pers glacier. Overall, the mean ice thickness and the total glacier volume are 2% larger than in the REFrun (Table 6.1).

When branch lines are removed (Fig. 6.4b), the modeled ice thickness is smaller, apart from the location where the deleted branch line was previously connected with another branch line, where the ice is thicker now. Overall the effect on the mean thickness and volume is small (-1%). With the maximum number of branch lines displayed in Figure 6.4c, the main pattern shows more ice at the glacier margins and less ice in the inner parts of the polygon. Mean ice thickness and total volume increased by 16% compared to the REFrun and the standard deviation ($\pm 23\ m$) is quite high.

With the intermediate branch line data sets (Fig. 6.4d/e), rather than getting deeper, the main overdeepening of the Morteratsch glacier becomes wider. The additional branch line at the orographic right side of the Pers glacier had an increase in ice thickness at the glacier margin resulting in a higher mean thickness and total (+10%).

Discussion

The sensitivity tests with different filtering, resolutions, and DEM sources revealed that surface smoothing yields higher thickness values. Furthermore, a decreased spatial

resolution has only local effects but not in the mean, and DEMs from SRTM and ASTER can also be applied when artifacts are corrected during pre-processing. These artifacts in the DEM cause much higher slope values locally and thus a strong underestimation of the ice thickness.

With the digitizing rules described in ***Paper I***, probably the best result is achieved. There is some flexibility in drawing these lines as they only need to cover all important branches and surround rock-outcrops. As a general rule, we found that the branch lines near the glacier margins function more sensitively than those in the middle. As an overall assessment based on the volume differences for the experiments as listed in Table 6.1, we estimate the uncertainty resulting from inaccuracies of the input data sets to be around $\pm 10\%$.

6.2 Spatial distribution of the ice volume

The analysis of ***Paper III*** revealed that about 80% of the glacierized area is less than 100 m thick and contributes not even half of the total ice volume of all Swiss glaciers with about half of the ice volume being stored in the 15 largest glaciers. The areas with the thickest ice (thickness >100 m) are thus highly relevant for the total and are located in the flat tongues of the largest glaciers. Figure 6.5 illustrates this for the Aletsch region with the modeled ice thickness distribution being compared to the elvation of the glacier beds. The ice of the thick tongues rests on bedrock at low elevations with altitudes even below 2000 m a.s.l. (e.g. Aletsch, Fiescher, Unteraar glacier). Hence the majority of ice from the largest glaciers is located in comparably flat tongues on weakly inclined beds at low elevations.

In Figure 2.3 three different types of valley glaciers are sketched to depict where the main part of the ice volume of glaciers can be found. The profiles of surface and bedrock elevation along the central flow line of Oberaletsch, Findelen and Mont Miné glacier illustrate this theoretical consideration (Fig. 6.6). In regard to Figure 2.3 the Oberaltesch glacier clearly belongs to type a); the thickest ice and the main part of the ice volume is found at low elevations and on a weakly inclined bed. The slope of Findelen glacier is over its entire elevation range sort of equally distributed, along with the ice thickness and ice volume (type b). Mont Miné glacier shows a flat and wide accumulation area and the main part of the glacier volume is located at high altitudes (type c). This glaciers has a comparably steep and thus thin tongue.

For a more in-depth analysis, a total of 20 larger valley glaciers were selected and profiles of surface and bedrock elevations extracted (Fig. 6.7). These profiles confirm that for many glaciers the thickest ice is found in the glacier tongues. Eleven glaciers belong

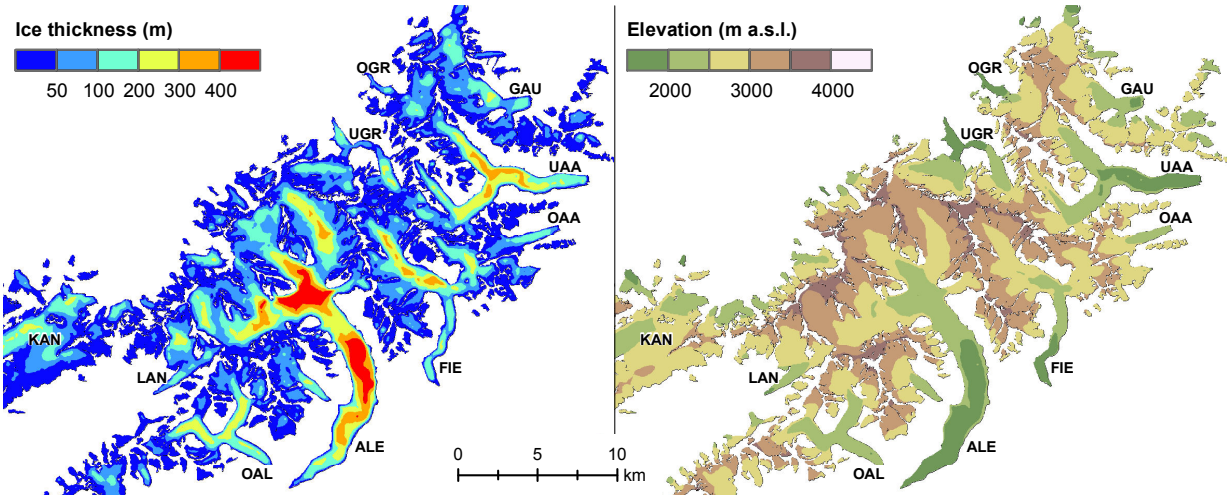

Figure 6.5: *Ice thickness distribution and bed topography for all glaciers in the Aletsch region as modeled by GlabTop according to* Linsbauer et al. *(2012b) referring to the 1973 outlines and the DEM from about 1985. Abbreviations refer to the following glaciers: UGR: Unterer Grindelwald, OGR: Oberer Grindelwald, GAU: Gauli, UAA: Unteraar, OAA: Oberaar, FIE: Fiescher, ALE: Grosser Aletsch, OAL: Oberaletsch, LAN: Lang and KAN: Kanderfirn.*

to type a) and have stored the main part of the volume in the tongues at low elevations. Four glaciers belong to type b) with no general preference of where the major part of the volume is stored. Five glaciers fit to type c) and show flat accumulation areas at high altitude and steep and thin tongues.

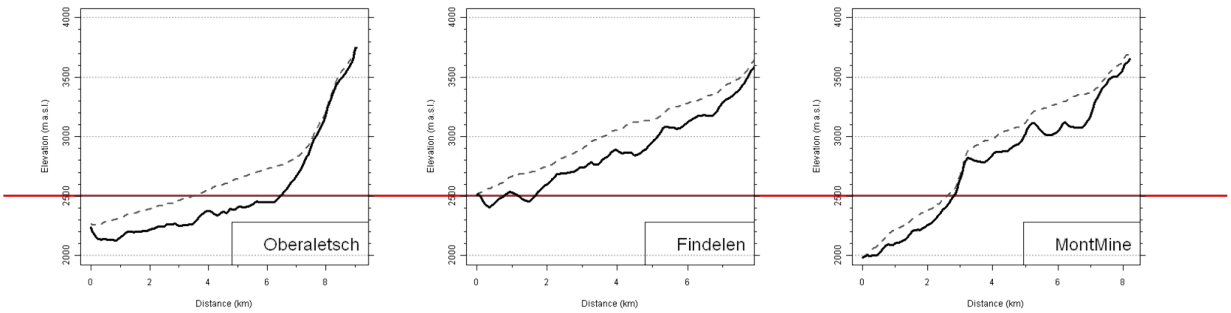

Figure 6.6: *Profiles of surface and bedrock elevation along the central flow line of Oberaletsch, Findelen and Mont Miné glacier to illustrate the theoretical consideration of Figure 2.3.*

This insight has important consequences for future glacier evolution. As large glaciers have response times of several decades (*Haeberli and Hoelzle*, 1995), they are still reacting to an air temperature increase which happened in the past. They are far away from an equilibrium and have to adjust their area by further retreat. However, equilibrium is

difficult to reach as the climate is in constant change and glaciers continuously adjust their extents to new climatic conditions depending on their specific geometry and response times. This implies that a rising snow line on glaciers with a flat ablation area has stronger consequences than for steep ablation area. On a flat tongue much more area is exposed to melt following a rise in ELA. Furthermore, due to the low mean slopes of the bedrock of type a) glaciers, a retreat of their terminus to higher elevations is hardly possible without loosing the main part of the ice volume.

In contrast, type c) glaciers with a wide and flat (and thus thick) accumulation area do not lose their main volume. They will become increasingly important with their ice reserves, when most of the flat, low-altitude tongues have already disappeared.

6.3 Overdeepenings – potential future lakes

The erosive power of glaciers can form large depressions at the bed and when such overdeepend parts are exposed due to glacier retreat and filled with water, rather than sediments, new lakes can form (*Clague and Evans*, 1994, *Haeberli et al.*, 2010). Hence, by detecting overdeepenings in the glacier bed, sites of potential future lake formation can be identified. As the glacier surface topography can be seen as a smoothed image of the underlying bed (*Oerlemans*, 2001), surface slope is a key factor in determining ice thickness variability (***Paper II***) and detecting such overdeepenings (*Frey et al.*, 2010).

Frey et al. (2010) presented a multi-level strategy for the identification of overdeepened parts of glacier beds. The strategy aims to cover large regions efficiently with low effort and then to apply more sophisticated and detailed approaches to focus on regions of particular interest. At all levels, overdeepenings were detected based on the geometry and characteristics of glacier surface topography. On the first level, a slope threshold of $< 5^\circ$ is applied. On the second level, the changes in surface slope, glacier width and crevasse patterns are evaluated. On Level 3, models to estimate ice-thickness distribution and bed topography are used. Finally, on Level 4, in-situ field measurements to obtain detailed, site-specific information are proposed.

Models like GlabTop are in the third level of this strategy and can be used to provide more quantitative information than in level 1 and 2. One of the results from ***Paper III*** is a quantification of all modeled overdeepenings under the Swiss glaciers. All sites were roughly classified according to their volume and time of appearance (Fig. 6.8). In total 500–600 overdeepneings with an area of 50–60 km^2 were found in still glacierized regions. The total volume of these potential lakes is about 2 km^3, i.e. about 3% of the remaining glacier volume. Most of these overdeepenings are less than 50 m deep, but some large ones have a mean depth of about 100 m. The largest overdeepenings

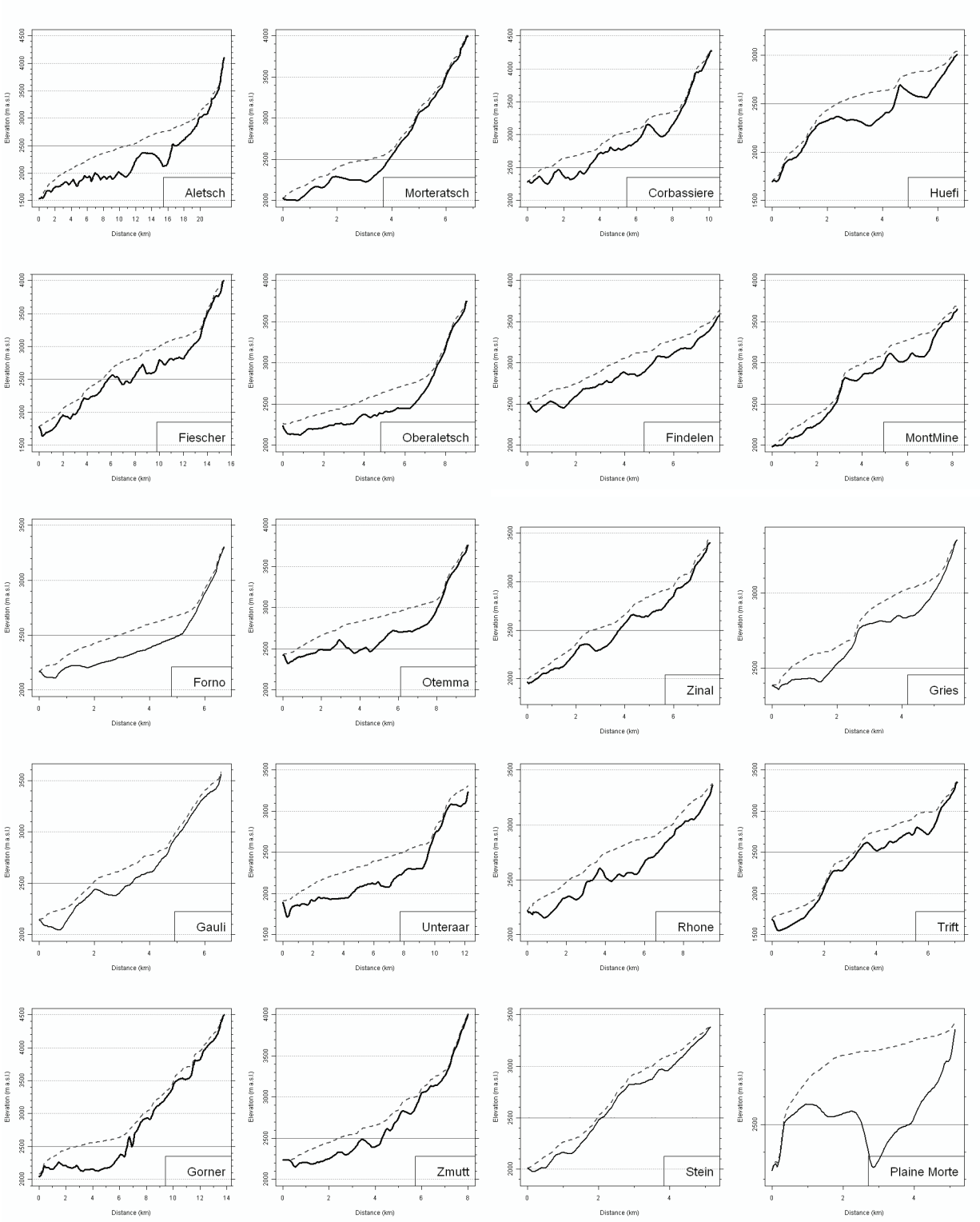

Figure 6.7: *Collection of profiles of surface and bedrock elevation along the central flow line of 20 larger valley glaciers.*

with volumes larger than 50 million m^3 are expected at Aletsch, Gorner, Otemma, Corbassière, Gauli and Plaine Morte glaciers. In the karst area of Plaine Morte a lake formation is doubtful, though (*Haeberli et al.*, 2012).

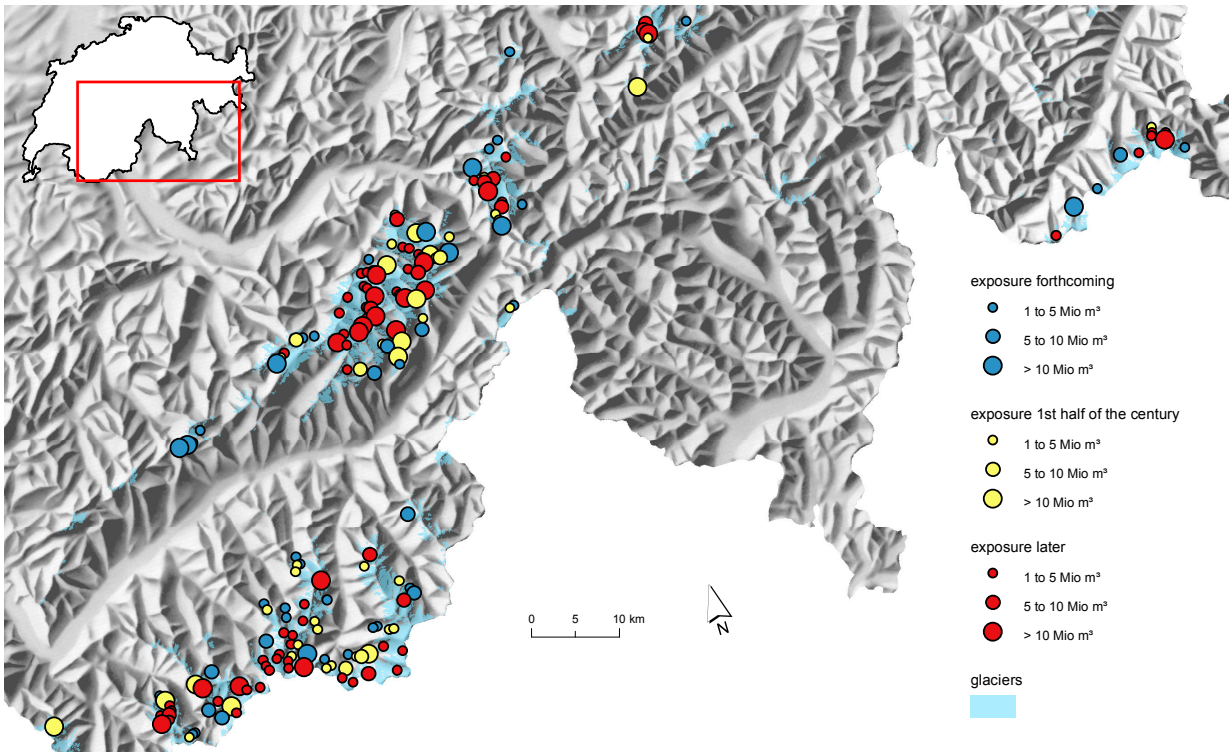

Figure 6.8: *Modeled overdeepenings (sites of potential lake formation) in the glacier beds of the Swiss Alps. The overdeepenings are classified according to their volume and time of appearance/exposure. Overdeepenings smaller than 1 million m^3 are not shown. (Fig. after* Haeberli et al., *2012)*

Within the next decades the formation of new lakes in deglaciated regions can be expected. Such lakes can become an attractive element in a high-mountain region and thus compensate the loss of attractiveness due to glacier disappearance to a certain degree (*Haeberli and Hohmann*, 2008). But these lakes also constitute a serious hazard potential as they form in an increasingly destabilized environment (*Künzler et al.*, 2010, *Schaub et al.*, 2013). On the other hand, they are of high interest for hydro-power production (*Terrier et al.*, 2011) and tourism (*Müller et al.*, 2012).

Based on the modeling results from ***Paper III***, the research project NELAK (New lakes in deglaciating high-mountain areas: climate-related development and challenges for sustainable use) – in the framework of the Swiss National Research Programme "Sustainable Water Management" (NRP 61) – was set up. This project investigated the questions where and when new lakes are likely to form, what their characteristics are (depth, vol-

ume, moraine/bedrock) and how the related potentials and risks can best be assessed and managed in an integrative way (*Haeberli et al.*, 2013).

A range of glacierized regions are located within the perimeter of protected areas. Such new lakes will likely be between the conflicting priorities of utilization (e.g. for hydro-power) and protection (e.g. for environmental protection). This pertains above all for combined projects related to flood protection, hydro power, water supply and tourism (*Haeberli et al.*, 2013). As an example, Figure 6.9 shows the Mattmark region without glaciers and their modeled overdeepenings filled with water. At the current terminus of Allalin glacier a lake will likely form behind a rocky barrier within the next decades. This lake possibly can be used for hydro-power production, as a retention basin, or as a reservoir for artificial snow production (*Haeberli et al.*, 2012).

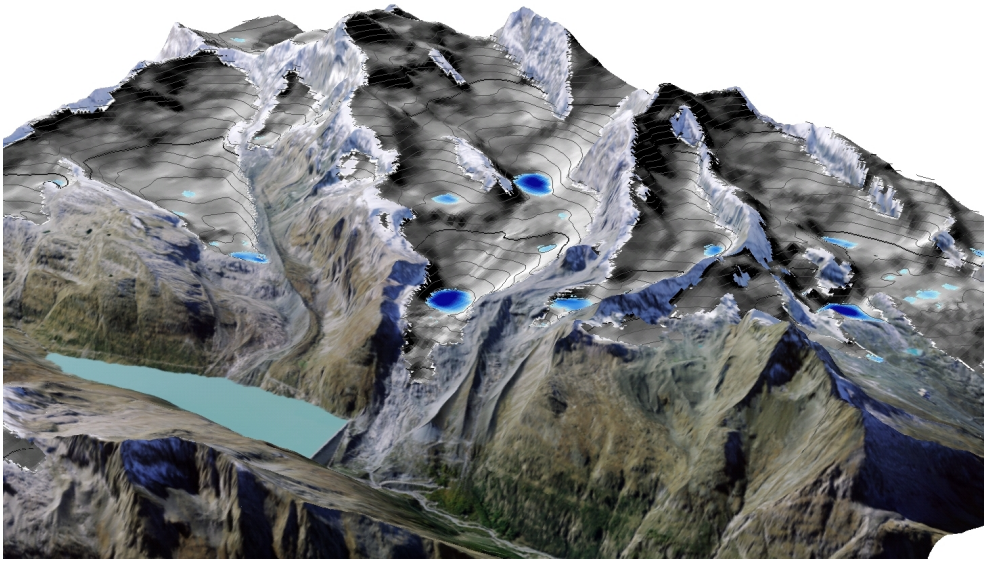

Figure 6.9: *The Mattmark region without glaciers; the contemporary glacierization is replaced by the modeled glacier bed topographies and the corresponding overdeepenings (potential future lakes). In the middle of the picture the bed of Allalin glacier with two larger overdeepenings is displayed.*

6.4 Future glacier evolution

As described in section 2.4.4 and in ***Paper IV***, a variety of approaches were applied to model future glacier evolution. All these models can be located in the range of model complexity and application scale (Fig. 2.11). Independently, the overall trends of the modeled future glacier evolution are clear and robust: a strong to almost complete loss

of glaciers in the Alps by the end of the 21^{st} century can be expected (e.g., *Zemp et al.*, 2006, *Paul et al.*, 2007b, *Radic and Hock*, 2011, *Huss*, 2012, ***Paper IV***), with air temperatures further increasing (cf. section 3). A short summary of findings in these studies are given in the following:

- *Zemp et al.* (2006) applied an integrated approach, combining in-situ measurements, remote sensing and numerical modeling to the European Alps to determine the past and future evolution of glaciers. Thereby, they showed that a 3 °C warming of summer air temperature within this century would reduce the Alpine glacier cover by about 80% and in the event of a 5 °C temperature increase the Alps would become almost completely ice-free.

- *Paul et al.* (2007b) applied an ELA-shift approach to the Swiss Alps resulting in new balanced-budgets ELAs and new glacier geometries according to given climate change scenarios (cf. ***Paper IV***). If an ELA-shift of +600 m due to a temperature increase of about 4 °C is assumed, the area of the Swiss glaciers will be reduced by about 86–95% and the volume by about 85–96% after full adjustment according to this study.

- *Radic and Hock* (2011) used multi-model projections to estimate and upscale the contribution of all mountain glaciers and ice caps to future sea-level rise with a regional differentiation. They found that the volume change (from initial volume in 2000) is largest in the European Alps with a reduction of 75±15% by 2100.

- *Huss* (2012) extrapolated the mass balance measurements of individual glaciers to the mountain range scale of the European Alps for the period 1900–2100. His model results indicate a glacier area reduction of 82–96% by 2100 relative to 2003.

All listed studies are based on different assumptions and models, but strongly support a strong reduction of glacier area (of about 80%) and volume in the Alps found also in ***Paper IV***. Though full geometric adjustment might not have taken place by 2100 in all studies, there is clear evidence that most of the glacier ice in the Alps (>80%) will finaly disappear for a 3–4 °C warming.

In discussions about strategies to limit the impacts of climatic change, politicians are focusing on a "2 °C temperature target", as the maximum allowable warming above preindustrial level to avoid dangerous anthropogenic interference in the climate (e.g., *Meinshausen et al.*, 2009, *UNFCCC*, 2009). Even such a modest warming above preindustrial level translates to a temperature increase beyond 2 °C in more continental regions such as the Alps and a related increase of the ELA by up to +600 m *Paul et al.* (2007b).

Salzmann et al. (2012) have shown the impact of the "2 °C temperature target" for the glaciers in the Swiss Alps. The model and climate data used in this study are the same as applied by method M3 in ***Paper IV***. The global 2 °C temperature target was defined to be a +2.5 °C temperature increase in the Alps reached around 2030, 2045 or 2055 (depending on the ensemble). The study showed that after a significant decrease of glacier extent and volume until the middle of this century both begin to stabilize around 2100 at about 20% for volume and at about 35% for area, relative to the values of the year 2000. Mean mass balance shows an increase after 2055, i.e. the ELA is shifted upwards mainly during the first half of the 21^{st} century and remains relativly stable afterwards. In contrast to the mean values, the high range of size and slope dependent glacier response times became also evident from this modeling experiment.

The moderate scenarios, used in ***Paper IV*** and also in *Salzmann et al.* (2012), work with an increase in air temperature of +2/+4 °C concerning two scenario periods centered around 2035 and 2085. So probably these scenarios are too low for the Alps and a stronger increase in air temperature must be expected. As the validation in ***Paper IV*** for the short period form 1970–2000 has shown, the modeled glacier terminus retreat is too slow. Hence, the modeled future development in glacier extent with the moderate scenarios can be seen as lower bound estimates.

7 Conclusions and perspectives

In the first section of this chapter the major findings of the research questions and papers are summarized. Overall conclusions are drawn in section 7.2 and finally an outlook on the outreach of this thesis and on ongoing as well as potential future research is given in section 7.3.

7.1 Major findings

The major findings are condensed and organized according to the research questions formulated in section 1.2. More details can be found in the full versions of the research papers in Part II of the thesis.

(**1**) ***What is the total volume of the glaciers in Switzerland and how is the ice thickness spatially distributed?***

- The total ice volume for all Swiss glaciers derived by GlabTop is about 75±22 km^3 for 1973 and 65±20 km^3 in 1999; differences to other independent estimates remain within the uncertainty range of ±30%.

- Ice thicknesses of less than 100 m are dominant; over 60% of the glacierized area (about 1300 km^2 in 1973) ice is less than 50 m and over another 20% between 50 and 100 m thick.
- About a quarter of the total volume is related to a small area (5%; 60–70 km^2) with ice thickness values exceeding 200 m.
- Overall, the 3, 6 and 15 largest glaciers contain $1/4$, $1/3$ and $1/2$ of the total ice volume, respectively.
- The thickest ice (and thus their main volume) of the largest glaciers is often found in their comparably flat glacier tongues.

(**2**) ***What are the characteristics of the glacier bed topography and where are potential overdeepenings located?***

- A subtraction of the estimated ice thickness distribution from the surface DEM gives a modeled glacier bed topography.
- In regions with large ice thickness, the elevations of the glacier beds are comparably low. As the thickest ice is generally found in the flat and low-lying tongues of the largest glaciers, large parts of the modeled beds are even below 2300 m a.s.l.
- These beds are furthermore weakly inclined, which implies that the corresponding glaciers have limited possibilities to retreat to higher elevations with cooler conditions and may continue to shrink until reaching much steeper slopes. For these glaciers downwasting will be the dominant response to increasing temperatures.
- About 500–600 overdeepenings with a total area of 50–60 km^2 were found in currently still glacierized regions. Most of these overdeepenings are less than 50 m deep, but some large ones have a mean depth of about 100 m.
- The largest overdeepenings with volumes exceeding 50 million m^3 are expected to appear at Aletsch, Gorner, Otemma, Corbassiere and Gauli glacier.
- If, due to glacier retreat, such overdeepend parts are exposed and filled with water, rather than sediments, new lakes can form. Hence the detected overdeepenings in the glacier beds helps with identifying sites of potential future lake formation.

(**3**) ***How does climate change influence the future development of glacier area (and volume) on a regional scale and what are the uncertainties?***

- As air temperature will likely further increase in the future, a strong to almost complete loss of glaciers by the end of the 21st century can be expected in the Swiss Alps. This overall trend of the modeled future glacier evolution is clear and robust.
- According to the investigated three models, a relative area loss between 60 and 80% by 2100 would result compared to the glacier extent in 1985; in reality glacier vanishing could be even more rapid.
- Due to the simplifications made by the parameterization schemes in the models, uncertainties are large at a local scale (individual glaciers), but likely average out at the regional scale (Swiss Alps) and over extended time periods (decades to a century).
- The choice of climate scenarios produces the largest spread concerning the long-term evolution of the modeled glacier area by 2100 (about 60%), while the uncertainty in present-day ice-thickness estimation causes a spread of about 30%.

7.2 Conclusions

Figure 7.1 shows a graphical summary of the content and the research papers of the thesis. This Figure is based on Figure 1.1, where it served to illustrate the framework and the research questions of the thesis. Here, the peer-reviewed research papers are additionally integrated and show how they build up on each other.

The thesis has a focus on the glaciers in the Swiss Alps. At the example of this mountain range, simple but robust methods working on a regional scale were developed to estimate ice thickness distribution and glacier bed topographies, to detect overdeepenings and potential lake formation sites and to model future glacier evolution according to a given change in climate.

The basic input data of the models developed and applied in this thesis are DEMs and glacier outlines. The approaches used are fast and robust and are implemented in a GIS to run automatically. Both the GlabTop model and the glacier evolution models still have a considerable range of uncertainty, but also have proved to be useful for treating large samples of glaciers at a regional scale. Validation and comparison of the models showed that the results are in line with the numerous recent studies about future glacier evolution. Thus, if all involved uncertainties are considered and the models are applied to a large glacier sample, the results should be valid as a whole and produce a comprehensive overview of the current conditions and characteristics of glaciers, as well as their potential future evolution.

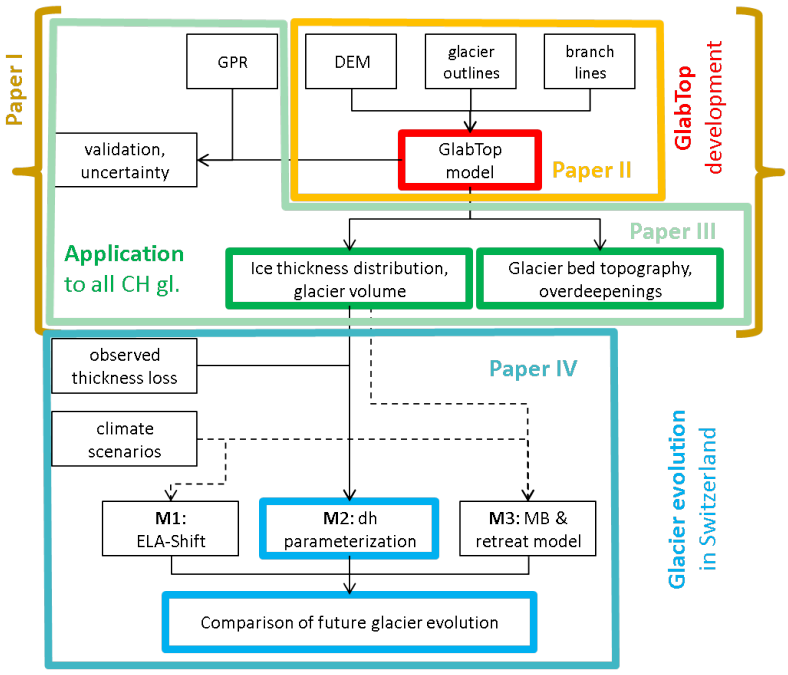

Figure 7.1: *Schematic overview of the elements of this thesis and their connections and relations as well as the grouping of topics into different research papers.*

At a more local scale (individual glaciers), the modeled glacier beds, as well as future glacier evolution, can have high uncertainties. Although deriving results for individual glaciers is easy as they are explicitly modeled, an interpretation of the results must be performed carefully. The model results can locally have large uncertainties, but nevertheless provide a first insight in ice thickness distribution and glacier evolution. When analyzed with the required care, the presented approaches can be used to anticipate potential future situations in advance.

7.3 Outreach and perspectives

As the knowledge of ice thickness distribution and glacier evolution is becoming increasingly important, and DEMs (section 4.1.1) as well as glacier outline data (section 4.1.3) are widely available, the application of the used approaches to other regions of the world is promising. The models and data produced within this thesis were already used in other studies in different regions. From the wide range of possibilities, the following sections give examples on research topics that could be addressed in future.

7.3.1 Outreach: Further use of the models and results

This thesis was carried out within the framework of the two research projects *CCHydro* and *Climate change and hydropower* (presented in section 1.1) with a strong hydrological focus. The achieved work is indeed a small but important piece of the puzzle for the questions to be answered by the projects. Some of the hydrological model results (*SGHL and CHy*, 2011, *BAFU*, 2012, *Köplin et al.*, 2012, and related works) are based on the modeled ice thickness distribution and glacier bed topography from ***Paper III*** and the glacier evolution scenarios of M1 and M2 presented in ***Paper IV***.

As mentioned in section 6.3, the DEM of Switzerland without glaciers was the baseline input data for the research project NELAK (*Haeberli et al.*, 2013). Based on the dataset on detected overdeepenings in the glacier beds, NELAK evaluates where and when lakes are likely to form and how potential risks and changes can be managed. Related to this project some further studies were published using the original data from ***Paper III*** (*Künzler et al.*, 2010, *Serraino*, 2011, *Terrier et al.*, 2011, *Haeberli et al.*, 2012, *Schaub et al.*, 2013).

The Method M3 in ***Paper IV*** also uses the ice thickness estimates from GlabTop. M3 was also applied in the study of *Salzmann et al.* (2012) and *Machguth et al.* (2013) and shows the potential of the use of ice thickness estimates for future glacier evolution.

The sensitivity tests (section 6.1.2) have shown that the DEMs from SRTM and ASTER can be used as an input data set for the GlabTop model. If glacier outlines exist and the branch lines can be digitized, applying GlabTop in remote regions is definitely possible. For example, to derive ice volume and ice thickness distributions, GlabTop was applied to large glacier samples on the Tibetan Plateau (*Bolch et al.*, 2011), in the Tien Shan (*Ender*, 2011, *Bolch*, 2012), in the Himalayas (*Conijn*, 2012, *Frey et al.*, 2012, *Stephan*, 2012) and in the Stauning Alper in Greenland (*Machguth et al.*, 2013). For very few glaciers in these samples measurements could be used for validation confirming the GlabTop uncertainty range of $\pm 30\%$.

The focus of the modeling approaches in this thesis is on mountain glaciers, whereas ice caps are neglected. It is without doubt that also ice caps are important for future sea-level rise and their ice thickness distribution and volume is thus equally important. In the thesis of *Meister* (2010) the suitability of the GlabTop-approach was tested at the Jostedalsbreen in Norway, a complex ice cap with several outlet glaciers and a large set of ice thickness measurements being available for model validation. The GlabTop model was adjusted to include a further input data set: a variable, slope-dependent grid with three distinct values for the basal shear stress. With this modification the GlabTop model provided reasonable results also for an ice cap like Jostedalsbreen.

Results from a GlabTop model run were used to illustrate the third step in the multi-level strategy for the identification of overdeepened parts of glacier beds by *Frey et al.* (2010). The derived subglacial topography was also used to model the flow path of potential future lake outbursts. In the work of *Rüesch* (2013) the multi-level strategy is applied to the Swiss Alps and the Cordillera Blanca in the Peruvian Andes to validate the strategy (cf. also *Schneider et al.*, 2012).

Moll (2012) applied the approaches developed in this thesis on a very local scale at the Tiefen glacier in Switzerland. Even though the approaches are not developed for application on individual glaciers, the results turned out to be reasonable enough for a first picture of future development of this region.

7.3.2 Perspectives: possible future developments

In the studies mentioned above, GlabTop was applied to different regions of the world, as it is described in ***Paper II*** and applied as described in ***Paper III***. But so far no adjustment to regional glacier characteristics were implemented, this also means that the applied basal shear stress parameterization is the same as in equation 2.9 (*Haeberli and Hoelzle*, 1995). It could be worth to reconsider this parameterization for regional characteristics as the glaciers for instance in the Tien Shan do not behave the same as (late-glacial) glaciers found in the Central Alps and their climatic regime is also rather different (dry/continental). As a first step it would be interesting to derive an upper-bound value for basal shear stress which could be applied for the largest glaciers. It remains to be seen, if the approach of *Fischer* (2012), who modeled basal shear stress of now ice-free LIA glaciers in the Swiss Alps, is transferable to other mountain ranges.

Driedger and Kennard (1986), *Haeberli and Schweizer* (1988) and recently *Huss and Farinotti* (2012) have shown that basal shear stress values in glaciers are not uniform. Using a glacier specific mean value with an upper-bound for large glaciers as in GlabTop is not per-se wrong. However, it would be an improvement of the approach when a variable slope-dependent parameterization of basal shear stress could be implemented.

The most time consuming work in applying GlabTop to a large glacier sample is related to the digitizing of branch lines. Although *Le Bris and Paul* (2013) and *Machguth* (2012) presented approaches to automatically derive flow lines of a glacier, it is only a small part of all branch lines required for GlabTop. To avoid the laborious digitization *Machguth et al.* (2013) presented a method based on GlabTop that is calculating ice thicknesses for random glacier points (defined percentage of all glacier cells), instead of points along glacier branch lines. If the procedure is repeated a few times and averaged to a final result, the outcome is quite satisfying and comparable to the one obtained from GlabTop using the branch-line approach. The new approach was applied in the

work of *Frey et al.* (2013) for Himalayan glaciers and to the Stauning Alper in Greenland by *Machguth et al.* (2013).

A GlabTop model run detects by default potential overdeepenings in the modeled glacier bed, but does not determine the probability of lake formation. Modeling the glacial sediment balance (*Zemp et al.*, 2005) could provide information on this, but a careful analysis of potential future lake formation sites is required nevertheless. A validation of the individual sites is only possible when the glacier has disappeared (as for instance at the terminus of Rhone, Trift or Gauli glaciers).

Further tests in other regions will show if the methods from this thesis can be developed to a real global scale application and hence provide an important alternative to already existing modeling approaches.

Bibliography

Alean, J. (2010). *Gletscher der Alpen*. Haupt Verlag, Bern.

Andreassen, L. M., Paul, F., Kääb, A., and Hausberg, J. E. (2008). Landsat-derived glacier inventory for Jotunheimen, Norway, and deduced glacier changes since the 1930s. *The Cryosphere*, 2 (2): 131–145. doi: 10.5194/tc-2-131-2008.

Anonymus (1969). Mass-balance terms. *Journal of Glaciology*, 8 (52): 3–7.

Arendt, A., Bolch, T., Cogley, J., Gardner, A., Hagen, J.-O., Hock, R., Kaser, G., Pfeffer, W., Moholdt, G., Paul, F., Radic, V., Andreassen, L., Bajracharya, S., Beedle, M., Berthier, E., Bhambri, R., Bliss, A., Brown, I., Burgess, E., Burgess, D., Cawkwell, F., Chinn, T., Copland, L., Davies, B., de Angelis, H., Dolgova, E., Filbert, K., Forester, R., Fountain, A., Frey, H., Giffen, B., Glasser, N., Gurney, S., Hagg, W., Hall, D., Haritashya, U., Hartmann, G., Helm, C., Herreid, S., Howat, I., Kapustin, G., Khromova, T., Kienholz, C., Koenig, M., Kohler, J., Kriegel, D., Kutuzov, S., Lavrentiev, I., LeBris, R., Lund, J., Manley, W., Mayer, C., Miles, E., Li, X., Menounos, B., Mercer, A., Moelg, N., Mool, P., Nosenko, G., Negrete, A., Nuth, C., Pettersson, R., Racoviteanu, A., Ranzi, R., Rastner, P., Rau, F., Rich, J., Rott, H., Schneider, C., Seliverstov, Y., Sharp, M., Sigurdsson, O., Stokes, C., Wheate, R., Winsvold, S., Wolken, G., Wyatt, F., and Zheltyhina., N. (2012). Randolph glacier inventory [v2.0]: A dataset of global glacier outlines.

Arnold, N., Willis, I., Sharp, M., Richards, K., and Lawson, W. (1996). A distributed surface energy-balance model for a small valley glacier. I. development and testing for Haut Glacier d'Arolla, Valais, Switzerland. *Journal of Glaciology*, 42 (140): 77–89.

Auer, I., Böhm, R., Jurkovic, A., Lipa, W., Orlik, A., Potzmann, R., Schöner, W., Ungersböck, M., Matulla, C., Briffa, K., Jones, P., Efthymiadis, D., Brunetti, M., Nanni, T., Maugeri, M., Mercalli, L., Mestre, O., Moisselin, J.-M., Begert, M., Müller-Westermeier, G., Kveton, V., Bochnicek, O., Stastny, P., Lapin, M., Szalai, S., Szentimrey, T., Cegnar, T., Dolinar, M., Gajic-Capka, M., Zaninovic, K., Majstorovic, Z., and Nieplova, E. (2007). HISTALP – historical instrumental climatological surface time series of the Greater Alpine Region. *International Journal of Climatology*, 27 (1): 17–46.

doi: 10.1002/joc.1377.

BAFU (2012). *Auswirkungen der Klimaänderung auf Wasserressourcen und Gewässer. Synthesebericht zum Projekt "Klimaänderung und Hydrologie in der Schweiz" (CCHydro).*, vol. 1217. Bundesamt für Umwelt, Bern. Umwelt-Wissen.

Bahr, D. B., Meier, M. F., and Peckham, S. D. (1997). The physical basis of glacier volume-area scaling. *Journal of Geophysical Research*, 102 (B9): 20,355–20,362. doi: 199710.1029/97JB01696.

Bahr, D. B., Dyurgerov, M., and Meier, M. F. (2009). Sea-level rise from glaciers and ice caps: A lower bound. *Geophysical Research Letters*, 36 (3): L03501. doi: 10.1029/2008GL036309.

Baltsavias, E. P., Favey, E., Bauder, A., Bosch, H., and Pateraki, M. (2001). Digital surface modelling by airborne laser scanning and digital photogrammetry for glacier monitoring. *The Photogrammetric Record*, 17 (98): 243–273. doi: 10.1111/0031-868X.00182.

Bauder, A., Funk, M., and Gudmundsson, G. H. (2003). The ice-thickness distribution of Unteraargletscher, Switzerland. *Annals of Glaciology*, 37 (6): 331–336. doi: 10.3189/172756403781815852.

Baumann, S. and Winkler, S. (2010). Parameterization of glacier inventory data from Jotunheimen/Norway in comparison to the European Alps and the Southern Alps of New Zealand. *Erdkunde*, 64: 155–177.

Begert, M., Schlegel, T., and Kirchhofer, W. (2005). Homogeneous temperature and precipitation series of Switzerland from 1864 to 2000. *International Journal of Climatology*, 25 (1): 65–80. doi: 10.1002/joc.1118.

Beniston, M. (2005). Mountain climates and climatic change: An overview of processes focusing on the European Alps. *Pure and Applied Geophysics*, 162 (8): 1587–1606. doi: 10.1007/s00024-005-2684-9.

Benn, D. I. and Evans, D. J. A. (1998). *Glaciers and glaciation*. Arnold, London <etc.>.

Benn, D. I. and Hulton, N. R. (2010). An ExcelTM spreadsheet program for reconstructing the surface profile of former mountain glaciers and ice caps. *Computers & Geosciences*, 36 (5): 605–610. doi: 10.1016/j.cageo.2009.09.016.

Benz, C. (1995). Die Gletscher des Unterwallis (Hochstand 1850 – Ausdehnung heute – Schwundszenarien). Master's thesis, Geographisches Institut, Universität Zürich.

Binder, D., Brückl, E., Roch, K., Behm, M., Schöner, W., and Hynek, B. (2009). Determination of total ice volume and ice-thickness distribution of two glaciers in the Hohe Tauern region, Eastern Alps, from GPR data. *Annals of Glaciology*, 50 (51): 71–79(9).

Blindow, N., Salat, C., Gundelach, V., Buschmann, U., and Kahnt, W. (2011). Performance and calibration of the helicoper GPR system BGR-P30. In: *2011 6th Inter-*

national Workshop on Advanced Ground Penetrating Radar (IWAGPR), pp. 1–5. doi: 10.1109/IWAGPR.2011.5963896.

Bolch, T. (2012). Veränderung und Bedeutung der Gletscher als Wasserressource Hochasiens – eine multiskalige Analyse. Vortrag am 8.10.2012, Universität Augsburg.

Bolch, T., Chen, F., Wei, Y., Buchroithner, M., Kang, S., Linsbauer, A., Schneider, C., Scherer, D., and Yao, T. (2011). Past and future glacier changes in the western Nyainqentanglha Range on the Tibetan Plateau. In: *AGU Fall Meeting , 4.-9.12.2011, San Francisco, USA.*

Bosshard, T. (2012). Hydrological climate-impact modelling in the Rhine catchment down to Cologne. Ph.D. thesis, ETH Zurich. doi: dx.doi.org/10.3929/ethz-a-007316898.

Bosshard, T., Kotlarski, S., Ewen, T., and Schär, C. (2011a). Spectral representation of the annual cycle in the climate change signal. *Hydrology and Earth System Sciences*, 15 (9): 2777–2788. doi: 10.5194/hess-15-2777-2011.

Bosshard, T., Kotlarski, S., and Schär, C. (2011b). Lokale Klimaszenarien für die Klimaimpaktforschung in der Schweiz. *Wasser Energie Luft*, 4: 267–272.

Braithwaite, R. (1981). On glacier energy balance, ablation, and air temperature. *Journal of Glaciology*, 27 (97): 381–391.

Braithwaite, R. J. (1989). Calculation of glacier ablation from air temperature. In: *Glacier fluctuations and climatic change*, (edited by Oerlemans, J.). Dordrecht, Kluwer.

Braithwaite, R. J. and Zhang, Y. (2000). Sensitivity of mass balance of five Swiss glaciers to temperature changes assessed by tuning a degree-day model. *Journal of Glaciology*, 46 (152): 7–14. doi: 10.3189/172756500781833511.

Brock, B., Willis, I., Sharp, M., and Arnold, N. (2000). Modelling seasonal and spatial variations in the surface energy balance of Haut Glacier d'Arolla, Switzerland. *Annals of Glaciology*, 31: 53–62.

Burrough, P. and McDonnell, R. (1998). *Principles of Geographical Information Systems*. Oxford University Press, New York.

Carey, M. (2007). The history of ice: How glaciers became an endangered species. *Environmental History*, 12 (3): 497–527. doi: 10.1093/envhis/12.3.497.

Casty, C., Wanner, H., Luterbacher, J., Esper, J., and Böhm, R. (2005). Temperature and precipitation variability in the European Alps since 1500. *International Journal of Climatology*, 25 (14): 1855–1880. doi: 10.1002/joc.1216.

Ceppi, P., Scherrer, S. C., Fischer, A. M., and Appenzeller, C. (2012). Revisiting Swiss temperature trends 1959–2008. *International Journal of Climatology*, 32 (2): 203–213. doi: 10.1002/joc.2260.

CH2011 (2011). *Swiss Climate Change Scenarios CH2011*. C2SM, MeteoSwiss, ETH, NCCR Climate, and OcCC, Zurich, Switzerland.

Chen, J. and Ohmura, A. (1990). Estimation of Alpine glacier water resources and their change since the 1870s. In: *Hydrology in Mountainous Regions. I – Hydrological Measurements; the Water Cycle*, (edited by Lang, H. and Musy, A.), vol. 193 of *IAHS*. Proceedings of two Lausanne Symposia, August 1990.

Clague, J. and Evans, S. (1994). Formation and failure of natural dams in the Canadian Cordillera. *Geological Survey of Canada Bulletin*, 464: 35p.

Clarke, G. (1987). A short history of scientific investigations on glaciers. *Journal of Glaciology*, Special Issue: 4–24.

Clarke, G. K. C., Berthier, E., Schoof, C. G., and Jarosch, A. H. (2009). Neural networks applied to estimating subglacial topography and glacier volume. *Journal of Climate*. doi: 10.1175/2008JCLI2572.1.

Cogley, J., Hock, R., Rasmussen, L., Arendt, A., Bauder, A., Braithwaite, R., Jansson, P., Kaser, G., Möller, M., Nicholson, L., and Zemp, M. (2011). Glossary of glacier mass balance and related terms. IHP-VII Technical Documents in Hydrology No. 86, IACS Contribution No. 2, UNESCO-IHP, Paris.

Cogley, J. G. (1999). Effective sample size for glacier mass balance. *Geografiska Annaler: Series A, Physical Geography*, 81 (4): 497–507. doi: 10.1111/1468-0459.00079.

Cogley, J. G. (2009). A more complete version of the World Glacier Inventory. *Annals of Glaciology*, 50 (53): 32–38. doi: 10.3189/172756410790595859.

Cohen, D., Hooke, R. L., Iverson, N. R., and Kohler, J. (2000). Sliding of ice past an obstacle at Engabreen, Norway. *Journal of Glaciology*, 46 (155): 599–610. doi: 10.3189/172756500781832747.

Condom, T., Coudrain, A., Sicart, J. E., and Théry, S. (2007). Computation of the space and time evolution of equilibrium-line altitudes on Andean glaciers (10°N–55°S). *Global and Planetary Change*, 59 (1–4): 189–202. doi: 10.1016/j.gloplacha.2006.11.021.

Conijn, C. J. (2012). Glacier changes in the Kokshaal-Too, Central Asia. Master's thesis, Geographisches Institut, Universität Zürich.

Driedger, C. and Kennard, P. (1986). Glacier volume estimation on Cascade volcanos: an analysis and comparison with other methods. *Annals of Glaciology*, 8: 59–64.

Eineder, N. (2001). Interferometric DEMs in rugged terrain. In: *Geoscience and Remote Sensing Symposium, 2001. IGARSS '01. IEEE 2001 International*, vol. 5, pp. 2040 –2042. doi: 10.1109/IGARSS.2001.977896.

Ender, A. (2011). Glacier volume and mass balance in the Ala Archa National Park (Kyrgyz Ala-Too/Kyrgyzstan). Master's thesis, TU Dresden.

ESRI (2011). *ArcGIS Desktop: Release 10*. Environmental Systems Research Institute, Redlands, CA.

Etzelmüller, B. and Björnsson, H. (2000). Map analysis techniques for glaciological applications. *International Jounral of Geographical Information Science*, 14 (6): 567–581. doi: 10.1080/136588100415747.

Farinotti, D., Huss, M., Bauder, A., and Funk, M. (2009a). An estimate of the glacier ice volume in the Swiss Alps. *Global and Planetary Change*, 68 (3): 225–231. doi: 10.1016/j.gloplacha.2009.05.004.

Farinotti, D., Huss, M., Bauder, A., Funk, M., and Truffer, M. (2009b). A method to estimate the ice volume and ice-thickness distribution of alpine glaciers. *Journal of Glaciology*, 55: 422–430. doi: 10.3189/002214309788816759.

Farinotti, D., Usselmann, S., Huss, M., Bauder, A., and Funk, M. (2012). Runoff evolution in the Swiss Alps: projections for selected high-alpine catchments based on ENSEMBLES scenarios. *Hydrological Processes*, 26 (13): 1909–1924. doi: 10.1002/hyp.8276.

Farr, T. G., Rosen, P. A., Caro, E., Crippen, R., Duren, R., Hensley, S., Kobrick, M., Paller, M., Rodriguez, E., Roth, L., Seal, D., Shaffer, S., Shimada, J., Umland, J., Werner, M., Oskin, M., Burbank, D., and Alsdorf, D. (2007). The Shuttle Radar Topography Mission. *Reviews of Geophysics*, 45 (2). doi: 10.1029/2005RG000183.

Finsterwalder, R. (1954). Photogrammetry and glacier research with special reference to glacier retreat in the Eastern Alps. *Journal of Glaciology*, 2 (11): 306–315.

Fischer, A. (2009). Calculation of glacier volume from sparse ice-thickness data, applied to Schaufelferner, Austria. *Journal of Glaciology*, 55: 453–460. doi: 10.3189/002214309788816740.

Fischer, A., Span, N., Kuhn, M., and Butschek, M. (2007). Radarmessungen der Eisdicke österreichischer Gletscher; Band II: Messungen 1999 bis 2006. *Österreichische Beiträge zu Meteorologie und Geophysik*, 39.

Fischer, A., Olefs, M., and Abermann, J. (2011). Glaciers, snow and ski tourism in Austria's changing climate. *Annals of Glaciology*, 52 (58): 89–96. doi: 10.3189/172756411797252338.

Fischer, M. (2012). Application of a refined perfect-plasticity approach for empirical GIS-based basal shear stress modelling to now ice-free LIA glacier forefields in the Swiss Alps. Master's thesis, Geographisches Institut, Universität Zürich.

Fountain, A. G. and Vecchia, A. (1999). How many stakes are required to measure the mass balance of a glacier? *Geografiska Annaler: Series A, Physical Geography*, 81 (4): 563–573. doi: 10.1111/1468-0459.00084.

Fowler, H. J., Blenkinsop, S., and Tebaldi, C. (2007). Linking climate change modelling to impacts studies: recent advances in downscaling techniques for hydrological modelling. *International Journal of Climatology*, 27 (12): 1547–1578. doi: 10.1002/joc.1556.

Frey, H. (2011). Compilation and applications of glacier inventories using satellite data and digital terrain information. Ph.D. thesis, Schriftenreihe Physische Geographie, Universität Zürich, 62.

Frey, H. and Paul, F. (2012). On the suitability of the SRTM DEM and ASTER GDEM for the compilation of topographic parameters in glacier inventories. *International Journal of Applied Earth Observation and Geoinformation*, 18: 480–490. doi: 10.1016/j.jag.2011.09.020.

Frey, H., Haeberli, W., Linsbauer, A., Huggel, C., and Paul, F. (2010). A multi-level strategy for anticipating future glacier lake formation and associated hazard potentials. *Natural Hazards and Earth System Sciences*, 10 (2): 339–352.

Frey, H., Machguth, H., Huggel, C., Bajracharya, S., Bolch, T., Linsbauer, A., Stoffel, M., and Salzmann, N. (2012). Ice volumes in the Himalayas and Karakoram: evaluating different assessment methods. In: *10th Swiss Geoscience Meeting, Bern 2012*.

Frey, H., Machguth, H., Huss, M., Huggel, C., Bajracharya, S., Bolch, T., Kulkarni, A., Linsbauer, A., Salzmann, N., and Stoffel, M. (2013). Ice volume estimates for the Himalaya–Karakoram region: evaluating different methods. *The Cryosphere Discussions*, 7 (5): 4813–4854. doi: 10.5194/tcd-7-4813-2013.

Geist, T. and Stötter, J. (2007). Documentation of glacier surface elevation change with multi-temporal airborne laser scanner data – case study: Hintereisferner and Kesselwandferner, Tyrol, Austria. *Zeitschrift für Gletscherkunde und Glazialgeologie*, 41: 77–106.

Giesen, R. H. and Oerlemans, J. (2010). Response of the ice cap Hardangerjøkulen in southern Norway to the 20th and 21st century climates. *The Cryosphere*, 4 (2): 191–213. doi: 10.5194/tc-4-191-2010.

Giesen, R. H. and Oerlemans, J. (2012). Global application of a surface mass balance model using gridded climate data. *The Cryosphere Discussions*, 6 (2): 1445–1490. doi: 10.5194/tcd-6-1445-2012.

Giorgi, F. and Mearns, L. O. (1999). Introduction to special section: regional climate modeling revisited. *Journal of Geophysical Gesearch*, 104 (D6): 6335–6352.

Glen, J. (1958). The flow law of ice. A discussion of the assumptions made in glacier theory, their experimental foundations and consequenses. *International Association of Scientific Hydrology*, 47: 171–183.

Greuell, W. and Genthon, C. (2004). Modelling land-ice surface mass balance. In: *Mass balance of the cryosphere: observations and modelling of contemporary and future changes.*, (edited by Bamber, J. and Payne, A.), pp. 117–168. Cambridge University Press.

Greuell, W. and Oerlemans, J. (1987). Sensitivity studies with a mass balance model including temperature profile calculations inside the glacier. *Zeitschrift für Gletscherkunde und Glazialgeologie*, 22: 101–124.

Haeberli, W. (1983). Permafrost – glacier relationships in the Swiss Alps today and in the past. In: *Proceedings of the Fourth International Conference on Permafrost, Fairbanks AK.*, pp. 415–420. National Academy of Sciences, Washington D.C.

Haeberli, W. (1991). Alpengletscher im Treibhaus der Erde. *Regio Basiliensis*, 35 (2): 59–72.

Haeberli, W. (2006). Integrated perception of glacier changes: A challenge of historical dimensions. In: *Glacier Science and Environmental Change*, (edited by Knight, P. G.), pp. 423–430. Blackwell Publishing.

Haeberli, W. and Beniston, M. (1998). Climate change and its impacts on glaciers and permafrost in the Alps. *Ambio Special Report*, 27 (4): 258–265.

Haeberli, W. and Burn, C. R. (2002). Natural hazards in forests: Glacier and permafrost effects as related to climate change. In: *Environmental Change and Geomorphic Hazards in Forests. IUFRO Research Series*, (edited by Sidle, R. C.), p. 256. CABI Publishing, Wallingford/New York.

Haeberli, W. and Dedieu, J.-P. (2004). Cryosphere monitoring in mountain biosphere reserves: Challenges for integrated research on snow and ice. In: *Global change in mountain regions (GLOCHAMORE): Global environmental and social monitoring*, (edited by Lee, C. and Schaaf, T.), pp. 29–33. UNESCO, Vienna.

Haeberli, W. and Fisch, W. (1984). Electrical resisitvitiy soundings of glacier beds: a test study on Grubengletscher, Wallis, Swiss Alps. *Journal of Glaciology*, 30 (106): 373–376.

Haeberli, W. and Hoelzle, M. (1995). Application of inventory data for estimating characteristics of and regional climate-change effects on mountain glaciers: a pilot study with the European Alps. *Annals of Glaciology*, 21: 206–212.

Haeberli, W. and Hohmann, R. (2008). Climate, glaciers and permafrost in the Swiss Alps 2050: Scenarios, consequences and recommendations. In: *Ninth International Conference on Permafrost, Fairbanks, Alaska*.

Haeberli, W. and Linsbauer, A. (2013). Brief communication "Global glacier volumes and sea level – small but systematic effects of ice below the surface of the ocean and of new local lakes on land". *The Cryosphere*, 7 (3): 817–821. doi: 10.5194/tc-7-817-2013.

Haeberli, W. and Maisch, M. (2007). Klimawandel im Hochgebirge. In: *Der Klimawandel – Einblicke, Rückblicke, Ausblicke*, (edited by Endlicher, W. and Gerstengarbe, F.), pp. 98–107. Potsdam-Institut für Klimafolgenforschung.

Haeberli, W. and Schweizer, J. (1988). Rhonegletscher 1850: Eismechanische Ueberlegungen zu einem historischen Gletscherstand. *Mitteilung VAW/ETHZ*, 94: 59–70.

Haeberli, W., Wächter, H., Schmid, W., and Sidler, C. (1982). *Erste Erfahrungen mit dem US Geological Survey-Monopuls Radioecholot im Firn, Eis und Permafrost der Schweizer Alpen*. Arbeitsheft, Versuchsanstalt für Wasserbau, Hydrologie und Glaziologie ETH Zürich.

Haeberli, W., Alean, J., Müller, P., and Funk, M. (1989). Assessing risks from glacier hazards in high mountain regions: some experiences in the Swiss Alps. *Annals of Glaciology*, 13: 96–102.

Haeberli, W., Frauenfelder, R., Hoelzle, M., and Maisch, M. (1999). On rates and acceleration trends of global glacier mass changes. *Geografiska Annaler*, 81A (4): 585–591. doi: 10.1111/1468-0459.00086.

Haeberli, W., Hoelzle, M., Paul, F., and Zemp, M. (2007). Integrated monitoring of mountain glaciers as key indicators of global climate change: the European Alps. *Annals of Glaciology*, 46: 150–160. International Symposium on Cryospheric Indicators of Global Climate Change, Cambridge, England, Aug 21-25, 2006.

Haeberli, W., Hoelzle, M., Paul, F., and Zemp, M. (2008). Integrated glacier monitoring strategies: comments on a recent correspondence. *Journal of Glaciology*, 54 (188): 947–948. doi: 10.3189/002214308787779870.

Haeberli, W., Clague, J., Huggel, C., and Kääb, A. (2010). Hazards from lakes in high-mountain glacier and permafrost regions: Climate change effects and process interactions. In: *Avances de la Geomorphología en España, 2008-2010, XI Reunión Nacional de Geomorphología, Solsona*, pp. 439–446.

Haeberli, W., Paul, F., and Zemp, M. (2011). Vanishing glaciers in the European Alps. *The Pontifical Academy of Sciences, Scripta Varia 118, Fate of Mountain Glaciers in the Anthropocene, Working Group 2-4 April 2011, Vatican City.*

Haeberli, W., Schleiss, A., Linsbauer, A., Künzler, M., and Bütler, M. (2012). Gletscherschwund und neue Seen in den Schweizer Alpen: Perspektiven und Optionen im Bereich Naturgefahren und Wasserkraft. *Wasser Energie Luft*, 2: 93–102.

Haeberli, W., Bütler, M., Huggel, C., Müller, H., and Schleiss, A. (eds.) (2013). *NELAK (2013): Neue Seen als Folge des Gletscherschwundes im Hochgebirge – Chancen und Risiken. Formation des nouveux lacs suite au recul des glaciers en haute montagne – chances et risques. Forschungsbericht NFP 61.* Zürich, vdf Hochschulverlag AG an der ETH Zürich.

Hambrey, M. and Alean, J. (2004). *Glaciers*. Cambridge University Press, Cambridge.

Haug, T., Rolstad, C., Elvehøy, H., Jackson, M., and Maalen-Johansen, I. (2009). Geodetic mass balance of the western Svartisen ice cap, Norway, in the periods 1968–1985 and 1985–2002. *Annals of Glaciology*, 50 (50): 119–125. doi: 10.3189/172756409787769528.

Hawkins, E. and Sutton, R. (2009). The potential to narrow uncertainty in regional climate predictions. *Bulletin of the American Meteorological Society*, 90 (8): 1095–1107. doi: 10.1175/2009BAMS2607.1.

Hayakawa, Y. S., Oguchi, T., and Lin, Z. (2008). Comparison of new and existing global digital elevation models: ASTER G-DEM and SRTM-3. *Geophysical Research Letters*, 35 (17): L17404. doi: 10.1029/2008GL035036.

Hilbich, C. (2010). Time-lapse refraction seismic tomography for the detection of ground ice degradation. *The Cryosphere*, 4 (3): 243–259. doi: 10.5194/tc-4-243-2010.

Hirabayashi, Y., Döll, P., and Kanae, S. (2010). Global-scale modeling of glacier mass balances for water resources assessments: Glacier mass changes between 1948 and 2006. *Journal of Hydrology*, 390 (3–4): 245–256. doi: 10.1016/j.jhydrol.2010.07.001.

Hock, R. (1999). A distributed temperature-index ice- and snowmelt model including potential direct solar radiation. *Journal of Glaciology*, 45 (149): 101–111.

Hock, R. (2003). Temperature index melt modelling in mountain areas. *Journal of Hydrology*, 282 (1–4): 104–115. doi: 10.1016/S0022-1694(03)00257-9.

Hock, R. (2005). Glacier melt: a review of processes and their modelling. *Progress in Physical Geography*, 29 (3): 362–391. doi: 10.1191/0309133305pp453ra.

Hock, R., de Woul, M., Radic, V., and Dyurgerov, M. (2009). Mountain glaciers and ice caps around Antarctica make a large sea-level rise contribution. *Geophysical Research Letters*, 36 (L07501): 5 PP. doi: 200910.1029/2008GL037020.

Hoelzle, M. and Haeberli, W. (1995). Simulating the effects of mean annual air-temperature changes on permafrost distribution and glacier size: an example from the Upper Engadin, Swiss Alps. *Annals of Glaciology*, 21: 399–405.

Hoelzle, M., Haeberli, W., Dischl, M., and Peschke, W. (2003). Secular glacier mass balances derived from cumulative glacier length changes. *Global and Planetary Change*, 36 (4): 295–306. doi: 10.1016/S0921-8181(02)00223-0.

Hoelzle, M., Paul, F., Gruber, S., and Frauenfelder, R. (2005). Glaciers and permafrost in mountain areas: Different modeling approaches. In: *Global change impacts in mountain biosphere reserves*, (edited by UNESCO), pp. 28–39.

Hoelzle, M., Chinn, T., Stumm, D., Paul, F., Zemp, M., and Haeberli, W. (2007). The application of glacier inventory data for estimating past climate change effects on mountain glaciers: A comparison between the European Alps and the South-

ern Alps of New Zealand. *Global and Planetary Change*, 56 (1–2): 69–82. doi: {10.1016/j.gloplacha.2006.07.001}.

Huss, M. (2009). Past and future changes in glacier mass balance. Ph.D. thesis, Laboratory of Hydraulics, Hydrology and Glaciology (VAW), ETH-Zurich, Mitteilung VAW Nr. 213.

Huss, M. (2011). Present and future contribution of glacier storage change to runoff from macroscale drainage basins in Europe. *Water Resources Research*, 47: W07511, 14pp. doi: doi:10.1029/2010WR010299.

Huss, M. (2012). Extrapolating glacier mass balance to the mountain-range scale: the European Alps 1900–2100. *The Cryosphere*, 6 (4): 713–727. doi: 10.5194/tc-6-713-2012.

Huss, M. and Farinotti, D. (2012). Distributed ice thickness and volume of all glaciers around the globe. *Journal of Geophysical Research*, 117 (F4): F04010. doi: 10.1029/2012JF002523.

Huss, M., Bauder, A., Funk, M., and Hock, R. (2008a). Determination of the seasonal mass balance of four Alpine glaciers since 1865. *Journal of Geophysical Research*, 113: F01015. doi: 10.1029/2007JF000803.

Huss, M., Farinotti, D., Bauder, A., and Funk, M. (2008b). Modelling runoff from highly glacierized alpine drainage basins in a changing climate. *Hydrological Processes*, 22 (19, Sp. Iss. SI): 3888–3902. doi: 10.1002/hyp.7055.

Huss, M., Bauder, A., and Funk, M. (2009). Homogenization of long-term mass-balance time series. *Annals of Glaciology*, 50 (50): 198–206. doi: 10.3189/172756409787769627.

Huss, M., Hock, R., Bauder, A., and Funk, M. (2010a). 100-year glacier mass changes in the Swiss Alps linked to the Atlantic Multidecadal Oscillation. *Geophyiscal Research Letters*, 37: L10501. doi: doi:10.1029/2010GL042616.

Huss, M., Jouvet, G., Farinotti, D., and Bauder, A. (2010b). Future high-mountain hydrology: a new parameterization of glacier retreat. *Hydrology and Earth System Sciences*, 14 (5): 815–829.

Hutchinson, M. (1989). A new procedure for gridding elevation and stream line data with automatic removal of spurious pits. *Journal of Hydrology*, 106: 211–232. doi: 10.1016/0022-1694(89)90073-5.

Hutchinson, M. F. (1995). Interpolating mean rainfall using thin plate smoothing splines. *International Journal of Geographical Information Systems*, 9 (4): 385–403. doi: 10.1080/02693799508902045.

Immerzeel, W., van Beek, L., Konz, M., Shrestha, A., and Bierkens, M. (2012). Hydrological response to climate change in a glacierized catchment in the Himalayas. *Climatic Change*, 110 (3): 721–736. doi: 10.1007/s10584-011-0143-4.

IPCC (2007). Climate Change 2007. The scientific basis. Contribution of the Working Group I to the Forth Assessment Report of the Intergovernmental Panel on Climate Change. Tech. rep., WMO/UNEP. Cambridge University Press: New York.

Jaeggi, M. (2007). The flood of August 22-23, 25 in Switzerland: some facts and challenges. *Developments in Earth Surface Processes*, 11: 587–603.

Jansson, P., Hock, R., and Schneider, T. (2003). The concept of glacier storage: a review. *Journal of Hydrology*, 282 (1–4): 116–129. doi: {10.1016/S0022-1694(03)00258-0}.

Joerg, P. C., Morsdorf, F., and Zemp, M. (2012). Uncertainty assessment of multitemporal airborne laser scanning data: A case study on an Alpine glacier. *Remote Sensing of Environment*, 127: 118–129. doi: 10.1016/j.rse.2012.08.012.

Johannesson, T., Raymond, C., and Waddington, E. (1989). Time-scale for adjustment of glaciers to changes in mass balance. *Journal of Glaciology*, 35 (121): 355–369.

Jones, C. (1997). *Geographical informations systems and computer cartography*. Addison-Wesley, Harlow.

Jones, P. D. and Mann, M. E. (2004). Climate over past millennia. *Reviews of Geophysics*, 42 (2): RG2002. doi: 10.1029/2003RG000143.

Jouvet, G., Huss, M., Blatter, H., Picasso, M., and Rappaz, J. (2009). Numerical simulation of Rhonegletscher from 1874 to 2100. *Journal of Computational Physics*, 228 (17): 6426–6439. doi: 10.1016/j.jcp.2009.05.033.

Jouvet, G., Huss, M., Funk, M., and Blatter, H. (2011). Modelling the retreat of Grosser Aletschgletscher, Switzerland, in a changing climate. *Journal of Glaciology*, 57 (206): 1033–1045.

Kääb, A., Paul, F., Maisch, M., Hoelzle, M., and Haeberli, W. (2002). The new remote-sensing-derived Swiss glacier inventory: II. First results. *Annals of Glaciology*, 34 (1): 362–366. doi: 10.3189/172756402781817473.

Kamb, B. and Echelmeyer, K. A. (1986). Stress-gradient coupling in glacier flow: I. longitudinal averaging of the influence of ice thickness and surface slope. *Journal of Glaciology*, 32 (111): 267–284.

Kaser, G., Grosshauser, M., and Marzeion, B. (2010). Contribution potential of glaciers to water availability in different climate regimes. *Proceedings of the National Academy of Sciences*, 107 (47): 20223–20227. doi: 10.1073/pnas.1008162107.

Klok, E. L. and Oerlemans, J. (2002). Model study of the spatial distribution of the energy and mass balance of Morteratschgletscher, Switzerland. *Journal of Glaciology*, 48 (163): 505–518. doi: 10.3189/172756502781831133.

Koboltschnig, G. R., Schoener, W., Zappa, M., Kroisleitner, C., and Holzmann, H. (2008). Runoff modelling of the glacierized Alpine Upper Salzach basin (Austria): multi-

criteria result validation. *Hydrological Processes*, 22 (19, Sp. Iss. SI): 3950–3964. doi: 10.1002/hyp.7112.

Köplin, N., Schädler, B., Viviroli, D., and Weingartner, R. (2012). The importance of glacier and forest change in hydrological climate-impact studies. *Hydrology and Earth System Sciences Discussions*, 9 (5): 5983–6021. doi: 10.5194/hessd-9-5983-2012.

Kuhn, M. (1981). Climate and glaciers. In: *Sea level, ice and climatic change (Proceedings of the Canberra Symposium, December 1979)*, vol. IAHS Publ. 131 of *IAHS Publ.*, pp. 3–20.

Kuhn, M. (1990). Energieaustausch Atmosphäre – Schnee und Eis. In: *Schnee, Eis und Wasser der Alpen in einer wärmeren Atmosphäre*, vol. 108, pp. 21–32. Mitteilungen der VAW, ETH Zurich.

Kuhn, M. (1993). Methods of assessing the effects of climatic changes on snow and glacier hydrology. In: *Snow and Glacier Hydrology (Proceedings of the Kathmandu Symposium, November 1992)*, (edited by Young, G. J.), vol. 218, pp. 135–144. IAHS.

Künzler, M., Huggel, C., Linsbauer, A., and Haeberli, W. (2010). Emerging risks related to new lakes in deglaciating areas of the Alps. In: *Mountain Risks: Bringing Science to Society. Proceedings of the "Mountain Risk" International Conference, 24–26 November 2010, Firenze, Italy*, (edited by Malet, J.-P., Glade, T., and Casagli, N.), pp. 453–458. CERG Editions, Strasbourg, France.

Le Bris, R. and Paul, F. (2013). An automatic method to create flow lines for determination of glacier length: A pilot study with alaskan glaciers. *Computers & Geosciences*, 52: 234–245. doi: 10.1016/j.cageo.2012.10.014.

Le Meur, E., Gerbaux, M., Schäfer, M., and Vincent, C. (2007). Disappearance of an Alpine glacier over the 21st century simulated from modeling its future surface mass balance. *Earth and Planetary Science Letters*, 261 (3–4): 367–374. doi: 10.1016/j.epsl.2007.07.022.

Leclercq, P. and Oerlemans, J. (2012). Global and hemispheric temperature reconstruction from glacier length fluctuations. *Climate Dynamics*, 38: 1065–1079. doi: 10.1007/s00382-011-1145-7.

Leung, L. R. and Ghan, S. J. (1999). Pacific northwest climate sensitivity simulated by a regional climate model driven by a GCM. part I: Control simulations. *Journal of Climate*, 12 (7): 2010–2030. doi: 10.1175/1520-0442(1999)012<2010:PNCSSB>2.0.CO;2.

Leysinger Vieli, G. J.-M. C. and Gudmundsson, G. H. (2004). On estimating length fluctuations of glaciers caused by changes in climatic forcing. *Journal of Geophysical Research*, 109: F01007. doi: 10.1029/2003JF000027.

Li, H., Li, Z., Zhang, M., and Li, W. (2011). An improved method based on shallow ice approximation to calculate ice thickness along flow-line and volume of mountain

glaciers. *Journal of Earth Science*, 22 (4): 441–448. doi: 10.1007/s12583-011-0198-1.

Li, H., Ng, Z., F.and Li, Qin, D., and Cheng, G. (2012). An extended "perfect-plasticity" method for estimating ice thickness along the flow line of mountain glaciers. *Journal of Geophysical Research*, 117: F01020. doi: 10.1029/2011JF002104.

Lie, O., Dahl, S. O., and Nesje, A. (2003). A theoretical approach to glacier equilibrium-line altitudes using meteorological data and glacier mass-balance records from southern Norway. *The Holocene*, 13 (3): 365–372. doi: 10.1191/0959683603hl629rp.

Linsbauer, A., Paul, F., Hoelzle, M., Frey, H., and Haeberli, W. (2009). The Swiss Alps without glaciers – a GIS-based modelling approach for reconstruction of glacier beds. In: *Proceedings of Geomorphometry 2009*, (edited by Purves, R., Gruber, S., Straumann, R., and Hengl, T.), pp. 243–247. University of Zurich, Zurich, Switzerland.

Linsbauer, A., Paul, F., and Haeberli, W. (2012a). Grossräumige Modellierung von Schwundszenarien für alle Schweizer Gletscher: Modellvergleich, Unsicherheiten und eine Analyse bezogen auf Grosseinzugsgebiete. Tech. rep., CCHydro-Schlussbericht des Geographischen Instituts der Universität Zürich (GIUZ).

Linsbauer, A., Paul, F., and Haeberli, W. (2012b). Modeling glacier thickness distribution and bed topography over entire mountain ranges with GlabTop: Application of a fast and robust approach. *Journal of Geophysical Research*, 117: F03007. doi: 10.1029/2011JF002313.

Linsbauer, A., Paul, F., Machguth, H., and Haeberli, W. (2013). Comparing three different methods to model scenarios of future glacier change in the Swiss Alps. *Annals of Glaciology*, 54 (63): 241–253. doi: 10.3189/2013AoG63A400.

Lliboutry, L. (1971). The glacier theory. *Advances in Hydroscience*, 7: 81–167.

Longley, P., Goodchild, M., and Maguire, D. (2011). *Geographic information systems and science*. Wiley, Hoboken, N.J, 3rd ed.

Machguth, H. (2008). On the use of RCM data and gridded climatologies for regional scale glacier mass balance modeling in high mountain topography; the example of the Swiss Alps. Ph.D. thesis, Departement of Geography, University of Zurich.

Machguth, H. (2012). A straightforward method for the automated calculation of glacier flow lines. In: *10th Swiss Geoscience Meeting, Bern 2012*.

Machguth, H., Purves, R. S., Oerlemans, J., Hoelzle, M., and Paul, F. (2008). Exploring uncertainty in glacier mass balance modelling with Monte Carlo simulation. *The Cryosphere*, 2 (2): 191–204. doi: 10.5194/tc-2-191-2008.

Machguth, H., Paul, F., Kotlarski, S., and Hoelzle, M. (2009). Calculating distributed glacier mass balance for the Swiss Alps from regional climate model output: A methodical description and interpretation of the results. *Journal of Geophysical Research*,

114: D19106. doi: 200910.1029/2009JD011775.

Machguth, H., Paul, F., and Haeberli, W. (2012). Mass-balance parameters derived from a synthetic network of mass-balance glaciers. *Journal of Glaciology*, 58 (211): 965–979. doi: 10.3189/2012JoG11J223.

Machguth, H., Rastner, P., Bolch, T., Mölg, N., Sørensen, L. S., Aðalgeirsdottir, G., Angelen, J. H. v., Broeke, M. R. v. d., and Fettweis, X. (2013). The future sea-level rise contribution of Greenland's glaciers and ice caps. *Environmental Research Letters*, 8 (2): 025005. doi: 10.1088/1748-9326/8/2/025005.

Maisch, M. (1992). *Die Gletscher Graubündens – Rekonstruktion und Auswertung der Gletscher und deren Veränderungen seit dem Hochstand von 1850 im Gebiet der östlichen Schweizer Alpen (Bündnerland und angrenzende Regionen)*, vol. 33a. Schriftenreihe Physische Geographie Universität Zürich.

Maisch, M. and Haeberli, W. (1982). Interpretation geometrischer Parameter von Spätglazialgletschern im Gebiet Mittelbünden, Schweizer Alpen. In: *Beiträge zur Quartärforschung in der Schweiz*, (edited by Gamper, M.), vol. 1, pp. 111–126. Schriftenreihe Physische Geographie Universität Zürich.

Maisch, M., Wipf, A., Denneler, B., Battaglia, J., and Benz, C. (2000). *Die Gletscher der Schweizer Alpen: Gletscherhochstand 1850, aktuelle Vergletscherung, Gletscherschwundszenarien. Schlussbericht NFP 31; 2. Auflage*. vdf Hochschulverlag. Zürich.

Marshall, S., White, E., Demuth, M., Bolch, T., Wheate, R., Menounos, B., Beedle, M., and Shea, J. (2011). Glacier water resources on the eastern slopes of the Canadian Rocky Mountains. *Canadian Water Resources Journal*, 36 (2): 109–134. doi: 10.4296/cwrj3602823.

Marzeion, B., Hofer, M., Jarosch, A. H., Kaser, G., and Mölg, T. (2012a). A minimal model for reconstructing interannual mass balance variability of glaciers in the European Alps. *The Cryosphere*, 6 (1): 71–84. doi: 10.5194/tc-6-71-2012.

Marzeion, B., Jarosch, A. H., and Hofer, M. (2012b). Past and future sea-level change from the surface mass balance of glaciers. *The Cryosphere*, 6 (6): 1295–1322. doi: 10.5194/tc-6-1295-2012.

Mauser, W. and Bach, H. (2009). PROMET – large scale distributed hydrological modelling to study the impact of climate change on the water flows of mountain watersheds. *Journal of Hydrology*, 376 (3-4): 362–377. doi: 10.1016/j.jhydrol.2009.07.046.

McGuffie, K. and Henderson-Sellers, A. (2001). Forty years of numerical climate modelling. *International Journal of Climatology*, 21 (9): 1067–1109. doi: 10.1002/joc.632.

Mearns, L. (2010). The drama of uncertainty. *Climatic Change*, 100 (1): 77–85. doi: 10.1007/s10584-010-9841-6.

Mearns, L., Easterling, W., Hays, C., and Marx, D. (2001). Comparison of agricultural impacts of climate change calculated from high and low resolution climate change scenarios: Part I. the uncertainty due to spatial scale. *Climatic Change*, 51 (2): 131–172. doi: 10.1023/A:1012297314857.

Meier, M. F., Dyurgerov, M. B., Rick, U. K., O'Neel, S., Pfeffer, W. T., Anderson, R. S., Anderson, S. P., and Glazovsky, A. F. (2007). Glaciers dominate Eustatic sea-level rise in the 21st century. *Science*, 317 (5841): 1064–1067. doi: {10.1126/science.1143906}.

Meinshausen, M., Meinshausen, N., Hare, W., Raper, S. C. B., Frieler, K., Knutti, R., Frame, D. J., and Allen, M. R. (2009). Greenhouse-gas emission targets for limiting global warming to 2°C. *Nature*, 458 (7242): 1158–1162. doi: 10.1038/nature08017.

Meister, I. (2010). Modelling and analysis of the subglacial topography of Jostedalsbreen, Norway. Master's thesis, Geographisches Institut, Universität Zürich.

METI/NASA/USGS (2009). ASTER GDEM validation summary report. Tech. rep., ASTER GDEM Validation Team: METI/ERSDAC, NASA/LPDAAC, USGS/EROS. In cooperation with NGA and other Collaborators.

Mitas, L. and Mitasova, H. (1999). Spatial interpolation. In: *Geographical Information Systems: Principles, Techniques, Management and Applications*, (edited by Longley, P. A., Maguire, D. J., Goodchild, M. F., and Rhind, D. W.), pp. 481–492. John Wiley, New York.

Moll, A. (2012). Tiefengletscher, Uri: Vergangenheits- und Gegenwartsanalyse, Eisradarmessungen zum Stand 2011 sowie Modellierungen einer zukünftigen möglichen Gletscherentwicklung. Master's thesis, Geographisches Institut, Universität Zürich.

Moore, R. D., Fleming, S. W., Menounos, B., Wheate, R., Fountain, A., Stahl, K., Holm, K., and Jakob, M. (2009). Glacier change in western North America: influences on hydrology, geomorphic hazards and water quality. *Hydrological Processes*, 23 (1): 42–61. doi: 10.1002/hyp.7162.

Mothes, H. (1927). Seismische Dickenmessung von Gletschereis. *Zeitschrift für Geophysik*, 5: 120–144.

Müller, F., Caflisch, T., and Müller, G. (1976). Firn und Eis der Schweizer Alpen: Gletscherinventar. *Publ. Nr. 57. Geographisches Institut der ETH Zurich, Zurich*.

Müller, F., Caflisch, T., and Müller, G. (1977). *Instructions for the compilation and assemblage of data for a world glacier inventory*. IAHS(ICSI)/UNESCO report, Temporal Technical Secretariat for the World Glacier Inventory (TTS/WGI), ETH Zurich, Switzerland.

Müller, H., Lehmann Friedli, T., Haeberli, W., and Bütler, M. (2012). Neue Gletscherseen als Folge der Entgletscherung im Alpenraum – Herausforderungen für den Touris-

mus. In: *Tourismus 2020+ interdisziplinär, Herausforderungen für Wirtschaft, Umwelt und Gesellschaft, Schriften zu Tourismus und Freizeit, Band 15*, (edited by Zehrer, A. and Grabmüller, A.). Erich Schmidt Verlag, Berlin.

Nakicenovic, N. and Swart, R. (eds.) (2000). *Emissions Scenarios*. Cambridge University Press, UK.

Narod, B. and Clarke, G. (1994). Miniature high-power impulse transmitter for radio-echo sounding. *Journal of Glaciology*, 40 (134): 190–194.

Navarro, F. J., Macheret, Y. Y., and Benjumea, B. (2005). Application of radar and seismic methods for the investigation of temperate glaciers. *Journal of Applied Geohysics*, 57 (3): 193–211. doi: 10.1016/j.jappgeo.2004.11.002.

Nemec, J., Huybrechts, P., Rybak, O., and Oerlemans, J. (2009). Reconstruction of the annual balance of Vadret da Morteratsch, Switzerland, since 1865. *Annals of Glaciology*, 50 (50): 126–134. doi: 10.3189/172756409787769609.

Ng, F. S., Barr, I. D., and Clark, C. D. (2010). Using the surface profiles of modern ice masses to inform palaeo-glacier reconstructions. *Quaternary Science Reviews*, 29 (23–24): 3240–3255. doi: 10.1016/j.quascirev.2010.06.045.

Nye, J. (1952). The mechanics of glacier flow. *Journal of Glaciology*, 2 (12): 82–93.

Nye, J. (1960). The response of glaciers and ice-sheets to seasonal and climatic changes. *Proceedings Royal Society, London, Series A*, 256: 559–584.

Nye, J. (1965). The flow of a glacier in a channel of rectangular, elliptic or parabolic cross-section. *Journal of Glaciology*, 5 (41): 661–690.

Oerlemans, J. (1991). A model for the surface balance of ice masses: part I. Alpine glaciers. *Zeitschrift für Gletscherkunde und Glazialgeologie*, 27/28: 63–83.

Oerlemans, J. (1992). Climate sensitivity of glaciers in southern Norway: application of an energy-balance model to Nigardsbreen, Hellstugubreen and Alfotbreen. *Annals of Glaciology*, 38: 223–232.

Oerlemans, J. (1994). Quantifying global warming from the retreat of glaciers. *Science*, 264 (5156): 243–245. doi: 10.1126/science.264.5156.243.

Oerlemans, J. (2001). *Glaciers and Climate Change*. A.A. Balkema Publishers.

Oerlemans, J. (2005). Extracting a climate signal from 169 glacier records. *Science*, 308 (5722): 675–677. doi: 10.1126/science.1107046.

Oeschger, H., Schotterer, U., Stauffer, B., Haeberli, W., and Röthlisberger, H. (1977). First results from Alpine core drilling projects. *Zeitschrift für Gletscherkunde und Glazialgeologie*, 13 (1/2): 193–208.

Ohmura, A. (2001). Physical basis for the temperature-based melt-index method. *Journal of Applied Meteorology*, 40 (4): 753–761. doi: 10.1175/1520-0450(2001)040<0753:PBFTTB>2.0.CO;2.

Ohmura, A. (2009). Completing the world glacier inventory. *Annals of Glaciology*, 50 (53): 144–148. doi: 10.3189/172756410790595840.

Ohmura, A., Kasser, P., and Funk, M. (1992). Climate at the equilibrium line of glaciers. *Journal of Glaciology*, 130: 397–411.

Oppikofer, T., Jaboyedoff, M., and Keusen, H. (2008). Collapse at the eastern Eiger flank in the Swiss Alps. *Nature Geoscience*, 1 (8): 531–535. doi: 10.1038/ngeo258.

Østrem, G. and Haakensen, N. (1999). Map comparison or traditional mass-balance measurements: Which method is better? *Geografiska Annaler: Series A, Physical Geography*, 81A (4): 703–711. Doi:10.1111/j.0435-3676.1999.00098.x.

O'Sullivan, D. and Unwin, D. J. (2002). *Geographic Information Analysis*. John Wiley & Sons, Inc., Hoboken, New Jersey.

Paterson, W. (1994). *The physics of glaciers*. Pergamon-Press.

Paul, F. (2007). The New Swiss Glacier Inventory 2000 – Application of Remote Sensing and GIS. Ph.D. thesis, Schriftenreihe Physische Geographie, Universität Zürich, 52.

Paul, F. and Haeberli, W. (2008). Spatial variability of glacier elevation changes in the Swiss Alps obtained from two digital elevation models. *Geophysical Research Letters*, 35 (21): L21502. doi: {10.1029/2008GL034718}.

Paul, F. and Kääb, A. (2005). Perspectives on the production of a glacier inventory from multispectral satellite data in Arctic Canada: Cumberland Peninsula, Baffin Island. *Annals of Glaciology*, 42: 59–66. doi: 10.3189/172756405781813087.

Paul, F. and Linsbauer, A. (2012). Modeling of glacier bed topography from glacier outlines, central branch lines, and a DEM. *International Journal of Geographical Information Science*, 26 (7): 1173–1190. doi: 10.1080/13658816.2011.627859.

Paul, F. and Svoboda, F. (2010). A new glacier inventory on southern Baffin Island, Canada, from ASTER data: II. Data analysis, glacier change and applications. *Annals of Glaciology*, 50 (53): 22–31. doi: 10.3189/172756410790595921.

Paul, F., Kääb, A., Maisch, M., Kellenberger, T., and Haeberli, W. (2002). The new remote-sensing-derived Swiss Glacier Inventory: I. Methods. *Annals of Glaciology*, 34 (1): 355–361.

Paul, F., Kääb, A., Maisch, M., Kellenberger, T., and Haeberli, W. (2004). Rapid disintegration of Alpine glaciers observed with satellite data. *Geophysical Research Letters*, 31 (21): L21402. doi: 10.1029/2004GL020816.

Paul, F., Kääb, A., and Haeberli, W. (2007a). Recent glacier changes in the Alps observed by satellite: Consequences for future monitoring strategies. *Global Planet Change*, 56 (1–2): 111–122. doi: 10.1016/j.gloplacha.2006.07.007.

Paul, F., Maisch, M., Rothenbuehler, C., Hoelzle, M., and Haeberli, W. (2007b). Calculation and visualisation of future glacier extent in the Swiss Alps by means of hypsographic modelling. *Global Planet Change*, 55 (4): 343–357. doi: 10.1016/j.gloplacha.2006.08.003.

Paul, F., Machguth, H., Hoelzle, M., Salzmann, N., and Haeberli, W. (2008). Alpine-wide distributed glacier mass balance modelling: a tool for assessing future glacier change? In: *Darkening Peaks: Glacier Retreat, Science, and Society*, (edited by Orlove, B., Wiegandt, E., and Luckman, B.), pp. 111–125. University of California Press, Berkeley and Los Angeles.

Paul, F., Barry, R., Cogley, J., Frey, H., Haeberli, W., Ohmura, A., Ommanney, C., Raup, B., Rivera, A., and Zemp, M. (2009). Recommendations for the compilation of glacier inventory data from digital sources. *Annals of Glaciology*, 50 (53): 119–126. doi: 10.3189/172756410790595778.

Paul, F., Linsbauer, A., and Haeberli, W. (2011). Grossräumige Modellierung von Schwundszenarien für alle Schweizer Gletscher, Klimaänderung und Wasserkraft, Sektorielle Studie Wallis, Modul B Gletscherszenarien. Tech. rep., WWK Schlussbericht des Geographischen Instituts der Universität Zürich (GIUZ).

Pelto, M. S. (2006). The current disequilibrium of north cascade glaciers. *Hydrological Processes*, 20 (4): 769–779. doi: 10.1002/hyp.6132.

Prudhomme, C., Reynard, N., and Crooks, S. (2002). Downscaling of global climate models for flood frequency analysis: where are we now? *Hydrological Processes*, 16 (6): 1137–1150. doi: 10.1002/hyp.1054.

Rabus, B., Eineder, M., Roth, A., and Bamler, R. (2003). The shuttle radar topography mission – a new class of digital elevation models acquired by spaceborne radar. *ISPRS Journal of Photogrammetry and Remote Sensing*, 57 (4): 241–262. doi: 10.1016/S0924-2716(02)00124-7.

Radic, V. and Hock, R. (2010). Regional and global volumes of glaciers derived from statistical upscaling of glacier inventory data. *Journal of Geophysical Research*, 115: F01010. doi: 10.1029/2009JF001373.

Radic, V. and Hock, R. (2011). Regionally differentiated contribution of mountain glaciers and ice caps to future sea-level rise. *Nature Geoscience*, 4 (2): 91–94. doi: 10.1038/ngeo1052.

Randall, D., Wood, R., Bony, S., Colman, R., Fichefet, T., Fyfe, J., Kattsov, V., Pitman, A., Shukla, J., Srinivasan, J., Stouffer, R., Sumi, A., and Taylor, K. (2007). Cilmate models

and their evaluation. In: *Climate Change 2007: The Physical Science Basis. Contribution of Working Group I to the Fourth Assessment Report of the Intergovernmental Panel on Climate Change*, (edited by Solomon, S., Qin, D., Manning, M., Chen, Z., Marquis, M., Averyt, K., M.Tignor, and Miller, H.), pp. 589–662. Cambridge University Press, Cambridge, United Kingdom and New York, NY, USA.

Raper, S., Brown, O., and Braithwaite, R. (2000). A geometric glacier model for sea-level change calculations. *Journal of Glaciology*, 46 (154): 357–368. doi: 10.3189/172756500781833034.

Raper, S. C. B. and Braithwaite, R. J. (2005). The potential for sea level rise: New estimates from glacier and ice cap area and volume distributions. *Geophysical Research Letters*, 32 (5): L05502. doi: 10.1029/2004GL021981.

Raup, B., Racoviteanu, A., Khalsa, S. J. S., Helm, C., Armstrong, R., and Arnaud, Y. (2007). The GLIMS geospatial glacier database: A new tool for studying glacier change. *Global Planet Change*, 56 (1–2): 101–110. doi: 10.1016/j.gloplacha.2006.07.018.

Reuter, H. I., Nelson, A., and Jarvis, A. (2007). An evaluation of void-filling interpolation methods for SRTM - data. *International Journal of Geographical Information Science*, 21 (9): 983. doi: 10.1080/13658810601169899.

Rickenbacher, M. (1998). Die digitale Modellierung des Hochgebirges im DHM25 des Bundesamtes für Topographie. *Wiener Schriften zur Geographie und Kartographie*, 11: 49–55.

Rothenbühler, C. (2006). GISALP – Räumlich-zeitliche Modellierung der klimasensitiven Hochgebirgslandschaft des Oberengadins. Ph.D. thesis, Geographisches Institut, Universität Zürich.

Röthlisberger, H. and Vögtli, K. (1967). Recent D.C. resistivity soundings on Swiss glaciers. *Journal of Glaciology*, 6 (47): 607–621.

Rüesch, R. (2013). Validierung und Anwendung einer mehrstufigen Strategie zur Identifikation zukünftiger Gletscherseen. Master's thesis, Geographisches Institut, Universität Zürich.

Salzmann, N., Frei, C., Vidale, P.-L., and Hoelzle, M. (2007). The application of Regional Climate Model output for the simulation of high-mountain permafrost scenarios. *Global and Planetary Change*, 56 (1–2): 188–202. doi: 10.1016/j.gloplacha.2006.07.006.

Salzmann, N., Machguth, H., and Linsbauer, A. (2012). The Swiss Alpine glaciers' response to the global '2°C air temperature target'. *Environmental Research Letters*, 7 (4): 044001. doi: 10.1088/1748-9326/7/4/044001.

Schädler, B., Weingartner, R., and Zappa, M. (2011). Auswirkungen der Klimaänderung auf die Wasserkraftnutzung. *Wasser Energie Luft*, 103 (4): 265–267.

Schaefli, B., Hingray, B., and Musy, A. (2007). Climate change and hydropower production in the Swiss Alps: quantification of potential impacts and related modelling uncertainties. *Hydrology and Earth System Sciences*, 11 (3): 1191–1205. doi: 10.5194/hess-11-1191-2007.

Schaub, Y., Haeberli, W., Huggel, C., Künzler, M., and Bründl, M. (2013). Landslides and new lakes in deglaciating areas: A risk management framework. In: *Landslide Science and Practice*, (edited by Margottini, C., Canuti, P., and Sassa, K.), pp. 31–38. Springer Berlin Heidelberg.

Schneider, D., Frey, H., Garcia, J., Giraldez, C., Guillen, S., Haeberli, W., Huggel, C., Rohrer, M., Salzmann, N., and Schleiss, A. (2012). Climate change adaptation and disaster risk reduction due to glacial recession in the Cordillera Blanca, Peru. Tech. rep., Institute of Geography, University of Zurich, Switzerland.

Serraino, M. (2011). Fels- und Eisstürze in Hochgebirgsseen der Schweizer Alpen: Eine GIS-basierte Analyse von Gefahrenpotentialen im 21. Jahrhundert. Master's thesis, Geographisches Institut, Universität Zürich.

SGHL and CHy (2011). *Auswirkungen der Klimaänderung auf die Wasserkraftnutzung – Synthesebericht*, vol. 38. Schweizerische Gesellschaft für Hydrologie und Limnologie (SGHL) und Hydrologische Kommission (CHy), Beiträge zur Hydrologie der Schweiz, Bern.

Shean, D., Head, J., and Marchant, D. (2007). Shallow seismic surveys and ice thickness estimates of the Mullins Valley debris-covered glacier, McMurdo Dry Valleys, Antarctica. *Antarctic Science*, 19 (04): 485–496. doi: 10.1017/S0954102007000624.

Shumsky, P. A. (1964). *Principles of structural glaciology*. Translated from the Russian by D. Kraus. Dover Publications, Inc., New York.

Span, N., Fischer, A., Kuhn, M., Massimo, M., and Butschek, M. (2005). Radarmessungen der Eisdicke österreichischer Gletscher; Band I: Messungen 1995 bis 1998. *Österreichische Beiträge zu Meteorologie und Geophysik*, 33.

Stahl, K., Moore, R. D., Shea, J. M., Hutchinson, D., and Cannon, A. J. (2008). Coupled modelling of glacier and streamflow response to future climate scenarios. *Water Resources Research*, 44 (2): W02422. doi: 10.1029/2007WR005956.

Stephan, C. (2012). Analysis of past and future glacier changes in the Langtang Valley, Nepal, using remote sensing. Master's thesis, ETH Zürich.

swisstopo (2005). *DHM25 – Das digitale Höhenmodell der Schweiz*. Swisstopo, Bundesamt für Landestopographie, Wabern (CH).

Terrier, S., Jordan, F., Schleiss, A., Haeberli, W., Huggel, C., and Künzler, M. (2011). Optimized and adapted hydropower management considering glacier shrinkage sce-

narios in the Swiss Alps. In: *Proceedings of the International Symposium on Dams and Reservoirs under Changing Challenges - 79th Annual Meeting of ICOLD, Swiss Committee on Dams, Lucerne, Switzerland*, (edited by Schleiss, A. and Boes, R.), pp. 497–508. Taylor & Francis Group, London.

Tomlin, C. D. (1991). Cartographic modelling. In: *Geographical Information Systems: principles and applications*, (edited by Maguire, D. J., Goodchild, M. F., and Rhind, D. W.), vol. 1, pp. 361–374. Longman, London.

Toutin, T. (2008). ASTER DEMs for geomatic and geoscientific applications: a review. *International Journal of Remote Sensing*, 29 (7): 1855–1875. doi: 10.1080/01431160701408477.

UNESCO (1970). Perennial ice and snow masses. A guide for compilation and assemblage of data for a World Glacier Inventory. *UNESCO/IAHS Technical Papers in Hydrology*, 1.

UNFCCC (2009). Decision 2/CP.15 Copenhagen Accord. In: *Report of the Conference of the Parties on its fifteenth session, held in Copenhagen from 7 to 19 December 2009. Addendum. Part Two: Action taken by the Conference of the Parties at its fifteenth session.* UNFCCC (United Nations Framework Convention on Climate Change).

Van de Wal, R. S. W. and Wild, M. (2001). Modelling the response of glaciers to climate change by applying volume-area scaling in combination with a high resolution GCM. *Climate Dynamics*, 18 (3): 359–366. doi: 10.1007/s003820100184.

van der Linden, P. and Mitchell, J. (2009). *ENSEMBLES: Climate Change and its Impacts: Summary of research and results from the ENSEMBLES project*. Met Office Hadley Centre, FitzRoy Road, Exeter EX1 3PB, UK.

Vanuzzo, C. and Pelfini, M. (1999). Assessing area and volume changes from deglaciated areas, Valle d'Aoste, Italy. *Annals of Glaciology*, 28: 129–134.

Verbunt, M., Gurtz, J., Jasper, K., Lang, H., Warmerdam, P., and Zappa, M. (2003). The hydrological role of snow and glaciers in alpine river basins and their distributed modeling. *Journal of Hydrology*, 282 (1–4): 36–55. doi: 10.1016/S0022-1694(03)00251-8.

Viviroli, D., Zappa, M., Gurtz, J., and Weingartner, R. (2009). An introduction to the hydrological modelling system PREVAH and its pre- and post-processing-tools. *Environmental Modelling & Software*, 24 (10): 1209–1222. doi: 10.1016/j.envsoft.2009.04.001.

Wahba, G. (1990). *Spline Models for Observational Data*. SIAM.

Watson, D. F. and Philip, G. M. (1985). A refinement of inverse distance weighted interpolation. *Geoprocessing*, 2: 315–327.

Watson, R. and Haeberli, W. (2004). Environmental threats, mitigation strategies and high-mountain areas. *Ambio Special Report*, 13: 2–10.

Watts, R. D. and England, A. W. (1976). Radio-echo sounding of temperate glaciers: ice properties and sounder design criteria. *Journal of Glaciology*, 17 (75): 39–48.

Watts, R. D. and Wright, D. L. (1981). Systems for measuring thickness of temperate and polar ice from the ground or from the air. *Journal of Glaciology*, 27 (97): 459–469.

Welch, B., Pfeffer, W., Harper, J., and Humphrey, N. (1998). Mapping subglacial surfaces of temperate valley glaciers by two-pass migration of a radio-echo sounding survey. *Journal of Glaciology*, 40 (146): 164–170.

WGMS (1989). *World Glacier Inventory – Status 1988*. IAHS (ICSI) / UNEP / UNESCO, World Glacier Monitoring Service, Zurich, Switzerland.

WGMS (2008a). *Fluctuations of Glaciers 2000-2005 (Vol. IX)*. ICSU (FAGS) / IUGG (IACS) / UNEP / UNESCO / WMO, World Glacier Monitoring Service, Zurich, Switzerland.

WGMS (2008b). *Global Glacier Changes: facts and figures*. UNEP, World Glacier Monitoring Service, Zurich, Switzerland.

WGMS (2011). *Glacier Mass Balance Bulletin No. 11(2008-2009)*. ICSU(WDS) / IUGG(IACS) / UNEP / UNESCO/WMO, World Glacier Monitoring Service, Zurich, Switzerland.

Wilby, R., Charles, S. P., Zorita, E., Timbal, B., Whetton, P., and Mearns, L. (2004). Guidelines for use of climate scenarios developed from statistical downscaling methods. Tech. rep., Data Distribution Centre of the International Panel of Climate Change (IPCC).

Wipf, A. (1999). Die Gletscher der Berner, Waadtländer und nördlichen Walliser Alpen. Ph.D. thesis, Geographisches Institut, Universität Zürich.

Zappa, M., Pos, F., Strasser, U., Warmerdam, P., and Gurtz, J. (2003). Seasonal water balance of an alpine catchment as evaluated by different methods for spatially distributed snowmelt modelling. *Nordic Hydrology*, 34 (3): 179–202. doi: 10.2166/nh.2003.012.

Zemp, M., Kääb, A., Hoelzle, M., and Haeberli, W. (2005). GIS-based modelling of glacial sediment balance. *Zeitschrift für Geomorphologie*, 138: 113–129.

Zemp, M., Haeberli, W., Hoelzle, M., and Paul, F. (2006). Alpine glaciers to disappear within decades? *Geophysical Research Letters*, 33 (13): L13504. doi: 10.1029/2006GL026319.

Zemp, M., Haeberli, W., Bajracharya, S., Chinn, T., Fountain, A., Hagen, J., Huggel, C., Kääb, A., Kaltenborn, B., Karki, M., Kaser, G., Kotlyakov, V., Lambrechts, C., Li, Z., Molnia, B., Mool, P., Nellemann, C., Novikov, V., Osipova, G., Rivera, A., Shrestha, B., Svoboda, F., Tsvetkov, D., and Yao, T. (2007). Glaciers and ice caps. Part I: Global overview and outlook. Part II: Glacier changes around the world. In: *UNEP: Global*

outlook for ice & snow, pp. 115–152. UNEP/GRID-Arendal, Norway.

Zemp, M., Paul, F., Hoelzle, M., and Haeberli, W. (2008). Glacier fluctuations in the European Alps 1850-2000: an overview and spatio-temporal analysis of available data. In: *The darkening peaks: Glacial retreat in scientific and social context*, (edited by Orlove, B., Wiegandt, E., and Luckman, B.), pp. 152–167. University of California Press.

Zemp, M., Hoelzle, M., and Haeberli, W. (2009). Six decades of glacier mass balance observations - a review of the worldwide monitoring. *Annals of Glaciology*, 50: 101–111.

Zumbühl, H., Steiner, D., and Nussbaumer, S. (2008). 19th century glacier representations and fluctuations in the central and western European Alps: An interdisciplinary approach. *Global and Planetary Change*, 60 (1–2): 42–57. doi: 10.1016/j.gloplacha.2006.08.005.

Part II

Research papers

Paper I

Linsbauer, A., Paul, F., Hoelzle, M., Frey, H., and Haeberli, W. (2009). The Swiss Alps without glaciers – a GIS-based modelling approach for reconstruction of glacier beds. In: *Proceedings of Geomorphometry 2009*, (edited by Purves, R., Gruber, S., Straumann, R., and Hengl, T.), pp. 243–247. University of Zurich, Zurich, Switzerland

The Swiss Alps Without Glaciers – A GIS-based Modelling Approach for Reconstruction of Glacier Beds

A. Linsbauer[1], F. Paul[1], M. Hoelzle[2], H. Frey[1], W. Haeberli[1]

[1]Glaciology, Geomorphodynamics and Geochronology
Department of Geography, University of Zurich
Winterthurerstrasse 190
CH-8057 Zurich, Switzerland
Telephone: +41 44 635 51 57
Fax: +41-44-635 68 41
Email: andreas.linsbauer@geo.uzh.ch

[2]Department of Geosciences, University of Fribourg
Chemin du Musée 4
CH-1700 Fribourg, Switzerland

1. Introduction

Due to the ongoing and expected future increase in global mean temperature, the Alpine environment will continue to depart from equilibrium (Watson and Haeberli 2004). As glaciers form a significant part of the mountain cryosphere and their changes are considered to be the best natural indicators of climatic change (IPCC 2007), they constitute a key indicator within global climate related observing programs (Haeberli 2004). The already observed as well as the expected changes in glacier geometry and volume could have large impacts on global (sea level rise), regional (water supplies) and local scales (natural hazards, hydropower). The calculation and visualization of future glacier development thus plays a vital role in communicating climate change effects to a wider public (Paul et al. 2007).

Of particular interest regarding hydrological aspects is the water volume that is stored in the glaciers (Jansson et al. 2002). This requires information on the glacier bed which is only accessible after the glacier has disappeared (e.g. Maisch and Haeberli 1982). Otherwise, glacier thickness has to be obtained in the field at discrete points or profiles using a range of techniques (e.g. GPR, seismic or drilling). The spatial extra- and interpolation of this local thickness information for reconstruction of the entire glacier bed is again based on a wide range of methods and assumptions with related uncertainties, but at least mean glacier thickness values can be derived. In order to overcome the scarcity of available measurements, a set of empirical (e.g. Chen and Ohmura 1990, Maisch and Haeberli 1982) or more physically based (Driedger and Kennard 1986, Haeberli and Hoelzle 1995) relationships have been proposed to obtain glacier volume for large samples of glaciers.

Apart from the amount of available water stored in glaciers, there is also an urgent need to have topographic information on the glacier bed itself. Anticipation and quantitative modelling of changes in surface topography and characteristics in large regions related to future climate change, and corresponding developments (landscape evolution, water cycle modifications, natural hazard potentials, tourism, hydropower, etc.) in cold mountain regions has become an important task. In this respect, an estimated topography of the glacier bed would facilitate a large number of applications including the visualization of future ice-free ground. Using examples from the Swiss Alps, this contribution presents a fast and robust GIS-based approach to construct digital elevation models (DEMs) “without glaciers” in currently glacierized mountain chains from a minimum set of input data (DEM, glacier outlines and flowlines).

2. Method

The glacier surface reflects a smoothed image of the underlying bed. One basic parameter that influences glacier thickness is mean slope: the steeper the glacier, the thinner the ice and vice versa. This relation is also given from the so-called shallow ice approximation (SIA) which is a theoretical concept for highly idealized glacier geometries (Paterson 1994), but has been shown to reveal good results compared to more comprehensive approaches (Leysinger Vieli and Gudmundsson 2004). The required calculation of the mean basal shear stress in our approach is based on data from late glacial glacier geometries (Maisch and Haeberli 1982) and a concept that calculates average shear stress as a function of mass turnover determined by vertical extent (Haeberli and Hoelzle 1995). This concept was applied to large glacier ensembles, using numerical information as available in detailed glacier inventories (Haeberli and Hoelzle 1995). Corresponding thickness and volume estimates for individual glaciers thereby became much more realistic as glaciers are 3-dimensional rather than planar bodies, and flow-related glacier thickness is primarily slope rather than area dependent. A decisive further step is introduced by combining this approach with geomorphometric analysis of DEMs and automated GIS-based data processing, which now make ice-depth estimates possible for individual parts of glaciers (Linsbauer 2008).

The method requires only the DEM, glacier outlines and a set of flowlines for individual glacier branches. For each glacier, an average basal shear stress is then estimated as a function of vertical extent, and ice depth is calculated along selected points of the flowlines as a function of surface slope (Fig. 1). The subsequent spatial interpolation of the thickness values is performed with the topogrid interpolation as implemented in the GIS software Arc/Info from ESRI. Topogrid has been designed to generate hydrologically consistent DEMs from elevation contours/points and other vector data (Hutchinson 1989), resulting in preferably concave-shaped landforms. It is thus well suited to mimic the typical parabolic shape of glacier beds without explicitly considering mass fluxes as applied in the approach by Farinotti et al. (in press). The most time consuming part of the work is the determination of flowlines on the individual glacier branches. For various reasons, this digitizing is still best and most reliably made by hand, starting at the lower end of the glacier tongue and cutting at a right angle through the elevation contour lines of the glacier surface.

The developed method is a raster-based GIS-tool, which is implemented in a short Arc Macro Language (AML) script. The basic steps of modelling are illustrated in Fig. 1 along with a schematic diagram of the modelled parameters. The steps are: (a) data preparation, (b) calculation of glacier thickness for base points of the flowlines from the SIA using mean slope for 50 m elevation bands, (c) spatial densification of base points along the flow lines using an IDW interpolation, and (d) the interpolation of the bed with topogrid and addition of the bed elevations to the DEM. When all input data (DEM, glacier outlines, flowlines) are prepared, a few hundred glacier beds are automatically calculated in a short time (minutes).

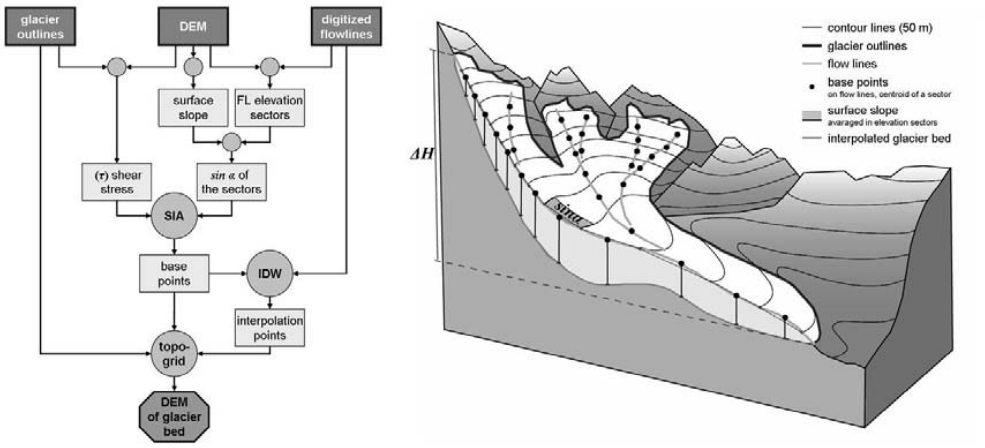

Figure 1. Flowchart of the method and schematic diagram of the modelled parameters.

3. Fields of Application

As mentioned above, the basic intention behind the development of this approach lies in the reconstruction of glacier beds over large regions, e.g. the entire Swiss Alps. The direct result is (1) an ice thickness distribution of all glaciers (Fig. 2) and (2) a DEM without glaciers (Fig. 3). From these data sets a number of further products and applications can be derived. At first, (3) mean thickness and (4) total volumes can be derived for each glacier in the sample. A comparison of (1) and (3) with direct measurements or results from other (more generalized/sophisticated) approaches can be performed, while (4) yields improved estimates of available water resources in the respective region.

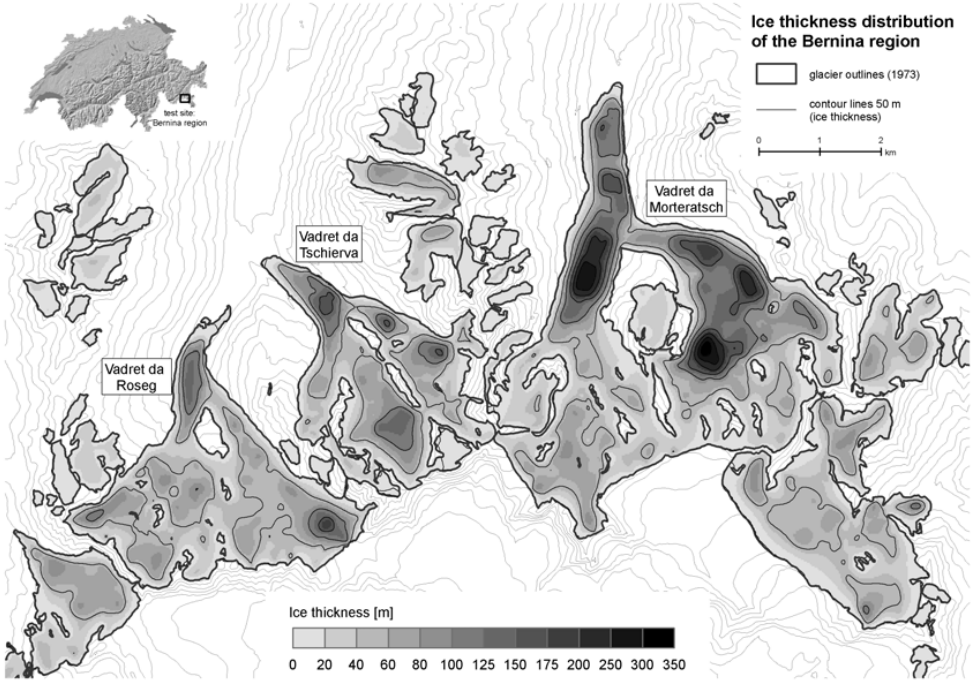

Figure 2. Modelled ice thickness distribution of the entire Bernina region, Switzerland. Reproduced by permission of swisstopo (BA091300).

A direct application of (2) is (5) the detection of overdeepenings in the glacier bed which can be easily visualized in the GIS by filling-up the depressions (Fig. 3). Dependent on the sedimentary nature of the glacier bed (Maisch et al., 1999), the depressions can fill with water and form lakes in the glacier forefield after the glacier has disappeared. These potential future lake formation sites can pose a hazard to downstream communities when the lake is located underneath steep rock walls or hanging glaciers (e.g. Haeberli and Hohman 2008). The glacier bed topography will also (6) facilitate the modelling of flow paths of potential outburst floods, which might help for the planning of mitigation measures (Rothenbühler 2006).

Furthermore, (7) a more realistic visualization of future glacier change than in Paul et al. (2007) can be achieved when the lost volume is eroded from the DEM and the bedrock becomes visible. Combined with a mass balance and hydrological model, the glacier beds can also be used for (8) improved modelling of changes in run-off from glacierized catchments (Huss et al. 2008). Finally, the bedrock can also serve as (9) an input for glacier flow models.

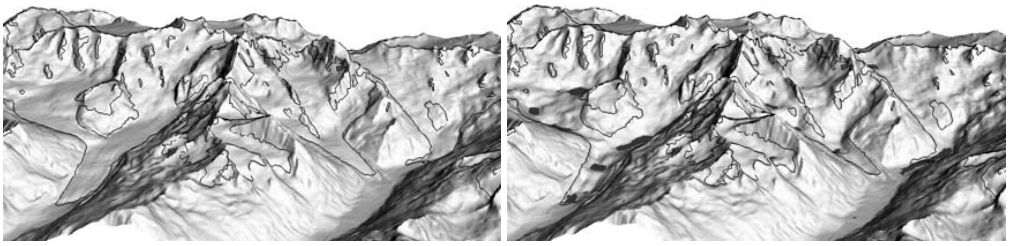

Figure 3. Input data and modelled glacier bed topographies with detected overdeepenings (potential lake formation sites) in the Bernina region, Switzerland. Reproduced by permission of swisstopo (BA091300).

4. Discussion and Conclusion

This simple approach of calculating glacier beds from geomorphometric properties of the glacier surface alone has of course several shortcomings. However, the modelled glacier beds were in a good agreement with field measurements (GPR profiles) and results from more complex approaches as described by Farinotti et al. (in press). Our approach is independent of glacier size and can be adjusted to different glacier types or climatic settings by considering glacier specific values of the form factor or a different calculation of the basal shear stress (τ) from the elevation range, respectively. It is also possible to incorporate a more localized (slope-dependent) calculation of τ for each glacier (e.g. Driedger and Kennard 1986) to consider the effect of higher shear stresses in steep ice falls than in flat glacier parts (Haeberli and Schweizer 1988). However, these modifications only change the estimated ice thickness of a glacier without influencing the general shape of the modelled glacier bed. Changing of the latter can only be achieved by digitizing new flowlines.

Apart from the required further validation of our approach with independent field data and more specific calculation of some parameters, we see a large potential for Alpine-wide application of the approach in the context of forthcoming climate change impact studies and hydrological assessments.

References

Chen J and Ohmura A, 1990, Estimation of Alpine glacier water resources and their change since the 1870s. *IAHS* 193:127-135.

Driedger C and Kennard P, 1986, Glacier volume estimation on cascade volcanos: an analysis and comparison with other methods. *Annals of Glaciology* 8:59-64.

Farinotti D, Huss M, Bauder A, Funk M and Truffer M, 2009, A method to estimate ice volume and ice thickness distribution of alpine glaciers. *Journal of Glaciology* 55(191):422-430.

Haeberli W, 2004, Glaciers and ice caps: historical background and strategies of world-wide monitoring. In: Bamber JL and Payne AJ (eds), *Mass Balance of the Cryosphere*, Cambridge University Press, Cambridge, 559-578.

Haeberli W and Hoelzle M, 1995, Application of inventory data for estimating characteristics of and regional climate-change effects on mountain glaciers: a pilot study with the European Alps. *Annals of Glaciology* 21:206-212.

Haeberli W and Hohmann R, 2008, Climate, Glaciers and Permafrost in the Swiss Alps 2050: Scenarios, Consequences and Recommendations. In: *Proceeding of the 9th International Conference on Permafrost*, Fairbanks, Alaska, USA.

Haeberli W and Schweizer J, 1988, Rhonegletscher 1850: Eismechanische Überlegungen zu einem historischen Gletscherstand. *Mitteilung VAW/ETHZ* 94:59-70.

Huss M, Farinotti D, Bauder A and Funk M, 2008, Modelling runoff from highly glacierized alpine drainage basins in a changing climate. *Hydrological Processes* 22(19):3888-3902.

Hutchinson M, 1989, A new procedure for gridding elevation and stream line data with automatic removal of spurious pits. *Journal of Hydrology* 106(3-4):211-232.

IPCC, 2007, *Climate Change 2007. The scientific basis*. Technical report, WMO/UNEP. Cambridge University Press, New York.

Jansson P, Hock R and Schneider T, 2003, The concept of glacier storage: a review. *Journal of Hydrology* 282(1-4):116-129.

Leysinger Vieli GJMC and Gudmundsson GH, 2004, On estimating length fluctuations of glaciers caused by changes in climatic forcing, *Journal of Geophysical Research – Earth Surface* 109:F01007.

Linsbauer A, 2008, *Modellierung von Gletscherbetten mit GIS*. Diploma thesis, Geographisches Institut, Universität Zürich.

Maisch M and Haeberli W, 1982, *Interpretation geometrischer Parameter von Spätglazialgletschern im Gebiet Mittelbünden, Schweizer Alpen*. Schriftenreihe Physische Geographie, Universität Zürich 1:111-126.

Maisch M, Haeberli W, Hoelzle M and Wenzel J, 1999, Occurrence of rocky and sedimentary glacier beds in the Swiss Alps as estimated from glacier-inventory data, *Annals of Glaciology* 28:231-235.

Paterson W, 1994, *The physics of glaciers*, Pergamon-Press, Oxford.

Paul F, Maisch M, Rothenbuehler C, Hoelzle M and Haeberli W, 2007, Calculation and visualisation of future glacier extent in the Swiss Alps by means of hypsographic modelling. *Global and Planetary Change* 55(4):343-357.

Rothenbühler C, 2006, *GISALP - Räumlich-zeitliche Modellierung der klimasensitiven Hochgebirgslandschaft des Oberengadins*. Schriftenreihe Physische Geographie, Universität Zürich 50.

Watson R and Haeberli W, 2004, Environmental threats, mitigation strategies and high-mountain areas. *Ambio Special Report* 13:2-10.

Paper II

Paul, F. and Linsbauer, A. (2012). Modeling of glacier bed topography from glacier outlines, central branch lines, and a DEM. *International Journal of Geographical Information Science*, 26 (7): 1173–1190. doi: 10.1080/13658816.2011.627859

International Journal of Geographical Information Science
Vol. 26, No. 7, July 2012, 1173–1190

Modeling of glacier bed topography from glacier outlines, central branch lines, and a DEM

Frank Paul* and Andreas Linsbauer

Department of Geography, University of Zurich, Zurich, Switzerland

(*Received 10 June 2011; final version received 15 September 2011*)

Due to the expected future climate change, glacier ice as a resource will be further diminished and its sea-level rise contribution further increased. A key for a more accurate determination of future glacier evolution is to improve our currently sparse knowledge on glacier bedrock topography. Here, we present a simplified method implemented in a geographic information system to approximate subglacial topography at a regional scale from spatial interpolation of local ice thickness values. The latter were derived from an ice-dynamical approach, which relates glacier thickness to its local surface slope, total vertical extent, and basal shear stress. The only input data required are glacier outlines, a set of central branch lines, and a digital elevation model (DEM). The modeled glacier beds are in good agreement with other, more complex modeling approaches and direct measurements. The observed local deviations can be explained with the sensitive dependence of our approach on the surface slope and the different methods used for spatial interpolation. The mean glacier thickness derived here for a sample of 40 glaciers in the Swiss Alps is slightly smaller than that derived from a similar, but scalar approach. Further adjustments of the data processing are possible to achieve agreement with available validation data. However, despite its local inaccuracies, the resulting DEM without glaciers can facilitate several applications such as the detection of overdeepenings or the modeling of future glacier evolution.

Keywords: glacier thickness; subglacial topography; DEM; surface slope; spatial interpolation; topogrid; map algebra

1. Introduction

Apart from the observed decline of glaciers around the world since their last maximum extent at the end of the Little Ice Age around 1850 (WGMS 2008), very rapid loss of glacier ice has been observed in the past two decades in the European Alps (e.g., Paul *et al.* 2004, Paul and Haeberli 2008) and many other parts of the world (e.g., Cogley 2009, Barry 2006, Kaser *et al.* 2006, Larsen *et al.* 2007). This rapid ice loss will continue or even accelerate in the future because (1) most glaciers have still not adjusted to current climatic conditions (Pelto 2006, Paul *et al*. 2007b, WGMS 2008), (2) a further increase in temperature can be expected according to recent climate change scenarios (IPCC 2007), and (3) reinforcement feedbacks (surface and albedo lowering, rock outcrops) increasingly influence glacier wastage (Raymond *et al.* 2005, Paul *et al*. 2007a, Oerlemans *et al.* 2009). As meltwater from glaciers plays an important role in local (hydropower, streamflow), regional

*Corresponding author. Email: frank.paul@geo.uzh.ch

ISSN 1365-8816 print/ISSN 1362-3087 online

http://dx.doi.org/10.1080/13658816.2011.627859
http://www.tandfonline.com

(freshwater, agriculture), and global hydrology (sea-level rise), a wide range of approaches have been developed to assess future glacier change and volume loss in glaciological or hydrological models.

With a focus on the regional scale, hydrological models are frequently used to assess climate change impacts on glaciers. Although these models can work with updated glacier-covered areas only (e.g., Verbunt *et al.* 2003, Koboltsching *et al* 2008, Stahl *et al*. 2008, Viviroli *et al*. 2009), more realistic and transient simulations of future glacier evolution require the knowledge of the subglacial topography also (e.g., Huss *et al.* 2008). As information about glacier beds is only sparsely available from direct measurements (e.g., transects from ground penetrating radar – GPR), numerical models are applied to reconstruct the bed of individual glaciers and assess their future evolution (e.g., Le Meur *et al.* 2007, Jouvet *et al*. 2009). Compared to these rather complex modeling approaches, recent studies have presented simplified approaches for glacier bed reconstruction that work for several glaciers (Farinotti *et al*. 2009b) or at the regional scale (Clarke *et al*. 2009). Still, these approaches are also computationally demanding and our goal is to develop a less challenging approach in terms of required input data, computational complexity, and processing speed that can be applied at a regional scale.

The research objectives of our new approach are (1) to obtain more realistic estimates of mean glacier thickness and total glacier volume for large samples of glaciers and (2) to have a digital elevation model (DEM) of the landscape without glaciers to facilitate the modeling and visualization of future glacier retreat scenarios over large regions. Further analysis of the modeled glacier beds might allow the detection of overdeepenings, which can be considered as potential sites of future lake formation. Such lakes can strongly enhance glacier melt and are also of interest for hydropower companies.

The developed method for the reconstruction of glacier beds is based on the study by Linsbauer (2008) and fully implemented in a processing scheme written in Arc Macro Language from the GIS software Arc/Info 9.0 (ESRI 2004). The method only requires glacier outlines, a DEM, and a set of digitized branch lines as input. It calculates slope-dependent ice thickness values according to Haeberli and Hoelzle (1995) for sectors of 50 m vertical equidistance along the branch lines. The glacier bed is then reconstructed (i.e., spatially extrapolated) from these local thickness values and the glacier outline with the *topogrid* routine developed by Hutchinson (1989) that was also applied by Fischer (2009) for spatial extrapolation of measured ice thickness values. Our method is largely based on map algebra combining several input grids (Etzelmüller and Bjørnsson 2000). It is thus computationally slim and applicable at a regional scale while maintaining the characteristics of individual glaciers.

In the following, we shortly describe the study region and the input datasets used, before we explain in Section 3 the physical background of the slope-dependent thickness-modeling approach along with a short review of previous works on the topic. We then describe the GIS implementation of our method and the rules for digitizing the branch lines. After the presentation of the results, we provide a quantitative evaluation of them and discuss the approach in more general terms. Major conclusions are given in the last section.

2. Study region

The test site for this study is the Bernina region (Grisons, Switzerland), a strongly glacierized mountain range in the Alps. Piz Bernina (46.4°N, 9.9°E) is at 4049 m a.s.l., the highest mountain peak in this region. We focus on the glaciers located mainly on the north-faced

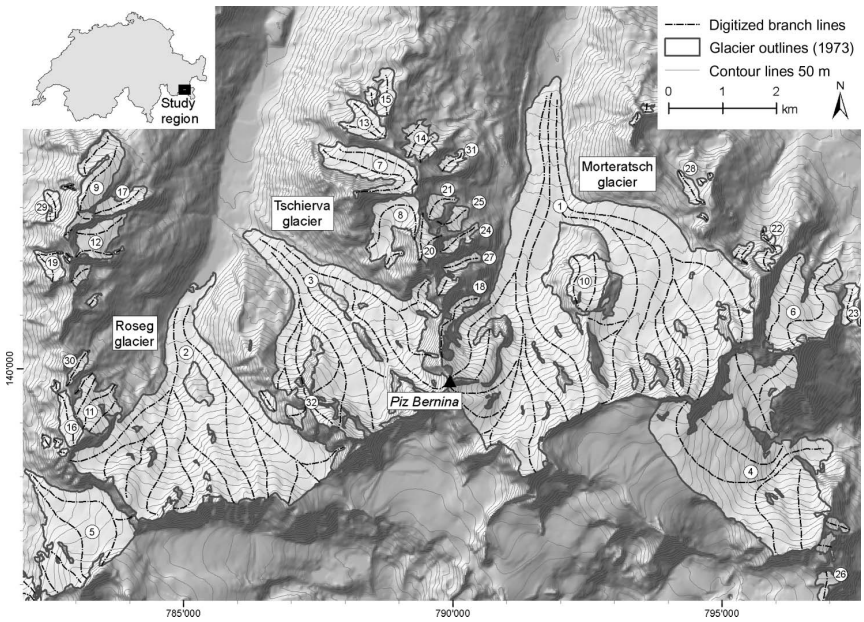

Figure 1. Location of the test site Bernina Group (see inset map) and input data (DEM25, contour lines, glacier outlines and branch lines) used drawn on a hillshade of the DEM25 from swisstopo.

Swiss side of the region, which includes three large valley glaciers (Morteratsch, Tschierva, and Roseg) and several (35) smaller mountain glaciers (Figure 1). Due to its easy access and impressive appearance, the Morteratsch glacier is maybe the most famous in the region. It stretches from nearly 4000 m down to 2020 m a.s.l., covers an area of about 16 km^2, and has been the target of several field and modeling studies (e.g., Hoelzle and Haeberli 1995, Klok and Oerlemans 2002, Paul *et al*. 2007b, Nemec *et al*. 2009). There is also a large interest in the impact of climate change on landscape evolution in this region, as tourism is a vital economic factor (Rothenbühler 2006).

3. Methods

3.1. Physical background

While large parts of the current subglacial topography originated from glacial erosion during the Last Glacial Maximum (e.g., Brocklehurst *et al*. 2008, Benn and Evans 2010), contemporary glaciers also contribute by erosion and sedimentation processes to the further evolution of the bedrock (e.g., Boulton 1979, Hallet *et al*. 1996, Burki *et al*. 2009). Assuming that the latter contribution is small compared to the already existing bedrock, today's glaciers basically fill this bedrock, with the glacier surface being a smoothed mirror of the underlying bed (Oerlemans 2001). Thereby, the thickness of the ice is largely governed by its surface slope (the steeper the surface, the thinner the ice and vice versa). The related equation can be derived by introducing some simplifications to the force budget that acts on a cube of ice (e.g., Oerlemans 2001): if ideal plasticity of the ice is assumed,

basal sliding is neglected, and the ice body has a horizontal extent that is much larger (about 10 times) than its vertical extent, the ice thickness d (m) depends on the slope α (degrees) and basal shear stress τ (Pa) in the following way:

$$d = \frac{\tau}{(\rho g f \sin\alpha)} \tag{1}$$

where ρ is the density of the ice (900 kg/m^3), g the acceleration due to gravity (9.81 m/s^2), and f the shape factor (here set constant to 0.8). The latter refers to the ratio between the cross-sectional area of the glacier and its perimeter and is related to the friction of a real glacier with the valley walls. The value of 0.8 is typical for valley glaciers and can be smaller for other glacier types (cf. Paterson 1994). In Figure 2a, the ice thickness as calculated by Equation (1) is illustrated for different values of α and τ. The graph illustrates two general principles: (a) the smaller the slope, the thicker the ice and (b) thickness is increasingly sensitive to surface slope toward smaller values of slope. An ice mass with zero slope does not flow, that is, $\tau = 0$ and thus $d = 0$ (see Equation (1)).

When Equation (1) is used to calculate glacier thickness, τ must be derived by other means. While a constant value of 1 bar (10^5 Pa) often serves as a good starting point (Binder *et al*. 2009, Clarke *et al*. 2009), Haeberli and Hoelzle (1995; hereafter HH95) used a glacier-specific empirical relation proposed by Maisch and Haeberli (1982). The relation is based on the analysis of topographic parameters from 62 previously existing late-glacial ice bodies (that were rather similar in size and shape to today's glaciers) and is thus based on real glacier beds. It relates τ to the elevation range Δh of a glacier using a quadratic regression to all data points:

$$\tau = 0.005 + 1.598\Delta h - 0.435\Delta h^2 \tag{2}$$

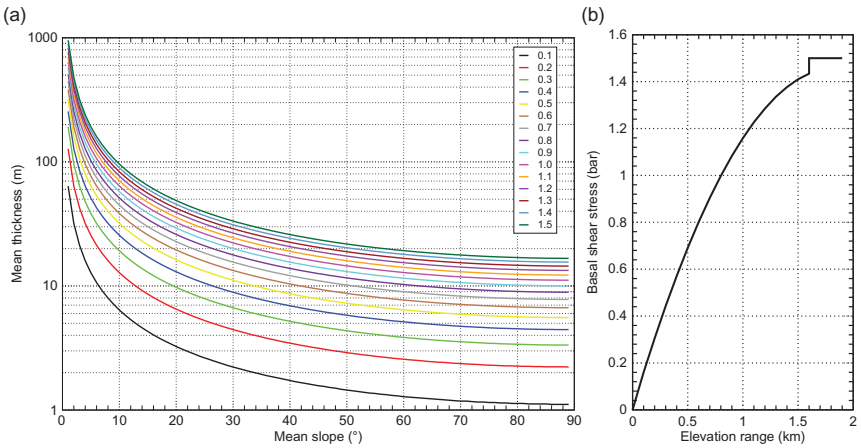

Figure 2. Illustration of the basic relations used for the ice thickness calculation. (a) Mean thickness versus slope for 15 distinct values of τ (from 0.1 to 1.5) according to Equation (1). (b) Mean basal shear stress τ versus elevation range Δh according to Equation (2). For an elevation range >1.6 km τ is set constant to 1.5 bar.

with Δh in km and τ in bar using a maximum value of $\tau = 1.5$ bar for Δh equal to or larger than 1.6 km (see Figure 2b). By relating τ to the elevation range of a glacier, the approach implicitly accounts for variations in mass turnover for differently sized glaciers (Haeberli and Schweizer 1988). For the same mean slope, a smaller glacier (i.e., with a smaller elevation range) gets a lower mean thickness. For special cases such as hanging glaciers, cold-based ice, or very small glaciers (<0.1 km^2), the method might give inaccurate results.

3.2. Previous works

With Equations (1) and (2), a scalar method (named here as type A) is available to calculate the mean thickness (and hence volume) for entire glaciers. The related method was applied in the case study by HH95 to all glaciers in the Alps larger than 0.2 km^2 using tabulated glacier inventory data. With the calculation of a slope-dependent mean thickness, the approach can reproduce that glaciers with the same size can have different mean thickness values and hence volumes. This is not possible when only glacier size is used to approximate mean thickness, like in the approaches by Müller *et al.* (1976) and Maisch *et al*. (2000). However, these are based on empirical relationships and can also be used for thickness determination of large glacier samples with small computational effort.

Another type of calculating mean glacier thickness can be applied when a reconstructed DEM of the glacier bed is available (type B). In this case, mean thickness results from the arithmetic mean of all grid cells with depth information within the respective glacier extent. Primarily, these glacier beds are derived from more or less dense field measurements of glacier thickness (e.g., along transects with a GPR) that are inter- and extrapolated to a continuous glacier bed using a variety of methods (e.g., Brückl 1970, Welch *et al*. 1998, Bauder *et al*. 2003, Span *et al*. 2005, Binder *et al*. 2009, Fischer 2009). In principle, these beds can be considered as a ground truth, but in regions without GPR measurements glacier thickness is only computed and might be rather different from reality. The thickness values also vary with the interpolation method applied (Fischer 2009). Due to the workload related to the field work and the later calculations, glacier bed topographies (i.e., a reconstructed DEM of the bedrock under the glacier) are only available for a few glaciers.

In order to largely extend the sample of reconstructed glacier beds for improved assessment of climate change impacts (e.g., future glacier volume evolution), simplified modeling approaches have been developed in the recent past to obtain glacier bed topography from other data. As the real glacier bed becomes only visible after the respective glacier has disappeared (Vanuzzo and Pelfini 1999), general relations for real glacier beds can be derived from currently ice-free regions that were glaciated in the past. Such an approach was presented by Clarke *et al*. (2009), who used the analogy of contemporary glacier beds to deglaciated terrain to train an artificial neural network (ANN) for modeling of glacier beds in western Canada. Considering the limitations of such a statistical approach to reflect the large variability of real glaciers, the ANN reconstructed subglacial topography rather well. However, the computational costs of the approach are high and a repeated application in overlapping 50 × 50 km tiles is required to cover a larger mountain range (Clarke *et al*. 2009).

When additional data on glacier mass balance and flow are available, the glacier bed can also be approximated from a numerical glacier flow model (e.g., Hubbard *et al*. 1998) that calculates glacier thickness along a given central flow line from an iterative adjustment of the glacier cross section to the prescribed mass flux. A similar approach was applied with some further simplifications by Farinotti *et al*. (2009a) to individual glaciers

of the Swiss Alps in combination with a distributed mass balance model and measured surface elevation changes. Measured cross sections derived by GPR profiles were used to calibrate the model parameters. This method also worked well for a larger sample of glaciers where the required input and calibration data were definitely available (Farinotti *et al*. 2009b).

Our approach is closer to Clarke *et al*.'s (2009), but has lower computational costs and considers the characteristics of individual glaciers explicitly. It basically transforms the approach by HH95 (type A) for calculation of glacier thickness from slope and elevation range to a spatially explicit reconstruction of the glacier bed (type B) using a DEM, digitized glacier outlines, and a set of branch lines in combination with the *topogrid* tool. *Topogrid* is based on the so-called ANUDEM algorithm and has been designed to build hydrologically correct DEMs from elevation data by Hutchinson (1989). For continuous depth data inside an outer polygon with a constant elevation (e.g., the glacier outline), *topogrid* automatically generates a depression with a parabolic shape. It is thus well suited to mimic the typical shape of glacier beds. *Topogrid* was also used by Fischer (2009) to interpolate GPR soundings of Austrian glaciers. In contrast to that study, our approach uses modeled rather than measured depth points for the interpolation.

3.3. Input data

Three input data sets are required for our method: a DEM, glacier outlines, and a set of manually digitized centre lines of major glacier branches (named branch lines in the following). The DEM used here is the 25 m spaced level 2 DEM from swisstopo (DEM25) with glacier surface elevations referring to ca.1991 in this region and covering 700 × 540 cells (17.5 × 13.5 km). Glacier outlines were taken from the digitized Swiss glacier inventory (Maisch *et al.* 2000, Paul 2007) and refer to the 1973 glacier extent. Due to the small overall area changes for most glaciers between 1973 and 1985 (Paul *et al.* 2004), these outlines still fit to the DEM25. However, for some of the large glaciers in the region, the retreat between 1973 and 1991 is recognizable, but without impacting the modeling (see Section 3.4). For the purpose of raster-based processing, the glacier polygons were additionally converted to a 25 m grid. The digitizing of the branch lines is based on the national topographic maps (1:25,000), a shaded relief of the DEM25, and the elevation contour lines with 50 m equidistance (Figure 1). The applied digitizing rules are based on empirical tests (see Section 4.1).

3.4. GIS implementation

To a large degree, the procedure used here for raster-based modeling of glacier beds with a GIS is based on map algebra, that is, the main calculations are arithmetical operations on input map layers on a cell-by-cell basis. Such a procedure was also applied by Etzelmüller and Björnsson (2000), who calculated glacial and subglacial parameters for the Vatnajøkull icecap in Iceland. The implementation of our modeling approach is illustrated in Figure 3 with a flowchart illustrating the individual processing steps and a schematic diagram of a glacier displaying the modeled parameters. To give the implementation some structure, we have separated it into four basic steps that are discussed in more detail below. These steps are (1) data preparation, (2) calculation of glacier thickness for the base points, (3) a spatial densification of the base points along the branch lines, and (4) the interpolation of the ice thickness distribution with *topogrid*. Mean ice thickness is finally calculated for each glacier as the arithmetic mean of all thickness values within the respective glacier outline.

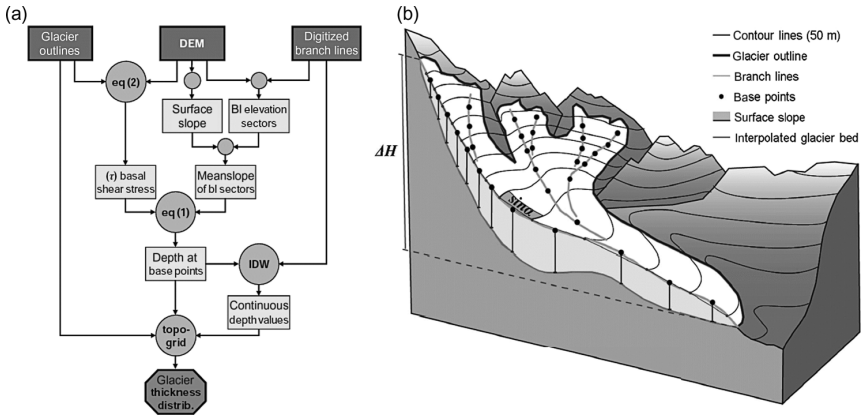

Figure 3. (a) Schematic summary of the basic processing steps for glacier bed interpolation in a flowchart (squares denote datasets and circles denote GIS-based calculations), with eq, equation; IDW, inverse distance weighting; bl, branch line. (b) This schematic perspective view illustrates the basic parameters used for glacier bed modeling.

Data preparation (step (1)) includes the digitization of branch lines (see Section 4.1), as well as the calculation of τ and α from the DEM. While τ is calculated from Δh using Equation (2) and stored in a separate grid with identical values for each cell of a specific glacier, the slope is derived from the DEM and smoothed with a focal mean filter of variable kernel size. For slopes $<5°$, a 7×7 kernel was applied; for a slope range from 5° to 20°, a 5×5 kernel was used; and for slopes $>20°$, a 3×3 kernel was used. This distinction is required because towards flat slopes the calculated thickness is increasingly sensitive to the slope values (Figure 2a). Moreover, the DEM25 reflects several small-scale topographic structures of the glacier surface (e.g., crevasses, seracs, moulins, moraines) that can have an influence on the calculated local slope value and should thus be smoothed.

In the next step (2), the branch lines were converted to 100 m raster cells and then segmented in sectors of 50 m elevation range using the DEM. For each branch line sector, the mean slope is calculated from the smoothed slope grid and assigned to the centroid cell of each sector. This procedure guarantees that slope is automatically averaged over a longer distance in flat glacier parts than in steeper parts as required to apply Equation (1). Glacier thickness is then calculated for the centroid cells of each elevation sector from Equation (1) using the mean slope values and the grid with glacier-specific values of τ. The centroid cells were then converted to point features (vector) with the thickness values assigned. They form the base points for the interpolation in the next step.

In order to have continuous thickness values along the branch lines at the bed (see Section 4.1), additional thickness values are calculated between the base points (step (3)). For this purpose, an inverse distance weighted (IDW) interpolation is applied to all thickness values at the base points using a standard set-up (radius: 5 times the cell size; minimum number of points: 2; power: 2.0). From the resulting interpolated grid with thickness values (for the entire glacier), only the cells under the branch lines are selected and converted back to the vector format (point features). We thus have now a continuous (25 m spacing) set of depth values along the branch lines (similar to the depth values from GPR profiles) that can be used for spatial interpolation.

In the final step (4), the *topogrid* interpolation uses the thickness values from steps (2) and (3) and the glacier outlines (that act as breaklines for the interpolation and have an elevation of 0) to interpolate the thickness values for each glacier to a continuous grid. Subtraction of this thickness grid from the original DEM gives a DEM without glaciers and hence the glacier bed topography.

4. Results

4.1. Digitizing of branch lines

The correct digitizing of the branch lines is a rather critical issue for our approach. We have thus tested beforehand which rules have to be followed for the digitizing to achieve adequate results with *topogrid*. The empirical tests were performed with a set of artificial branch lines at a specific depth (100 m) and an outer polygon of rectangular shape on flat and inclined planes (Figures 4 and 5). These tests helped to constrain (1) whether the interpolation should be performed on a flat (entire outline at zero elevation) or inclined plane, (2) the density of required branch lines per glacier/tributary, (3) the location of their start and end points, and (4) the required point density for an interpolation without artifacts. For the tests described below, the specifications for tolerances and iterations of *topogrid* were set to default and the 'drainage enforcement' was turned off (ESRI 2004).

Test (1) revealed that interpolation on an inclined plane resulted in considerable local artifacts (increasing with steepness) and was thus disregarded. Test (2) is illustrated in Figure 4a (upper panel) and b. For the given width of the depression, two branch lines

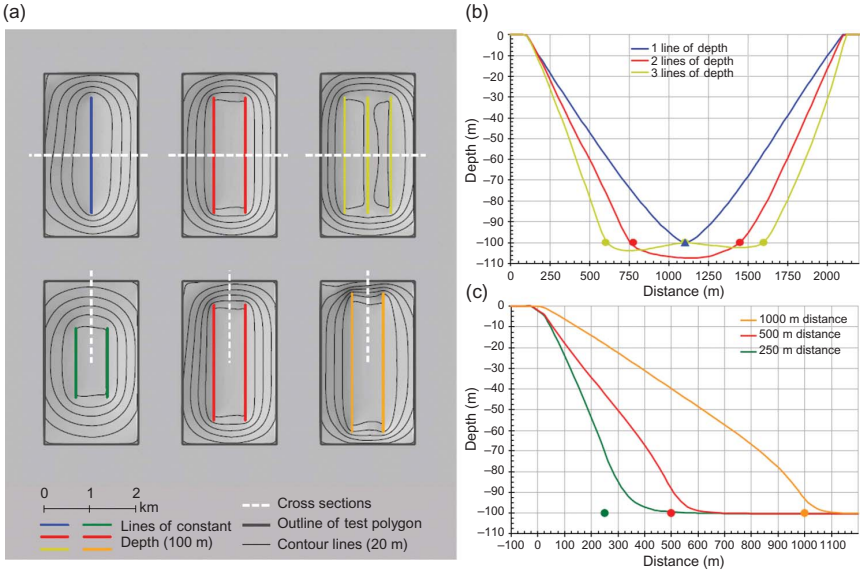

Figure 4. (a) Conceptual design of the experiments to determine the digitizing rules for the branch lines. Rectangular outer polygons with a variable number and length of branch lines at a constant depth of 100 m. (b) Cross sections through the interpolated glacier beds using one, two, and three parallel flowlines. (c) Longitudinal profiles through the interpolated glacier beds to determine the required distance of the branch line endpoints from the outer polygon.

revealed the most realistic (U-shaped) bed profile. With one branch line the cross section resulted in a V-shape; with three branch lines an undulating pattern at the bottom was modeled. This implies that for tributaries with more than one branch line, the distance to the glacier boundary should be sufficiently large. The endpoint location test (3) is depicted in Figure 4a (lower panel) and c. When the start/end point of the branch line comes too close to the boundary, an unrealistic abrupt transition is visible in the longitudinal cross section. When these points are placed some 100 m away from the glacier boundary, the *topogrid* interpolation creates a smooth and much more realistic transition (first of concave, then of convex curvature).

Test (4) is related to the required spacing of interpolation points and is depicted in Figure 5. Typically, the base points used for calculation of ice thickness can have a horizontal spacing of several hundred meters in flat parts of the glacier. While this spacing is required for averaging mean slope, it would result in local artifacts (bulls' eyes) at the location of each base point. For a decreasing distance, the amplitude of the artifacts becomes smaller and disappears at a 25 m spacing (Figure 5). This implies that additional thickness values have to be inserted between the base points before the bed is interpolated by *topogrid*.

The tests described above along with further tests on the 'real' glaciers in the Bernina region resulted in the following set of rules for the branch line digitizing (cf. Figure 1 for location):

- The lines should be digitized from bottom to top (easier than vice versa) and perpendicular to the elevation contour lines.

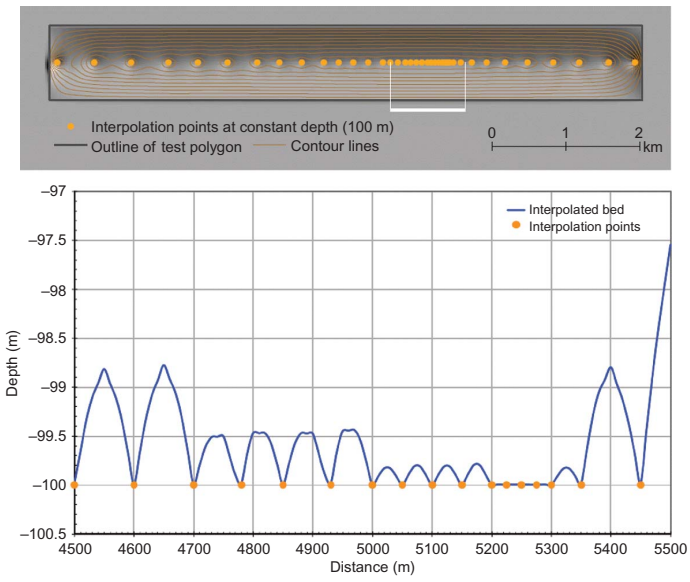

Figure 5. Illustration of interpolation artifacts resulting from a different spacing of the base points. At the top the entire bed is shown along with contour lines. The region marked in white is depicted in the cross section of the lower panel in detail.

- They should end about 100 m before the glacier outline (at the bottom and top).
- All important branches of a glacier should be covered. At confluence points, they should merge but without snapping (Figure 1).
- Local surface structures, which are related to erosion or accumulation processes (e.g., moraines, lakes, water channels, moulins), should not be crossed.
- For the tongues of larger valley glaciers, the branch lines should be digitized in parallel (one line for every 200–400 m of glacier width).

4.2. Modeling results

The modeled distribution of glacier thickness for the entire test site is illustrated in Figure 6. The image reveals that the thickest ice (200–300 m) is located in the large valley glaciers while the smaller mountain glaciers are comparably thin (20–30 m). Very small glaciers (<0.1 km^2) can have mean thickness values below 5 m which might be unrealistic. As assumed, overdeepenings are closely related to very flat regions of the respective glaciers. These flat parts are typically located in front of or behind steep slopes where the effects of glacier erosion are particularly strong (Haeberli and Schweizer 1988). However, such local overdeepenings can be found at all elevations and are not restricted to the glacier tongues (see Figure 6). For the Tschierva glacier tongue, we calculated some cross sections (see Figure 6 for location) to elevation values of the original DEM and the modeled bedrock (Figure 7a). While the parabolic shape of the bedrock can be recognized, it is also evident from Figure 7a that the elevations of the bed are derived by subtracting the modeled ice

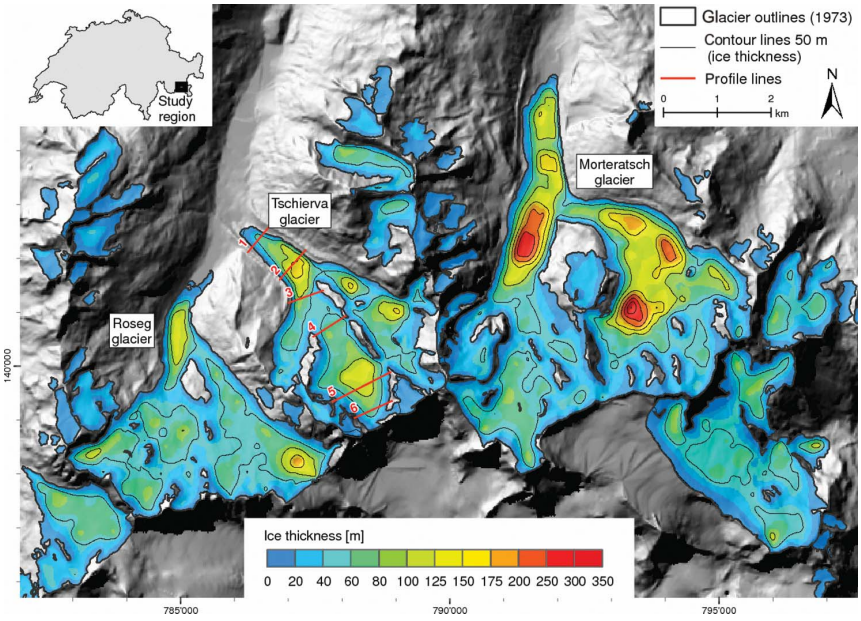

Figure 6. Modeled ice thickness distribution for the test site Bernina Group superimposed on a hillshade of the DEM25 from swisstopo.

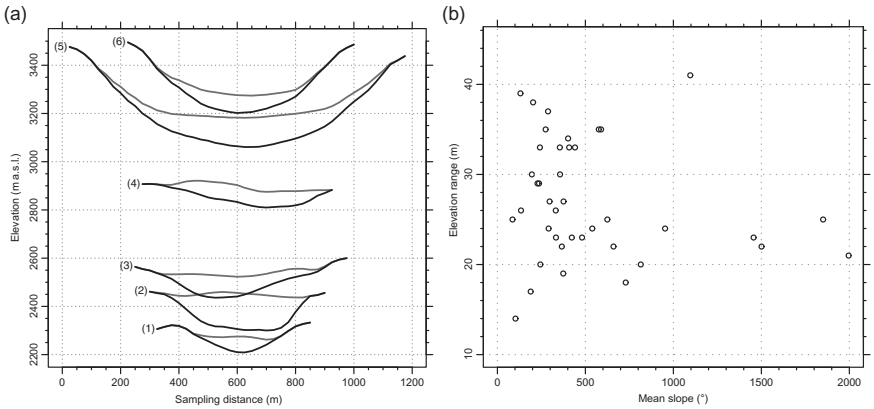

Figure 7. (a) Six cross sections through the original DEM (grey) and the modeled bedrock (black) for the Tschierva glacier (see Figure 6 for location of the numbered lines). (b) Scatter plot of glacier elevation range versus mean slope; both are derived from the DEM.

thickness from the surface DEM. Hence, the variability and artifacts of the surface DEM are transferred to the bedrock. This has to be considered when the modeled bedrock is used for other specific purpose (e.g., dynamical modeling).

Mean arithmetic (area-weighted) thickness for the entire sample of 40 glaciers is 20 m (50 m) for the method by HH95 and 16 m (46 m) for our GIS-based method. This relates to total glacier volumes of 2.62 and 2.43 km^3, respectively. The five largest glaciers account for about 91% of the total volume. In Table 1, the values for the glaciers >0.1 km^2 are summarized; values for smaller glaciers are not listed due to their high uncertainties.

The most important parameters for glacier thickness calculation in this study are elevation range Δh and mean slope α. In Figure 7b, we present the values in a scatter plot for the entire sample of 40 glaciers. In principle, large glaciers cover large elevation ranges and have small mean slopes and vice versa. This dependence is also obvious from Figure 7b, where elevation range increases with decreasing mean slopes. However, the scatter increases strongly towards glaciers with a smaller elevation range and some small glaciers with a small mean slope do exist as well. The figure also illustrates that only two glaciers have $\Delta h > 1.6$ km and thus $\tau = 1.5$ while for most glaciers Δh is < 500 m and τ thus below 0.7 bar. From Figure 2b, typical mean thickness values between 5 and 20 m can be derived for these values of Δh and τ.

5. Quantitative evaluation

As described before, a sound validation of the modeled glacier beds is difficult as the model is not designed to be exact at the local scale (e.g., GPR profiles) and available glacier beds in raster format were interpolated between the measurements as well (see Section 3). To nevertheless get an idea of the accuracy, we compare our results with datasets derived by three other methods: (1) the scalar method by HH95, (2) averaged thickness values obtained by GPR soundings at the Tschierva glacier, and (3) a modeled glacier bed obtained with the method developed by Farinotti *et al*. (2009b) for a glacier in a different location. We are aware that this way of comparing results might not be called validation, but it is at least compliant with the expected quality of our model results.

Table 1. Summary of glacier inventory parameters from 1973 and derived mean ice thickness and glacier volume for all glaciers >0.1 km^2 in the Bernina test region.

							h_{mean}		Volume	
No.	Name	Area	Δh	α	L_0	τ	HH95	GIS	HH95	GIS
1	MORTERATSCH VAD.	16.84	1996	21	7.49	1.5	65	65	1.091	1.094
2	ROSEG VADRET DA	8.78	1501	22	5.04	1.42	55	49	0.487	0.43
3	TSCHIERVA VAD.	7.03	1851	25	5.41	1.5	52	50	0.362	0.347
4	PALUE VADRET DA	6.64	1456	23	4.15	1.41	47	38	0.314	0.248
5	TREMOGGIA VAD.	2.53	729	18	2.98	0.94	44	40	0.111	0.099
6	CAMBRENA VADRET	1.72	953	24	2.36	1.13	34	32	0.058	0.055
7	MISAUN VADRET DA	1.02	815	20	2.82	1.02	41	39	0.041	0.039
8	TSCHIERVA V.IN	0.78	660	22	2.00	0.87	31	25	0.024	0.019
9	CORVATSCH VAD.	0.72	625	25	1.54	0.83	25	19	0.018	0.014
10	FORTEZZA VAD.	0.61	481	23	1.09	0.67	18	18	0.011	0.011
11	CHAPUETSCHIN VAD	0.60	539	24	1.11	0.74	19	19	0.011	0.011
12	MURTEL VADRET	0.47	374	19	1.09	0.54	19	15	0.009	0.007
13	MISAUN V.IN DA S	0.36	423	23	0.97	0.60	17	15	0.006	0.005
14	BOVAL DADOUR VAD	0.33	376	27	0.69	0.54	13	12	0.004	0.004
15	MISAUN V.IN DA N	0.31	333	23	0.88	0.49	15	8	0.005	0.002
16	CHAPUETSCH. V.IN	0.28	244	20	1.08	0.37	19	9	0.005	0.002
17	ALP OTA VAD. DA	0.26	366	22	1.11	0.53	19	10	0.005	0.003
18	X	0.22	1096	41	1.54	1.23	24	15	0.005	0.003
19	X	0.20	332	26	0.72	0.49	13	11	0.003	0.002
20	X	0.20	402	34	0.88	0.58	16	9	0.003	0.002
21	BOVAL DADAINS N	0.17	408	33	0.74	0.58	13	8	0.002	0.001
22	ARLAS VADRET D'	0.17	576	35	0.47	0.78	11	9	0.002	0.002
23	X	0.17	297	27	0.66	0.44	12	7	0.002	0.001
24	X	0.15	589	35	0.89	0.79	16	10	0.002	0.002
25	BOVAL DADAINS NE	0.15	356	30	0.71	0.52	13	8	0.002	0.001
26	VARUNA VED. DI	0.14	103	14	0.62	0.17	11	3	0.002	0.001
27	PRIEVLUS VADRET	0.13	441	33	0.76	0.63	14	9	0.002	0.001
28	X	0.13	189	17	0.81	0.29	14	8	0.002	0.001
29	MURTEL VADREC	0.13	355	33	0.57	0.52	11	8	0.001	0.001
30	X	0.11	291	24	0.80	0.43	14	9	0.002	0.001
31	BOVAL D'MEZ. VAD.	0.11	237	29	0.59	0.36	11	6	0.001	0.001
32	X	0.11	242	33	0.45	0.37	9	6	0.001	0.001

Note: Abbreviations denote (unit): Area (km^2); Δh, elevation range (m); α, mean slope (°); L_0, length (m); τ, basal shear stress (bar); h_{mean}, mean thickness (m); volume (km^3); HH95, according to Haeberli and Hoelzle (1995); GIS, according to the here presented approach.

5.1. Comparison with Haeberli and Hoelzle (1995)

The comparison with the study by HH95 might be considered as not fully independent as it is based on the same set of equations. However, the used input datasets are different (elevation range and length vs. slope from the DEM) and the way of calculating the mean thickness is also not the same (type A calculation vs. type B: mean slope for the entire glacier vs. local slope from a DEM). We thus consider both methods as independent enough for a direct comparison which is depicted in Figure 8a. Our approach gives values that are systematically smaller (–4.0 m) than those obtained by HH95 with a correlation coefficient of $R^2 = 0.97$. To a large extent, the difference can be explained with a higher mean slope as calculated from the DEM compared to the calculation from elevation range and length in HH95. We speculate that the systematic nature of the difference to HH95 will not be found in other samples.

5.2. Comparison with Tschierva and Morteratsch glaciers

In a recent study by Joerin *et al*. (2008), ice depth soundings were made at selected points of the lower part of the Tschierva glacier. These soundings revealed ice depths of about 130–160 m (measured from the 2007 glacier surface) in an overdeepening behind a steeper part of the glacier. This overdeepening is also modeled with our approach (Figure 6) and has a depth of about 150–170 m with reference to the glacier surface of 1991. Considering an overall surface lowering of about 10–20 m since that time and at this place, the modeled thickness agrees with the measured one. A comparison with GPR soundings from the Morteratsch glacier compiled by P. Huybrechts (Vrije Universiteit Brussel) indicates that the general shape of the glacier bed including the major overdeepenings is well captured, but locally larger deviations exist. In part, these are due to errors in the measurements (P. Huybrechts, personal communication) rather than in our model. We thus conclude that our approach is more suitable to reproduce the regional characteristics of a glacier bed rather than accurate values at a local scale (i.e., point locations).

5.3. Comparison with the Zinal glacier

We have also applied our model to the Zinal glacier in the Canton of Valais (Switzerland) to compare it with the result of the model developed by Farinotti *et al.* (2009b). This glacier has five major and comparably steep tributaries and a flat, debris-covered tongue. Of course, for a sound direct comparison, the same input datasets must be used. As these were not available for this study, we here provide only an image comparison of the derived ice thickness values (Figure 8b), but using the same grey shades and depth contour lines as in the related figure by Farinotti *et al.* (2009b). In that study, the bed was calibrated with several GPR profiles across the glacier tongue, so we assume that their result is realistic. Both thickness distributions are very similar at this visual scale, in depth as well as in the location of the deeper or shallower parts. As expected, local deviations exist, but

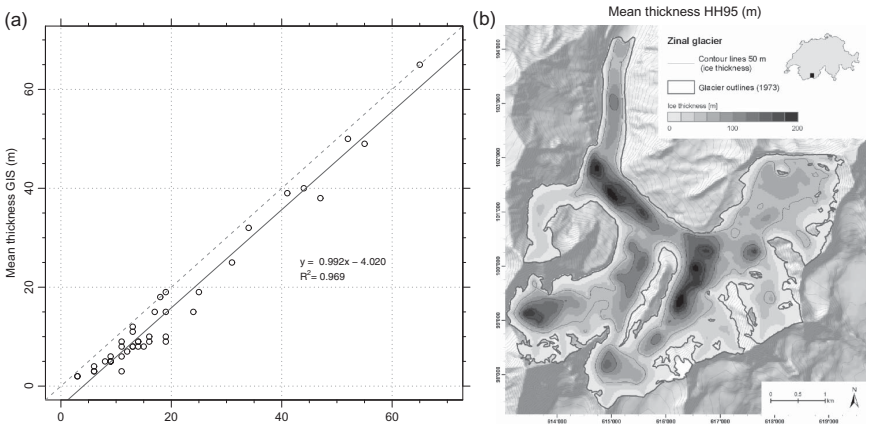

Figure 8. (a) Mean thickness obtained with our approach versus HH95, the approach by Haeberli and Hoelzle (1995). The dashed line is the identity and the solid line a linear regression. (b) Modeled ice thickness distribution of the Zinal glacier (Valais, Switzerland) in comparison with the results obtained by Farinotti *et al*. (2009b). The hillshade in the background is derived from the DEM25 from swisstopo.

they could be explained with the constraints imposed by the different input datasets and modeling approaches. The mean thickness of this glacier is 66 m for the year 2006 according to Farinotti *et al.* (2009a) and 55 m with our approach for the year 1998 (DEM from 1995), which is a difference of –17% in this case.

6. Discussion

6.1. Improvements of the input parameters

The presented approach of calculating glacier bed topography has been optimized to work very fast with few and widely available input data (glacier outlines, DEM, branch lines). The calculation of mean slope values for equidistant elevation intervals automatically adjusts the averaging distance to the mean slope and thus the thickness of the ice. However, the 50 m equidistance used here gives only distances that are about 5 times larger than the thickness (should be 10 times). This has to be considered when the model results are interpreted. The core of the fast performance lies in the raster-based calculation of glacier thickness values for an entire region that does not loop through individual glaciers. The interpolation of the thickness values with *topogrid* has the advantage of reproducing the parabolic shape of glacier beds very well, as the implemented ANUDEM algorithm is optimized for generating DEMs with concave shapes for correct hydrologic flow (Figure 7a). Of course, the rules for the digitization of branch lines have to be followed (see Section 4.1). Considering today's wide availability of DEM data (e.g., from Shuttle Radar Topography Mission (SRTM) or the Advanced Spaceborne Emission and reflection Radiometer (ASTER-GDEM)) and glacier outlines (e.g., from the Global Land Ice Measurements from Space (GLIMS) database), the main effort is in the digitization of the branch lines. With the acquired know-how from the digitizing tests (Section 4.1), it took about 1 hour to digitize all branch lines for the Bernina region.

The modeled glacier beds can be adjusted to local conditions when validation data (i.e., reconstructed glacier beds) are available. Such adjustments include re-digitizing of branch lines at a new position, the smoothing of the original DEM or the slope grid (with other filters or thresholds), the use of more glacier-specific shape factors (instead of 0.8), the application of a different interpolation technique for the densification of the base points (instead of IDW), or the consideration of a locally variable shear stress, for example, following the approach by Driedger and Kennard (1986), to further improve the slope-dependent variability of τ (Haeberli and Schweizer 1988). We have not tested these adjustments here as the obtained results for the larger glacier tongues were rather satisfactory, and because the required validation data for the small glaciers (e.g., to adjust the shape factors) are missing. In our approach, one value of τ is calculated for the entire glacier from an empirical relationship and thickness values are derived locally. Accordingly, for a very flat surface mean slope can get close to 0 and thickness can reach high values at these locations. To avoid such singularities in the modeled ice thickness, slope values need to be properly analyzed and maybe filtered before the method is applied.

6.2. Modeled glacier beds

The spatial pattern of glacier thickness distribution as modeled with our GIS-based approach (visually determined; Figure 6) is in good agreement with the typical characteristics of a glacier bed as known from measurements or the now deglaciated terrain. However, absolute values seem to be underestimated for small glaciers. This is likely due to the high shape factor of 0.8 for valley glaciers used here, which is smaller for mountain glaciers as

they have less lateral drag from the valley walls. However, we think that the shape of the modeled bed topography is still plausible for glaciers >0.5 km^2 and that glaciers >0.1 km^2 can be considered for volume estimates (see Table 1). The three larger valley glaciers in the study region contain most of the volume and have much higher mean thickness values than all other glaciers. This has to be considered when the potential future mass change of the catchment is modeled: most glaciers are thin (mean thickness <25 m), but the major mass loss will come from the flat, thick, and low-lying tongues of the largest valley glaciers (Paul and Haeberli 2008). The modeled overdeepenings in the glacier bed are widespread and can be found at glaciologically realistic places, for example in front of or behind steep slopes (Frey et al. 2010).

6.3. Accuracy

The systematic difference to the mean thickness values derived by HH95 is interesting but might be specific for this sample. The higher mean slope values as derived from the DEM can explain the lower mean thickness values to some degree. As the local and DEM-derived slope used here is independent from the elevation range and length of a glacier as used by HH95, the high correlation is promising. It might hint of the robustness of both approaches.

We are aware that our approach might fail at a local scale, as not all details of the bedrock topography are expressed in the surface slope. However, the comparison with the result of the approach by Farinotti *et al*. (2009b) for the Zinal glacier confirmed its general suitability in regard to the location of overdeepenings and the thickness of the steeper parts. With the mean thickness for the entire glacier being 17% smaller with our approach, we conclude that our modeling approach is unable to reproduce the highest thickness values found by Farinotti *et al*. (2009b). This would only be possible with ca. 20% higher maximum value of τ, for which we need to have additional evidence (and a revised Equation (2)). Together with the uncertainty of about $\pm$20–30% in the basal shear stress as derived from the regression with measured values (cf. Haeberli and Hoelzle 1995), we conclude that the accuracy of the modeled ice thickness is also not better than $\pm$20–30%. This is in line with earlier accuracy estimates of mean glacier thickness (e.g., Müller *et al*. 1976, Maisch 1982).

6.4. Computational effort

The raster-based modeling approach presented here is based on simple map algebra and hence comes with little computational cost and complexity. A looping by glacier, tiling of subregions, complex statistical computations, or glacier-specific iterations are not required. The approach works fully automatic and does not require any user interaction. The calculations for the entire Bernina region took about 1 minute, whereas the digitizing of the branch lines (165 km in total) took about 1 hour. The major effort is thus in the branch line digitization that needs to be done beforehand (but only once). The other two required input datasets (DEM, glacier outlines) are widely available and have very limited preprocessing demands (vector–raster conversion of the outlines, calculation of a slope grid, and contour lines from the DEM). The only computational constraints are imposed by the *topogrid* (ANUDEM) interpolation for the size of the input grids. Applying the method to all glaciers in Switzerland might require the use of a 50 m cell size instead of the 25 m grid used here, but this is still sufficient to adequately model glaciers down to a size of 0.1 km^2.

7. Conclusion

This study presented a new GIS-based approach of estimating the thickness distribution of glaciers from sparse input data (glacier outlines, DEM) and an empirical relation between the elevation range of a glacier and basal shear stress. It makes full use of the topographic information that is available today for glacier surfaces from DEMs and thus greatly expands previous approaches that only calculated a mean thickness value for a glacier. Compared to other recently presented distributed approaches, our method is computationally less expensive while fully retaining the characteristics of individual glaciers. The spatial extrapolation of the local thickness values with *topogrid* proved to be favorable for the shape of glacier beds, as *topogrid* is optimized for concave shapes of the terrain.

Glacier volume and mean thickness as derived here are about 20% smaller compared to another approach. However, by adjusting parameters like τ or f for individual glaciers in our approach, the differences can be strongly reduced. Of course, identical initialization conditions (outlines, DEM) are required in both approaches to do such a calibration exactly. On the other hand, a satisfying agreement with a more complex modeling approach was found for the modeled pattern of the regional thickness variability for the Zinal glacier. We thus conclude that the presented approach is robust in regard to the general shape of a glacier bed, but absolute values might require adjustment.

The obtained DEM without glaciers revealed characteristics of the glacier beds (e.g., overdeepenings) that can be used for several further applications. This includes improved glacier volume estimations for large glacier samples, visualization and modeling of future glacier retreat scenarios, or identification of potential lake formation sites. In our opinion, the quality and level of detail of the modeled glacier beds is already sufficient for such applications. We will investigate this in future studies.

Acknowledgements

We acknowledge the ice2sea project, funded by the European Commission's 7th Framework Programme through grant number 226375, ice2sea manuscript number 002, and financial support from the ESA project GlobGlacier (21088/07/I-EC). We would like to thank the anonymous reviewers for their very detailed and constructive comments that helped improve the article. Also W. Haeberli and M. Hoelzle have provided valuable comments on the article.

References

Barry, R.G., 2006. The status of research on glaciers and global glacier recession: a review. *Progress in Physical Geography*, 30 (3), 285–306.

Bauder, A., Funk, M., and Gudmundsson, G.H., 2003. The ice-thickness distribution of Unteraargletscher, Switzerland. *Annals of Glaciology*, 37, 331–336.

Benn, D. and Evans, D.J.A., 2010. *Glaciers and glaciation*. London: Hodder Arnold, 816 pp.

Binder, D., et al., 2009. Determination of total ice volume and ice thickness distribution of two glaciers in the Hohen Tauern region, Eastern Alps, from GPR data. *Annals of Glaciology*, 50 (51), 71–79.

Boulton, G.S., 1979. Processes of glacier erosion on different substrata. *Journal of Glaciology*, 23 (89), 15–38.

Brocklehurst, S.A., Whipple, K.X., and Foster, D., 2008. Ice thickness and topographic relief in glaciated landscapes of the western USA. *Geomorphology*, 97, 35–51.

Brückl, E., 1970. Eine Methode zur Volumenbestimmung von Gletschern auf Grund der Plastizitätstheorie. *Archives for Meteorology, Geophysics, and Bioklimatology Series A*, 19 (3), 317–328.

Burki, V., et al., 2009. Glacial remobilization cycles as revealed by lateral moraine sediment, Bødalsbreen glacier foreland, western Norway. *The Holocene*, 19 (3), 415–426.

Clarke, G.K.C., et al., 2009. Neural networks applied to estimating subglacial topography and glacier volume. *Journal of Climate*, 22 (8), 2146–2160.

Cogley, J.G., 2009. Geodetic and direct mass-balance measurements: comparison and joint analysis. *Annals of Glaciology*, 50 (50), 96–100.

Driedger, C.L. and Kennard, P.M., 1986. Glacier volume estimation on Cascade volcanoes: an analysis and comparison with other methods. *Annals of Glaciology*, 8, 59–64.

ESRI, 2004. *ARC 9.0*. Redlands, CA: Environmental Systems Research Institute, Inc.

Etzelmüller, B. and Bjørnsson, H., 2000. Map analysis techniques for glaciological applications. *International Journal of Geographical Information Science*, 14 (6), 567–581.

Farinotti, D., et al., 2009a. An estimate of the glacier ice volume in the Swiss Alps. *Global and Planetary Change*, 68, 225–231.

Farinotti, D., et al., 2009b. A method to estimate the ice volume and ice-thickness distribution of alpine glaciers. *Journal of Glaciology*, 55 (191), 422–430.

Fischer, A., 2009. Calculation of glacier volume from sparse ice-thickness data, applied to Schaufelferner, Austria. *Journal of Glaciology*, 55 (191), 453–460.

Frey, H., et al., 2010. A multi-level strategy for anticipating future glacier lake formation and associated hazard potentials. *Natural Hazards and Earth System Science*, 10, 339–352.

Haeberli, W. and Hoelzle, M., 1995. Application of inventory data for estimating characteristics of and regional climate-change effects on mountain glaciers: a pilot study with the European Alps. *Annals of Glaciology*, 21, 206–212.

Haeberli, W. and Schweizer, J., 1988. Rhonegletscher 1850: Eismechanische Überlegungen zu einem historischen Gletscherstand. *Mitteilung VAW/ETHZ*, 94, 59–70.

Hallet, B., Hunter, L., and Bogen, J., 1996. Rates of erosion and sediment evacuation by glaciers: a review of field data and their implications. *Global and Planetary Change*, 12, 213–235.

Hoelzle, M. and Haeberli, W., 1995. Simulating the effects of mean annual air-temperature changes on permafrost distribution and glacier size: an example from the Upper Engadin, Swiss Alps. *Annals of Glaciology*, 21, 399–405.

Hubbard, A., et al., 1998. Comparison of a three-dimensional model for glacier flow with field data from Haut Glacier d'Arolla, Switzerland. *Journal of Glaciology*, 44 (147), 368–378.

Huss, M., et al., 2008. Modelling runoff from highly glacierized alpine drainage basins in a changing climate. *Hydrological Processes*, 22, 3888–3902.

Hutchinson, M.F., 1989. A new procedure for gridding elevation and stream line data with automatic removal of spurious pits. *Journal of Hydrology*, 106, 211–232.

IPCC, 2007. *Fourth assessment report*. Cambridge and New York: Intergovernmental Panel on Climate Change.

Joerin, U.E., et al., 2008. Holocene optimum events inferred from subglacial sediments at Tschierva Glacier, Eastern Swiss Alps. *Quaternary Science Reviews*, 27 (3–4), 337–350.

Jouvet, G., et al., 2009. Numerical simulation of Rhonegletscher from 1874 to 2100. *Journal of Computational Physics*, 228 (17), 6426–6439.

Kaser, G., et al., 2006. Mass balance of glaciers and ice caps: consensus estimates for 1961–2004. *Geophysical Research Letters*, 33, L19501.

Klok, E.J. and Oerlemans, J., 2002. Model study of the spatial distribution of the energy and mass balance of Morteratschgletscher, Switzerland. *Journal of Glaciology*, 48 (163), 505–518.

Koboltschnig, G.R., et al., 2008. Runoff modelling of the glacierized Alpine Upper Salzach basin (Austria): multi-criteria result validation. *Hydrological Processes*, 22 (19), 3950–3964.

Larsen, C.F., et al., 2007. Glacier changes in southeast Alaska and northwest British Columbia and contribution to sea level rise. *Journal of Geophysical Research*, 112, F01007.

Le Meur, E., et al., 2007. Disappearance of an Alpine glacier over the 21st century simulated from modeling its future surface mass balance. *Earth and Planetary Science Letters*, 261 (3–4), 367–374.

Linsbauer, A., 2008. Modellierung von Gletscherbetten mit GIS. Thesis (Diploma). University of Zurich, Department of Geography, 142 pp.

Maisch, M. and Haeberli, W., 1982. Interpretation geometrischer parameter von Spätglazialgletschern im Gebiet Mittelbünden, Schweizer Alpen. *Physische Geographie Universität Zürich*, 1, 111–126.

Maisch, M., et al., 2000. *Die Gletscher der Schweizer Alpen. Gletscherhochstand 1850, Aktuelle Vergletscherung, Gletscherschwund-Szenarien*. Zurich: vdf Hochschulverlag.

Müller, F., Caflisch, G., and Müller, G., 1976. *Firn und Eis der Schweizer Alpen, Gletscherinventar*. Zurich: ETH Zurich, Publication, 57, 57a.

Nemec, J., et al., 2009. Reconstruction of the annual balance of Vadret da Morteratsch, Switzerland, since 1865. *Annals of Glaciology*, 50 (50), 126–134.

Oerlemans, J., 2001. *Glaciers and climate change*. Lisse: A. A. Balkema Publishers.

Oerlemans, J., Giesen, R.H. and van den Broeke M.R., 2009. Retreating alpine glaciers: increased melt rates due to accumulation of dust (Vadret da Morteratsch, Switzerland). *Journal of Glaciology*, 55 (192), 729–736.

Paterson, W.S.B., 1994. *The physics of glaciers*. 3rd ed. Oxford: Elsevier.

Paul, F., 2007. The New Swiss Glacier Inventory 2000 – application of remote sensing and GIS. *Schriftenreihe Physische Geographie, University of Zurich*, 52, 210 pp.

Paul, F. and Haeberli, W., 2008. Spatial variability of glacier elevation changes in the Swiss Alps obtained from two digital elevation models. *Geophysical Research Letters*, 35, L21502.

Paul, F., et al., 2004. Rapid disintegration of Alpine glaciers observed with satellite data. *Geophysical Research Letters*, 31, L21402.

Paul, F., Kääb, A., and Haeberli, W., 2007a. Recent glacier changes in the Alps observed from satellite: consequences for future monitoring strategies. *Global and Planetary Change*, 56, 111–122.

Paul, F., et al., 2007b. Calculation and visualisation of future glacier extent in the Swiss Alps by means of hypsographic modelling. *Global and Planetary Change*, 55 (4), 343–357.

Pelto, M.S., 2006. The current disequilibrium of North Cascade Glaciers. *Hydrological Processes*, 20, 769–779.

Raymond, C., et al., 2005. Retreat of Glaciar Tyndall, Patagonia, over the last half-century. *Journal of Glaciology*, 51 (173), 239–247.

Rothenbühler, C., 2006. GISALP: räumlich -zeitliche Modellierung der klimasensitiven Hochgebirgslandschaft des Oberengadins. Geographisches Institut, Universität Zürich. *Schriftenreihe Physische Geographie*, 50, 175 pp.

Span, N., et al., 2005. Radarmessungen der Eisdicke österreichischer Gletscher. Band 1: Messungen 1995 bis 1998. *Österreichische Beiträge zur Meteorologie und Geophysik*, 33, 145 pp.

Stahl, K., et al., 2008. Coupled modelling of glacier and streamflow response to future climate scenarios. *Water Resources Research*, 44, W02422.

Vanuzzo, C. and Pelfini, M., 1999. Assessing area and volume changes from deglaciated areas, Valle d'Aoste, Italy. *Annals of Glaciology*, 28, 129–134.

Verbunt, M., et al., 2003. The hydrological role of snow and glaciers in alpine river basins and their distributed modeling. *Journal of Hydrology*, 282, 36–55.

Viviroli, D., et al., 2009. An introduction to the hydrological modelling system PREVAH and its pre- and post-processing-tools. *Environmental Modelling and Software*, 24 (10), 1209–1222.

Welch, B.C., et al., 1998. Mapping subglacial surfaces of temperate valley glaciers by twopass migration of a radio-echo sounding survey. *Journal of Glaciology*, 44 (146), 164–170.

WGMS, 2008, Global glacier changes: facts and figures. *In*: M. Zemp, et al., eds. *UNEP*. Zurich: World Glacier Monitoring Service, 88 pp.

Paper III

Linsbauer, A., Paul, F., and Haeberli, W. (2012b). Modeling glacier thickness distribution and bed topography over entire mountain ranges with GlabTop: Application of a fast and robust approach. *Journal of Geophysical Research*, 117: F03007. doi: 10.1029/2011JF002313

JOURNAL OF GEOPHYSICAL RESEARCH, VOL. 117, F03007, doi:10.1029/2011JF002313, 2012

Modeling glacier thickness distribution and bed topography over entire mountain ranges with GlabTop: Application of a fast and robust approach

A. Linsbauer,[1] F. Paul,[1] and W. Haeberli[1]

Received 23 December 2011; revised 16 May 2012; accepted 27 May 2012; published 31 July 2012.

[1] The combination of glacier outlines with digital elevation models (DEMs) opens new dimensions for research on climate change impacts over entire mountain chains. Of particular interest is the modeling of glacier thickness distribution, where several new approaches were proposed recently. The tool applied herein, GlabTop (Glacier bed Topography) is a fast and robust approach to model thickness distribution and bed topography for large glacier samples using a Geographic Information System (GIS). The method is based on an empirical relation between average basal shear stress and elevation range of individual glaciers, calibrated with geometric information from paleoglaciers, and validated with radio echo soundings on contemporary glaciers. It represents an alternative and independent test possibility for approaches based on mass-conservation and flow. As an example for using GlabTop in entire mountain ranges, we here present the modeled ice thickness distribution and bed topography for all Swiss glaciers along with a geomorphometric analysis of glacier characteristics and the overdeepenings found in the modeled glacier bed. These overdeepenings can be seen as potential sites for future lake formation and are thus highly relevant in connection with hydropower production and natural hazards. The thickest ice of the largest glaciers rests on weakly inclined bedrock at comparably low elevations, resulting in a limited potential for a terminus retreat to higher elevations. The calculated total glacier volume for all Swiss glaciers is 75 ± 22 km^3 for 1973 and 65 ± 20 km^3 in 1999. Considering an uncertainty range of ±30%, these results are in good agreement with estimates from other approaches.

Citation: Linsbauer, A., F. Paul, and W. Haeberli (2012), Modeling glacier thickness distribution and bed topography over entire mountain ranges with GlabTop: Application of a fast and robust approach, *J. Geophys. Res.*, *117*, F03007, doi:10.1029/2011JF002313.

1. Introduction

[2] The ongoing increase in global mean temperature has caused substantial decline for most glaciers in the world [*World Glacier Monitoring Service* (*WGMS*), 2008; *Lemke et al.*, 2007; *Watson and Haeberli*, 2004]. Accelerated glacier loss in high-mountain regions, [e.g., *Paul et al.*, 2007a] can have strong environmental as well as economic impacts at local to regional and even continental to global scales (hydro-power, water resources, sea level rise [e.g., *Zemp et al.*, 2007; *WGMS*, 2008]). When observed glacier changes are combined with digitized glacier inventories and digital elevation models (DEMs), an important knowledge basis for timely anticipation and quantitative modeling of such changes is at hand [e.g., *Huss et al.*, 2010; *Künzler et al.*, 2010; *Paul et al.*, 2007b]. A most prominent application of the combined data sets is the modeling of the ice thickness distribution for larger samples of glaciers from simplified glaciological principles [e.g., *Paul and Linsbauer*, 2012; *Li et al.*, 2012, 2011; *Farinotti et al.*, 2009b; *Clarke et al.*, 2009]. Beside the improved calculation of glacier volume that is an urgent demand also on a global scale [*Radic and Hock*, 2010], a further simple step is the subtraction of the modeled ice thickness from a surface DEM providing a DEM without glaciers, i.e., an approximation of the subglacial topography [e.g., *Linsbauer et al.*, 2009; *Binder et al.*, 2009]. This type of information is important for the modeling of future glacier evolution according to given climate change scenarios [e.g., *Jouvet et al.*, 2009, 2011]. The calculated glacier bed further allows assessment of related impacts, for example on changing runoff regimes [*Huss et al.*, 2010], the potential formation of new lakes in subglacial depressions or of future hazard conditions [*Frey et al.*, 2010; *Künzler et al.*, 2010; *Quincey et al.*, 2007; *Rothenbühler*, 2006]. There are still high uncertainties involved in all methods used for

[1]Department of Geography, University of Zurich, Zurich, Switzerland.

Corresponding author: A. Linsbauer, Department of Geography, University of Zurich, Winterthurerstr. 190, CH-8057 Zurich, Switzerland. (andreas.linsbauer@geo.uzh.ch)

0148-0227/12/2011JF002313

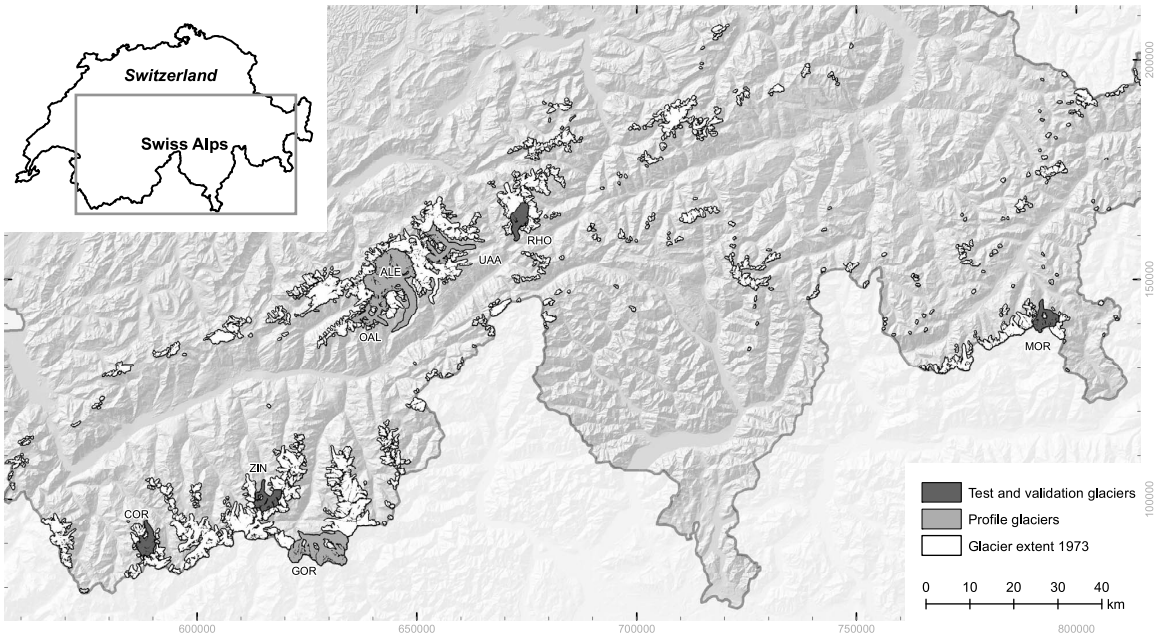

Figure 1. Model domain showing all Swiss glacier with their extend from 1973. Abbreviations refer to the following glaciers: MOR, Morteratsch; RHO, Rhone; UAA, Unteraar; ALE, Great Aletsch; OAL, Oberaletsch; GOR, Gorner; ZIN, Zinal; COR, Corbassière.

estimating glacier thickness, but even approximately reconstructed glacier beds justifies their application.

[3] The modeling approach GlabTop (Glacier bed Topography) as presented in *Paul and Linsbauer* [2012] and applied here is based on the assumption that glacier thickness depends on surface slope via an average basal shear stress (assuming perfect plasticity [cf. *Paterson*, 1994]), which depends on the mass turnover and, hence, the mass balance gradient and the elevation range of the considered glacier [*Haeberli and Hoelzle*, 1995], with an upper-bound value of 150 kPa for large glaciers (cf. also *Li et al.* [2012]). Using only three input data sets (glacier outlines, a DEM and a set of digitized central branch lines), GlabTop calculates thickness values at point locations and spatially interpolates them to a continuous bed within the limits of the glacier using the ANUDEM algorithm by *Hutchinson* [1989]. This algorithm is designed to create hydrologically correct DEMs and is thus especially suitable for glacier beds with their concave shapes [*Fischer*, 2009]. Based on the concept of simple map algebra (adding or subtracting grids) [e.g., *Etzelmüller and Björnsson*, 2000], GlabTop can be applied to large samples of glaciers in a computationally efficient manner.

[4] The regional scale application of the modeling framework presented in *Paul and Linsbauer* [2012] is presented in this study by applying GlabTop to all glaciers in Switzerland along with a detailed analysis and validation of the results. The main objectives of this study are thus: (a) the calculation of the ice thickness distribution for all glaciers in Switzerland, (b) the analysis of the geomorphometric characteristics of the modeled glacier beds with a focus on overdeepenings as sites of potential future lake formation, (c) a comparison of the here derived glacier volumes with results from other approaches, (d) a validation of model results with data from Ground Penetrating Radar (GPR), and (e) a determination of the sensitivity of GlabTop in regard to uncertainties of the input parameters used. For (d) we selected three differently shaped larger valley glaciers and for (c) we compared the modeled mean glacier thickness to the results from (i) a modeling approach based on principles of mass conservation and flow dynamics developed by *Farinotti et al.* [2009a] and (ii) the approach by *Haeberli and Hoelzle* [1995] using tabular data as stored in glacier inventories as an input.

[5] After describing the study region and input data sets, we summarize the previously and here-applied methods. We then present the results of the modeled ice thickness distribution together with the derived glacier volumes and potential lake formation sites. After presenting the model validation and comparison with other approaches, the results achieved and the accuracy and uncertainty of the model are discussed. The conclusions summarize the main findings.

2. Study Region

[6] The Swiss Alps cover an area of about 25000 km^2 (Figure 1) with glaciers in this region stretching from about 1500 up to 4500 m a.s.l. and a mean elevation of about 2900 m a.s.l. [*Paul et al.*, 2007a]. The 71 glaciers with an area larger than 3 km^2 (in 1973) contribute 58% to the total glacierized area but only about 3% to the total number. On the other hand, glaciers smaller than 1 km^2 account for 91% of the number but only 24% of the area (Figure 2a). However, these small glaciers contributed strongly to the overall area loss between 1985 and 1999 [*Paul et al.*, 2004] and are

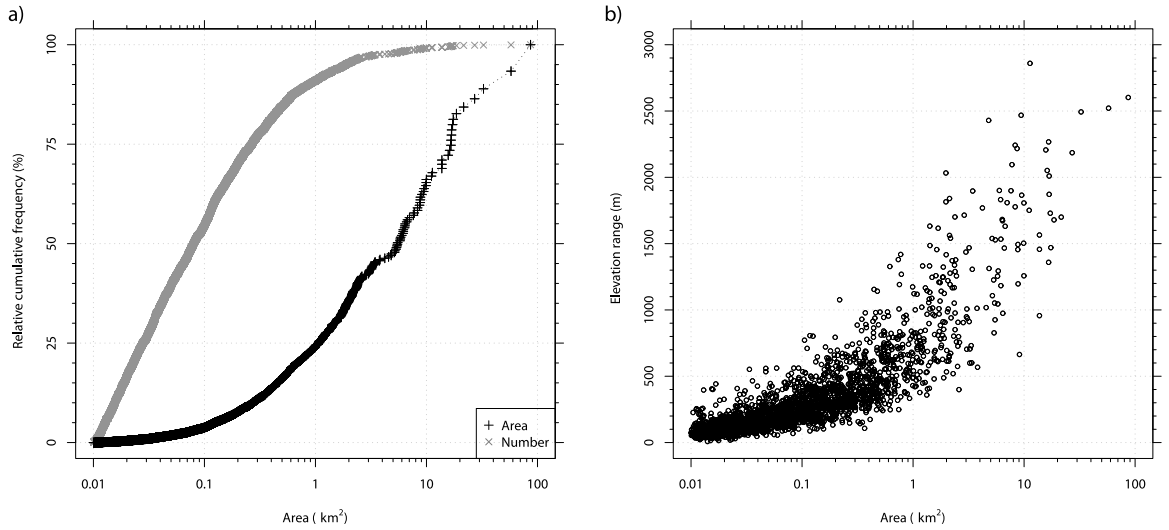

Figure 2. (a) Glacier size and the number of glacier versus the relative cumulative frequency of both values in the same plot. (b) Relation between glacier area and elevation range of all Swiss glaciers.

thus also considered in GlabTop. The strongly biased number and size distribution has to be considered when mean glacier thickness is interpreted.

[7] In total, we considered 2365 glaciers and glacierets larger than 0.01 km^2 (highlighted in Figure 1). Their elevation range is plotted against glacier area in Figure 2b. For glaciers with a size of about 10 km^2 the elevation range can vary between 700 and 2800 m and 38 glaciers stretch over more than 1600 m. From this sample of modeled glaciers, four sub-samples were selected for various purposes: (A) 71 glaciers larger than 3 km^2 for the comparison with thickness values modeled by *Farinotti et al.* [2009a], (B) five glaciers with large tongues reaching down to low altitudes for visualization of modeled glacier beds (in long profiles), (C) three glaciers (Rhone, Zinal and Corbassière) for validation of the model results with GPR soundings, and (D) one glacier (Morteratsch) for uncertainty tests. Morteratsch glacier (16 km^2) is composed of two main branches (Pers and Morteratsch glaciers) which merge in the lower third of the main valley. Rhone glacier (17 km^2) flows from its gently sloping accumulation basin to the comparably flat ablation area in an increasingly narrow valley, where the tongue ends today in a rapidly enlarging lake that fills an overdeepening behind a bedrock barrier. Zinal glacier (16 km^2) is composed of five major, comparably steep tributaries and has a flat, nearly completely debris-covered tongue. And finally Corbassière glacier (16 km^2) mainly consists of two flat basins in the accumulation area which are connected by moderately steep icefalls with a wide, flat and largely debris-free tongue as ablation area.

3. Data Sets

[8] GlabTop requires three different input data sets: (1) a DEM, (2) glacier outlines and (3) a set of branch lines for each glacier.

[9] The DEM used here was produced by the Swiss Federal Office of Topography (swisstopo) from aerial photography and has a cell size of 25 m. The DEM is based on the interpolation of contour lines from the Swiss topographic map sheets (1:25000) and includes digitized lake perimeters, main break lines and spot heights [*Rickenbacher*, 1998]. Two versions of this data set are available: a Level 1 (DHM25L1) from around 1985 and a Level 2 (DHM25L2) from around 1995. Apart from the acquisition date, the two DEMs primarily differ in regard to the algorithms used for the contour line interpolation [*Swiss Federal Office of Topography*, 2005]. For the Bernina region both DEMs refer to 1991. For the purpose of this study, we have evaluated the suitability of both DEMs.

[10] Digital glacier outlines from two sources were used: First, outlines based on the digitized Swiss Glacier Inventory from 1973 by *Müller et al.* [1976], in the revised version by *Maisch et al.* [2000]. These glacier polygons fit well to the glacier extent in the DHM25L1, as only small overall area changes took place for most glaciers in the Alps between 1973 and 1985 [*Paul et al.*, 2004]. Second, the glacier outlines from the Swiss Glacier Inventory 2000 (SGI2000) [*Paul*, 2007] as derived from Landsat images acquired in the years 1998 and 1999 are used. In this case the DHM25L2 corresponds much better to the extent of the glaciers. We only consider perennial ice bodies larger than 0.01 km^2 from these two samples containing 2365 glaciers and glacierets for 1973 and 1182 for 1998/1999. The difference in number is mainly due to the number of small glaciers considered (<0.1 km^2); many of them have disappeared during this time period or were not recognizable in the satellite image (e.g., due to increased debris cover) [*Paul et al.*, 2007a].

[11] The manually digitized central branch lines cover all important tributaries of a glacier and merge at confluences (they are thus not flow lines in a strict glaciological sense). The shaded relief of the DEM, elevation contour lines in 50 m equidistance, and if necessary, the Swiss topographic maps (1:25000) were used as background information to digitize them. According to the guidelines described in *Paul and Linsbauer* [2012], the branch lines were digitized from

bottom to top, perpendicular to the contour lines of surface elevation, ending about 100 m before the glacier outline with one parallel line for every 200–400 m of glacier width. The fully digitized branch line data set for the 1973 glacier extent was clipped and if necessary manually modified until the branch lines also matched the SGI2000 glacier outlines. Additionally, one central flowline, which directly connects the lowest with the highest point, was digitized for each glacier. In total, the digitizing of all vector lines (branch lines (4400 km) and central flowlines (2100 km) for the 1973 glacier extent, branch lines (3500 km) and central flowlines (1400 km) for the SGI2000) was performed in less than a week.

[12] GPR profiles for the three glaciers Rhone (7 profiles), Zinal (8 pr.) and Corbassière (11 pr.) were used for validation of the model results. They were provided by the Laboratory of Hydraulics, Hydrology and Glaciology (VAW), ETH-Zurich and for Corbassière digitized from the report by *Laboratory of Hydraulics, Hydrology and Glaciology* (*VAW*) [1998] and the work of *Farinotti* [2010]. The profiles from Rhone and Zinal have also been used in the study by *Farinotti et al.* [2009b] for model validation and the profiles of all three glaciers for estimating their glacier volume by *Farinotti et al.* [2009a]. They were acquired during different field campaigns (Rhone: 2003; Zinal 2006/2007; Corbassière: 1988/1998) [*Farinotti et al.*, 2009b, 2009a; *Farinotti*, 2010; *VAW*, 1998]. These profiles only provide glacier depth information at the respective cross sections and have uncertainties as well (2D-analysis, lateral effects not considered, smoothing effect of the sounding method). For the bed between these profiles a direct validation is not possible.

4. Previous Works on Glacier Thickness Modeling

[13] Thickness estimates for glaciers were long made using empirical relations between measured surface areas and (geophysically) measured ice depths [e.g., *Müller et al.*, 1976; *Maisch and Haeberli*, 1982; *Driedger and Kennard*, 1986; *Maisch et al.*, 2000] or volume/area correlations [e.g., *Chen and Ohmura*, 1990; *Bahr et al.*, 1997; *Luethi et al.*, 2008]. Neither area-related estimates nor other scalar approaches [e.g., *Haeberli and Hoelzle*, 1995] yield information about subglacial topography, a severe limitation which can now be overcome using digital terrain information and distributed thickness estimates [e.g., *Clarke et al.*, 2009].

[14] The topographic information which became available in detailed glacier inventories of the past century first made it possible to derive mean glacier thicknesses and hence volumes for large samples of glaciers using listed elevation ranges and lengths to derive mean slope values for each glacier [*Haeberli and Hoelzle*, 1995; *Hoelzle et al.*, 2007]. Corresponding thickness estimates for individual glaciers are considered to be more realistic than area-dependent estimates, because flow-related glacier thickness is strongly slope-dependent [*Paterson*, 1994; *Kamb and Echelmeyer*, 1986].

[15] The application of DEMs in combination with vector outlines of glacier extent now makes ice-depth estimates for individual parts of glaciers possible. Though such approaches have been presented long ago [*Driedger and Kennard*, 1986], they only recently became rather popular. Two examples of such recently developed methods with a focus on modeling glacier thickness distribution for large samples of glaciers were presented by *Clarke et al.* [2009] and *Farinotti et al.* [2009b].

[16] *Clarke et al.* [2009] used an Artificial Neural Network (ANN) to transfer the characteristics of now ice free glacier beds to contemporary glaciers. The ANN method yielded plausible subglacial topography with an error of ± 70 m, but is computationally very intensive and requires a repeated application in overlapping 50 km by 50 km subregions to cover a larger mountain range [*Clarke et al.*, 2009].

[17] The model ITEM (Ice Thickness Estimation Method) by *Farinotti et al.* [2009b] uses a method based on mass conservation and principles of ice flow dynamics to estimate the ice thickness distribution of larger alpine glaciers (>3 km^2). It requires a detailed parameterization of the involved physical processes and rough assumptions about several only vaguely determined processes (e.g., surface accumulation, mass balance gradient, rate factor in the ice flow law, basal sliding velocity). As a consequence, it must be tuned for each glacier [*Farinotti et al.*, 2009b] by comparing it with selected glacier cross sections derived from GPR profiles to make it realistic. The required model input data are glacier surface topography, glacier outlines delineating ice flow catchments and meteorological data to calculate mass balance distribution and estimate ice flow. The method also worked well for a larger number of glaciers, when the required amount of input (and calibration) data was available [*Farinotti et al.*, 2009a].

[18] *Li et al.* [2012] developed a method that is also based on the perfect-plastic rheology assumption (see equation (1)), for estimating the flow line thickness of glaciers. The novelty is the inclusion of side drag in the force-balance calculation; thus it requires accurate determination of the width of each cross-section from observations. The key advantage of this model is its simplicity: only few input data sets are required, they are straightforward to derive, and the physical basis is easy to understand. The uncertainty relates to the basal shear stress (τ), which has to be assumed where independent ice-thickness data are lacking, or to be calibrated in case such data is available.

[19] A critical step for the use of modeled glacier beds in other applications is the assessment of their quality, which requires validating them with ground truth data. For still existing glaciers, bedrock information can be derived from (hot-water) drilling, geophysical soundings like ground penetrating radar (GPR) or – optimally – a combination of both [*Haeberli and Fisch*, 1984]. Such reference information, however, is only sparsely available and in many cases biased toward crevasse-free, flat and thus thick glacier parts with compressing flow [e.g., *Frey et al.*, 2010]. The bed between the profiles remains unknown and a modeled product [e.g., *Fischer*, 2009; *Binder et al.*, 2009].

5. Methods

5.1. The GlabTop Approach

[20] The GlabTop approach introduced by *Linsbauer et al.* [2009] and *Paul and Linsbauer* [2012] is intermediate between the two approaches of *Clarke et al.* [2009] and

Farinotti et al. [2009b] and close to the idea by *Li et al.* [2012]: it is based on a very basic consideration of flow dynamics and it enables all glacier beds to be calculated at once which makes it computationally very fast. It is calibrated with geometric (shear stress) information from vanished (late glacial) glaciers and validated with independent GPR measurements.

[21] The technical details of GlabTop are described by *Paul and Linsbauer* [2012] and are thus only shortly summarized here. The core of GlabTop is the parameterization scheme presented by *Haeberli and Hoelzle* [1995] for analyzing tabular data in detailed glacier inventories. In that approach, a constant basal shear stress along the central flowline of the entire glacier is assumed to derive ice thickness along the central flowline:

$$h = \frac{\tau}{f \cdot \rho \cdot g \cdot \sin \alpha}, \quad (1)$$

with h = ice thickness, τ = basal shear stress, f = shape factor (0.8), ρ = ice density (900 kgm^{-3}), g = acceleration due to gravity (9.81 ms^{-2}) and α = glacier surface slope ($\alpha \neq 0$). For each glacier, a value for τ is estimated from an empirical relation between τ and elevation range (ΔH) according to a regression with a sample of values calculated for 62 vanished late glacial glaciers [*Maisch and Haeberli*, 1982; *Haeberli and Hoelzle*, 1995]:

$$\tau = 0.005 + 1.598\Delta H - 0.435\Delta H^2, \quad \textit{and } \tau = 150 \text{ kPa } \textit{for } \Delta H > 1600 \text{ m}. \quad (2)$$

[22] A maximum value of 150 kPa is assumed for glaciers with $\Delta H > 1600$ m (38 in our sample) and the basal shear stress of the smallest glaciers is set to 0.005 kPa. The maximum value of 150 kPa is empirically estimated [*Maisch and Haeberli*, 1982; *Haeberli and Hoelzle*, 1995] and 50% higher than the 100 kPa used in other studies as a mean value for all glaciers. For example *Marshall et al.* [2011] mentioned that this value tend to underestimate the shear stress for large glaciers and overestimate it for small glaciers. This is in line with the study by *Driedger and Kennard* [1986] who found size-dependent values between 30 and 160 kPa for a group of comparably steep glaciers on the Cascade volcanoes and *Li et al.* [2012] who found values of 50–175 kPa for five Chinese glaciers.

[23] The variable parameters in the model are the basal shear stress (τ) and the surface slope (α). The shape factor (f), which is related to the lateral drag on a glacier through friction at the valley walls and the general form of the glacier cross section, ranges according to *Paterson* [1994] from 0.5 to 0.9. For alpine glaciers and based on empirical evidence *Maisch and Haeberli* [1982] used a shape factor of 0.7 for the glacier tongues in the ablation area and 0.9 for the much wider accumulation areas. *Haeberli and Hoelzle* [1995] chose $f = 0.8$ for the entire glacier in their parameterization scheme. To keep the processing in GlabTop simple, we also used a constant shape factor ($f = 0.8$) for all glaciers.

[24] Application of the perfect plasticity assumption of equation (1) including effects of longitudinal stress coupling requires that surface slope (α) is averaged over a reference distance, which is about one order of magnitude larger than the local ice thickness [*Paterson*, 1994; *Haeberli and Schweizer*, 1988; *Kamb and Echelmeyer*, 1986; *Maisch and Haeberli*, 1982]. Averaging surface slope within 50 m elevation bins results in reference distances of about 5–10 times the ice thickness.

[25] The basal shear stress (τ) is calculated from equation (2). The large spread of the data points found in *Haeberli and Hoelzle* [1995] reflects the general variability of flow dynamics (rate factor for ice deformation and relative amount of sliding) and cannot easily be overcome in any quantitative approach. The scatter relates to an uncertainty of ±30% and for some individual glaciers even ±45%.

5.2. GIS Implementation and Application to All Swiss Glaciers

[26] The spatial variability in ice thickness for an individual glacier is considered by calculating an averaged surface slope for equidistant elevation intervals of 50 m directly from the DEM. The reference distance for the slope determination is thereby automatically adjusted to the local glacier thickness, i.e., it is long where the glacier is relatively flat/thick and relatively short where it is steep/thin. Typical ratios of such reference distances versus local thickness vary here from 1:5 to 1:10.

[27] The subsequent spatial interpolation of the thickness values is performed with the ANUDEM (TopoToRaster in ArcGIS [*ESRI*, 2008]) interpolation scheme [*Hutchinson*, 1989] that was also used by *Fischer* [2009] for spatial interpolation of thickness profiles measured by GPR. The resulting digital map (raster data) of ice thickness distribution is subtracted from the surface DEM to obtain the bed topography, i.e., a DEM without glaciers. By calculating zonal statistics in the GIS, the key values for mean (h_{mean}) and maximum (h_{max}) ice thickness and total volume (V) are obtained. This mean thickness is also used for a comparison with the values derived by *Haeberli and Hoelzle* [1995] and from the ITEM approach [*Farinotti et al.*, 2009a].

[28] Both ice thickness distribution and bed topography were modeled for all ice bodies larger than 0.01 km^2, but a statistical analysis of the results is only performed for glaciers larger 0.1 km^2. Similar to *Haeberli and Hoelzle* [1995] we treat glacierets between 0.01 km^2 and 0.1 km^2 separately, using a mean ice thickness of 5 m and calculating the volume by multiplication with the ice-covered area. The overdeepenings in the glacier beds are detected by filling them with the ArcGIS hydrology-tool 'fill' [*ESRI*, 2008] and a slope grid derived from the filled DEM. By selecting slope values smaller than one degree within the glacier outlines, the overdeepenings in the glacier beds are found. The difference grid between the filled DEM and the former DEM without glaciers is used to quantify the area and volume of the overdeepenings. The mean and maximum depths of the potential lakes are also calculated with zonal statistics.

[29] In the implementation of GlabTop as presented by *Paul and Linsbauer* [2012], a standard Inverse Distance Weighted (IDW) interpolation was applied to have continuous thickness values between the base points, where the ice thickness is estimated according to the physical background (see section 5.1). Changing this 'IDW'-interpolation in GlabTop to the 'TopoToRaster'-algorithm entails a stronger smoothing of the subglacial topography with less artefacts and somewhat larger mean thickness values. To also consider the uncertainty related to the interpolation methods, we show selectively results from both modeling approaches.

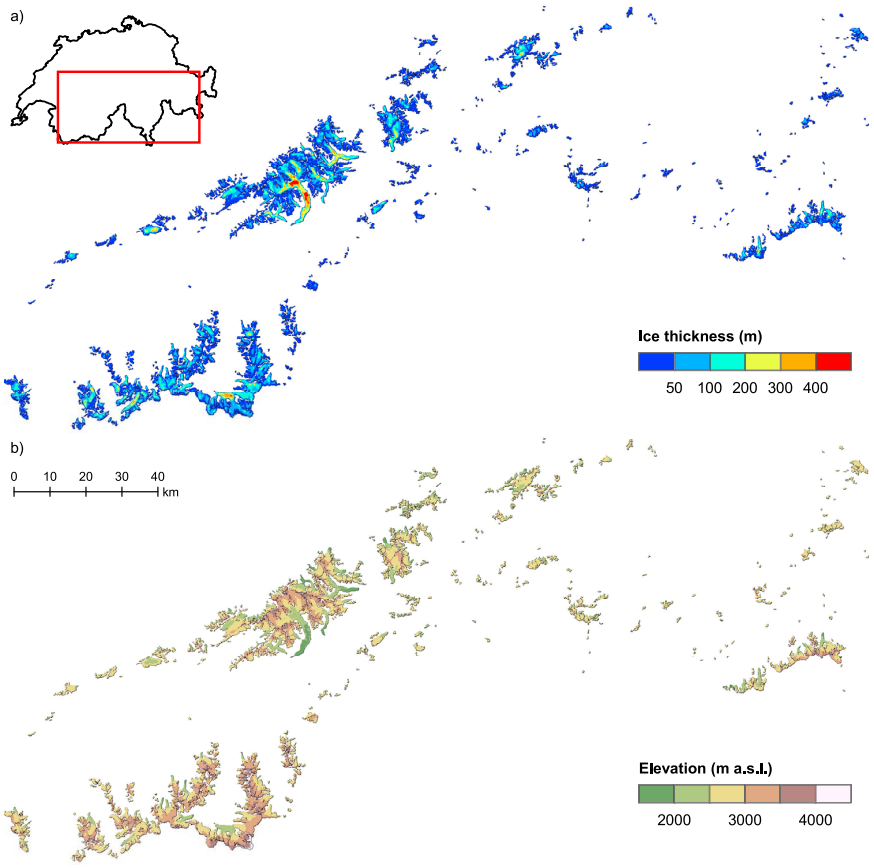

Figure 3. Output of GlabTop model run 73L1 (with the DHM25L1, the outlines from 1973 and the corresponding branch lines): (a) ice thickness distribution and (b) glacier bed elevation for all Swiss glaciers.

5.3. Accuracy Assessment, Uncertainty and Comparison of Methods

[30] For a validation of the model calculations, the results of GlabTop are compared to GPR cross sections (z values at given x, y coordinates) from three valley glaciers (Rhone, Zinal and Corbassière). The GPR profiles are typically located on accessible, flat and uncrevassed parts of the glacier surface (see Figure 8 and *Fischer* [2009]), i.e., where the glacier ice is thickest. To illustrate the differences resulting from the two applied interpolation methods in GlabTop (IDW and TopoToRaster), we show results from both methods in the cross-section comparisons.

[31] As also the input parameters shear stress, surface slope and shape factor have an uncertainty, we tested the impact of this uncertainty on the modeled ice thickness by a systematic variation of their values within typical uncertainty ranges (τ: ±30%, α: ±10%, f: ±12.5%). The uncertainty for f assumes that typical values range from 0.7 to 0.9 instead of the here used value of 0.8 (see section 5.1). The assumed uncertainty in the slope value mainly results from local artefacts in the DEM, as elevation values (and hence also slope) of neighboring cells are otherwise highly correlated. This experiment revealed that the uncertainty in the modeled ice thickness is dominated by the uncertainty of τ. We have thus also modeled all glacier beds with 30% higher and lower values of τ and include the resulting thickness values in the comparison with the GPR profiles.

[32] For the comparison with the results from the ITEM approach we computed mean glacier thickness from the areas and volumes listed in *Farinotti et al.* [2009a]. As their values refer to the 1999 period, we used glacier outlines from the SGI2000 and the DHM25L2 as an input to GlabTop. As glacier outlines and input DEMs differ, also thickness values will likely not be the same. However, mean thickness is at least much less sensitive to differences in the glacier size than volume.

[33] We also compared our modeled thickness values with the approach by *Haeberli and Hoelzle* [1995], who used a set of widely available glacier inventory data (glacier length (L_0), maximum and minimum elevation (H_{max}, H_{min}) and surface area (A) to estimate glacier mean thickness. For this purpose we used the DEM, glacier outlines and central flowlines to derive the above parameters. Though both approaches are based on the same equations for calculation of mean ice thickness and τ, we consider them as independent enough for a comparison as the input data sets used are

Table 1. Glacierized Area (A) and Ice Volume (V) of Five Ice Thickness Classes as Modeled for the Year 1973 With GlabTop and the Two Different Interpolation-Methods for the Basepoints

Ice Thickness (m)	IDW(73L1)				TopoToRaster(73L1)			
	A (km^2)	%	V (km^3)	%	A (km^2)	%	V (km^3)	%
0–50	821	63	15	21	795	61	15	20
50–100	274	21	19	27	274	21	19	24
100–200	156	12	22	30	170	13	24	30
>200	52	4	16	22	65	5	21	26
Total	1304	100	72	100	1304	100	79	100

calculated differently and are statistically independent. Moreover, we are interested in the effects of a change in the source data (locally derived mean surface slope versus slope calculated from length and elevation range of a glacier) when equations are the same. Of course, this is a model intercomparison rather than validation.

6. Results

6.1. Ice Thickness Distribution and Total Volume of the Swiss Glaciers

[34] GlabTop was applied to the DHM25L1 with the glacier outlines from 1973 (GlabTop_73L1) and to the DHM25L2 with the outlines from the SGI2000 (GlabTop_2kL2) and corresponding branch lines for both combinations. We focus in the following on the results obtained with 'GlabTop_73L1' with the TopoToRaster-interpolation. In Figure 3 the ice thickness distribution (Figure 3a) and elevation of the resulting glacier beds (Figure 3b) for all Swiss glaciers is visualized.

[35] The ice thickness distribution reveals that ice thicknesses of less than 100 m (blue colors) are clearly dominant. Over approximately 60% of the glacierized area the ice is less than 50 m and over another 20% between 50 and 100 m thick. The large area of ice (about 800 km^2) which is only up to 50 m thick, contributes about the same amount or even less to the total volume of all glaciers than the small area (60–70 km^2) with ice thicknesses exceeding 200 m (cf. Table 1). Overall, the 3, 6 and 15 largest glaciers contain 1/4, 1/3 and 1/2 of the total ice volume respectively (cf. also Table 5).

[36] For the year 1973, we have estimated the total ice volume of all Swiss glaciers to be around 79 $\pm$ 23 km^3. Dividing the total ice volume by the total area of 1304 km^2 yields a corresponding (area weighted) mean ice thickness of 61 m (cf. Table 2). When excluding the largest 3, 6 or 15 glaciers, the mean thickness of all other glaciers is 50 m, 47 m and 40 m respectively. The mean thickness value is thus strongly influenced by the (few) largest glaciers. The comparison of modeled mean and maximum ice thickness per glacier (Figure 4a) reveals a high correlation of $R^2 = 0.95$ (linear regression with a slope of $y = 2.99x$ and an intercept of 0). This implies that maximum ice thickness is generally about three times larger than mean ice thickness, which is in good agreement with the value of 2.9 found by *Raper and Braithwaite* [2009] from theoretical considerations.

[37] When glacier area is plotted against modeled mean glacier thickness for each glacier in the analysis (Figure 4b), the wide range of possible mean thickness values for glaciers of the same size becomes obvious, although the double logarithmic plot strongly reduces the scattering. It also seems that a simple power law does not accurately fit the data points.

[38] An ice volume of 68 $\pm$ 20 km^3 and a mean ice thickness of 65 m is obtained by the model run 'GlabTop_2kL2' for the year 2000 (cf. Table 2). This gives a total volume loss of 11 km^3 between 1973 and 2000, which is in good agreement with the 12.2 km^3 volume loss derived from direct DEM differencing and comparison with surface mass balance measurements [*Paul and Haeberli*, 2008]. Assuming little volume change between 1973 and 1985 [*Paul et al.*, 2004] this gives a volume loss of about -17% for the Swiss glaciers in 15 years or a loss rate of about 1% per year. Further results for individual glaciers and distinct area classes can be found in Table 5.

6.2. Glacier Bed Topography

[39] The modeled glacier bed elevations are shown in Figure 3b. In regions with large ice thickness, the elevations of the glacier beds are comparably low. This can also be seen in the direct comparison of bed elevation profiles along the central flowline of five large glacier tongues in Figure 5. Large parts of these tongues are located on bedrock with elevations below 2400 m a.s.l.. Great Aletsch and Unteraar glacier have major parts of their beds even below 2000 m a.s.l. (Figure 5). The profile lines also illustrate the large number of modeled overdeepenings (cf. section 6.3). This "step-pool" character of glacier beds is found in several deglaciated mountain ranges and will likely facilitate the formation of dead ice during glacier retreat and hence its rapid melt down [*Vacco et al.*, 2010], as well as possible lake formation in the future [*Frey et al.*, 2010]. Further

Table 2. Total Glacierized Area (A), Mean Ice Thickness (h_{mean}) and Total Volume (V) of 3 GlabTop Model Runs With Different Input Data for the IDW and the TopoToRaster-Interpolation

Run	Outlines	DEM	A (km^2)	IDW		TopoToRaster	
				h_{mean} (m)	V (km^3)	h_{mean} (m)	V (km^3)
73L1	1973	DHM25L1	1304	55	72	61	79
2kL1	SGI2000	DHM25L1	1040	61	64	67	70
2kL2	SGI2000	DHM25L2	1035	59	61	65	68

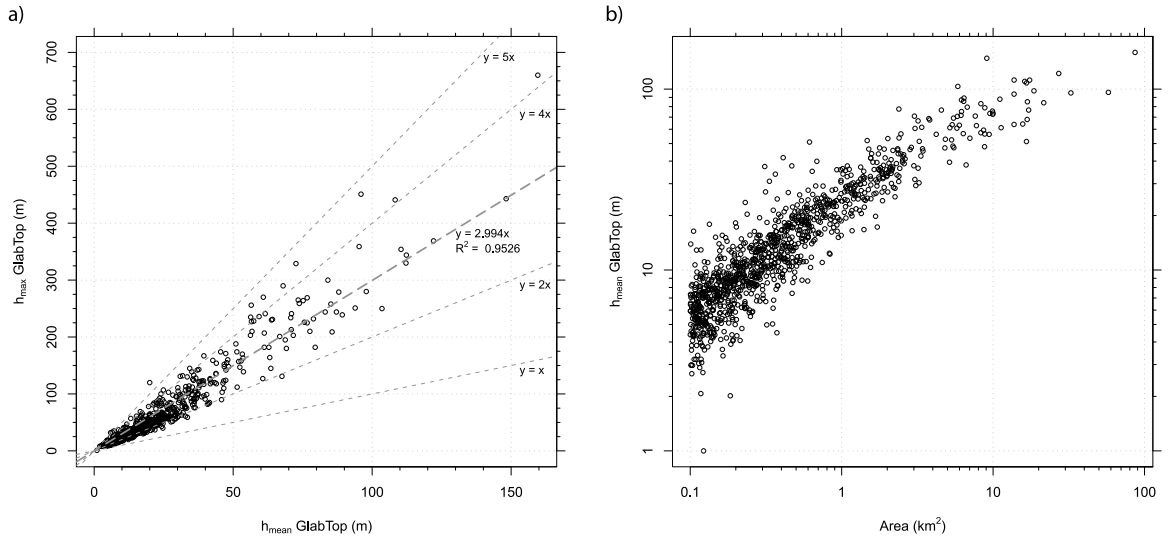

Figure 4. (a) Scatterplot of mean thickness versus maximum thickness and (b) mean thickness versus area.

profiles through other glaciers (not shown) illustrate the variability of the location of the thickest glacier parts. While for most of the larger valley glaciers the thickest ice is found in the flat tongues of the ablation region, for some glaciers (e.g., Trient, Giétro, Mont Miné, Ried, and Hüfi glacier) it is found in the accumulation region. These glaciers have comparably steep and thus thin tongues and a wide and flat (and thus thick) accumulation area at high altitude. This has important consequences for the future evolution of glaciers in regard to water resources (cf. section 8.3).

[40] The mean ice thickness for distinct elevation intervals with reference to the modeled glacier bed is depicted in Figure 6, along with the hypsography of the glacier surface and the volume distribution of the ice (both for 1973). While the glacierized area is about normally distributed around the mean elevation of 2900 m a.s.l., the mean ice thickness reaches its largest values at much lower elevations, i.e., 1900 m a.s.l..To some extent, this peak can be related to the large overdeepening found at Konkordia (the confluence of three large branches) of Great Aletsch glacier (cf. section 6.3). But also in general, much higher ice thickness values are found over bedrock situated below 2500 m a.s.l. The volume distribution resulting from the distribution of areas and thickness with elevation follows the hypsometry of the surface area with a downward shift of about 200 m. Despite the rapid decrease of glacier area below 2500 m a.s.l. (with reference to the surface), the ice volume situated above such low altitudes remains important (Figures 3 and 6).

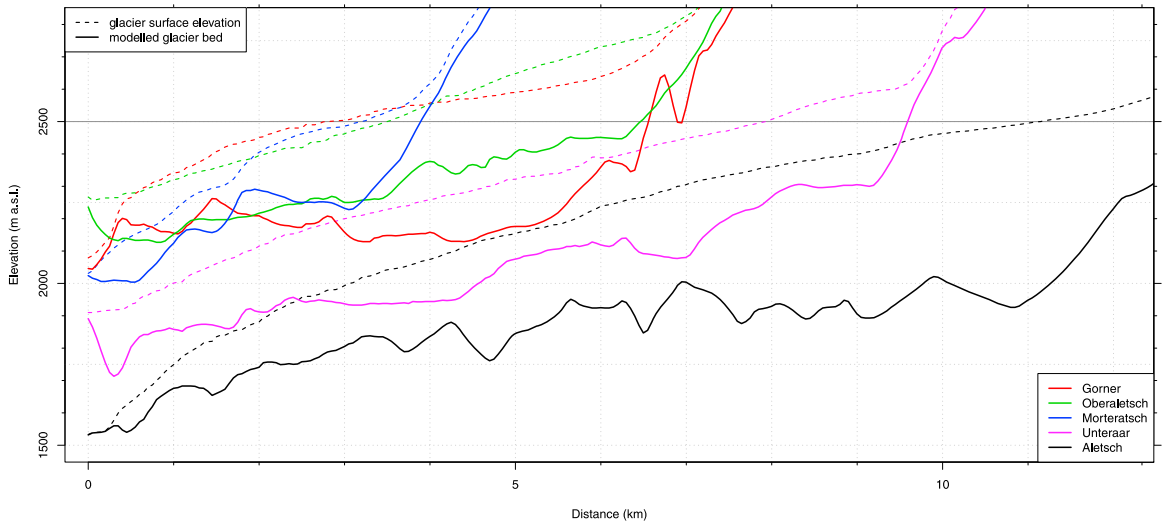

Figure 5. A direct comparison of profiles of bed elevations along the central flowline for a subset of 5 larger glacier tongues. For location see Figure 1.

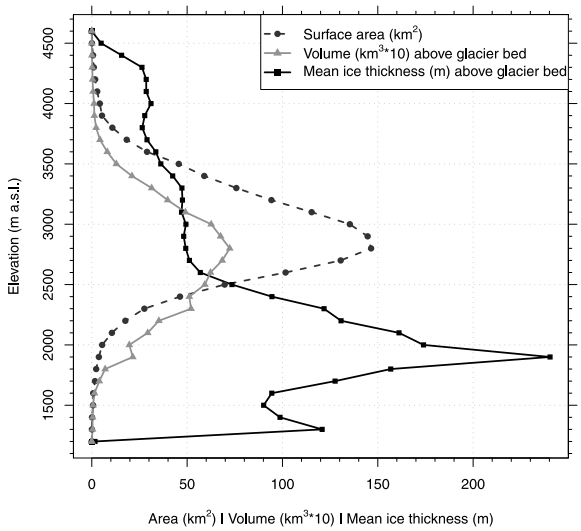

Figure 6. The hypsographic distribution of the glacier area and volume for the year 1973 and the corresponding mean ice thickness for distinct elevation intervals related to the modeled glacier bed.

6.3. Overdeepenings and Potential Future Lakes

[41] The detected overdeepenings in the modeled glacier beds indicate a high number of sites enabling potential future lake formation [cf. *Frey et al.*, 2010]. Using a threshold of 1 ha (10000 m^2) for the lake area (to exclude insignificant water bodies and model artifacts), 500–600 sites remain for the GlabTop_73L1 model run and 400–500 for the GlabTop_2kL2 run. For the Aletsch region a map with outlines of the modeled overdeepenings from both model runs is shown in (Figure 7a). The congruence of many outlines indicates that the location of these features is rather robust i.e., not much influenced by the DEM selected. These local depressions may, depending on the rocky/sedimentary nature of the glacier bed [e.g., *Maisch et al.*, 2000; *Zemp et al.*, 2005], be either filled with water and form lakes (deep depressions, rock beds) or trap sediments and become floodplains (shallow depressions, sediment beds) in the glacier forefield after the glacier has disappeared. Disregarding the latter case for a first order assessment, a total of about 50–60 km^2 of potential new lake area can form (Table 3) once all glacier ice has vanished [cf. *Künzler et al.*, 2010]. This is slightly more than the area of Lake Thun (48.4 km^2) in Switzerland (Bundesamt für Umwelt (BAFU), Seen in der Schweiz, unpublished data, 2007, http://www.bafu.admin.ch/hydrologie/01835/02118/index.html).

Table 3. Summary of the Overdeepenings Detected in the Modeled Glacier Bed Geometries for Two GlabTop Runs and Two Interpolation-Algorithms[a]

	IDW		TopoToRaster	
	73L1	2kL2	73L1	2kL2
Number of overdeepening	625	523	515	394
Total area (km^2)	65	52	56	44
Total volume (km^3)	2.3	1.6	1.9	1.2
Arithmetic mean depth (m)	35	31	35	28
Area weighted mean depth (m)	15	15	14	13

[a](IDW, TopoToRaster): 73L1 refers to the year 1973 and 2kL2 refers to the year 1999.

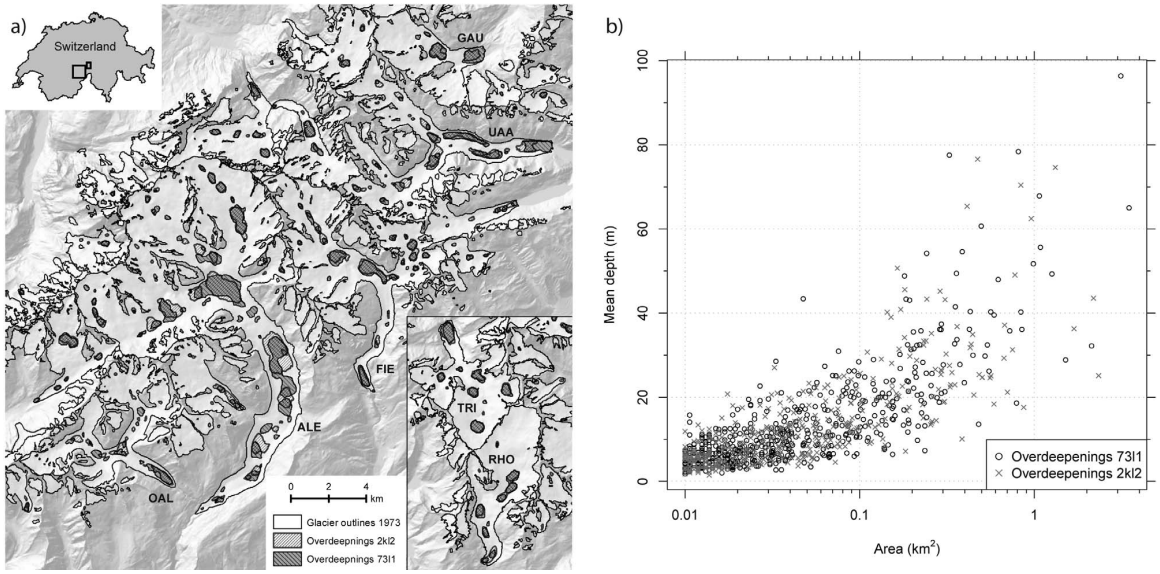

Figure 7. (a) An illustration of the modeled overdeepnings for both model runs for the Aletsch region (see inset for location; abbreviations refer to the following glaciers: GAU, Gauli; UAA, Unteraar; FIE, Fiescher; ALE, Great Aletsch; OAL, Oberaletsch; TRI, Trift; RHO, Rhone) and (b) scatterplot of mean depth of the overdeepenings versus their area as modeled for the year 1973 (73L1) and 1999 (2kL2).

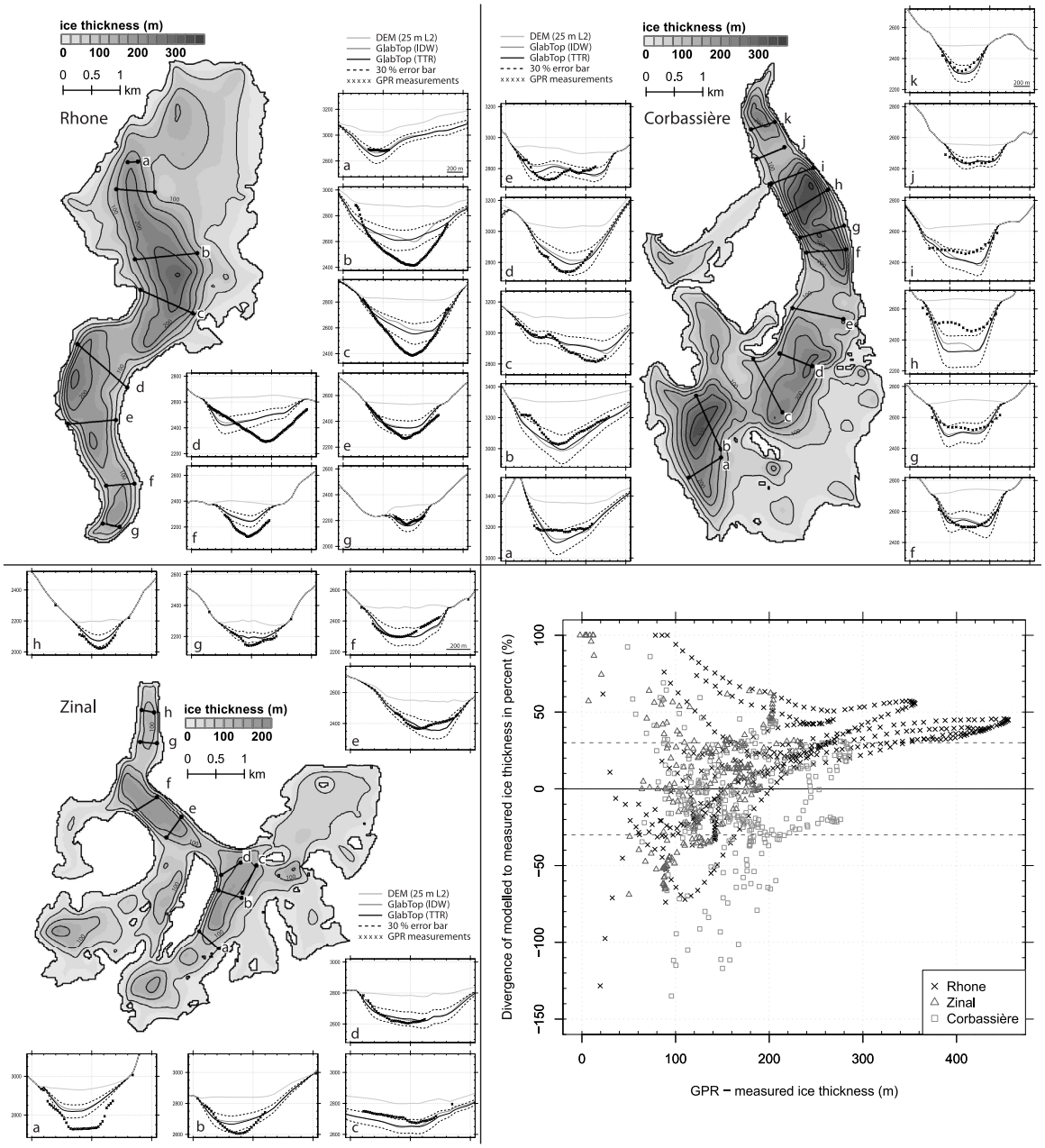

Figure 8. (top left) Calculated ice-thickness distribution of Rohne, (top right) Corbassière and (bottom left) Zinal glacier. The insets show the marked cross-sections with the two different GlabTop model versions (IDW versus TopoToRaster), the GPR measurements and an error range of ±30% for validation. All profile plots have the same horizontal extent and vertical exaggeration. On the y-axis the elevation is displayed. (bottom right) Divergence of modeled to measured ice thickness value in percent of the three validation glaciers is assigned to the measured thickness value from GPR.

[42] More than half of the 500–600 overdeepenings are smaller than 5 ha and their mean depth is smaller than 20 m (Figure 7b). The two largest overdeepenings are located underneath Great Aletsch glacier with a combined area of about 5 km^2. The depression located at Konkordia, for instance, has an area of about 2.5 km^2, a mean (max) depth of approximately 100 m (300 m) and a volume of about 250 million m^3 (Figure 7a). This roughly corresponds to the Lac d'Emosson, which is the second largest hydropower lake in the Swiss Alps (BAFU, unpublished data, 2007) with an

Table 4. Mean Thickness in Meters of the Three Validation Glaciers (Rhone, Zinal and Corbassière) Derived With the Approach From *Haeberli and Hoelzle* [1995] and GlabTop (Two Interpolation Methods) From the DEM25L2 and the SGI2000 Outline and Also for the ITEM Approach Where the Calculated Volume was Divided With the Area as Listed in *Farinotti et al.* [2009a]

	HH95	GT(idw)	GT(ttr)	ITEM
Rhone	105	101	105	132
Zinal	54	58	61	66
Corbassière	84	91	96	93

area 3.27 km^2 and a volume of 227 million m^3, respectively. The largest mean depth of the potential lakes would reach 100 m, but most of them have a mean depth of less than 50 m (Figure 7b). Two-thirds of the overdeepenings have a volume below 1 million m^3 and about 50 have a volume larger than 10 million m^3. The total volume of all modeled overdeepenings is about 2 km^3 or about 3% of the estimated ice volume in the Swiss Alps today.

7. Evaluation of Model Performance

7.1. Comparison With GPR Profiles

[43] In Figure 8 the calculated ice thickness distributions of the validation sites (Rhone, Corbassière and Zinal glacier) are shown within the SGI2000 outlines and the location of the GPR-measurements. The cross-section plots show elevation versus distance as modeled by GlabTop with two interpolation methods, a ±30% uncertainty range for the TopoToRaster-interpolation and the GPR measurements. This comparison reveals that GlabTop generally models the parabolic shape of glacier beds in good agreement with the shape of the GPR measurements. In absolute terms, the GPR data often show lower elevations (or higher ice thickness, in particular for Rhone glacier), but they are nearly always within the ±30% uncertainty range. Comparing the measured and modeled mean and maximum ice thickness within a profile at the locations of the GPR measurements, only 6 (mean) or 10 (maximum) out of 26 profiles deviate more than 30% and only 1 (mean and max) by more than 50%. For Zinal and Corbassière glacier the differences are not systematic and GlabTop is sometimes closer to the GPR data than ITEM. Only few profiles differ obviously from the measurements and need further explanation. Mean thickness values for the entire glacier are compared in Table 4. For Rhone glacier the value derived by GlabTop is about 20% smaller than with ITEM, for the other two glaciers there is not a large difference.

[44] At *Zinal glacier* (Figure 8, bottom left) ice thickness with GlabTop and ITEM is underestimated at profiles (a) by about 90 m and (b) by about 60 m. Compared to the ice thickness distribution modeled by ITEM [*Farinotti et al.* 2009b, Figure 7], GlabTop produces very similar results at the visual scale, in depth as well as in the location of the deeper and shallower parts. For 9 out of 11 profiles at *Corbassière glacier* (see Figure 8, top right) the measured GPR values are within the 30% uncertainty range of the modeled ice thickness with GlabTop. Only at profile (h) GlabTop strongly overestimates ice thickness (by about 150 m). This is different for *Rhone glacier* (see Figure 8, top left), where both methods often underestimate the GPR-derived thickness value, in particular the thickest parts (by more than 100 m). To obtain a better fit at these places (profiles b and c), a 50% higher ice thickness and hence a shear stress of about 225 kPa would be required for GlabTop. This seems unrealistically high for such flat regions and hints to specific local processes that are not accounted for by either model. Also special is profile (d), where GlabTop modeled an overdeepening at the orographic right side of the glacier tongue (where the surface is very flat) that does not appear in the GPR data. This illustrates that local surface slope might not in all cases be a good predictor of glacier thickness. However, based on visual inspection there is a good general agreement of the modeled thickness distribution pattern between GlabTop (Figure 8, top left) and ITEM [*Farinotti et al.* 2009b, Figure 6].

[45] The point-to-point comparison between modeled and measured ice thickness as shown in Figure 8 (bottom right) can be used for an integrative uncertainty assessment. In total, 54% of the differences are smaller than ±30% while 82% are smaller than ±50%. In particular for the large ice thicknesses at Rhone glacier the modeled values are out of the range of ±30%. For Zinal and Corbassière glacier 58% and 67% of the modeled values are within the ±30% uncertainty range. Some values differ by more than ±100%, but this concerns a small number of points with mostly thin ice. The overall mean difference is 6% with a standard deviation of 46%. Given that both models (GlabTop and ITEM) are not really designed to reproduce glacier thickness value at a point scale (i.e., the GPR profiles) we consider the agreement as sufficient for the intended purposes. The general pattern of the ice thickness distribution as well as the location of overdeepenings in the bed rock are rather robust and thus appropriate for application in other models.

7.2. Uncertainties in Input Parameters

[46] The uncertainty of each factor (cf. equation (1)) propagates in the same way to the overall uncertainty of the modeled ice thickness as the latter results from a linear combination of all factors. This implies that the parameter with the highest uncertainty (τ) governs the uncertainty of the thickness estimates. With our assumed uncertainty ranges for the other parameters, we can also calculate a worst-case scenario where possible uncertainties act in the same direction. Under such conditions τ would be 30% lower (or higher), slope would be overestimated (or underestimated) by 10%, and f is 0.9 (0.7) rather than 0.8. In these cases the thickness values would be underestimated by 42% or overestimated by 62% compared to a reference value. This range might indicate a possible minimum and maximum deviation for individual glaciers. For most of the other combinations the difference to the reference value does not exceed ±30%.

7.3. Model Intercomparison

[47] Glacier thickness values derived from the approach by *Haeberli and Hoelzle* [1995] are listed in Table 5 for 71 glaciers larger than 3 km^2 and are compared in the scatterplot of Figure 9a with the values derived from GlabTop with the TopoToRaster-interpolation. The mean ice thickness of

Table 5. The Parameters Area (A_{73}), Elevation Range (ΔH) and Mean Slope (α) for 71 Glaciers >3 km^2 and a Comparison of Mean (h_{mean}) and Maximum Thickness (h_{max}) and Volume (V) as Modeled With GlabTop_73L1 With the IDW-Interpolation ($GlabTop_{idw}$) and the TopoToRaster-Interpolation ($GlabTop_{ttr}$) and the Parameterization Scheme From *Haeberli and Hoelzle* [1995] (HH95)[a]

	Glacier Parameter			h_{mean} (m)			h_{max} (m)			Volume (km^3)		
					GlabTop			GlabTop			GlabTop	
	A_{73} (km^2)	ΔH (m)	α (°)	HH95	idw	ttr	HH95	idw	ttr	HH95	idw	ttr
Grosser Aletsch Gletscher	86.63	2602	15.3	148	144	160	606	669	660	12.86	12.51	13.82
Gornergletscher	57.77	2522	18.9	91	87	96	442	416	451	5.26	5.00	5.55
Fieschergletscher VS	32.65	2493	18.2	104	87	95	429	365	359	3.39	2.83	3.11
Unteraargletscher	27.15	2186	17.9	103	112	122	683	369	369	2.80	3.04	3.31
Oberaletschgletscher	21.62	1700	21.5	91	78	84	465	298	300	1.96	1.68	1.82
Findelengletscher	18.62	1679	14.9	85	89	98	428	290	280	1.59	1.66	1.82
Rhonegletscher	17.44	1470	14.8	103	99	112	451	339	330	1.80	1.72	1.96
Triftgletscher	17.18	1729	19.5	71	69	77	252	282	269	1.21	1.19	1.32
Zmuttgletscher	16.85	1872	19.1	74	78	85	435	274	258	1.24	1.31	1.43
Morteratsch Vadret da	16.79	2010	21.6	64	66	68	296	304	290	1.08	1.11	1.15
Otemma Glacier d'	16.64	1359	16.9	110	96	108	601	398	441	1.83	1.60	1.80
Feegletscher	16.62	2267	23.4	42	51	51	184	178	174	0.70	0.84	0.85
Corbassière Glacier de	16.18	2052	16.8	84	97	110	431	392	354	1.36	1.57	1.79
Zinal Glacier de	15.70	2206	23.3	59	56	64	281	219	231	0.93	0.87	1.01
Hüfifirn	13.77	1565	14.7	70	99	112	241	356	344	0.97	1.37	1.55
Kanderfirn	13.76	956	14.1	88	80	94	379	252	251	1.22	1.11	1.29
Gauligletscher	13.76	1458	20.2	72	59	64	346	231	230	0.99	0.82	0.88
Fieschergletscher BE	11.31	2860	24.0	51	57	61	237	212	207	0.58	0.65	0.69
Mont Miné Glacier du	11.09	1751	16.9	80	79	88	290	279	279	0.89	0.87	0.98
Allalingletscher	9.98	1807	17.8	63	62	74	275	253	259	0.62	0.62	0.74
Brenay Glacier du	9.96	1257	19.7	71	59	73	346	253	329	0.71	0.59	0.72
Ferpècle Glacier de	9.90	1503	17.1	69	65	76	254	217	226	0.69	0.64	0.75
Langgletscher	9.52	1866	20.2	64	67	73	302	272	265	0.61	0.63	0.70
Oberer Grindelwaldgletscher	9.42	2468	24.5	48	54	56	169	203	203	0.45	0.51	0.53
Plaine Morte Glacier de la	9.09	664	7.70	76	124	148	272	402	443	0.69	1.12	1.35
Forno Vadrec del	8.82	1197	19.0	82	76	79	403	238	232	0.72	0.67	0.70
Steingletscher	8.81	1494	21.8	57	52	57	247	269	256	0.50	0.46	0.50
Roseg Vadret da	8.78	1455	21.9	57	49	48	234	167	160	0.50	0.43	0.42
Obers Ischmeer	8.65	2217	24.8	54	54	59	227	237	236	0.47	0.47	0.51
Mittelaletschgletscher	8.31	1778	24.0	53	54	57	284	216	228	0.44	0.45	0.48
Riedgletscher	8.31	2242	19.5	50	80	83	203	248	244	0.42	0.66	0.69
Saleina Glacier de	7.77	2096	22.2	54	60	63	221	188	182	0.42	0.46	0.49
Mont Durand Glacier du	7.63	1900	20.4	54	67	71	293	240	241	0.41	0.51	0.54
Tschierva Vadret da	7.03	1809	25.4	53	49	54	254	163	163	0.37	0.34	0.38
Brunegggletscher	6.75	1631	18.3	51	72	80	267	182	182	0.34	0.48	0.54
Palü Vadret da	6.64	1466	22.8	47	38	38	206	130	122	0.31	0.25	0.25
Griesgletscher	6.43	975	13.5	76	79	89	371	250	239	0.49	0.51	0.57
Trient Glacier du	6.40	1672	17.4	52	76	86	171	222	209	0.33	0.48	0.55
Moming Glacier de	6.36	1682	25.3	42	53	57	219	199	210	0.27	0.34	0.36
Tschingelfirn	6.19	1184	17.1	46	67	75	291	283	264	0.29	0.41	0.47
Arolla Glacier d'	6.18	1534	17.1	56	76	87	232	257	244	0.35	0.47	0.54
Rosenlauigletscher	6.14	1832	20.1	49	66	72	202	203	203	0.30	0.40	0.44
Turtmanngletscher	5.99	1901	19.3	58	59	63	252	168	164	0.35	0.35	0.38
Giétro Glacier du	5.85	1295	13.5	55	99	104	242	251	250	0.32	0.58	0.61
Arolla Haut Glacier d'	5.81	1045	18.5	57	69	71	338	231	234	0.33	0.40	0.41
Moiry Glacier de	5.77	1254	18.8	60	53	61	242	217	270	0.35	0.31	0.35
Hohlichtgletscher	5.51	1529	23.2	49	46	47	213	146	142	0.27	0.25	0.26
Schwarzberggletscher	5.48	925	14.9	58	67	69	311	183	180	0.32	0.37	0.38
Furgg-Gletscher	5.43	1053	20.6	54	47	48	283	142	148	0.25	0.22	0.22
Mellichgletscher	5.37	827	16.2	50	60	64	320	137	145	0.27	0.32	0.34
Oberaargletscher	5.32	1226	19.8	36	48	52	181	150	147	0.19	0.26	0.28
Dammagletscher	5.18	1107	20.3	63	60	61	302	181	182	0.33	0.31	0.32
Üsser Baltschiedergletscher	5.16	1539	26.1	37	38	39	165	114	117	0.19	0.20	0.20
Bisgletscher	4.84	1312	22.5	35	49	53	181	157	158	0.17	0.24	0.26
Paradiesgletscher	4.81	2429	28.0	32	43	47	131	177	171	0.15	0.20	0.23
Cheilon Glacier de	4.56	1017	16.9	50	66	77	322	215	225	0.23	0.30	0.35
Stufesteigletscher	4.21	1770	27.1	35	53	56	180	240	235	0.15	0.22	0.24
Tsanfleuron Glacier de	3.81	569	10.0	55	64	68	243	134	131	0.21	0.25	0.26
Castel Nord Vadrec dal	3.76	1013	18.9	57	61	69	415	186	195	0.22	0.23	0.26
Hohbergletscher	3.45	1897	25.1	41	45	45	180	192	174	0.14	0.15	0.16
Breithorngletscher	3.42	1307	23.5	41	45	47	219	152	148	0.14	0.15	0.16
Oberer Theodulgletscher	3.38	602	12.7	38	47	62	223	110	241	0.13	0.16	0.21
Wildstrubelgletscher	3.34	731	18.2	39	37	43	169	121	159	0.13	0.12	0.14
Silvrettagletscher	3.25	707	13.7	53	48	51	252	112	112	0.17	0.16	0.17
Grialetsch Vadret da	3.24	599	19.5	24	30	30	88	65	61	0.08	0.10	0.10

Table 5. (continued)

	Glacier Parameter			h_{mean} (m)			h_{max} (m)			Volume (km^3)		
					GlabTop			GlabTop			GlabTop	
	A_{73} (km^2)	ΔH (m)	α (°)	HH95	idw	ttr	HH95	idw	ttr	HH95	idw	ttr
Tiefengletscher	3.20	912	22.2	39	37	37	181	138	128	0.13	0.12	0.12
Tsijiore Nouve Glacier de	3.20	1469	21.6	54	56	67	222	194	201	0.17	0.18	0.21
Flachensteinfirn	3.09	937	25.4	30	29	29	125	59	57	0.09	0.09	0.09
Glatt Firn	3.05	1007	17.3	40	58	61	137	134	127	0.12	0.18	0.19
Alpjergletscher	3.04	703	19.1	32	31	32	123	81	78	0.10	0.09	0.10
Brunnifrin	3.02	949	18.1	44	57	71	211	220	213	0.13	0.17	0.21
	Glacier Parameter			h_{mean} (m)			h_{max} (m)			Volume (km^2)		
					GlabTop			GlabTop			GlabTop	
	A_{73} (km^2) sum	ΔH (m) mean	α (°) mean	HH95 mean	idw mean	ttr mean	HH95 mean	idw mean	ttr mean	HH95 sum	idw sum	ttr sum
Glaciers >3 km^2	750.1	1522.5	19.4	78.9	80.4	88.7	279.8	225.7	228.3	59.2	60.3	66.5
Glaciers 0.1–3 km^2	504.9	482.7	26.8	24.8	22.4	24.0	63.6	35.3	336.9	12.5	11.3	12.1
Glaciers 0.1–0.01 km^2	49.0	156.8	30.5	5.0	5.0	5.0	18.0	7.0	6.4	0.2	0.2	0.2
Glaciers >0.01 km^2	1304.1	336.4	28.6	55.1	55.1	60.5	45.3	25.6	26.1	71.9	71.9	78.9

[a]At the end of the table the totals or average values of distinct glacier size classes are shown.

glaciers larger than 3 km^2 (1 km^2) is about 15% (5%) higher with the latter interpolation. When the mean slope per glacier is directly derived from the DEM, but h_{mean} calculated with the approach by *Haeberli and Hoelzle* [1995], much smaller thickness values result for these larger glaciers, as the mean slope based on DEM cells is higher than the value from length and elevation range in these cases. On the other hand, for the smallest glaciers (h_{mean} < 30 m) the mean slope is smaller and the thickness becomes higher in GlabTop. The histogram of thickness classes in Figure 9b illustrates these differences. Most glaciers (65%–75%) have a mean ice thickness smaller than 40 m. The total volume derived from GlabTop is between 2% (using the IDW interpolation of base points) and 12% (with TopoToRaster) higher than with the *Haeberli and Hoelzle* [1995] approach.

[48] The equivalent comparison with the ITEM approach by *Farinotti et al.* [2009a] is displayed in the scatterplot of Figure 10a (R^2 = 0.69), indicating smaller mean thickness values from GlabTop, in particular for the three thickest glaciers as modeled by ITEM. These three glaciers (Aletsch, Unteraar, Rhone) are partly responsible for the 8 km^2 higher

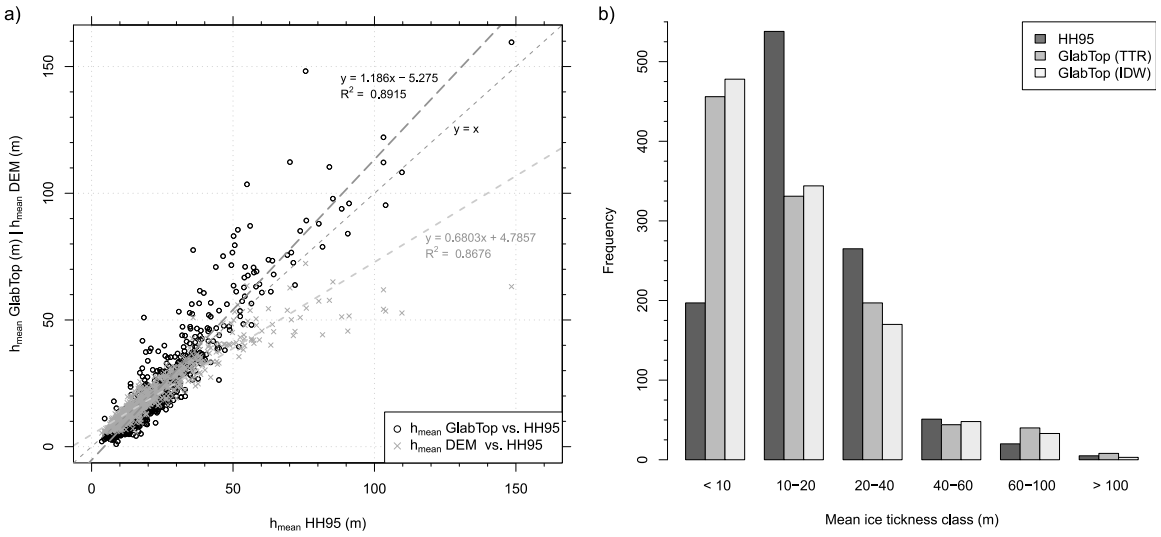

Figure 9. (a) Mean ice thickness of GlabTop and as derived from DEM-slope are displayed versus mean ice thickness derived by the approach from *Haeberli and Hoelzle* [1995]. (b) Frequency distribution of modeled mean ice thickness values.

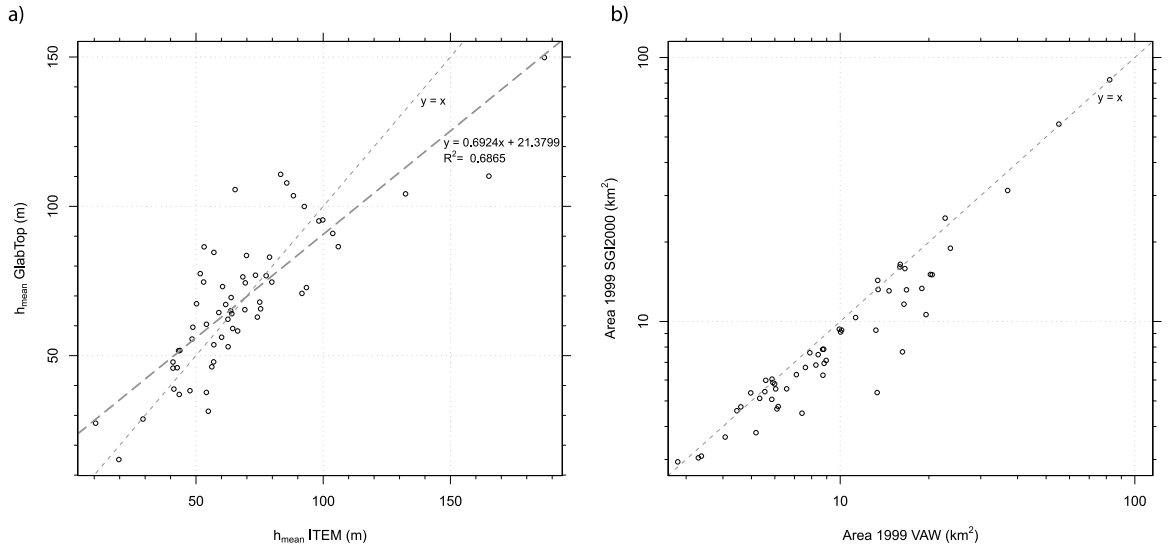

Figure 10. Comparison of GlabTop versus ITEM with (a) the mean thickness and (b) the area.

total volume of 65 ± 8 km^3 with ITEM for the year 1999 and glaciers larger than 3 km^2 compared to GlabTop. For all glaciers the difference is slightly smaller (74 ± 9 km^3 with ITEM and 68 ± 20 km^3 with GlabTop). The total volume from GlabTop for all Swiss glaciers is in this case around 10% smaller than that derived with ITEM.

8. Discussion

8.1. Ice Volume and Thickness

[49] The total ice volume for all Swiss glaciers as modeled with GlabTop (72–79 km^3 for 1973, 61–68 km^3 for 1999) is in good agreement with earlier studies by *Müller et al.* [1976] (67 km^3 for the 1970's) and *Maisch et al.* [2000] (74 km^3 for 1973), but overall 10–20% smaller than calculated with the ITEM approach by *Farinotti et al.* [2009a] (74 km^3 for 1999). The thickness and volume estimates from the different approaches nevertheless agree within the estimated general uncertainty (about 30%) with the ITEM results probably providing upper-bound values.

[50] According to our model, most glaciers smaller than 1 km^2 have mean thickness values below 20 m, or even below 10 m if they are smaller than 0.2 km^2 (cf. Figure 4b). Considering that a 10 m mean thickness translates to a maximum thickness of about 30 m (cf. section 6.1 and Figure 4a), the modeled values can still be regarded as being realistic. The more or less constant scatter in mean thickness for glaciers larger than 1 km^2, (e.g., from 50 to 100 m for glaciers with a size of 10 km^2) indicates a variability of the glacier volume by a factor of two for glaciers of the same size.

8.2. Accuracy and Uncertainties

[51] Concerning direct ice thickness measurements, GPR had started to replace earlier seismic soundings (cf., for instance *Haeberli and Fisch* [1984] and *Narod and Clarke* [1994]) and is now widely used [cf. *Farinotti*, 2010]. However, the point density of measurements per km^2 of a glacier can vary by orders of magnitude, because measurements are difficult to carry out in very steep, crevassed, avalanche- or ice-/rockfall affected areas of a glacier [*Fischer*, 2009]. For simple logistic reasons, therefore, ground-based GPR profiles mainly cover the crevasse-free flat (and thick) parts of glaciers with compressing flow (often in overdeepened parts of the bed) and might thus not be representative for the entire glacier. In order to derive the spatial distribution of ice thickness variability over entire glaciers, GPR data has therefore to be inter- and extrapolated from measured profiles using model assumptions [e.g., *Bauder et al.*, 2003; *Binder et al.*, 2009]. Smoothing techniques to reflect longitudinal stress coupling in the ice are thereby especially critical with respect to estimating thinner ice depths underneath steeper glacier parts with extending flow and intense crevasse formation: fitting models for thickness estimations to selected radar profiles is not trivial.

[52] The direct comparison with the thickness values of three glaciers shown in the GPR profiles by *Farinotti et al.* [2009b, 2009a] and *VAW* [1998] reveals that the maximum ice thickness values obtained by GlabTop are within an uncertainty range of ±30% in flat regions. For individual glaciers, ITEM gives 20–30% higher ice thickness values than GlabTop, but GlabTop can also predict higher values locally. The former largely explains the observed differences in the total glacier volume, but the area used in the ITEM model is also slightly higher (see Figure 10b). However, neither GlabTop nor ITEM is designed to resolve the glacier bed topography at a high spatial resolution. Both approaches rather allow sketching plausible bed configurations that are important to model future glacier evolution [e.g., *Jouvet et al.*, 2011]. Though absolute modeled ice thickness of places with overdeepenings have an uncertainty of ±30%, the locations of the modeled overdeepenings in the glacier bed are rather robust. To this end, the validation with the GPR profiles reveals that the locally averaged slope values of the surface topography are indeed well suited to model general glacier bed characteristics.

8.3. Glacier-Bed Topography and Future Glacier Evolution

[53] The modeled glacier beds (cf. sections 6.1 and 6.2) lead to three important implications concerning possible future glacier evolution:

[54] (i) Due to the low mean slope of the bedrock in the ablation region of the largest glaciers, a retreat of the corresponding tongues to higher elevations is hardly possible in the longer term (>50 a). As a consequence of the mass balance altitude feedback [e.g., *Raymond et al.*, 2005], such tongues cannot easily adjust their geometries to increasing temperatures, and a self-acceleration of the mass loss for surfaces located at increasingly lower elevations will occur. While this reinforcement feedback might be slowed down for some glaciers by an increasing amount of debris-cover on the surface [*Jouvet et al.*, 2011] or increased shading from adjacent slopes [*Paul*, 2010], the already observed albedo reduction (caused by small particles) might strongly enhance mass loss [*Oerlemans et al.*, 2009; *Paul et al.*, 2005].

[55] (ii) The formation of lakes in the modeled overdeepenings could strongly enhance mass loss by calving and draw-down of ice from higher areas. In contrast to current time-dependent modeling approaches [e.g., *Jouvet et al.*, 2009], the ice will probably not remain longest where the glacier ice is thickest (i.e., in the overdeepenings), but early development of pro-glacial lakes at these places may well enhance and accelerate ice loss through thermokarst effects [e.g., *Kääb and Haeberli*, 2001; *Kirkbride and Warren*, 1999] and calving processes [e.g., *Benn et al.*, 2007]. Once the ice is decoupled from the glacier it will rapidly meltdown independent of its location in a lake or on land [*Vacco et al.*, 2010], as many examples worldwide show. Due to the sedimentary characteristics of some (especially debris-covered) glaciers, shallow lakes can be filled with sediment rather than water. This aspect is a matter of further investigations, in particular in view of the potential use of such lakes for hydro-power-production, either as a reservoir or a sediment trap [*Terrier et al.*, 2011].

[56] (iii) The observation that the ice thickness in the ablation area – in particular for the largest glaciers – is often larger than in the accumulation area has important consequences for future water availability in regions with similar glacier types. After the ice in the flat and thick tongues has melted away (possibly rather fast due to reinforcement feedbacks), not much ice volume will remain in the steep back walls and summer runoff can decrease sharply in the future [*Huss et al.*, 2010]. This steep/high-altitude ice may remain there for extended times, as it is less sensitive to rising snow lines. On the other hand, medium-sized valley glaciers that have flat and thus thick accumulation regions (e.g., Trient, Giétro, Mont Miné, Ried, and Hüfi glacier) will become increasingly important with their ice reserves in terms of supplying meltwater, when most of the flat, low-altitude tongues have already disappeared.

9. Conclusions

[57] We here applied a model (named GlabTop) to obtain the ice thickness distribution for large glacier samples to the entire Swiss Alps and analyzed the characteristics of the resulting glacier beds in terms of potential future lake formation sites among others. The model provides an important alternative to mass conservation/flow models and works with limited and widely available input data (a DEM, glacier outlines and a set of central branch lines). While the uncertainty of mean thickness and volume values for unmeasured glaciers unavoidably remains high (about ±30% on average) due to uncertainties in the parameterization of ice flow components, the spatial pattern of ice thickness and bed topography (including the location of overdeepenings) primarily depends on surface slope and is found to be rather robust. GlabTop provides information on a possible future (ice-free) surface topography and sites of potential lake formation, both of which are key elements for studies related to climate change impacts on landscape and glacier evolution in mountain regions [e.g., *Huss*, 2012]. The results of the here presented application of the GlabTop approach to all glaciers in the Swiss Alps reveal the following main findings:

[58] 1. While absolute values of ice thickness estimates are still affected by a relatively large uncertainty range (±30% on average and even more in individual cases), relative spatial patterns of modeled glacier-bed topography primarily depend on surface slope as contained in DEMs and are quite robust.

[59] 2. The total ice volume for all Swiss glaciers produced by GlabTop is about 75 ± 22 km^3 for 1973 and 65 ± 20 km^3 in 1999; differences to other independent estimates remain within the uncertainty range of ±30%.

[60] 3. The calculated mean glacier thickness – as determined over changing glacier areas and surface elevations between 1973 and 1999 – is around 60 m.

[61] 4. When excluding the largest 15 glaciers from the sample (that contain 50% of the total volume), mean ice thickness of all other glaciers is about 40 m.

[62] 5. The modeled maximum glacier thickness is about three times larger than mean thickness (as found in earlier studies).

[63] 6. Mean thicknesses for individual glaciers of the same size vary by more than a factor of two, indicating a ±50% uncertainty or even more for area-related (planar) estimates of mean glacier thicknesses or volumes.

[64] 7. The ice of the largest glaciers is often found in comparably flat/thick glacier tongues situated above weakly inclined beds at comparably low elevations (below 2300 m a.s.l.). This implies that such glaciers cannot really retreat to higher elevations with cooler conditions and may continue to shrink until the slope of the glacier bed increases substantially.

[65] 8. A considerable number of (partly large) overdeepenings is found in the modeled glacier beds; they have a total area of about 50–60 km^2 and can be seen as sites of potential future lake formation. Such lakes are of high interest for hydropower production and tourism, but they could also enhance glacier mass loss and may constitute major hazard potentials.

[66] Applicability of the model to other mountain ranges and the necessary adjustments to differing climatic, topographic and data-quality conditions must be investigated as a next step.

[67] **Acknowledgments.** This study was funded by FOEN (Federal Office of Environment) and FMV (Forces Motrices Valaisannes) as part of the two research projects CCHydro and "Climate change and hydropower." Swisstopo provided the topographic maps and DEMs used and

the VAW/ETHZ the GPR measurements for Rhone and Zinal glacier. GPR data for Corbassière glacier were kindly provided by M. Funk from VAW/ETHZ. The constructive comments of the editors A. Densmore and B. Hubbard as well as the reviews of G. Clarke and the anonymous reviewers helped to improve the manuscript considerably.

References

Bahr, D. B., M. F. Meier, and S. D. Peckham (1997), The physical basis of glacier volume-area scaling, *J. Geophys. Res.*, *102*(B9), 20,355–20,362, doi:10.1029/97JB01696.

Bauder, A., M. Funk, and G. H. Gudmundsson (2003), The ice-thickness distribution of Unteraargletscher, Switzerland, *Ann. Glaciol.*, *37*, 331–336.

Benn, D. I., C. R. Warren, and R. H. Mottram (2007), Calving processes and the dynamics of calving glaciers, *Earth Sci. Rev.*, *82*(3–4), 143–179, doi:10.1016/j.earscirev.2007.02.002.

Binder, D., E. Brückl, K. Roch, M. Behm, W. Schöner, and B. Hynek (2009), Determination of total ice volume and ice-thickness distribution of two glaciers in the Hohe Tauern region, Eastern Alps, from GPR data, *Ann. Glaciol.*, *50*, 71–79.

Chen, J., and A. Ohmura (1990), Estimation of Alpine glacier water resources and their change since the 1870s, *IAHS AISH Publ.*, *193*, 127–135.

Clarke, G. K. C., E. Berthier, C. G. Schoof, and A. H. Jarosch (2009), Neural networks applied to estimating subglacial topography and glacier volume, *J. Clim.*, *22*, 2146–2160, doi:10.1175/2008JCLI2572.1.

Driedger, C., and P. Kennard (1986), Glacier volume estimation on Cascade volcanos: An analysis and comparison with other methods, *Ann. Glaciol.*, *8*, 59–64.

ESRI (2008), *ArcGIS Desktop: Release 9.3*, Environ. Syst. Res. Inst., Redlands, Calif.

Etzelmüller, B., and H. Björnsson (2000), Map analysis techniques for glaciological applications, *Int. J. Geogr. Inf. Sci.*, *14*(6), 567–581, doi:10.1080/136588100415747.

Farinotti, D. (2010), Simple methods for inferring glacier-thickness and snow accumulation distribution, PhD thesis, Lab. of Hydraulics, Hydrol. and Glaciol. (VAW), ETH-Zurich, Zurich, Switzerland.

Farinotti, D., M. Huss, A. Bauder, and M. Funk (2009a), An estimate of the glacier ice volume in the Swiss Alps, *Global Planet. Change*, *68*(3), 225–231, doi:10.1016/j.gloplacha.2009.05.004.

Farinotti, D., M. Huss, A. Bauder, M. Funk, and M. Truffer (2009b), A method to estimate the ice volume and ice-thickness distribution of alpine glaciers, *J. Glaciol.*, *55*, 422–430.

Fischer, A. (2009), Calculation of glacier volume from sparse ice-thickness data, applied to Schaufelferner, Austria, *J. Glaciol.*, *55*, 453–460.

Frey, H., W. Haeberli, A. Linsbauer, C. Huggel, and F. Paul (2010), A multi-level strategy for anticipating future glacier lake formation and associated hazard potentials, *Nat. Hazards Earth Syst. Sci.*, *10*(2), 339–352.

Haeberli, W., and W. Fisch (1984), Electrical resistivitiy soundings of glacier beds: A test study on Grubengletscher, Wallis, Swiss Alps, *J. Glaciol.*, *30*, 373–376.

Haeberli, W., and M. Hoelzle (1995), Application of inventory data for estimating characteristics of and regional climate-change effects on mountain glaciers: A pilot study with the European Alps, *Ann. Glaciol.*, *21*, 206–212.

Haeberli, W., and J. Schweizer (1988), Rhonegletscher 1850: Eismechanische Überlegungen zu einem historischen Gletscherstand, *Mitt. VAW/ETHZ*, *94*, 59–70.

Hoelzle, M., T. Chinn, D. Stumm, F. Paul, M. Zemp, and W. Haeberli (2007), The application of glacier inventory data for estimating past climate change effects on mountain glaciers: A comparison between the European Alps and the Southern Alps of New Zealand, *Global Planet. Change*, *56*(1–2), 69–82, doi:10.1016/j.gloplacha.2006.07.001.

Huss, M. (2012), Extrapolating glacier mass balance to the mountain range scale: The European Alps 1900–2100, *Cryosphere Discuss.*, *6*(2), 1117–1156, doi:10.5194/tcd-6-1117-2012.

Huss, M., G. Jouvet, D. Farinotti, and A. Bauder (2010), Future high-mountain hydrology: A new parameterization of glacier retreat, *Hydrol. Earth Syst. Sci.*, *14*(5), 815–829.

Hutchinson, M. (1989), A new procedure for gridding elevation and stream line data with automatic removal of spurious pits, *J. Hydrol.*, *106*, 211–232, doi:10.1016/0022-1694(89)90073-5.

Jouvet, G., M. Huss, H. Blatter, M. Picasso, and J. Rappaz (2009), Numerical simulation of Rhonegletscher from 1874 to 2100, *J. Comput. Phys.*, *228*(17), 6426–6439, doi:10.1016/j.jcp.2009.05.033.

Jouvet, G., M. Huss, M. Funk, and H. Blatter (2011), Modelling the retreat of Grosser Aletschgletscher, Switzerland, in a changing climate, *J. Glaciol.*, *57*(206), 1033–1045.

Kääb, A., and W. Haeberli (2001), Evolution of a high-mountain thermokarst lake in the Swiss Alps, *Arct. Antarct. Alp. Res.*, *33*(4), 385–390.

Kamb, B., and K. A. Echelmeyer (1986), Stress-gradient coupling in glacier flow: I. Longitudinal averaging of the influence of ice thickness and surface slope, *J. Glaciol.*, *32*(111), 267–284.

Kirkbride, M. P., and C. R. Warren (1999), Tasman glacier, New Zealand: 20th-century thinning and predicted calving retreat, *Global Planet. Change*, *22*(1–4), 11–28, doi:10.1016/S0921-8181(99)00021-1.

Künzler, M., C. Huggel, A. Linsbauer, and W. Haeberli (2010), Emerging risks related to new lakes in deglaciating areas of the Alps, in *Mountain Risks: Bringing Science to Society. Proceedings of the "Mountain Risk" International Conference, 24–26 November 2010, Firenze, Italy*, edited by J.-P. Malet, T. Glade, and N. Casagli, pp. 453–458, CERG Editions, Strasbourg, France.

Laboratory of Hydraulics, Hydrology and Glaciology (VAW) (1998), Mauvoisin, Giétrogletscher, Corbassièregletscher, Glaziologische Studie im Zusammenhang mit den Stauanlagen Mauvoisin, *Tech. rep. 55.05.7903*, Lab. of Hydraulics, Hydrol. and Glaciol., ETH-Zurich, Zurich, Switzerland.

Lemke, P., et al. (2007), Observations: Changes in snow, ice and frozen ground, in *Climate Change 2007: The Physical Science Basis. Contribution of Working Group I to the Fourth Assessment Report of IPCC*, edited by S. Solomon et al., pp. 337–383, Cambridge Univ. Press, New York.

Li, H., Z. Li, M. Zhang, and W. Li (2011), An improved method based on shallow ice approximation to calculate ice thickness along flow-line and volume of mountain glaciers, *J. Earth Sci.*, *22*(4), 441–448, doi:10.1007/s12583-011-0198-1.

Li, H., F. Ng, Z. Li, D. Qin, and G. Cheng (2012), An extended "perfect-plasticity" method for estimating ice thickness along the flow line of mountain glaciers, *J. Geophys. Res.*, *117*, F01020, doi:10.1029/2011JF002104.

Linsbauer, A., F. Paul, M. Hoelzle, H. Frey, and W. Haeberli (2009), The Swiss Alps without glaciers: A GIS-based modelling approach for reconstruction of glacier beds, in *Proceedings of Geomorphometry 2009*, edited by R. Purves et al., pp. 243–247, Univ. of Zurich, Zurich, Switzerland.

Luethi, M., M. Funk, and A. Bauder (2008), Comment on 'Integrated monitoring of mountain glaciers as key indicators of global climate change: The European Alps' by Haeberli and others, *J. Glaciol.*, *54*(184), 199–200.

Maisch, M., and W. Haeberli (1982), Interpretation geometrischer Parameter von Spätglazialgletschern im Gebiet Mittelbünden, Schweizer Alpen, in *Beiträge zur Quartärforschung in der Schweiz*, pp. 111–126, Schriftenr. Phys. Geogr. Univ. Zürich, Zurich, Switzerland.

Maisch, M., A. Wipf, B. Denneler, J. Battaglia, and C. Benz (2000), Die Gletscher der Schweizer Alpen: Gletscherhochstand 1850, aktuelle Vergletscherung, Gletscherschwundszenarien, *Final rep. 31*, vdf Hochschulverlag, Zürich, Switzerland.

Marshall, S., E. White, M. Demuth, T. Bolch, R. Wheate, B. Menounos, M. Beedle, and J. Shea (2011), Glacier water resources on the eastern slopes of the Canadian Rocky Mountains, *Can. Water Resour. J.*, *36*(2), 109–134, doi:10.4296/cwrj3602823.

Müller, F., T. Caflisch, and G. Müller (1976), *Firn und Eis der Schweizer Alpen: Gletscherinventar*, Geogr. Inst. der ETH Zurich, Zurich, Switzerland.

Narod, B., and G. Clarke (1994), Miniature high-power impulse transmitter for radio-echo sounding, *J. Glaciol.*, *40*(134), 190–194.

Oerlemans, J., R. Giesen, and M. Van Den Broeke (2009), Retreating alpine glaciers: Increased melt rates due to accumulation of dust (Vadret da Morteratsch, Switzerland), *J. Glaciol.*, *55*(192), 729–736.

Paterson, W. (1994), *The Physics of Glaciers*, Pergamon, Tarrytown, N. Y.

Paul, F. (2007), The new Swiss glacier inventory 2000: Application of remote sensing and GIS, PhD thesis, Schriften. Phys. Geogr., Univ. Zürich, Zürich, Switzerland.

Paul, F. (2010), The influence of changes in glacier extent and surface elevation on modeled mass balance, *Cryosphere*, *4*(4), 569–581, doi:10.5194/tc-4-569-2010.

Paul, F., and W. Haeberli (2008), Spatial variability of glacier elevation changes in the Swiss Alps obtained from two digital elevation models, *Geophys. Res. Lett.*, *35*, L21502, doi:10.1029/2008GL034718.

Paul, F., and A. Linsbauer (2012), Modeling of glacier bed topography from glacier outlines, central branch lines and a DEM, *Int. J. Geograph. Inf. Sci.*, doi:10.1080/13658816.2011.627859, in press.

Paul, F., A. Kääb, M. Maisch, T. Kellenberger, and W. Haeberli (2004), Rapid disintegration of Alpine glaciers observed with satellite data, *Geophys. Res. Lett.*, *31*, L21402, doi:10.1029/2004GL020816.

Paul, F., H. Machguth, and A. Kääb (2005), On the impact of glacier albedo under conditions of extreme glacier melt: The summer of 2003 in the Alps, *EARSeL eProc.*, *4*(2), 139–149.

Paul, F., A. Kääb, and W. Haeberli (2007a), Recent glacier changes in the Alps observed by satellite: Consequences for future monitoring strategies,

Global Planet. Change, *56*(1–2), 111–122, doi:10.1016/j.gloplacha.2006.07.007.

Paul, F., M. Maisch, C. Rothenbuehler, M. Hoelzle, and W. Haeberli (2007b), Calculation and visualization of future glacier extent in the Swiss Alps by means of hypsographic modelling, *Global Planet. Change*, *55*(4), 343–357, doi:10.1016/j.gloplacha.2006.08.003.

Quincey, D., S. Richardson, A. Luckman, R. Lucas, J. Reynolds, M. Hambrey, and N. Glasser (2007), Early recognition of glacial lake hazards in the Himalaya using remote sensing datasets, *Global Planet. Change*, *56*(1–2), 137–152, doi:10.1016/j.gloplacha.2006.07.013.

Radic, V., and R. Hock (2010), Regional and global volumes of glaciers derived from statistical upscaling of glacier inventory data, *J. Geophys. Res.*, *115*, F01010, doi:10.1029/2009JF001373.

Raper, S. C. B., and R. J. Braithwaite (2009), Glacier volume response time and its links to climate and topography based on a conceptual model of glacier hypsometry, *Cryosphere*, *3*(2), 183–194.

Raymond, C., T. A. Neumann, E. Rignot, K. Echelmeyer, A. Rivera, and G. Casassa (2005), Retreat of Glaciar Tyndall, Patagonia, over the last half-century, *J. Glaciol.*, *51*(173), 239–247.

Rickenbacher, M. (1998), Die digitale Modellierung des Hochgebirges im DHM25 des Bundesamtes für Topographie, *Wiener Schr. Geograph. Kartographie*, *11*, 49–55.

Rothenbühler, C. (2006), GISALP: Räumlich-zeitliche Modellierung der klimasensitiven Hochgebirgslandschaft des Oberengadins, PhD thesis, Geograph. Inst., Univ. Zürich, Zürich, Switzerland.

Swiss Federal Office of Topography (2005), Das digitale Höhenmodell der Schweiz, report, Bundesamt für Landestopographie, Wabern, Switzerland.

Terrier, S., F. Jordan, A. Schleiss, W. Haeberli, C. Huggel, and M. Künzler (2011), Optimized and adapted hydropower management considering glacier shrinkage scenarios in the Swiss Alps, in *Proceedings of the International Symposium on Dams and Reservoirs under Changing Challenges: 79th Annual Meeting of ICOLD, Swiss Committee on Dams, Lucerne, Switzerland*, edited by A. Schleiss and R. Boes, pp. 497–508, Taylor and Francis, London.

Vacco, D. A., R. B. Alley, D. Pollard, and D. B. Reusch (2010), Numerical modeling of valley glacier stagnation as a paleoclimatic indicator, *Quat. Res.*, *73*(2), 403–409, doi:10.1016/j.yqres.2009.09.006.

Watson, R., and W. Haeberli (2004), Environmental threats, mitigation strategies and high-mountain areas, *Ambio*, *13*, 2–10.

World Glacier Monitoring Service (WGMS) (2008), Global glacier changes: Facts and figures, report, U. N. Environ. Prog., Zurich, Switzerland.

Zemp, M., A. Kääb, M. Hoelzle, and W. Haeberli (2005), GIS-based modelling of glacial sediment balance, *Z. Geomorphol.*, *138*, 113–129.

Zemp, M., et al. (2007), *UNEP: Global Outlook for Ice and Snow*, pp. 115–152, U. N. Environ. Prog., Nairobi.

Paper IV

Linsbauer, A., Paul, F., Machguth, H., and Haeberli, W. (2013). Comparing three different methods to model scenarios of future glacier change in the Swiss Alps. *Annals of Glaciology*, 54 (63): 241–253. doi: 10.3189/2013AoG63A400

Comparing three different methods to model scenarios of future glacier change in the Swiss Alps

Andreas LINSBAUER,[1] Frank PAUL,[1] Horst MACHGUTH,[1,2] Wilfried HAEBERLI[1]

[1]*Department of Geography, University of Zürich, Zürich, Switzerland*
E-mail: andreas.linsbauer@geo.uzh.ch
[2]*Geological Survey of Denmark and Greenland, Copenhagen, Denmark*

ABSTRACT. Ongoing atmospheric warming causes rapid shrinking of glaciers in the European Alps, with a high chance of their near-complete disappearance by the end of the 21st century. Here we present a comparison of three independent approaches to model the possible evolution of the glaciers in the Swiss Alps over the 21st century. The models have different levels of complexity, work at a regional scale and are forced with three scenarios of temperature increase (low, moderate, high). The moderate climate scenario gives an increase in air temperature of ~2°C and ~4°C for the two scenario periods 2021–50 and 2070–99, respectively, resulting in an area loss of 60–80% by 2100. In reality, the shrinkage could be even faster, as the observed mean annual thickness loss is already stronger than the modelled one. The three approaches lead to rather similar results with respect to the overall long-term evolution. The choice of climate scenarios produces the largest spread (~40%) in the final area loss, while the uncertainty in present-day ice-thickness estimation causes about half this spread.

1. INTRODUCTION

Ongoing glacier shrinkage in the European Alps is of increasing interest because of the expected changes in the hydrologic regime of major river catchments (e.g. Mauser and Bach, 2009; Huss, 2011) and its influence on hydropower production (e.g. Schaefli and others, 2007; Terrier and others, 2011; Farinotti and others, 2012), tourism (Fischer and others, 2011) and natural hazards (e.g. Moore and others, 2009; Frey and others, 2010; Haeberli and others, 2010; Künzler and others, 2010). Scenarios of future climate change with further increasing temperatures (Solomon and others, 2007) involve continued, if not accelerated, glacier shrinkage, and even the possibility of complete loss of glaciers in entire mountain ranges (e.g. Zemp and others, 2006). Several methods, based on different basic concepts, complexity and application scales, have been developed to determine future glacier evolution (i.e. change in glacier area and/or volume) along with the related changes in runoff. Such glacier models can either be regionally calibrated empirical/statistical models or process-oriented models, which are more physically based (Hoelzle and others, 2005).

For modelling glacier evolution at the scale of entire mountain ranges, a variety of simple techniques and approaches (requiring only few input data) have been applied in the past. Examples are a shift of the equilibrium-line altitude (ELA), according to given changes in temperature and/or precipitation and the related change of the accumulation area (e.g. Lie and others, 2003; Zemp and others, 2006; Condom and others, 2007; Paul and others, 2007), the application of various spatio-temporal extrapolation techniques (Huss, 2012) or the parameterization scheme for glacier inventory data introduced by Haeberli and Hoelzle (1995). Using even more simplified methods, future glacier changes are also modelled at a global scale, for example to assess the future contribution of glaciers to sea-level rise, mostly as a combination of analogy concepts and multivariate analysis with strongly abstracted glaciers (e.g. Raper and Braithwaite, 2005; Bahr and others, 2009; Marzeion and others, 2012). Radić and Hock (2011) and Raper and others (2000) considered the change in a standardized area/elevation distribution (hypsometry) to account for the adjustment of glacier area to future climate conditions. A more direct way to determine future glacier evolution is the calculation of glacier volume loss based on observed overall changes in glacier thickness, as derived from geodetic measurements (e.g. differencing of two digital elevation models (DEMs)) over a longer time period (e.g. Huss and others, 2010a). Based on these observations, simple parameterizations of thickness evolution can be derived and, in combination with calculated ice-thickness distributions (e.g. Farinotti and others, 2009; Linsbauer and others, 2012) and mass balances (e.g. Giesen and Oerlemans, 2012), be applied to large glacier samples (e.g. Huss, 2011; Salzmann and others, 2012).

A variety of more complex approaches exist to model future glacier evolution, based on mass-balance modelling and glacier flow (e.g. Le Meur and others, 2007; Jouvet and others, 2009, 2011). These models are computationally expensive and only applicable to individual well-studied glaciers, where sufficient data (also for calibration and validation) exist.

Ultimately, the glacier-evolution models described above must be linked to a climate scenario, and changes should be time-dependent. Although models that are based on mass-balance calculations can be directly linked to climate model output (e.g. Machguth and others, 2009), the modelled mass change is not identical to thickness change, as the geometric adjustment of a glacier (change in area or length) to a mass-balance forcing will only occur after a delay. Using a (surface) mass-balance model to determine future glacier evolution has thus to implement a parameterization of mass transport. This can be obtained by a comparison of the modelled cumulative mass budget and the observed overall volume loss over the same period (Huss and others, 2010a). For the simpler approaches (e.g. shift in the ELA) the link to a certain climate scenario can be established, based on atmospheric lapse rates or known relations between ELA change and changes in temperature, precipitation and the energy balance

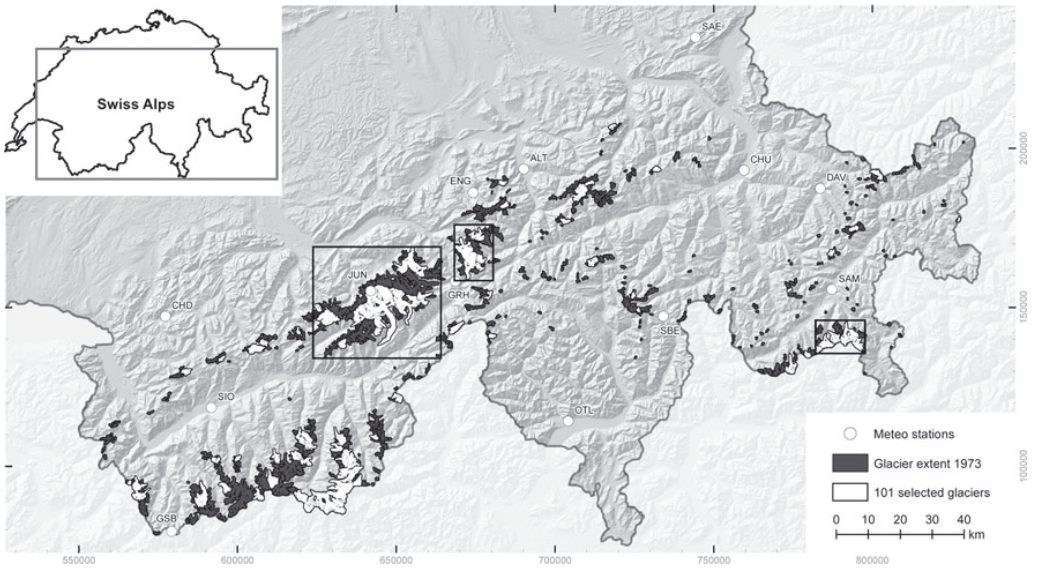

Fig. 1. The model domain 'Swiss Alps' with the subsample of 101 selected glaciers marked. The white points denote the locations of the MeteoSwiss weather stations with homogenized annual mean temperature data for the period 1980–2009. ALT: Altdorf (438 m a.s.l.), CHD: Chateau-d'Oex (985 m a.s.l.), CHU: Chur (556 m a.s.l.), DAV: Davos (1594 m a.s.l.), ENG: Engelberg (1035 m a.s.l.), GRH: Grimsel Hospiz (1980 m a.s.l.), GSB: Col du Grand St Bernhard (2472 m a.s.l.), JUN: Jungfraujoch (3580 m a.s.l.), OTL: Locarno/Monti (366 m a.s.l.), SAE: Säntis (2502 m a.s.l.), SAM: Samedan (1708 m a.s.l.), SBE: S. Bernardino (1638 m a.s.l.) and SIO: Sion (482 m a.s.l.). Black rectangles show the extent for Figures 4 and 7.

(e.g. Kuhn, 1981). However, the involved time dependence of the geometric adjustment has to be introduced artificially, for example based on estimated response times for larger glacier samples (e.g. Haeberli and Hoelzle, 1995).

Although the various existing approaches have structurally different designs and use different climate forcings, they tend to provide similar results. A model intercomparison can help to tease out model-specific problems and hence sources of uncertainty for simulations and predictions. Thereby, the boundary conditions for the compared approaches are usually held constant and the models compared are conceptually rather similar. Models that use conceptually different approaches have not, so far, been analysed together. Here we compare three methods of variable complexity applicable to large glacier populations and focus on the glaciers of the Swiss Alps.

One model (M1; Section 3.1) provides future glacier area only, and is based on an adjustment of the hypsometric area distribution following an upward shift of the ELA (Paul and others, 2007) according to three scenarios of climate change.

A second approach (M2; Section 3.2) uses a modelled ice-thickness distribution in combination with observed geodetic volume changes for an extrapolation of the elevation-dependent thickness change and related area evolution into the future, assuming a constant rate of ice-thickness loss as a reaction to temperature increasing by 1°C in time-steps of 20, 25 and 30 years.

A third method (M3; Section 3.3) uses a distributed mass-balance model that is directly coupled to three ensembles of downscaled, de-biased, gridded and transient regional climate model (RCM) simulations (Machguth and others, 2009, 2012; Salzmann and others, 2012), in combination with a hypsometric change in glacier geometry using the parameterization by Huss and others (2010a).

Besides comparing the modelled glacier extents, hypsometric distributions and relative area loss for M1, M2 and M3, we also analysed the uncertainties introduced by model simplifications, the ice-thickness estimations and the climate change scenarios. Because future glacier extents or runoff from glacierized catchments cannot be validated, a validation can only be performed over the recent past. We thus compared the modelled area and/or volume changes over the 1985–2000 period with the observed ones, being well aware that none of the three models are designed to give reliable results over such a short timescale.

2. STUDY REGION AND INPUT ATA

The study region of the Swiss Alps comprises an area of ~25 000 km^2 including a glacierized area of ~1300 km^2 in 1973 (Müller and others, 1976) (Fig. 1). The DEM covering the study site was produced by the Swiss Federal Office of Topography (swisstopo), has a cell size of 25 m (termed DEM25 in the following) and approximately represents the glacier surfaces around 1985 (Rickenbacher, 1998; swisstopo, 2005). The accuracy of the DEM25 is reported to be 2.5–7.5 m in the horizontal direction and <10 m in the vertical direction (swisstopo, 2005). The digital glacier outlines are based on the digitized Swiss Glacier Inventory from 1973 (SGI1973) by Müller and others (1976), in the revised version by Maisch and others (2000) which includes 2365 glacier and glacierets >0.01 km^2. These glacier polygons fit well to the glacier extent in the DEM25, as only small overall area changes took place for most glaciers in the Alps between 1973 and 1985 (Paul and others, 2004).

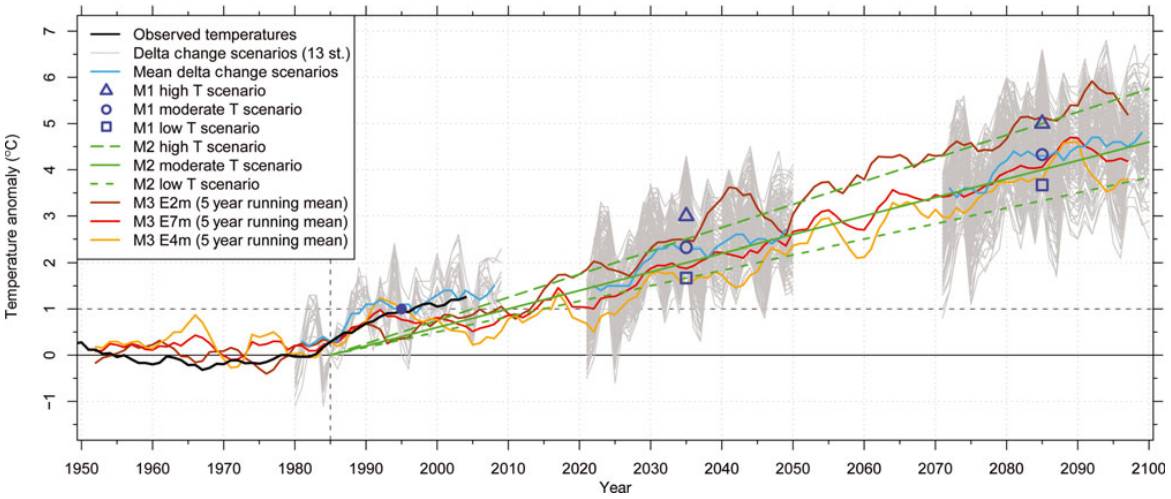

Fig. 2. Anomaly of 2 m air temperature of the observed temperatures and climate scenarios used, all normalized to the reference period from 1961–90 for Switzerland (after Rebetez and Reinhard, 2008). As a reference, the annual temperature anomalies (Rebetez and Reinhard, 2008) from 12 homogenized temperature series for 12 stations in Switzerland (Begert and others, 2005) are displayed in black. The grey lines show observed temperatures from 13 MeteoSwiss weather stations (Fig. 1) for the control period 1980–2009 and their projections to the two scenario periods 2021–50 and 2070–99 according to the delta change values and ten different model chains from Bosshard and others (2011). In light blue the 5 year running mean for the measurements and the projections for the 13 weather stations are shown. The blue point is the starting point for all three M1 scenarios, and the triangle, circle and square mark the low-, moderate- and high-temperature scenarios for M1. The lines of the linear extrapolated temperature trends, as used for M2, are shown in green. The 5 year running mean for three scenario ensembles (E2m, E7m and E4m) used for M3 are shown in in orange, red and brown.

While the first two models (M1 and M2) were applied to all glaciers in the Swiss Alps, M3 was restricted to a sample of 101 selected glaciers, as explained in Section 3.3, representing ~50% of the total glacierized area and ~75% of the ice volume in Switzerland.

The ice-thickness distribution for all Swiss glaciers is calculated with the GlabTop model (Linsbauer and others, 2012; Paul and Linsbauer, 2012) using the DEM25 and the glacier outlines from the SGI1973 as inputs. GlabTop spatially extrapolates locally (50 m elevation bins) estimated glacier thickness values that are derived from averaged values of surface slope and a mean basal shear stress per glacier (assuming perfect plasticity; see Paterson, 1994). The basal shear stress was empirically derived from the glacier elevation range, which can be seen as a proxy for mass turnover (Haeberli and Hoelzle, 1995), and has an upper-bound value of 150 kPa for glaciers exceeding an elevation range of 1.6 km (Li and others, 2012). The obtained model results have an uncertainty range of about ±30%, as shown by a comparison with independent radar profiles and an uncertainty analysis (Linsbauer and others, 2012).

The presence of glaciers, their number and characteristics are mainly linked to the elevation of their headwater catchment, which determines the seasonality of the runoff regime (mostly pluvio-nival or glacio-nival). Most Swiss glaciers (exceptions are found in the Val Bregaglia and the Val Fenga) are drained by seven major river catchments with gauging stations in the lowlands. In combination with the outlines of these major river catchments, the grid from the DEM differencing (Shuttle Radar Topography Mission DEM (SRTM3) – DEM25) by Paul and Haeberli (2008) was used to obtain catchment-specific elevation changes over the period 1985–99, based on zone statistics (with each major river catchment as a zone). Apart from a few regions with data voids over glaciers, this dataset covers nearly all glaciers in the Swiss Alps. The mean change of the DEM differencing (−11 m w.e.) is in good agreement with the mean cumulative mass budget of nine Alpine glaciers with measured mass balances (−10.8 m w.e.).

Both the reported temperature data from Rebetez and Reinhard (2008) and the measured temperatures from 13 selected weather stations (Fig. 2) run by the Swiss Federal Office of Meteorology and Climatology (MeteoSwiss) show a distinct temperature increase of ~1°C between 1980 and 1995. From the 1990s until the present the temperatures further increased (by ~0.5°C), but at a lower rate (Fig. 2).

The three climate scenarios applied here are derived from ten climate model chains (combination of a general circulation model (GCM) and an RCM) using an A1B emission scenario (Solomon and others, 2007) at a 25 km horizontal resolution from the EU-ENSEMBLES program (Van der Linden and Mitchell, 2009). Values for temperature and precipitation for several MeteoSwiss weather stations were downscaled for the scenario periods 2021–50 and 2070–99 (relative to the control period 1980–2009) by Bosshard and others (2011) using a delta change approach. From the resulting temperature increase at 13 weather stations we derived low, moderate and high scenarios, that cover the range of model chain variability. The moderate scenario gives an increase in air temperature of 2°C and 4°C for the two scenario periods centred around 2035 and 2085, respectively.

Glacier development until the first scenario period in model M1 is based on the reaction to the 1°C temperature increase that took place in the 1980s. After that, glaciers react to the three scenarios of temperature increase derived for the first scenario period. The three scenarios for model M2 follow three linear trend extrapolations, assuming that the above-mentioned temperature increase of 1°C is repeated every

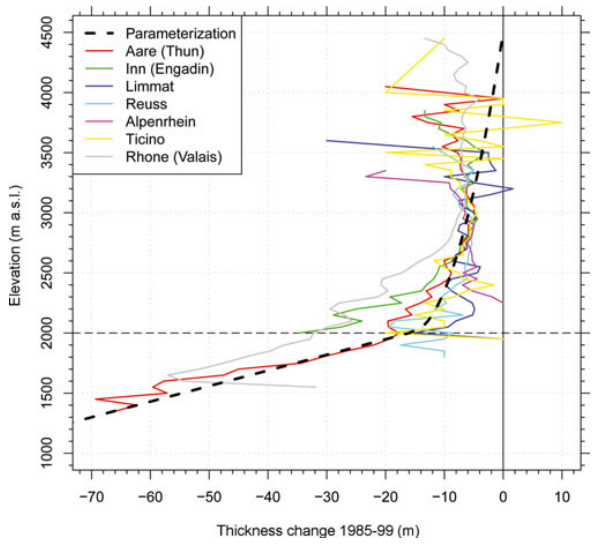

Fig. 3. Thickness changes from 1985 to 1999 (Paul and Haeberli, 2008) for seven major river catchments, together with an empirical elevation-dependent function to parameterize the thickness loss for all Swiss glaciers in model M2 (Eqn (1)).

20, 25 or 30 years. The 25 year repeat period (i.e. the moderate scenario) also gives a 2°C and 4°C temperature increase by 2035 and 2085 (Fig. 2). The distributed mass-balance model applied in M3 is directly forced with three ensemble means of the A1B scenario using RCM simulations from ENSEMBLES, assuming ensemble means are the most plausible scenario guess (e.g. Guo and others, 2007). Ensemble E7m consists of seven different RCM realizations (driven by ECHAM5-r3, HadCM3Q0 and the ARPEGE GCMs), E4m consists of four RCMs all driven with ECHAM5-r3 and E2m is the ensemble of the two HadCM3Q0-driven ensembles (Salzmann and others, 2012). Monthly resolution RCM grids were chosen because the daily resolution grids showed unrealistic variability in daily precipitation.

The climate model input datasets are thus different by source, but not by value (Fig. 2). The moderate scenarios from M1 and M2, as well as E7m from M3 (the moderate scenario used in this model), all project a 2°C temperature increase for the two scenario periods centred around 2035 and 2085.

3. METHODS

For all three models, the initial glacier extent is given by the glacier outlines from 1973 (SGI1973; Maisch and others, 2000) and the swisstopo DEM25 with 25 m resolution, referring to the glacier surfaces at around 1985. The starting point 1973/1985 was chosen as most glaciers were close to a dynamic steady state then. The required ice-thickness distribution for models M2 and M3 is taken from Linsbauer and others (2012).

3.1. ELA-shift model (M1)

The ELA-shift model is described by Paul and others (2007) and thus only briefly outlined here. The model is based on the fact that with rising temperatures the ELA of glaciers is shifted to higher elevations (here by 150 m K^{-1}; Kuhn, 1981), resulting in smaller accumulation areas and, after some time, smaller glacier extents. Using a balanced budget accumulation–area ratio, AAR_0, of 60% (WGMS, 2011), new total glacier sizes can be calculated and adjusted by removing the lowermost parts of a glacier. This model only provides information on how large glaciers will be after full adjustment, without saying when this will happen. To link the glacier adjustment to a timescale considering that response times vary from ~5 to maybe 100 years or more, the same mean response time of 50 years (Haeberli and Hoelzle, 1995) is assumed for all glaciers. This matches the years 2035 and 2085, the centred scenario periods when starting from 1985. In order to have model results in 5 year time-steps, the total area change over the 50 year response time was divided into ten single steps.

There are several restrictions to the validity of the model, due to the simplicity of the approach. The model calculates new glacier extents for given ELA shifts and a hypothetical new steady state. However, equilibrium is not reached in reality, as the climate is in constant change and glaciers continuously adjust their extents to new climatic conditions, depending on their specific geometry and response times. With a constant 50 year response time for all glaciers, the speed of area change is overestimated for the largest and underestimated for small glaciers. As this approach works in two dimensions only, the introduced response time only serves for adjustment of the area (thickness changes are not considered) to make the method time-dependent. Moreover, the balanced budget, AAR_0, might vary between 50% and 70% for individual glaciers (Machguth and others, 2012), while here it is assumed to be constant and the same for all glaciers.

M1 is coupled with climate in a retrospective manner. The 50 year response time period for all glaciers starts in 1985 (running to 2035 and 2085 in the model). In the first period all glaciers react to the 1°C temperature increase of the mid-1980s (Fig. 2 and Rebetez and Reinhard, 2008) that resulted in a 150 m increase of the ELA. In the second period, the glaciers react to the warming of the first 50 years according to three different temperature scenarios. These scenarios are derived from the means of the delta change values from ten RCM models yielding an increase in ELA of +100 m (low-temperature scenario), +200 m (moderate) and +300 m (high). Thus it is a step-change and retrospective response model, i.e. reacting to a forcing that has taken place in the past. The 5 year time-steps are only used to generate a smooth transition between the two steady-state extents.

3.2. Thickness change parameterization (M2)

Since the beginning of the 1980s, increasingly negative glacier mass balances have been observed in the Alps (WGMS, 2011). The related thickness change for the period 1985–99 was calculated for all Swiss glaciers from DEM differencing (Paul and Haeberli, 2008), revealing strong thickness losses for low-lying and flat glacier tongues. This illustrates that the adaptation of the glacier extent to a rapidly changing climate can be dominated by thickness loss (downwasting) rather than area change (Huss and others, 2008, 2010a). Plotting thickness loss vs altitude for the major river catchments reveals a rather similar and increasing thickness loss towards lower elevations for all regions (Fig. 3). To parameterize this for the entire study region, we used (similarly to Huss and others, 2010a) an empirically derived elevation-dependent function as an average for catchment-related mean values composed of a

lower (<2000 m) linear decline and an upper (>2000 m) quadratic decrease:

$$\frac{dh}{dt} = \begin{cases} -70 + (\mathrm{DEM}_i - 1300) \cdot \frac{54}{700} & \text{if } \mathrm{DEM}_i \leq 2000 \\ -16 + (\mathrm{DEM}_i - 2000)^{1/2} \cdot \frac{25}{8} & \text{if } \mathrm{DEM}_i > 2000 \end{cases} \quad (1)$$

with dh/dt the rate of thickness change (m a^{-1}) within the specified time period and DEM_i the elevation (m a.s.l.) of each gridcell. Of course, the assumption that all glaciers are subject to the same elevation-dependent thinning rates is not correct (e.g. delay due to debris cover or different shading conditions) and the resulting area changes can be strongly over- or underestimated for individual glaciers. Above 3000 m the approximation of the parameterization differs from the extracted thickness loss rates in Figure 3, but values in this elevation range are influenced by artefacts in the SRTM3 DEM. The decrease to zero at the highest elevations is implemented to keep small, steep and thus thin glaciers at high elevations from disappearing too fast. The function used is an empirical one, rather than derived by a regression, to better accommodate the DEM uncertainties and model needs mentioned above. In this regard it has to be stressed that the modelled area changes are assumed to be realistic only at the regional scale (e.g. for major river catchments).

M2 is coupled with climate by (1) relating the observed thickness change from 1985 to 1999 to the observed temperature increase of 1°C mentioned above and (2) assuming that the glacier surface will adjust to this forcing over a 20, 25 or 30 year time period (Fig. 2). This trend is then assumed to continue into the future (linear extrapolation), resulting in a 1°C temperature increase every 20, 25 and 30 years. Glacier area is removed once the cumulative ice-thickness loss exceeds the initial ice thickness. Each time the thickness change increment is subtracted from the initial DEM, the glacier surface gradually shifts to lower elevations, where the rate of thickness loss is higher.

3.3. Glacier mass-balance simulation and retreat modelling for 101 glaciers (M3)

Glacier mass balance is calculated using a distributed mass-balance model (Machguth and others, 2009). This is a simplified energy-balance model, which runs at daily time-steps and uses gridded RCM data of 2 m air temperature, T, precipitation, P, and total cloudiness, n, for input. Because of spurious values in the daily RCM fields, the data applied here are at monthly resolution. Daily values are generated from linear interpolation, and precipitation falls every fifth day (Salzmann and others, 2012). Cumulative mass balance, b_c, on day $t+1$ is calculated for every time-step and over each gridcell of the DEM, according to Oerlemans (2001):

$$b_c(t+1) = b_c(t) + \begin{cases} \Delta t \cdot (-Q_m)/l_m + P_{solid} & \text{if } Q_m > 0 \\ P_{solid} & \text{if } Q_m \leq 0 \end{cases} \quad (2)$$

where t is the discrete time variable, Δt is the time-step, l_m is the latent heat of fusion of ice (334 kJ kg^{-1}) and P_{solid} is solid precipitation (m w.e.). The energy available for melt, Q_m, is calculated as

$$Q_m = (1-\alpha)S_{in} + C_0 + C_1 T \quad (3)$$

where α is the surface albedo (three constant albedo values are applied: snow = 0.72, firn = 0.45 and ice = 0.27), S_{in} is the incoming shortwave radiation at the surface, calculated according to Greuell and others (1997) from n and clear-sky global radiation computed at DEM resolution and taking all effects of exposition and shading into account, T is in °C, and $C_0 + C_1 T$ is the sum of the longwave radiation balance and the turbulent exchange (Oerlemans, 2001). C_1 is set to 12 W m^{-2} K^{-1} and C_0 is tuned to −45 W m^{-2} (Machguth and others, 2009). Accumulation is equal to P_{solid}, the redistribution of snow is not taken into account and a threshold range of 1–2°C is used to distinguish between snowfall and rain. Any meltwater is considered as runoff, i.e. refreezing and internal storage of meltwater is neglected.

Glacier retreat is simulated based on the modelled mass balances and the so-called Δh glacier-retreat approach, following Huss and others (2010a). The latter parameterize glacier surface elevation change by distributing glacier mass loss or mass gain over the entire glacier surface, according to altitude-dependent functions of observed changes in glacier thickness. Here we use the glacier-size-dependent Δh functions as proposed for the Swiss Alps (Huss and others, 2010a, fig. 3b therein). Glacier geometry is updated annually, based on calculated surface elevation changes. Glacier surface mass balance is calculated on the updated topography and thus considers the mass-balance/altitude feedback, i.e. a reduction in glacier thickness results in a lower elevation of the glacier surface and consequently a more negative mass balance (e.g. Raymond and others, 2005). Glacierized gridcells become ice-free when their elevation falls below the elevation of the glacier bed.

Simplifications in the mass-balance model used (e.g. debris cover is not considered) limit the number of glaciers where reasonable mass balances can be calculated. Therefore, 101 glaciers are selected from the SGI1973, based on the following criteria: (1) no or little debris cover; (2) no or little influence of avalanches; (3) mass loss restricted to melting (the applied mass-balance model does not consider any processes like calving into lakes or over rock faces); and (4) sufficient size (>1 km^2), as small glaciers usually show accumulation patterns of a very local nature with strong influence from wind-drift and avalanching.

M3 is coupled to climate using gridded RCM fields for model input, rather than projected temperature change at weather station locations (cf. models M1 and M2). The direct use of the RCM fields involves the two steps of (1) downscaling the gridded 25 km resolution fields to the 100 m resolution of the mass-balance model, and (2) de-biasing the downscaled RCM fields. These two steps are implemented in the mass-balance modelling set-up and directly applied to each RCM grid while the model is running. The downscaling of T and P is based on interpolation of the RCM values with the subsequent application of simple subgrid parameterizations, while S_{in} is computed from high-resolution clear-sky global radiation and attenuation from clouds derived from interpolated total cloudiness, n (see Machguth and others, 2012, for full details).

The de-biasing of the RCM fields is done for each variable, according to the method described by Machguth and others (2012), where biases in RCM values of T and n are established from comparison with observations at 14 high-mountain weather stations in the Swiss Alps and spatial distribution of RCM precipitation is scaled to match the precipitation pattern of the Schwarb and others (2001) precipitation map. However, the accuracy of the downscaled and de-biased fields is limited, as knowledge of real meteorological conditions at the glacier sites is imperfect. In particular, the large uncertainties in observed high-mountain precipitation (Sevruk, 1997) hamper the de-biasing

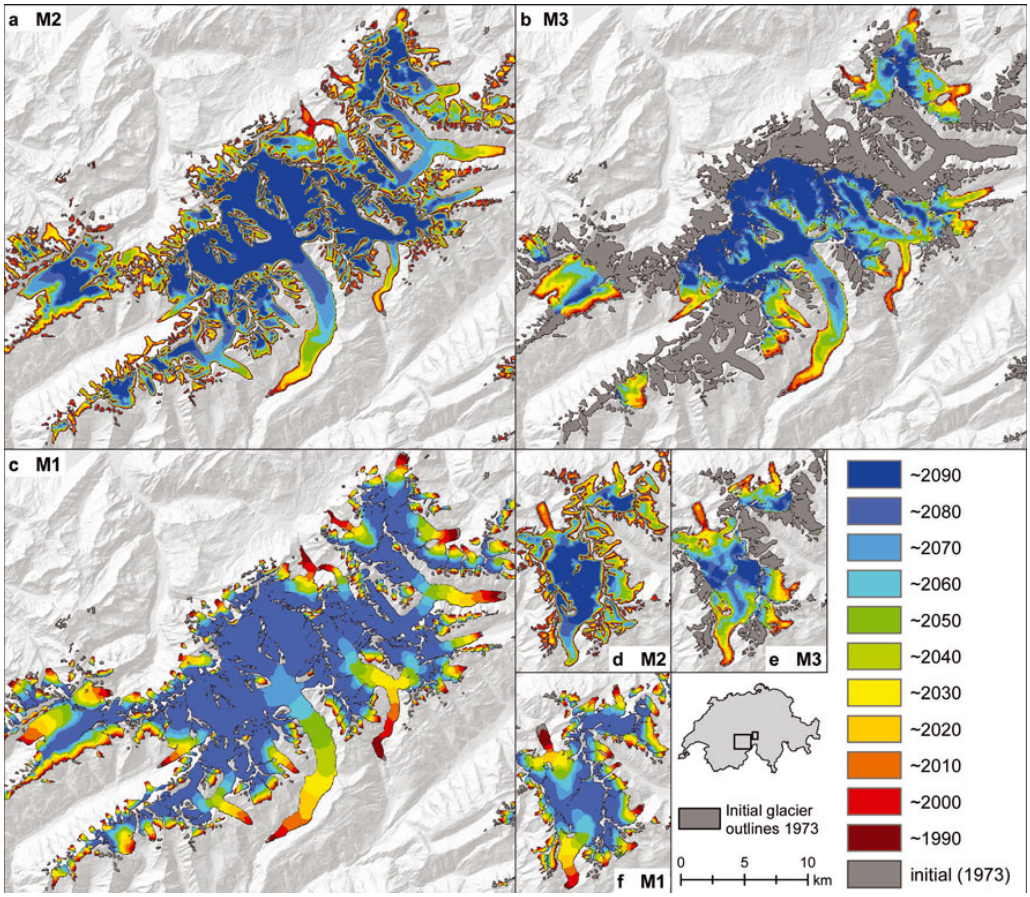

Fig. 4. Visualization of the results for the regions around Aletsch (a–c) and Rhone (d–f) glaciers for all three models (M1: (c) and (f); M2: (a) and (d); M3: (b) and (e)) with their moderate climate scenario, starting with their 1973 extent (i.e. DEM25). The colour steps depict 10 year changes and are the same for all models. The modelling with M3 was restricted to the subsample of 101 glaciers.

procedure and make it impossible to achieve a level of accuracy that would allow the calculation of accurate mass balances for each individual glacier. This issue is reflected in the successful model-calibration to observed melt during the summer period while at the same time winter mass balance strongly disagrees with measurements (Machguth and others, 2009). We have approached these limitations by applying a calibration procedure, where the mass-balance model is driven by the downscaled and de-biased RCM time series for the period 1970–2000 and precipitation is adjusted for each glacier individually to achieve a prescribed cumulative mass balance (Machguth and others, 2012). Choosing an appropriate value for the cumulative mass balance is challenging, as available observations differ: while Zemp and others (2008) report a mean cumulative mass balance of −13 m w.e. for nine Alpine glaciers, Huss and others (2010b,c) calculate −9 m w.e. from a combined approach of modelling and observations. We prescribe a cumulative mass balance of −11 m w.e., which is midway between the two values. Furthermore, all glaciers were calibrated to the same cumulative mass balance. This simplification had to be introduced because, for most of the 101 selected glaciers, no individual observational records are available. We are confident that the latter simplification only marginally affects the calculated future glacier volumes. Salzmann and others (2012) applied the same model chain and showed that using alternative sets of non-uniform cumulative mass balances in the calibration procedure has a negligible impact on future scenarios. The downscaled, de-biased and calibrated RCM data are subsequently used to run the mass-balance model over the entire scenario period.

4. RESULTS

The simulated glacier area loss for all three models is illustrated in Figure 4. For M1 the moderate scenario is displayed, with an ELA shift of 150 m until the first scenario period and a shift of another 200 m until the second scenario period. As this model is a two-dimensional simplification of a glacier, it is limited to providing area changes (on the initial unchanged DEM) with the lower ends of the glaciers simply cut off. This leads to glacier geometries with cropped ablation and unchanged accumulation areas. The visual comparison with the moderate M2 and the M3 E7m scenario is provided nevertheless.

Models M2 and M3 additionally require the ice-thickness distribution to calculate ice volume change, as a combination of surface lowering and area reduction. The resulting patterns of glacier shrinkage seem to be closer to reality than for M1, where for some glaciers the shrinkage starts along the edges (where the ice is thin) at the lowest elevations (where thinning is greatest). The visual comparison of M2

160

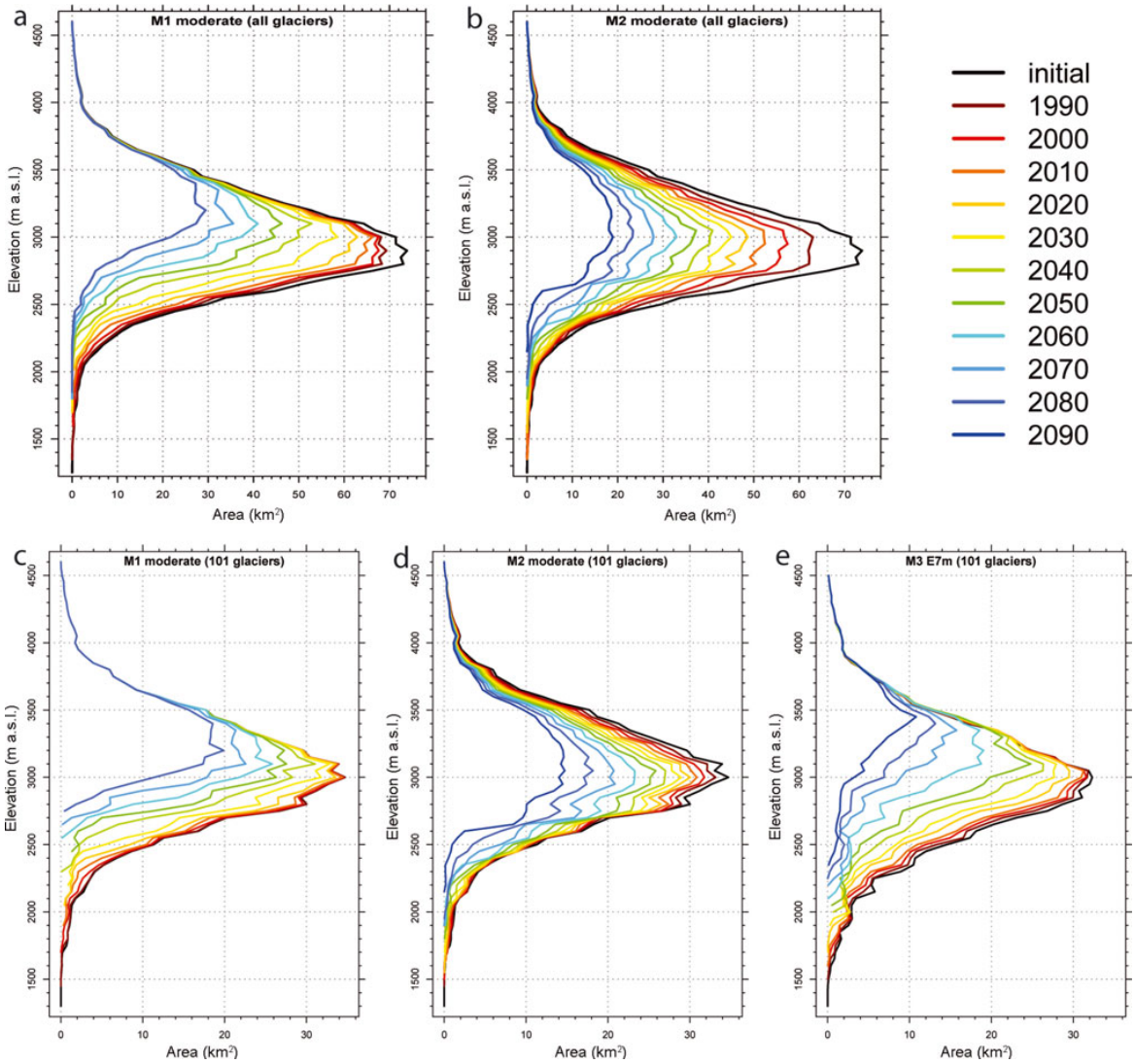

Fig. 5. Change in overall glacier hypsometry in 10 year steps (colour code is the same as in Fig. 4) until 2090 (2080 for M1) for all glaciers (a, b) and the 101 selected glaciers (c–e), calculated with the moderate temperature scenarios of M1 (a, c) and M2 (b, d) and ensembles scenario E7m from M3 (e).

and M3 in Figure 4 and the quantitative comparison in Figure 6d indicate that the area loss in M3 is slightly faster than for M2.

The evolution of the area/elevation distribution (hypsometry) for 10 year time-steps and the three moderate climate scenarios is depicted in Figure 5. While for model M1 the entire distribution, including the maximum value, is shifted upwards, model M2 shows a constant decrease at all elevations without a trend in the maximum. This is due to the implemented elevation feedback, i.e. large parts of the surface area shift to lower elevations (where melting is higher). Focusing on just the 101 selected glaciers from M3 using the other two models (Fig. 5, lower panels), the trends of the area distribution for M1 and M2 are the same as for the full sample. Interestingly, the hypsometric changes of M3 are rather similar to M1, but with an overall stronger loss in area at higher elevations and a reduced loss at lower elevations. In contrast to M1 and M2 which work at 25 m resolution, M3 operates at 100 m resolution. Therefore, the initial glacier areas in Figure 5c and d and Figure 5e are not exactly the same.

Figure 6a–d show the temporal development of the area loss (and volume loss for M3) during the 21st century for all three models and their different realizations, corresponding to the different applied climate scenarios, the thickness uncertainty (M2) and the full sample vs the 101 selected glaciers (M1, M2). The development of the relative area change along the various model pathways is, to a large extent, similar, but differences are also visible. There is a spread of ~10–20% around the near future (2035) and of ~30–50% at the end of the century for the various model realizations in all four plots. Considering the simulations for the sample of the selected 101 glaciers, the general trend for all model realizations is the same: by mid-century the area loss is still moderate, but it then increases sharply until the end of the century, especially with M3 and the high-temperature scenarios of M1. This is also reflected in the glacier hypsometry modelled by M3 (Fig. 5e), which shows a

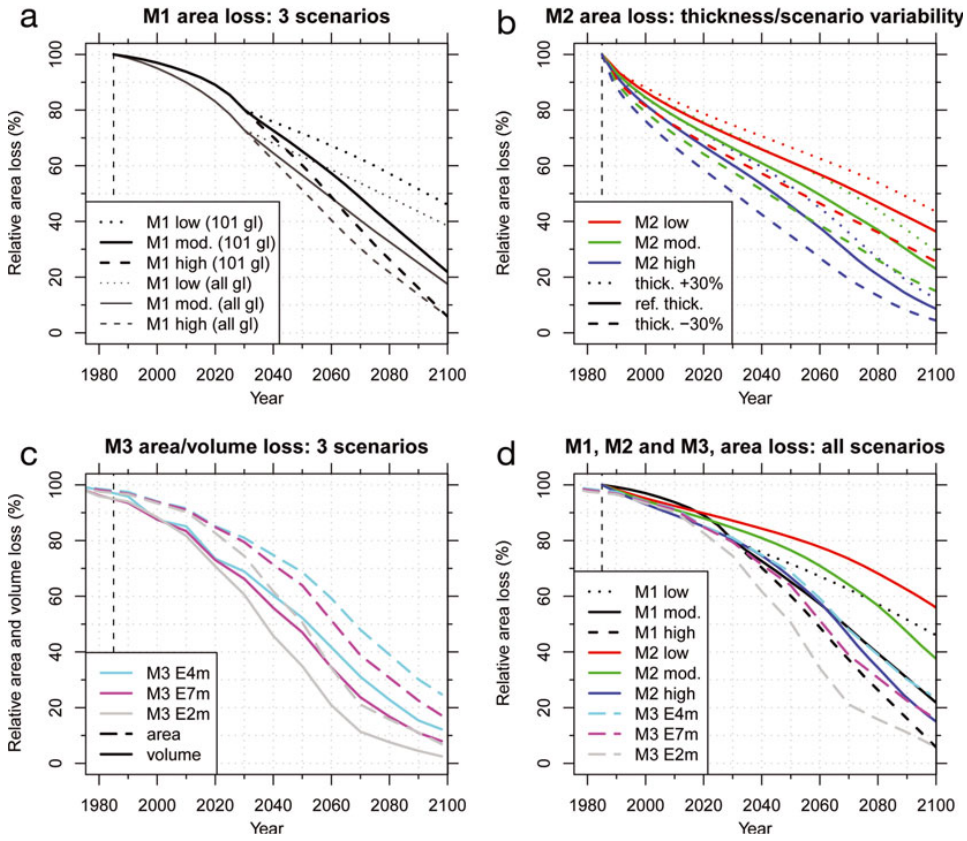

Fig. 6. Development of relative area loss from the model starting point (1985 for M1 and M2; 1970 for M3) until 2100 for all three models and their different realizations (scenarios, thickness, glacier samples). (a) The three retrospective applied scenarios for M1 represented by the grey lines for all glaciers and in black (bold) for the 101 glaciers. (b) The three different temperature trend extrapolations applied in M2 together with the corresponding ±30% uncertainty due to the ice-thickness modelling for all Swiss glaciers. (c) Area and volume loss for the selected 101 glaciers as modelled with the three climate scenario ensembles used in M3. (d) A comparison based on the sample of the selected 101 glaciers of the climate scenario runs from all three models.

marked increase in hypsometric area loss in the second half of the model simulation.

In Figure 6a the curves for the applied climate scenario realizations for M1 (Section 3.1), with a first ELA shift of 150 m until the first scenario period and a further ELA shift of 100, 200 and 300 m after the first scenario period, are shown (for all glaciers and the 101 glaciers) leading to a spread of the modelled glacier area of 40% at the end of the century (loss of 55–95% by 2100). There is no large difference between the curves for all glaciers and those for the 101 glaciers.

The 30% uncertainty in the glacier thickness (Fig. 6b) results in a spread of not more than 20%, considering area loss as modelled with M2 for the three climate scenarios. The spread of the lines reproducing area loss according to the three different scenarios is much larger (∼40% around the second scenario period), whereby the high-temperature scenario (+5.75°C temperature increase by 2100) results in an almost complete loss of glaciers (∼90%). The uncertainty in ice thickness (±30%) has a nonlinear impact on glacier retreat. With 30% thinner ice the extent of the reference thickness is reached 20 years earlier, while 30% thicker ice gives only 10 additional years before this extent is reached. Thus, differences in ice-thickness estimations directly impact the timescales of the scenarios, but might have a smaller effect on the remaining ice in 2100 than that resulting from the uncertainties in temperature change (Fig. 6b and d).

In Figure 6c the evolution of area and volume for the selected 101 glaciers as modelled with three scenario ensembles and with M3 is shown. The behaviour of the curves is rather similar, differing only in the speed of area loss, resulting in a spread of ∼20% at the second scenario period.

For the comparison in Figure 6d, all scenario runs for all three models for the 101 selected glaciers are displayed. It shows that the uncertainties introduced by different realizations of climate change are very similar during the first scenario period and rather large in the second scenario period. Thus, model results increasingly deviate when going into the future. The moderate scenarios of the three models (M1 mod., M2 mod. and M3 E7m) result in a total loss of glacier area of ∼60–80% by around the year 2100. In terms of area loss, the scenarios M1 mod., M2 high, M3 E4m and M3 E7m are close together, i.e. they do not differ by more than 15%. The area loss modelled by scenarios M1 low, M2 mod. and, in particular, M2 low is rather slow compared to the other scenarios and can be seen as a lower boundary.

The variable curvature of the lines reveals interesting details about the speed of glacier shrinkage at various phases of the recession, largely depending on the remaining area covered by thick ice. A key aspect is that all curves will

Table 1. Comparison of area and volume loss and cumulative mass budgets for all scenarios of M1, M2 and M3 from their model start until the validation year 2000, together with the derived area loss obtained by comparing the two relevant Swiss Glacier Inventories (SGI) from 1973 and 2000. Results are tabulated for all Swiss glaciers and for the subset of 101 glaciers

	Area		Volume		Cumulative mass budget	Time period
	%	km^2	%	km^3	m w.e.	
M1 all	−5	−61	–	–	–	1985–2000
M1 101	−3	−19	–	–	–	1985–2000
M2 low all	−13	−176	−8	−6.4	−5.6	1985–2000
M2 low 101	−5	−31	−6	−3.1	−5.1	1985–2000
M2 mod. all	−15	−202	−10	−7.6	−7.4	1985–2000
M2 mod. 101	−6	−36	−7	−3.7	−6.0	1985–2000
M2 high all	−19	−249	−13	−9.9	−10.1	1985–2000
M2 high 101	−7	−47	−9	−5.0	−8.6	1985–2000
M3 E4m 101	−6	−38	−13	−6.8	−11.0	1970–2000
M3 E7m 101	−6	−39	−12	−6.7	−11.0	1970–2000
M3 E2m 101	−7	−42	−12	−6.3	−11.0	1970–2000
SGI all	−20	−268	–	–	−11*	1973–2000
SGI 101	−9	−56	–	–	–	1973–2000

*The indicated cumulative mass budgets for 'SGI all' refers to the DEM differencing of Paul and Haeberli (2008) and the ice-thickness modelling of Linsbauer and others (2012).

finally approach 0, i.e. glaciers are unable to stabilize their extent for the given scenarios of climate change. This behaviour is also visible in the hypsometric changes in Figure 5b, where the area loss (all glaciers) is relatively large between the initial and the first step, whereas in Figure 5d there is not much difference between these two curves.

In contrast to M1 and M2, which have a fixed starting point in 1985, the model start of M3 is 1970. This is done to maximize the length of the calibration period. For the model comparison the earlier starting point of M3 is of negligible importance, as the climate was approximately stable and, according to M3, only 2.5% (15 km^2) of the area and 5% (2.8 km^3) of the initial volume were lost between 1970 and 1985.

5. VALIDATION

For M3 (and all three ensemble scenarios) the cumulative mass balance for the time period 1970–2000 is calibrated to an overall mass loss of −11 m w.e., the mean calculated from the observed cumulative mass budget of Zemp and others (2008) (−13 m w.e.) and Huss and others (2010b,c) (−9 m w.e.) (Salzmann and others, 2012). Within this calibration period, a model validation for M1, M2 and M3 would be possible, as corresponding and consistent glacier outlines for nearly all Swiss glaciers exist for 1973 and 2000 (SGI2000; Paul, 2007). In Table 1 the area (and where available the volume) of all model scenarios and the glacier inventories is displayed to allow comparison in a quantitative manner. The observed area loss is 20% for all glaciers and 9% for the 101 glaciers. The M3 scenarios and the moderate and high M2 scenarios do not differ by more than 5% from these values. The cumulative mass budgets for the M3 scenarios are calibrated, but the value obtained for the high M2 scenario for all glaciers corresponds rather well to the observations (Paul and Haeberli, 2008). Cumulative mass budget for the moderate M2 scenario is within the range of values of Huss and others (2010b,c). Area (and volume) losses for M1 and the low M2 scenario are probably too low. This is expected for M1, where only the lowermost parts of the glaciers were removed, according to an AAR_0 of 60%. As many of the lower parts of the larger glaciers in 1973 ended in narrow tongues, only minor parts of the area are deleted.

In Figure 7 a comparison of observed and modelled glacier extents for the year 2000 is shown for the glaciers in the Bernina region. It has to be kept in mind that M1 and M2 are designed to model glacier evolution on a regional scale, rather than individual glaciers, and that only three time-steps are applied until 2000. As can be seen, the changes in the observed glacier extents (1973–2000) for the large glaciers occur at the snout and along the edges. Some glaciers show a distinct retreat of the tongue from 1973 to 2000, but in general all glaciers lost area all over their margins due to the implemented surface lowering.

For the glaciers depicted in Figure 7, both M2 and M3 reproduce well the observed inward shift of glacier boundaries due to surface lowering. The agreement between observed and modelled terminus positions of Tremoggia, Tschierva and Morteratsch glaciers is good, while the modelled retreat for Palü and, especially, Roseg glaciers is too small (Fig. 7). Generally, the area and in particular the volume loss as modelled with M3 is larger than with M2, as mentioned above (Figs 4–6). This is also illustrated in the inset map of Figure 7. It shows the tongue of Tschierva glacier with outlines for the year 2000 as modelled by all models (and scenarios). M1 shows the typical pattern resulting from cutting off the lowermost part of the tongue, with a retreat of about 200 m compared to the mapped glacier outline, while the other two models achieve a glacier outline similar to the mapped tongue position.

6. DISCUSSION

6.1. Simplifications and uncertainties

Concerning the glacier change models and the climate change scenarios, several simplifications and uncertainties need to be discussed. Although there is general agreement concerning temperature development in the climate models used, changes in precipitation are highly uncertain and do not show a significant trend (e.g. Bosshard and others, 2011). They are only considered in M3 and have been neglected for

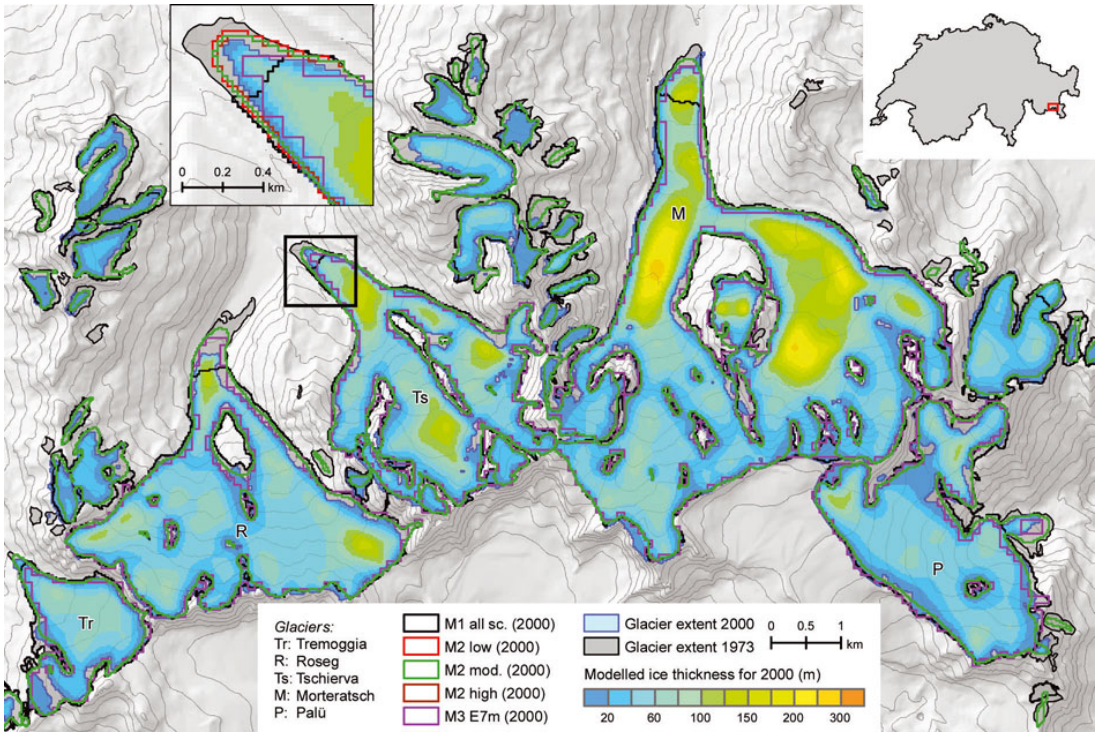

Fig. 7. The extents of glaciers in the Bernina region according to the inventories from 1973 and 2000 and the modelled ice thickness for the year 2000 according to Linsbauer and others (2012), compared to the modelled area evolution with the moderate scenarios of M1, M2 and M3 for the time-step corresponding to the year 2000. The inset shows the Tschierva glacier snout with all the glacier margins according to all model scenarios.

M1 and M2. A further simplification in M1 is that all glaciers have the same temperature sensitivity (150 m ELA rise per °C), response time (50 years) and AAR_0 (60%) (Section 3.1). Apart from the response time, these are typical mean values that certainly differ from glacier to glacier. Response time is somewhat biased towards larger glaciers, but this is required, as they are the main contributors to the overall area and volume change and should thus not shrink too fast. The parameterization of M2 is based on three linear extrapolations of an observed trend (elevation change in response to a 1°C increase), and all glaciers follow the same elevation-dependent thickness loss, using an empirical generalization rather than a regression. The three assumed time periods for glacier surface adjustment constitute a best guess to cover three scenarios for M2. The underlying climate scenarios of M3 are based on RCM simulations (ensemble means) and are thus beyond a simple linear extrapolation. M3 is also restricted to a subsample of selected glaciers that adhere to specific criteria (Section 3.3) to be suitable for the applied mass-balance model. Models M2 and M3 are based on a modelled ice-thickness distribution with an estimated uncertainty of about ±30%, that directly impacts on the timescale of the modelled glacier retreat.

We have not explicitly assessed the impact of all the simplifications mentioned above on glacier evolution. In general, many of the effects will average out when large samples are considered, as deviations from the mean values used are probably normally distributed (apart from the response-time bias). The hypothesis is not explicitly tested, but, for natural systems and large samples of independent data, deviations from a mean should be normally distributed. For individual glaciers the differences between the development modelled here and a model that considers glacier characteristics more explicitly may be large. However, for regional-scale assessment these differences are expected to contribute mainly to the variability rather than the trend, and both are governed by the implemented climate scenario.

All model approaches investigated here have advantages and disadvantages, and were designed for specific research questions. All three models operate on a regional scale, but M3 is rather glacier-specific. As a governing principle, a balance between computational effort and the required level of detail in the results has to be found.

6.2. Possibilities and limitations of model applications

For a sound model intercomparison, the models can only be compared against observed changes in the past. As the model starting point is 1985 for M1 and M2 and 1970 for M3, there is only a short time period available for a comparison. This comparison might not really be seen as a validation, as none of the models are expected to provide useful results over this timescale. However, for the year 2000, modelled glacier extents fit the mapped ones rather well. As the modelled future changes are much larger than the changes observed over this 15 year period, the significance of this comparison is limited.

The modelled area losses (Fig. 6) clearly reflect the temperature trends of the applied climate scenarios (Fig. 2). The three moderate scenarios that prescribe a 2°C or 4°C temperature increase for the two scenario periods centred around 2035 and 2085 show a comparable area loss over time (with a maximal spread of ~20%). The spread in area

loss of ~50% by 2100 is given by the low-temperature scenario of M2 (upper boundary) and the E2m scenario of M3 (lower boundary).

M1 and M2 are highly simplified models, but provide glacier change scenarios for large glacier samples at a regional scale with a small computational effort. This is in contrast to M3, that better considers characteristics of individual glaciers. Though the simplifications in M1 and M2 are substantial, they might be considered as being compliant with the uncertainties of the RCM scenarios, i.e. the variability in area change introduced by the simplifications is of the same order of magnitude as that resulting from the unknown future climate. According to the results of this comparison, the latter is somewhat larger. For studies seeking to establish future trends in the glacier cover of entire mountain ranges (e.g. the Swiss Alps), M1 and M2 are fast approaches providing results similar to the more detailed modelling of M3. As both models apply average parameter sets to all Swiss glaciers, the results are valid on the sample as a whole. We also found agreement with results from completely different studies (Jouvet and others, 2009, 2011; Huss and others, 2010a; Huss, 2012), which is not surprising as the strong future temperature increase dominates the response. The simple approach of M1 was designed to provide adjusted glacier areas as an input for hydrological models operating at a regional scale (e.g. Viviroli and others, 2009; Köplin and others, 2012). This study has shown that area loss is fastest in M1, which can be seen as a lower-bound timescale for the expected terminus retreat. For the hydrological model that generates additional runoff solely from the change in glacier area, the stronger area change in M1 might be well suited to mimic the expected future increase in runoff due to downwasting, a process that is not included in M1 but important in reality.

Although all three models are based on equivalent climate scenarios and RCM runs, the coupling to the climate model output is rather different: retrospective with M1; based on trend extrapolation with M2; and directly driven by RCM grids in M3. The modelled future development in glacier extent with the moderate scenarios can already be seen as lower-bound estimates, as the current temperature increase is already stronger and modelled mean annual thickness loss from 2000 to 2010 (with M2 mod. and M3 E7m; Fig. 8) is only 0.4 m a^{-1} according to the models, instead of the observed 0.8 m a^{-1} (Zemp and others, 2009). The decrease in mean annual thickness change in the last part of the modelling period for all scenarios in M3 (Fig. 8) may be related to the direct coupling with RCM data (allowing for positive and negative mass balances) and a possible future adjustment of the remaining small glaciers at high elevation.

Finally, it has to be considered that several feedbacks are not incorporated in any of the models, including the change of albedo (Oerlemans and others, 2009), development of new lakes (Frey and others, 2010), increasing debris cover (Jouvet and others, 2011) and changes in glacier thermal state (Vincent and others, 2007; Hoelzle and others, 2011). The local and general influence of these processes is difficult to assess because they partly act in opposite directions.

7. CONCLUSION

The three compared approaches for calculating future glacier evolution use robust (based on simple physical laws or observations) but simplified parameterizations that are applicable to large glacier samples. Two of the models are implemented in a GIS processing environment and enable glacier change scenarios to be simulated at a regional scale with small computational costs. From the comparison of the three models we conclude the following:

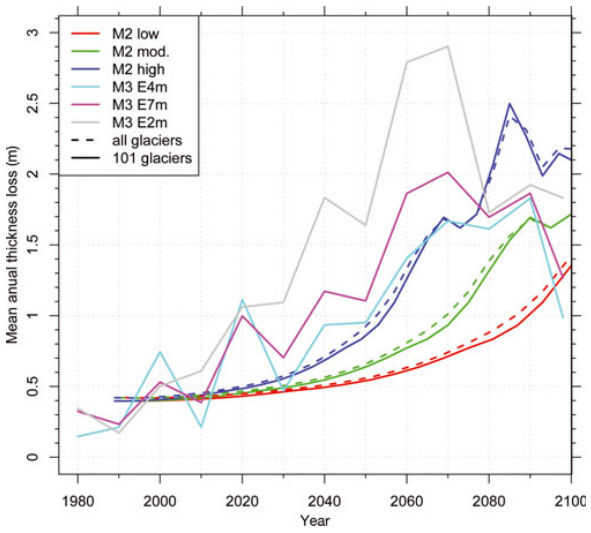

Fig. 8. Mean annual thickness loss over time, as derived from the three scenarios of M2 and the three ensemble means of M3.

The moderate scenarios of the three models give a relative area loss of 60–80% by 2100 compared to the glacier extent in 1985; in reality, glacier vanishing could be even more rapid.

Due to the simplifications induced by the parameterization schemes, uncertainties are large at a local scale (individual glaciers), but are likely to average out at the regional scale (Swiss Alps) and over extended time periods (decades to a century).

The overall trends of the modelled future glacier evolution – a strong to almost complete loss of glaciers by the end of the 21st century – are therefore clear and robust as air temperatures are expected to increase further.

The variability in the climate scenarios leads to a maximum spread of ~40% in the remaining area by 2100 (relative loss of 55–95%).

The uncertainty in estimations of present-day ice thickness (about ±30%) has a smaller but still considerable effect and impacts directly and non-symmetrically on the timescale of the modelled future glacier development.

The probably strong impact of unconsidered feedback processes (albedo change, lake formation, subglacial ablation, debris cover, etc.) needs further investigation.

All three models have advantages and disadvantages in their application. Which model to choose for a specific application depends on data availability and the level of detail required in the output. M1 and M2 have proven to provide fast and robust first-order estimates for glacier retreat, dominated by temperature increase. They might be less suitable when changes in precipitation have to be considered as well, but here the uncertainties are even larger.

ACKNOWLEDGEMENTS

This study was funded by BAFU (Swiss Federal Office for the Environment) and FMV (Forces Motrices Valaisannes) as part of two research projects CCHydro and 'Climate change and hydropower'. We acknowledge MeteoSwiss for providing the meteorological observations, and swisstopo for the DEM. The delta change scenario data were distributed by the Center for Climate Systems Modeling (C2SM). The data were derived from regional climate simulations of the European Union FP6 Integrated Project ENSEMBLES (contract No. 505539). The dataset was prepared by T. Bosshard at ETH Zürich, partly funded by swisselectric/Swiss Federal Office of Energy (BFE) and CCHydro/BAFU. We thank M. Hoelzle for helpful remarks. The constructive comments of the editor, V. Radić, and two anonymous reviewers helped to improve the manuscript considerably.

REFERENCES

Bahr DB, Dyurgerov M and Meier MF (2009) Sea-level rise from glaciers and ice caps: a lower bound. *Geophys. Res. Lett.*, **36**(3), L03501 (doi: 10.1029/2008GL036309)

Begert M, Schlegel T and Kirchhofer W (2005) Homogeneous temperature and precipitation series of Switzerland from 1864 to 2000. *Int. J. Climatol.*, **25**(1), 65–80 (doi: 10.1002/joc.1118)

Bosshard T, Kotlarski S, Ewen T and Schär C (2011) Spectral representation of the annual cycle in the climate change signal. *Hydrol. Earth Syst. Sci. Discuss.*, **8**(1), 1161–1192 (doi: 10.5194/hessd-8-1161-2011)

Condom TH, Coudrain A, Sicart JE and Théry S (2007) Computation of the space and time evolution of equilibrium-line altitudes on Andean glaciers (10° N–55° S). *Global Planet. Change*, **59**(1–4), 189–202 (doi: 10.1016/j.globplacha.2006.11.021)

Farinotti D, Huss M, Bauder A and Funk M (2009) An estimate of the glacier ice volume in the Swiss Alps. *Global Planet. Change*, **68**(3), 225–231 (doi: 10.1016/j.gloplacha.2009.05.004)

Farinotti D, Usselmann S, Huss M, Bauder A and Funk M (2012) Runoff evolution in the Swiss Alps: projections for selected high-alpine catchments based on ENSEMBLES scenarios. *Hydrol. Process.*, **26**(13), 1909–1924 (doi: 10.1002/hyp.8276)

Fischer A, Olefs M and Abermann J (2011) Glaciers, snow and ski tourism in Austria's changing climate. *Ann. Glaciol.*, **52**(58), 89–96 (doi: 10.3189/172756411797252338)

Frey H, Haeberli W, Linsbauer A, Huggel C and Paul F (2010) A multi-level strategy for anticipating future glacier lake formation and associated hazard potentials. *Natur. Hazards Earth Syst. Sci. (NHESS)*, **10**(2), 339–352

Giesen RH and Oerlemans J (2012) Global application of a surface mass balance model using gridded climate data. *Cryos. Discuss.*, **6**(2), 1445–1490 (doi: 10.5194/tcd-6-1445-2012)

Greuell W, Knap WH and Smeets PC (1997) Elevational changes in meteorological variables along a mid-latitude glacier during summer. *J. Geophys. Res.*, **102**(D22), 25 941–25 954 (doi: 10.1029/97JD02083)

Guo Z, Dirmeyer PA, Gao X and Zhao M (2007) Improving the quality of simulated soil moisture with a multi-model ensemble approach. *Q. J. R. Meteorol. Soc.*, **133**(624), 731–747 (doi: 10.1002/qj.48)

Haeberli W and Hoelzle M (1995) Application of inventory data for estimating characteristics of and regional climate-change effects on mountain glaciers: a pilot study with the European Alps. *Ann. Glaciol.*, **21** 206–212

Haeberli W, Clague JJ, Huggel C and Kääb A (2010) Hazards from lakes in high-mountain glacier and permafrost regions: climate change effects and process interactions. In Úbeda X, Vericat D and Batalla R eds. *Avances de la geomorfología en Espãna, 2008–2010*. Societat Espanyola de Geomorfologia, Barcelona, 439–446

Hoelzle M, Paul F, Gruber S and Frauenfelder R (2005) Glaciers and permafrost in mountain areas: different modeling approaches. In *Global change impacts in mountain biosphere reserves*. UNESCO, Paris, 28–39 http://unesdoc.unesco.org/images/0014/001424/142482E.pdf

Hoelzle M, Darms G, Lüthi MP and Suter S (2011) Evidence of accelerated englacial warming in the Monte Rosa area, Switzerland/Italy. *Cryosphere*, **5**(1), 231–243 (doi: 10.5194/tc-5-231-2011)

Huss M (2011) Present and future contribution of glacier storage change to runoff from macroscale drainage basins in Europe. *Water Resour. Res.*, **47**(W7), W07511 (doi: 10.1029/2010WR010299)

Huss M (2012) Extrapolating glacier mass balance to the mountain-range scale: the European Alps 1900–2100. *Cryosphere*, **6**(4), 713–727 (doi: 10.5194/tc-6-713-2012)

Huss M, Farinotti D, Bauder A and Funk M (2008) Modelling runoff from highly glacierized alpine drainage basins in a changing climate. *Hydrol. Process.*, **22**(19), 3888–3902 (doi: 10.1002/hyp.7055)

Huss M, Jouvet G, Farinotti D and Bauder A (2010a) Future high-mountain hydrology: a new parameterization of glacier retreat. *Hydrol. Earth Syst. Sci.*, **14**(5), 815–829 (doi: 10.5194/hess-14-815-2010)

Huss M, Hock R, Bauder A and Funk M (2010b) 100-year mass changes in the Swiss Alps linked to the Atlantic Multidecadal Oscillation. *Geophys. Res. Lett.*, **37**(10), L10501 (doi: 10.1029/2010GL042616)

Huss M, Usselmann S, Farinotti D and Bauder A (2010c) Glacier mass balance in the south-eastern Swiss Alps since 1900 and perspectives for the future. *Erdkunde*, **64**(2), 119–140 (doi: 10.3112/erdkunde.2010.02.02)

Jouvet G, Huss M, Blatter H, Picasso M and Rappaz J (2009) Numerical simulation of Rhonegletscher from 1874 to 2100. *J. Comput. Phys.*, **228**(17), 6426–6439 (doi: 10.1016/j.jcp.2009.05.033)

Jouvet G, Huss M, Funk M and Blatter H (2011) Modelling the retreat of Grosser Aletschgletscher, Switzerland, in a changing climate. *J. Glaciol.*, **57**(206), 1033–1045 (doi: 10.3189/002214311798843359)

Köplin N, Schädler B, Viviroli D and Weingartner R (2012) The importance of glacier and forest change in hydrological climate-impact studies. *Hydrol. Earth Syst. Sci. Discuss.*, **9**(5), 5983–6021 (doi: 10.5194/hessd-9-5983-2012)

Kuhn M (1981) Climate and glaciers. *IAHS Publ.* 131 (Symposium at Canberra 1979 – *Sea Level, Ice and Climatic Change*), 3–20

Künzler M, Huggel C, Linsbauer A and Haeberli W (2010) Emerging risks related to new lakes in deglaciating areas of the Alps. In Malet JP, Glade T and Casagli N eds. *Mountain risks: bringing science to society. Proceedings of the 'Mountain Risk' International Conference, 24–26 November, 2010, Firenze, Italy*. Centre Européen sur les Risques Géomorphologiques, Strasbourg, 453–458

Le Meur E, Gerbaux M, Schäfer M and Vincent C (2007) Disappearance of an Alpine glacier over the 21st century simulated from modeling its future surface mass balance. *Earth Planet. Sci. Lett.*, **261**(3–4), 367–374 (doi: 10.1016/j.epsl.2007.07.022)

Li H, Ng F, Li Z, Qin D and Cheng G (2012) An extended 'perfect-plasticity' method for estimating ice thickness along the flow line of mountain glaciers. *J. Geophys. Res.*, **117**(F1), F01020 (doi: 10.1029/2011JF002104)

Lie O, Dahl SO and Nesje A (2003) Theoretical equilibrium-line altitudes and glacier buildup sensitivity in southern Norway based on meteorological data in a geographical information system. *Holocene*, **13**(3), 373–380

Linsbauer A, Paul F and Haeberli W (2012) Modeling glacier thickness distribution and bed topography over entire mountain ranges with GlabTop: application of a fast and robust approach. *J. Geophys. Res.*, **117**(F3), F03007 (doi: 10.1029/2011JF002313)

Machguth H, Paul F, Kotlarski S and Hoelzle M (2009) Calculating distributed glacier mass balance for the Swiss Alps from regional climate model output: a methodical description and interpretation of the results. *J. Geophys. Res.*, **114**(D19), D19106 (doi: 10.1029/2009JD011775)

Machguth H, Haeberli W and Paul F (2012) Mass balance parameters derived from a synthetic network of mass-balance glaciers. *J. Glaciol.*, **58**(211), 965–979 (doi: 10.3189/2012JoG11J223)

Maisch M, Wipf A, Denneler B, Battaglia J and Benz C (2000) *Die Gletscher der Schweizer Alpen. Gletscherhochstand 1850, Aktuelle Vergletscherung, Gletscherschwund-Szenarien.* (Schlussbericht NFP 31) vdf Hochschulverlag AG ETH, Zürich

Marzeion B, Hofer M, Jarosch AH, Kaser G and Mölg T (2012) A minimal model for reconstructing interannual mass balance variability of glaciers in the European Alps. *Cryosphere*, **6**(1), 71–84 (doi: 10.5194/tc-6-71-2012)

Mauser W and Bach H (2009) PROMET – Large scale distributed hydrological modelling to study the impact of climate change on the water flows of mountain watersheds. *J. Hydrol.*, **376**(3–4), 362–377 (doi: 10.1016/j.jhydrol.2009.07.046)

Moore RD and 7 others (2009) Glacier change in western North America: influences on hydrology, geomorphic hazards and water quality. *Hydrol. Process.*, **23**(1), 42–61 (doi: 10.1002/hyp.7162)

Müller F, Caflisch T and Müller G (1976) *Firn und Eis der Schweizer Alpen: Gletscherinventar.* (Geographisches Institut Publ. 57) Eidgenössische Technische Hochschule, Zürich

Oerlemans J (2001) *Glaciers and climate change.* AA Balkema, Lisse

Oerlemans J, Giesen RH and Van den Broeke MR (2009) Retreating alpine glaciers: increased melt rates due to accumulation of dust (Vadret da Morterastch, Switzerland). *J. Glaciol.*, **55**(192), 729–736 (doi: 10.3189/002214309789470969)

Paterson WSB (1994) *The physics of glaciers*, 3rd edn. Elsevier, Oxford

Paul F (2007) The new Swiss glacier inventory 2000 – application of remote sensing and GIS. *Schr. Phys. Geogr.* 52

Paul F and Haeberli W (2008) Spatial variability of glacier elevation changes in the Swiss Alps obtained from two digital elevation models. *Geophys. Res. Lett.*, **35**(21), L21502 (doi: 10.1029/2008GL034718)

Paul F and Linsbauer A (2012) Modeling of glacier bed topography from glacier outlines, central branch lines, and a DEM. *Int. J. Geogr. Inf. Sci.*, **26**(7), 1173–1190 (doi: 10.1080/13658816.2011.627859)

Paul F, Kääb A, Maisch M, Kellenberger T and Haeberli W (2004) Rapid disintegration of Alpine glaciers observed with satellite data. *Geophys. Res. Lett.*, **31**(21), L21402 (doi: 10.1029/2004GL020816)

Paul F, Maisch M, Rothenbühler C, Hoelzle M and Haeberli W (2007) Calculation and visualisation of future glacier extent in the Swiss Alps by means of hypsographic modelling. *Global Planet. Change*, **55**(4), 343–357 (doi: 10.1016/j.gloplacha.2006.08.003)

Radić V and Hock R (2011) Regionally differentiated contribution of mountain glaciers and ice caps to future sea-level rise. *Nature Geosci.*, **4**(2), 91–94 (doi: 10.1038/ngeo1052)

Raper SCB and Braithwaite RJ (2005) The potential for sea level rise: new estimates from glacier and ice cap area and volume distributions. *Geophys. Res. Lett.*, **32**(5), L05502 (doi: 10.1029/2004GL021981)

Raper SCB, Brown O and Braithwaite RJ (2000) A geometric glacier model for sea-level change calculations. *J. Glaciol.*, **46**(154), 357–368 (doi: 10.3189/172756500781833034)

Raymond CF, Neumann TA, Rignot E, Echelmeyer K, Rivera A and Casassa G (2005) Retreat of Glaciar Tyndall, Patagonia, over the last half-century. *J. Glaciol.*, **51**(173), 239–247 (doi: 10.3189/172756505781829476)

Rebetez M and Reinhard M (2008) Monthly air temperature trends in Switzerland 1901–2000 and 1975–2004. *Theor. Appl. Climatol.*, **91**(1–4), 27–34 (doi: 10.1007/s00704-007-0296-2)

Rickenbacher M (1998) Die digitale Modellierung des Hochgebirges im DHM25 des Bundessamtes für Landestopographie. *Wien. Schrift. Geogr. Kartogr.*, **11**, 49–55

Salzmann N, Machguth H and Linsbauer A (2012) The Swiss Alpine glaciers' response to the global '2°C air temperature target'. *Environ. Res. Lett.*, **7**(4), 044001 (doi: 10.1088/1748-9326/7/4/044001)

Schaefli B, Hingray B and Musy A (2007) Climate change and hydropower production in the Swiss Alps: quantification of potential impacts and related modelling uncertainties. *Hydrol. Earth Syst. Sci.*, **11**(3), 1191–1205

Schwarb M, Daly C, Frei C and Schär C (2001) Mean annual precipitation throughout the European Alps, 1971–1990. In *Hydrological atlas of Switzerland.* National Hydrologic Service, Bern, plates 2.6–2.7

Sevruk B (1997) Regional dependency of precipitation–altitude relationship in the Swiss Alps. *Climatic Change*, **36**(3–4), 355–369 (doi: 10.1023/A:1005302626066)

Solomon S and 7 others eds. (2007) *Climate change 2007: the physical science basis. Contribution of Working Group I to the Fourth Assessment Report of the Intergovernmental Panel on Climate Change.* Cambridge University Press, Cambridge

swisstopo (2005) *DHM25, das digitale Höhenmodel der Schweiz.* Federal Office of Topography, swisstopo, Wabern

Terrier S, Jordan F, Schleiss A, Haeberli W, Huggel C and Künzler M (2011) Optimized and adapted hydropower management considering glacier shrinkage scenarios in the Swiss Alps. In Schleiss A and Boes RM eds. *Proceedings of the International Symposium on Dams and Reservoirs under Changing Challenges. 79th Annual Meeting of ICOLD, Swiss Committee on Dams, Lucerne, Switzerland.* Taylor and Francis, London, 497–508

Van der Linden P and Mitchell JFB (2009) *ENSEMBLES: climate change and its impacts: summary of research and results from the ENSEMBLES project.* Met Office Hadley Centre, Exeter

Vincent C, Le Meur E, Six D, Possenti P, Lefebvre E and Funk M (2007) Climate warming revealed by englacial temperatures at Col du Dôme (4250 m, Mont Blanc area). *Geophys. Res. Lett.*, **34**(16), L16502 (doi: 10.1029/2007GL029933)

Viviroli D, Zappa M, Gurtz J and Weingartner R (2009) An introduction to the hydrological modelling system PREVAH and its pre- and post-processing-tools. *Environ. Model. Softw.*, **24**(10), 1209–1222 (doi: 10.1016/j.envsoft.2009.04.001)

World Glacier Monitoring Service (WGMS) (2011) *Glacier Mass Balance Bulletin No. 11 (2008–2009)*, eds. Zemp M, Nussbaumer SU, Gärtner-Roer I, Hoelzle M, Paul F and Haeberli W. ICSU(WDS)/IUGG(IACS)/UNEP/UNESCO/WMO, World Glacier Monitoring Service, Zürich

Zemp M, Haeberli W, Hoelzle M and Paul F (2006) Alpine glaciers to disappear within decades? *Geophys. Res. Lett.*, **33**(13), L13504 (doi: 10.1029/2006GL026319)

Zemp M, Paul F, Hoelzle M and Haeberli W (2008) Glacier fluctuations in the European Alps, 1850–2000: an overview and a spatiotemporal analysis of available data. In Orlove B, Wiegandt E and Luckman BH eds. *Darkening peaks: glacier retreat, science, and society.* University of California Press, Berkeley, CA. 152–167

Zemp M, Hoelzle M and Haeberli W (2009) Six decades of glacier mass-balance observations: a review of the worldwide monitoring network. *Ann. Glaciol.*, **50**, 101–111 (doi: 10.3189/172756409787769591)

Part III

Appendix

Personal bibliography

Frey, H., Haeberli, W., Linsbauer, A., Huggel, C., and Paul, F. (2010). A multi-level strategy for anticipating future glacier lake formation and associated hazard potentials. *Natural Hazards and Earth System Sciences*, 10 (2): 339–352.

Frey, H., Machguth, H., Huss, M., Huggel, C., Bajracharya, S., Bolch, T., Kulkarni, A., Linsbauer, A., Salzmann, N., and Stoffel, M. (2013). Ice volume estimates for the Himalaya–Karakoram region: evaluating different methods. *The Cryosphere Discussions*, 7 (5): 4813–4854. doi: 10.5194/tcd-7-4813-2013.

Haeberli, W., Schleiss, A., Linsbauer, A., Künzler, M., and Bütler, M. (2012). Gletscherschwund und neue Seen in den Schweizer Alpen: Perspektiven und Optionen im Bereich Naturgefahren und Wasserkraft. *Wasser Energie Luft*, 2: 93–102.

Haeberli, W. and Linsbauer, A. (2013). Brief communication "Global glacier volumes and sea level – small but systematic effects of ice below the surface of the ocean and of new local lakes on land". *The Cryosphere*, 7 (3): 817–821. doi: 10.5194/tc-7-817-2013.

Künzler, M., Huggel, C., Linsbauer, A., and Haeberli, W. (2010). Emerging risks related to new lakes in deglaciating areas of the Alps. In: *Mountain Risks: Bringing Science to Society. Proceedings of the "Mountain Risk" International Conference, 24–26 November 2010, Firenze, Italy*, (edited by Malet, J.-P., Glade, T., and Casagli, N.), pp. 453–458. CERG Editions, Strasbourg, France.

Linsbauer, A., Paul, F., Hoelzle, M., Frey, H., and Haeberli, W. (2009). The Swiss Alps without glaciers – a GIS-based modelling approach for reconstruction of glacier beds. In: *Proceedings of Geomorphometry 2009*, (edited by Purves, R., Gruber, S., Straumann, R., and Hengl, T.), pp. 243–247. University of Zurich, Zurich, Switzerland.

Linsbauer, A., Paul, F., and Haeberli, W. (2012a). Grossräumige Modellierung von Schwundszenarien für alle Schweizer Gletscher: Modellvergleich, Unsicher-

heiten und eine Analyse bezogen auf Grosseinzugsgebiete. Tech. rep., CCHydro-Schlussbericht des Geographischen Instituts der Universität Zürich (GIUZ).

Linsbauer, A., Paul, F., and Haeberli, W. (2012b). Modeling glacier thickness distribution and bed topography over entire mountain ranges with GlabTop: Application of a fast and robust approach. *Journal of Geophysical Research*, 117: F03007. doi: 10.1029/2011JF002313.

Linsbauer, A., Paul, F., Machguth, H., and Haeberli, W. (2013). Comparing three different methods to model scenarios of future glacier change in the Swiss Alps. *Annals of Glaciology*, 54 (63): 241–253. doi: 10.3189/2013AoG63A400.

Paul, F., Linsbauer, A., and Haeberli, W. (2011). Grossräumige Modellierung von Schwundszenarien für alle Schweizer Gletscher, Klimaänderung und Wasserkraft, Sektorielle Studie Wallis, Modul B Gletscherszenarien. Tech. rep., WWK Schlussbericht des Geographischen Instituts der Universität Zürich (GIUZ).

Paul, F. and Linsbauer, A. (2012). Modeling of glacier bed topography from glacier outlines, central branch lines, and a DEM. *International Journal of Geographical Information Science*, 26 (7): 1173–1190. doi: 10.1080/13658816.2011.627859.

Salzmann, N., Machguth, H., and Linsbauer, A. (2012). The Swiss Alpine glaciers' response to the global '2°C air temperature target'. *Environmental Research Letters*, 7 (4): 044001. doi: 10.1088/1748-9326/7/4/044001.

Curriculum Vitae (short version)

Personal details

First names:	Andreas
Last name:	Linsbauer
Date of birth:	24 May 1977
Place of birth:	Frauenfeld, Switzerland
Citizenship:	Swiss

Education

08/1993–07/1998	Lehrerseminar Kreuzlingen, Switzerland
10/2002–06/2008	Studies in Geography at the University of Zurich Specialization: Physical Geography, Glaciology and GIS Thesis: *Modellierung von Gletscherbetten mit GIS*
10/2006–04/2010	Höheres Lehramt in Geography, University of Zurich
10/2008–12/2012	PhD student at the Department of Geography, University of Zurich

Work experience

1998–2001	Primarlehrer an der Mittelstufe in Rickenbach bei Wil (TG)
2002–2005	Diverse Vikariate und Stellvertretungen als Mittel- und Oberstufenlehrer
2005–2009	Umweltschutz Stadt Luzern: GIS-Beauftragter/Sachbearbeiter (20%)
03–05/2011	Zivildienstleistener Pro Natura, Basel: Implementierung eines GIS-Servers
08–12/2012	WGMS, University of Zurich, Project Assistant (Meta-Data-Browser, 60%)

Acknowledgements

Gegen das Ende meiner Diplomarbeit (2008), bewarb ich mich auf eine Stelle ausserhalb der akademischen Welt, bei der ich in die engere Auswahl kam. In diesem Zusammenhang fragte ich Frank Paul an, ob ich ihn als Referenz angeben dürfe. Frank stimmte zu, bot mir aber gleichzeitig auch eine Doktorarbeit an. Unverhofft kam ich so in die Situation, dass ich zwischen einer unbefristeten Stelle und einer Stelle als Doktorand auswählen konnte.

Nun, vier Jahre später bereue ich meinen Entscheid keineswegs. Ich bin sehr glücklich dass ich diesen Punkt erreicht habe und auf eine erfolgreiche Dissertation zurückblicken kann. Während meiner Arbeit haben mich viele Menschen begleitet und unterstützt. Ohne sie wäre das alles nicht möglich gewesen und dafür möchte ich mich herzlich bedanken. Ein besonders herzliches Dankeschön geht an:

- Frank Paul, den Betreuer meiner Dissertation, der bereits als Betreuer meiner Diplomarbeit fungierte und mich dabei in die wissenschaftliche Welt der Gletscherforschung eingeführt hat. Das meiste was ich für diese Arbeit benötigte, habe ich von ihm gelernt. Sein grosse vernetztes Wissen und seine vielen Ideen haben mich immer wieder beeindruckt und mir bei meiner Arbeit weitergeholfen. Obwohl Frank öfters mit (zu) viel Arbeit eingedeckt war und unter enormen Termindruck stand, hat er immer wieder Zeit gefunden, um auf meine Fragen und Probleme einzugehen, sie ausführlich zu beantworten, oder nach einer längeren Diskussion eine gute Lösung zu finden. Frank war immer da (7 Tage die Woche, bis abends um 23 Uhr) und das habe ich sehr geschätzt (und auch oft genutzt). Herzlichen Dank Frank!

- Wilfried Haeberli, der schon zu Beginn des Studiums meine Begeisterung für die vergletscherte Hochgebirgswelt geweckt und immer weiter genährt hat. Seine Begeisterung für die Sache und sein grosses Interesse an meinen Resultaten waren immer wieder ermutigend und motivierend. Wilfried hat den Überblick über meine Arbeit behalten, sie im grösseren Kontext betrachtet und damit verhindert, dass ich mich in den Details verliere. Seine Sicht- und Denkweise hat meine

akademische Karriere wesentlich geprägt und ich bin dankbar, dass mich Wilfried bis zum Schluss so eng begleitet hat.

- Martin Hoelzle, der meine Dissertation mit betreut hat und mit der nötigen Distanz die Resultate meiner Arbeit beurteilen konnte. Er hat mich in meiner Arbeit bestärkt und war da, wenn ich ihn brauchte.

- Der ganzen 3G-Gruppe und der tollen Arbeitsatmosphäre. Es gab immer wieder Gelegenheit und Raum für angeregte wissenschaftliche Debatten, aber auch persönliche und belanglose Gespräche. Vor allem dank der lebendigen 3G-Gruppe war es nie ein "Muss" an den Irchel zu kommen.

- Luzia Fischer, Demian Schneider, Lorenz Böckli, Joel Fiddes und Claudia Giraldez, die mit mir das Büro teilten und mithalfen die Pflanzen zu giessen; Lorenz Böckli und Stephanie Gubler, die ihre Diss etwa gleichzeitig begonnen und beendet haben; Raymond Le Bris, mit dem ich die Höhen und Tiefen des letzten Jahres geteilt habe; Holger Frey, mit dem ich thematisch viel zu tun hatte und der die tolle LaTeX-Vorlage lieferte; Matthias Künzler, für die vielen Gespräche und die gemeinsame Zeit an der Uni und bei ProNatura; Wilfried Haeberli, Christian Huggel, Yvonne Schaub, Nico Mölg und Matthias Künzler vom NELAK-Projekt, indem meine Daten verwendet wurden; Holger Frey, Lorenz Böckli, Andreas Hasler, Jeannette Nötzli, Vanessa Wirz, Philipp Rastner und Ralph Böhlert für die Joggingrunden im Wald; Michael Zemp, Isabelle Gärtner-Roer und Samuel Nussbauemer vom WGMS, bei dem ich das letzte halbe Jahr mitarbeiten durfte und auch Nadine Salzmann und Horst Machguth, für die gute Zeit mit und auf dem Findelengletscher.

- Meinen Eltern, meinen Brüdern und ihren Partnerinnen, den Semis und Pfadis, den Nachbarn im Hof und den anderen Freunden mit denen ich viel Zeit neben der Arbeit an meiner Dissertation verbracht habe.

- Ronja und Maja, die das Leben entscheidend bereichert haben und es mir sehr einfach machten "die abgehobene Welt der Wissenschaft" zu vergessen und mich auf den Boden zurückholten.

- Und vor allem auch an Andrea, die mich immer unterstützt und begleitet hat und immer für mich da war.

Herzlichen Dank!